

**CALIX[4]ARENE METAL COMPLEXES
AS NUCLEASE AND TRANSACYLASE MIMICS**

© A. Sartori, Enschede, 2004

Front cover: from left to right, pictures of Enschede, Roma, Parma.

Back cover: from top left, clockwise, pictures of Parma, Enschede, Roma, Enschede.

No part of this work may be reproduced by print, photocopy or any other means without the permission in writing of the author.

ISBN 90-365-2095-9

CALIX[4]ARENE METAL COMPLEXES AS NUCLEASE AND TRANSACYLASE MIMICS

PROEFSCHRIFT

ter verkrijging van
de graad van doctor aan de Universiteit Twente,
op gezag van de rector magnificus,
prof. dr. F.A. van Vught,
volgens besluit van het College van Promoties
in het openbaar te verdedigen
op vrijdag 25 november 2004 om 16.45 uur

door

Andrea Sartori

geboren op 05 november 1973
Te Parma, Italië

Dit proefschrift is goedgekeurd door:

Promotor: Prof. Dr. Ir. D. N. Reinhoudt

Assistent-promotor: Prof. A. Casnati

Contents

CHAPTER 1

General Introduction	1
-----------------------------------	---

CHAPTER 2

Enzymes and supramolecular catalysts for ester, amide and nucleotide cleavage

2.1 Introduction.....	5
2.2 Enzyme catalysis.....	7
2.2.1 Enzyme kinetics.....	7
2.2.2 Origin of the enzyme catalysis.....	8
2.3 Mechanisms of phosphoryl and acyl transfer reactions.....	11
2.3.1 Phosphate ester hydrolysis.....	11
2.3.2 Enzymatic cleavage of phosphodiester.....	13
2.3.3 Mechanism of amide and ester hydrolysis.....	17
2.3.4 Enzymatic amide cleavage.....	18
2.4 Enzyme mimics.....	19
2.5 Synthetic metallonucleases for RNA cleavage.....	20
2.5.1 Mononuclear catalysts.....	21
2.5.2 Di- and trinuclear nuclease mimics.....	23
2.5.3 Catalysts with a RNA recognition group.....	27
2.6 Synthetic supramolecular catalysts for amide cleavage.....	31
2.7 Synthetic supramolecular catalysts for ester cleavage.....	33
2.8 Calixarenes as enzyme models.....	35
2.9 Concluding remarks.....	38
2.10 References and notes.....	38

CHAPTER 3

Water soluble calix[4]arene based receptors and catalysts

3.1 Introduction.....	44
3.1.1 Water soluble calix[4]arenes.....	44
3.1.2 β -Cyclodextrins as solubilizing moieties.....	46
3.1.3 Aim of the work and contents of the chapter.....	47
3.2 Introduction of polyethyleneglycol chains at the lower rim.....	48
3.3 Synthesis of adamantyl calix[4]arenes.....	51
3.3.1 Water solubility measurements.....	53
3.3.2 Upper rim functionalization of adamantyl calixarenes	53
3.3.3 Microcalorimetric measurements.....	56
3.4 Alternative approach to obtain water soluble calix[4]arene trinuclear catalysts...	58
3.4.1 Water solubility and Zn(II) complexation.....	58
3.5 Catalysis.....	59
3.6 Conclusions.....	61
3.7 Experimental part.....	61
3.8 References and notes.....	79

CHAPTER 4

Synthesis and catalytic activity of upper rim proximal calix[4]arene dinuclear metal complexes

4.1 Introduction.....	82
4.2 Upper rim 1,2-difunctionalization of calix[4]arenes.....	83
4.3 Synthesis of bis(monoaza-18-crown-6)calix[4]arenes.....	88
4.4 Catalysis.....	89
4.4.1 Rate accelerations and synergism factors.....	90
4.4.2 Effective Molarities.....	92
4.4 Conclusions.....	95
4.5 Experimental part.....	96
4.6 References and notes.....	101

CHAPTER 5

Synthesis and catalytic activity of Zn(II) calix[4]arene complexes in aryl ester methanolysis

5.1 Introduction.....	106
5.2 Synthesis.....	108
5.2.1 Synthesis of 1,2-bisdiaminopyridine-calix[4]arene.....	108
5.2.2 Synthesis of [12]aneN ₃ -calix[4]arenes.....	109
5.3 Binding and catalysis.....	113
5.3.1 Methanolysis catalyzed by pyridine-calixarene Zn ^{II} complexes.....	114
5.3.2 Methanolysis catalyzed by [12]aneN ₃ -calixarene Zn ^{II} complexes.....	116
5.4 Conclusions.....	119
5.5 Experimental part.....	119
5.6 References and notes.....	131

CHAPTER 6

Cleavage of phosphate diester RNA models and dinucleotides by metallo(II) complexes of calix[4]arenes functionalized with nitrogen ligands

6.1 Introduction.....	134
6.2 Catalytic activity of Zn(II) complexes in HPNP transesterification.....	137
6.3 Catalytic activity of Cu(II) triazacalix[4]arene complexes in HPNP transesterification.....	139
6.4 Catalytic activity of Cu(II) complexes in dinucleotide cleavage.....	141
6.5 Conclusions.....	143
6.6 Experimental part.....	144
6.7 References and notes.....	146

CHAPTER 7

Oligoribonucleotide cleavage by copper(II) triazacalix[4]arene complexes

7.1 Introduction.....	148
7.1.1 Structural and base-pair sequence effects on the nonenzymatic cleavage of oligoribonucleotides.....	148
7.1.3 Contents of the Chapter.....	152
7.2 Catalytic activity of Cu(II) triazacalix[4]arene complexes in oligonucleotide cleavage.....	152
7.3 Conclusions.....	166
7.4 Experimental part.....	167
7.5 Appendix.....	168
7.6 References and notes.....	171
Summary.....	173
Samenvatting.....	177
Acknowledgements.....	181
The author.....	183

CHAPTER 1

General introduction

"Many organic chemists viewing the crystal structures of enzyme systems or nucleic acids and knowing the marvels of specificity of the immune system must dream of designing and synthesising simpler organic compounds that imitate the working features of these naturally occurring compounds."^{*} This statement was made by Donald Cram during his Nobel lecture and illustrates well the inspiration of biomimetic catalysis, which occupies a central position in supramolecular chemistry¹. The enormous accelerations with respect to the uncatalyzed reactions and the extreme substrate regio- and stereospecificity provided under mild conditions by enzymes² is obtained in Nature through the simultaneous operation of weak intermolecular interactions (electrostatic and van der Waals forces, hydrophobic effects, π - π stacking, metal coordination and hydrogen bonding). This feature has challenged many supramolecular chemists and led them to design systems that mimic the catalytic activity of enzymes.³ The general goal is the invention of simple systems, which exhibit catalytic functions analogous to those present in enzyme active sites, in order to create more robust catalysts with wider applicability, also at an industrial level. Moreover, the enzyme models are useful to better understand the mode of action of enzymes in terms of structure, mechanism and rate acceleration.⁴

Nucleases and peptidases are hydrolytic enzymes that catalyze the cleavage of phosphodiester and amide bonds, respectively, that under neutral conditions have a very high kinetic stability. Phosphodiester bonds are the linkages between the nucleosides in DNA and RNA. Because of the importance of these biological macromolecules in the storage and transmission of genetic information, there is large interest in the synthesis of compounds able to cleave selectively a target RNA or DNA. These biomimetic catalysts could be useful both for biotechnological applications in molecular biology and in medicine as therapeutic antisense oligonucleotides.⁵

Many nucleases and some peptidases exploit divalent metal ions as essential cofactors.⁶ The metal centers are directly involved in the catalytic mechanism by

^{*} D. J. Cram, "The Design of Molecular Hosts, Guests, and their complexes (Nobel Lecture)", *Angew. Chem. Int. Ed. Engl.*, **1988**, 27, 1009-1020.

activating the nucleophile and the electrophile, stabilizing the leaving group, or furnishing an acid-base catalysis by means of bound-water molecules. However, only a combination of these factors by an optimum preorganization of the metal centers in the active site,⁷ allows the hydrolytic enzymes to provide rate enhancements larger than 10^{12} .

Several models with two metal ions have been reported in recent years with the aim of mimicking the catalytic activity of dinuclear metallo-hydrolases.⁸ However, because of the many factors involved in the efficiency of a dinuclear catalyst (metal-metal distance and relative orientation, geometry of the metal coordination, rigidity/flexibility of the system, substrate-catalyst interaction, etc) it is often difficult to reach high degrees of cooperativity of the metal centers, and the rate enhancements are generally low.

Because of the different possibilities of functionalization in terms of number and position, the calix[4]arene skeleton⁹ has been used to preorganize the catalytic groups for cooperative catalysis. It turned out to be a useful scaffold.¹⁰

This thesis describes the synthesis of mono, di- and trinuclear metallo-catalysts based on calix[4]arenes and their catalytic activity in phosphate diester cleavage and ester methanolysis.

In Chapter 2 an introduction to enzyme catalysis and its origin is given. Examples of natural metallo-nucleases and peptidases are described and the most recent efforts in the development of metallo-enzyme mimics for the cleavage of ester, amide and phosphate bonds are reviewed. Particular attention is devoted to the role of the metal centers in the catalytic processes.

Chapter 3 describes three different approaches that have been explored to solubilize calix[4]arenes in water with the aim of preparing water soluble calixarene-based catalysts. The synthesis of water soluble para-guanidinium di- and tetra-adamantyl calix[4]arenes used as guest molecules to pattern β -cyclodextrin self-assembled monolayers is also reported.

In Chapter 4 a procedure to introduce functional groups on the 1,2-proximal positions of the calix[4]arene upper rim is described. Novel homodinuclear calix[4]arene ligands were prepared by functionalization of the proximal (1,2) or diametral (1,3) positions with monoaza-18-crown-6, and the catalytic activity of their Ba^{2+} complexes was investigated in the ethanolysis of esters.

Chapter 5 describes the synthesis of a calix[4]arene functionalized at the 1,2-positions with 2,6-bis[(dimethylamino)methyl]pyridine ligating groups and the synthesis of new calixarene ligands obtained by the introduction of one, two (in diametral or proximal positions) and three 1,5,9-triazacyclododecane ([12]aneN₃)

macrocycles at the upper rim. The catalytic activity of the Zn(II) complexes of these ligands is reported in the methanolysis of aryl esters (acyl transfer reactions).

Chapter 6 and Chapter 7 describe studies of the phosphodiesterase activity of the metal (II) complexes of the triaza-calix[4]arenes. In Chapter 6 the catalytic activity of the Zn(II) complexes in the transesterification of hydroxypropyl p-nitrophenyl phosphate (HPNP) is reported, while the corresponding Cu(II) complexes are studied as catalysts for the cleavage of both HPNP and dinucleotides. In Chapter 7 the nuclease activity of copper(II) triaza-calixarene complexes in the cleavage of six-, seven- and seventeen-base oligomers is reported.

References

- (1) a) Special Issue "Supramolecular Chemistry and Self Assembly": *Science* **2002**, *295*, 2400-2421. b) Lehn, J. M. *Supramolecular Chemistry: Concepts and Perspectives*; WILEY-VCH: Weinheim, 1995. c) *Comprehensive Supramolecular Chemistry*; Atwood, J. L.; Davies, J. E. D.; MacNicol, D. D.; Vögtle, F. Elsevier: Oxford, 1996.
- (2) Stryer, L. *Biochemistry*; New York, 1995.
- (3) a) Murakami, Y.; Kikuchi, J.; Hisaeda, Y.; Hayashida, O. *Chem. Rev.* **1996**, *96*, 721-758. b) Parkin, G. *Chem. Rev.* **2004**, *104*, 699-767. c) Motherwell, W. B.; Bingham, M. J.; Six, Y. *Tetrahedron* **2001**, *57*, 4663-4686.
- (4) Dugas, H. *Bioorganic Chemistry*; Springer-Verlag: New York, 1988.
- (5) a) Trawick, B. N.; Daniher, A. T.; Bashkin, J. K. *Chem. Rev.* **1998**, *98*, 939-960. b) Agrawal, S.; Zhao, Q. *Curr. Opin. Chem. Biol.* **1998**, *4*, 519-528.
- (6) Wilcox, D. E. *Chem. Rev.* **1996**, *96*, 2435-2458.
- (7) a) Strater, N.; Lipscomb, W. N.; Klabunde, T.; Krebs, B. *Angew. Chem. Int. Ed* **1996**, *35*, 2024-2055. b) Emilsson, G. M.; Nakamura, S.; Roth, A.; Breaker, R. R. *RNA* **2003**, *9*, 907-918.
- (8) a) Morrow, J. R.; Iranzo, O. *Curr. Opin. Chem. Biol.* **2004**, *8*, 192-200. b) Hegg, E. L.; Burstyn, J. N. *Coord. Chem. Rev.* **1998**, *173*, 133-165. c) Bashkin, J. K. *Curr. Opin. Chem. Biol.* **1999**, *3*, 752-758. d) Sreedhara, A.; Cowan, J. A. *J. Biol. Inorg. Chem.* **2001**, *6*, 166-172. e) Kimura, E. *Curr. Opin. Chem. Biol.* **2000**, *4*, 207-213. f) Chin, J. *Curr. Opin. Chem. Biol.* **1997**, *1*, 514-521.
- (9) a) *Calixarenes in Action*; Imperial College Press: London, 2000. b) *Calixarenes 2001*; Kluwer Academic Publishers: Dordrecht, 2001.
- (10) a) Cacciapaglia, R.; Mandolini, L. Calixarene based catalytic systems; In *Calixarenes in Action*; Mandolini, L., Ungaro, R., eds. Imperial College Press: London, 2000; pp 241-264. b) Molenveld, P.; Engbersen, J. F. J.; Reinhoudt, D. N. *Chem. Soc. Rev.* **2000**, *29*, 75-86.

CHAPTER 2

Enzymes and supramolecular catalysts for ester, amide and nucleotide cleavage

An introduction to enzyme catalysis and its origin is reported in the first part of this chapter. Then the mechanism of phosphodiester bond cleavage in a RNA strand both in uncatalyzed and catalyzed reactions is described. Examples of nucleases are discussed with particular attention to the role of the metals in their catalytic mechanisms. Also the catalytic activation of amide bonds by metal ions is described and some examples of metallopeptidases are reported. Enzyme models which exploit metal ions for the cleavage of ester, amide and phosphate bonds are reviewed. In the last part of the chapter some examples of calixarene enzyme mimics are described.

2.1 Introduction

Enzymes are an important class of biomolecules. With the exception of few catalytic RNAs named ribozymes, they are mainly proteins that can catalyze reactions very efficiently and with a high degree of specificity.^{1;2} They show substrate regio- and stereospecificity, but the most impressive property is their ability to accelerate reactions under mild conditions (37 °C, pH 7.4) in some cases up to 10^{15} times with respect to the uncatalyzed reaction. Although enzymes generally have a molecular weight higher than 20 kDa, the catalytic process takes place only in a specific region referred to as the active site. This consists of the amino acid residues primarily involved in the selective binding and subsequent transformation of the substrate. The enzyme catalytic activity is therefore apparently determined only by a limited number of groups highly preorganized in the active site. The goal of supramolecular chemists interested in catalysis is the synthesis of artificial systems able to mimic the enzyme active site with the aim of reaching the catalytic accelerations of natural enzymes.³ These systems are called enzyme models and are generally organic molecules that contain one or more features present in the enzyme active sites.

Nucleases and peptidases are hydrolytic enzymes (hydrolases) able to cleave very efficiently phosphate ester and amide bonds, respectively (Figure 2.1). The importance of biomimetic nucleases for the hydrolysis of DNA and RNA is their possible application in biotechnology (manipulation of genes, DNA sequencing) and in medicine (gene therapy).^{4;5} Synthetic peptidases, on the other hand, could be used in determining the sequence of large proteins.⁶ Nevertheless, the achievement of the enzyme-like activity (and/or selectivity) by synthetic compounds is far from being reached and the research of true enzyme models is still in its infancy. However, the importance of these synthetic systems is in the possibility that they offer of a better understanding the mechanism of action of natural enzymes.

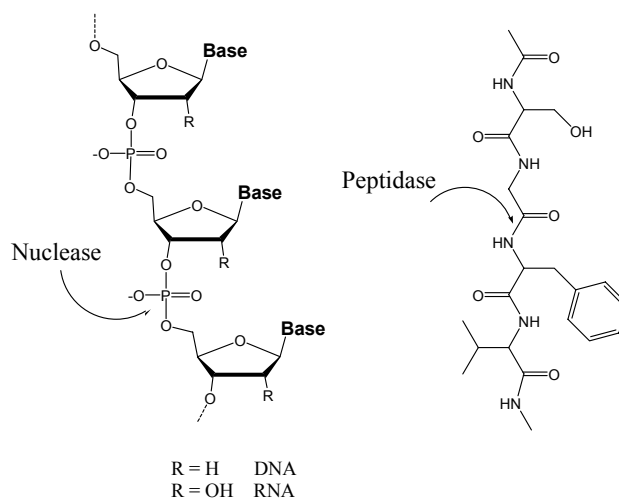


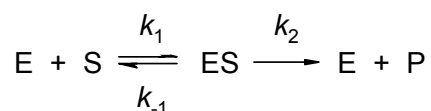
Figure 2.1

In this chapter an introduction to the enzyme catalysis and its origin is reported. A discussion of the reactivity of phosphate diester, and carboxy amide and ester bonds will be followed by the description of some examples of natural nucleases and peptidases with particular attention to their catalytic mechanisms. The state of the art in supramolecular biocatalysis will be illustrated with several recent examples of synthetic hydrolytic enzyme models.

2.2 Enzyme catalysis

2.2.1 Enzyme kinetics

In 1913 Michaelis and Menten were the first to develop a quantitative scheme for enzyme kinetics. The difference between enzyme catalyzed and conventional bimolecular reactions is the large excess of substrate concentration with respect to the enzyme concentration ($[S] \gg [E]$). For a simple reaction involving only one substrate:



the rate equation is given by (1) and it is a function of the concentration of ES, that cannot be directly measured.

$$v = \frac{d[P]}{dt} = k_2 [ES] \quad (1)$$

The Michaelis-Menten kinetic model was developed on the hypothesis of the "steady-state".

$$\frac{d[ES]}{dt} = 0$$

After a brief transient period the $[ES]$ is kept at a constant level, while $[S]$ decreases and $[P]$ increases, both of them linearly. This phenomenon is called saturation because the enzyme is saturated by the substrate. Using this assumption, the rate equation can be written as:

$$v = \frac{k_2 [E_{\text{tot}}] [S]}{[S] + K_M} = \frac{V_{\text{max}} [S]}{[S] + K_M} \quad (2)$$

where K_M is the Michaelis-Menten constant and V_{max} is reached when the enzyme is completely saturated.

$$K_M = \frac{k_{-1} + k_2}{k_1}$$

$$V_{\max} = k_2 [ES] = k_2 [E_{\text{tot}}]$$

In equation (2) the rate is governed by two parameters (V_{\max} and K_M) and the concentration of the substrate, which can be experimentally measured.

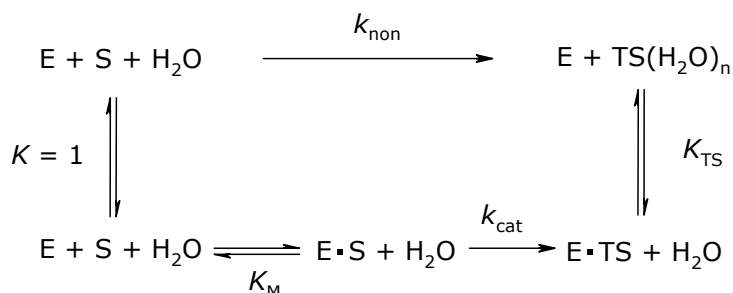
It is important to underline that K_M is correlated to the binding of the enzyme with the substrate. When $k_2 \ll k_{-1}$ (rapid equilibrium), K_M is given by the ratio k_{-1}/k_1 , so it is a direct measure of the enzyme-substrate affinity, while nothing can be said when the k_2 value is unknown. Moreover, K_M is a constant specific for every enzyme. In a process like that described above, k_2 is the same as k_{cat} (catalytic rate constant). k_{cat} is also the turnover frequency ($k_{\text{cat}} = V_{\max}/[E_{\text{tot}}]$) because it represents the number of substrate molecules converted into product in the unit of time per one enzyme molecule.

The ratio k_{cat}/K_M is named the specificity constant. When $[S] \ll K_M$, k_{cat}/K_M becomes an apparent second order rate constant and the reaction shows clean second order kinetics. When $k_2 \gg k_{-1}$ and $k_{\text{cat}}/K_M = k_1$, this ratio is the rate constant for binding of the substrate to the enzyme. In this case the reaction rate approaches the diffusion limit.

Almost every enzyme reaction is more complicated, but the Michaelis-Menten equation describes well the reactions catalyzed by enzyme mimics.

2.2.2 Origin of enzyme catalysis

Pauling's idea^{7;8} that the active site of an enzyme binds more strongly to the transition state (TS) than to the substrate (S) and by doing so, stabilizes the TS and lowers the activation energy of the reaction is still largely accepted. The pseudothermodynamic cycle shown in Scheme 2.1 has been used to compare the uncatalyzed reaction in solution with the enzyme catalyzed one, calculating the equilibrium constant ($1/K_{\text{TS}}$) for binding of various transition states by their respective enzymes. The numerical value calculated for $K_{\text{TS}} = (k_{\text{non}}K_M)/k_{\text{cat}}$ is a measure of the efficiency of the catalysis.



Scheme 2.1

Nevertheless, a still open question is how enzymes achieve their catalytic rate enhancements relative to the corresponding uncatalyzed reactions. Many researchers in the field have pointed out the possible relationship between enzyme catalysis and intramolecularity. Indeed, huge accelerations ($\geq 10^8$) are often observed when an intermolecular reaction is converted into its intramolecular counterpart. These values are comparable to rate accelerations found in enzyme catalyzed reactions.^{9;10} This has suggested that in the activity of enzymes and in intramolecular systems accelerations have a similar origin.

Page and Jencks have emphasized entropic factors, pointing out that the translational and rotational freedom of motion of reactants in a bimolecular reaction would be frozen out on conversion to an intramolecular reaction or an enzymatic reaction.¹¹ The estimated entropic contributions should be sufficient to provide a 10^8 increase in rate. Their calculations are considered largely overestimated by many researchers. Warshel found that many of the motions that are free in solution are also free in the transition state¹² and the binding of substrate to the enzyme does not completely freeze out the motion of the fragments. Thus the entropic contributions are not so different in the enzyme and in solution. Menger^{9;10;13} has also pointed out that activation entropy is a mixture of factors (changes in solvation, conformation, molecularity, etc...) that cannot be rationalized or predicted. He proposed the "spatiotemporal principle" considering the reactivity as a function of the distance and time: "fast reactions between two functionalities are achieved when the reacting centers are held at contact distances either by covalent framework (intramolecular systems) or by noncovalent forces (enzymes); meaning with "contact" an atomic separation too small to permit intervening solvent ($< 3 \text{ \AA}$)". In the active site of an enzyme the reactive groups are held in an arrangement such that a water molecule cannot be situated between them and the TS formation is under enthalpic control.

The idea that the driving force in an enzyme reaction is enthalpic is also supported by the studies of Bruice and Lightstone.¹⁴ They reinterpreted¹⁵ the data of intramolecular lactonizations,¹⁶ used for a long time as a support for the importance of entropic factors in the activation energy (ΔG^\ddagger), concluding that these reactions are enthalpy driven. They introduced the definition of the Near Attack Conformation (NAC) as the required conformation for reactants to enter a transition state (TS). The ΔG^\ddagger of each intramolecular reaction is directly dependent on the fraction of ground state conformations present as NACs, and the formation of NACs is under enthalpic control. Examining several enzymatic reactions, that did not involve covalent intermediates, Bruice^{17;18} concluded that the kinetic advantage of enzymatic reactions compared to the nonenzymatic ones is the ease of formation of NAC structures. The enzymes are

able to desolvate the substrate and orient the reactants into a NAC, increasing the mole percent of conformers that are NACs.

Recently, enzyme catalysis has been studied using a combination of quantum and molecular mechanics obtaining very interesting results. From these studies, concepts like "orbital steering",¹⁹ "low-barrier hydrogen bonds"²⁰ or "pK_a matching"²¹, which have been used to explain the high enzyme accelerations, remain unproven. Warshel introduced the concept of the "solvent cage" comparing calculations regarding a specific reaction in an enzyme and in solution.¹² In the enzyme the total activation free energy can be divided into the binding free energy of the Michaelis complex (ΔG_{bind} , related to the dissociation constant K_M) and the free energy needed to reach the TS from the complex, $\Delta g_{\text{cat}}^\ddagger$, which corresponds to the rate constant k_{cat} .

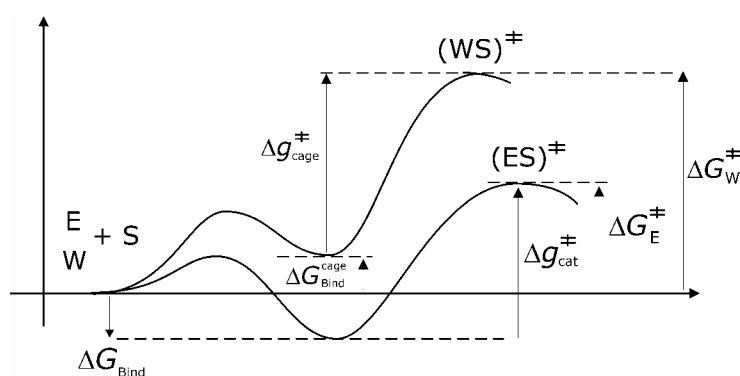


Figure 2.2 Comparing the free energy surfaces for an enzyme reaction and the corresponding reaction in solution. E = enzyme, W = water molecules (uncatalyzed reaction), S = substrate.

Direct comparison between $\Delta g_{\text{cat}}^\ddagger$ and $\Delta g_{\text{cage}}^\ddagger$ can be made. From calculations the $\Delta g_{\text{cat}}^\ddagger$ is considerably smaller than $\Delta g_{\text{cage}}^\ddagger$ and this reduction results mainly from electrostatic interactions that stabilize the TS in the enzyme more than the corresponding TS in water. This is because the folded enzyme provides a preorganized dipolar environment that is already partially oriented so as to stabilize the charge distribution in the TS. In water, on the other hand, the solvent must pay a significant reorganization energy to orient the polar environment towards the TS charges. The enzyme has already paid much of its reorganization energy to create the active site during the folding process.

Similar conclusions were reached by Kollman,^{22;23} although he considered that Warshel underestimated the free energy cost of prealigning the groups for catalysis in solution. Kollman has introduced $\Delta G_{(\text{crat})}$ for the solution reaction (assuming it is zero for the enzyme-catalyzed reaction). This is the free energy required to bring the reactant molecules together and to orient them properly, in other words the free energy cost to preorganize the solution reaction. His conclusions were that the enzyme rate enhancement is given by electrostatic stabilization of the TS better than solution, and by the preorganization of the reacting groups ($\Delta G_{(\text{crat})}$ in the enzyme < $\Delta G_{(\text{crat})}$ in

solution). Finally Moliner and co-workers,²⁴ studying the chorismate mutase, have found not only that this enzyme is organized to accommodate and stabilize the TS (by means of electrostatic interactions), but also that the same enzyme structure has an effect on the reactants, and it is able to promote those reactant conformations closer to the TS.

2.3 Mechanisms of phosphoryl and acyl transfer reactions

Phosphate diester and peptide bonds are extremely important in all living organisms. The former are the bonds linking together the nucleosides in DNA and RNA, and to them is entrusted the maintenance and transmission of the genetic code. Peptide bonds instead keep together the amino acids in proteins, which cover many different fundamental biological functions (enzymatic, structural, storage, transport, hormonal, defensive...). For these reasons the importance of the kinetic stability of phosphodiester and peptide bonds under physiological conditions is easily understood. The half-life for hydrolysis of phosphodiester bonds in DNA and RNA at neutral pH and 25 °C has been estimated to be at least 130,000 and 110 years,^{25,26} respectively. The large difference in the reactivity of these two phosphate diester bonds is due to the presence of the OH in the 2' position on the ribose, which can intramolecularly attack the phosphate group (paragraph 2.4). Under identical conditions, peptide bonds have a half-life between 350 and 600 years.^{27;28}

However, these bonds have also to be hydrolyzed (for example foreign DNA and proteins need to be destroyed, mutations in native DNA need to be excised and repaired, messenger RNA must be degraded after it has performed its function) and as such the natural organisms utilize hydrolytic enzymes called nucleases and peptidases (Figure 2.1). For many nucleases and for some peptidases metal ions are essential cofactors and are directly involved in the hydrolytic mechanism.

2.3.1 Phosphate ester hydrolysis

Because of the important role played by phosphate hydrolysis in many biological processes (molecular switches in signal transduction, DNA transcription, etc.), several studies to understand both the nonenzymatic and the enzymatic hydrolytic mechanism have been performed.²⁹⁻³¹ In this paragraph we will focus the attention on the mechanism of RNA phosphate diester hydrolysis.

In the phosphate ester hydrolysis a pentacoordinate transition state is involved, in which the entering and leaving groups occupy the axial positions. The character of the transition state varies for mono-, di- and phosphotriester cleavage.

Phosphate monoester hydrolysis shows a marked dependence on the leaving group reactivity and a small dependence on nucleophile, indicating a dissociative transition state with extensive bond cleavage of the leaving group and little bond formation to the nucleophile. Phosphotriesters, on the other hand, exhibit increased sensitivity to the nucleophile and decreased sensitivity to the leaving group revealing an associative transition state, with bond formation to the nucleophile more advanced than bond breaking of the leaving group.

The transition state for phosphodiester hydrolysis is in the middle between that found for the phosphomono- and triester cleavages. The mechanism is considered to be concerted involving simultaneous bond formation and bond cleavage.

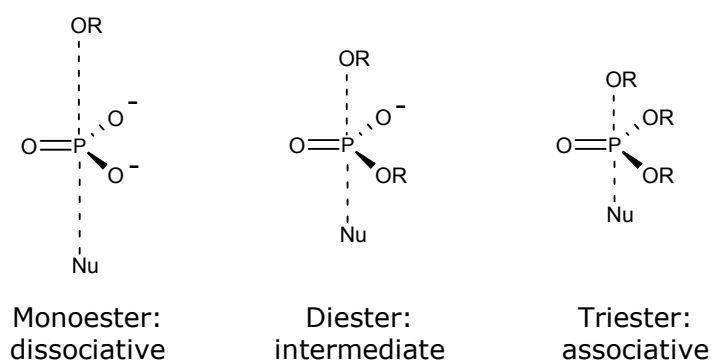


Figure 2.3 Transition state model for phosphoryl transfer.

In RNA, under physiological conditions (pH \sim 7), the hydroxide ion catalyzed cleavage of phosphodiester bonds is the predominant reaction mechanism (Figure 2.4).³¹⁻³⁴ The 2'-oxyanion, which is deprotonated in a rapid pre-equilibrium step, acts as an internal nucleophile and attacks the adjacent phosphate group (transition state TS1, Figure 2.4), resulting in the formation of a dianionic pentacoordinated species. In the second step, the bond with the 5'-oxygen of the leaving nucleotide is broken to give a 2',3'-cyclic phosphate and a 5'-OH terminus (transition state TS2, Figure 2.4). According to the rules proposed by Westheimer,³⁵ the cleavage of the P-5'O bond is allowed only when the attacking and departing groups are collinear with the phosphorus atom. The step which leads to transition state TS2 is rate-limiting,³⁶ in other words the attack of 2'-OH on the phosphorous atom is easier than cleavage of the exocyclic P-O(5') bond. It is not quite clear, whether the reaction is a two step process with a marginally stable dianionic phosphorane intermediate or whether it is a concerted process going *via* a phosphorane-like transition state. Most of the researchers are in favor of the first hypothesis (as depicted in Figure 2.4), because, even if *ab initio* calculations have revealed that in the gas phase the dianionic phosphorane intermediate does not exist, water solvation can stabilize this species that can be an intermediate of the reaction in solution.

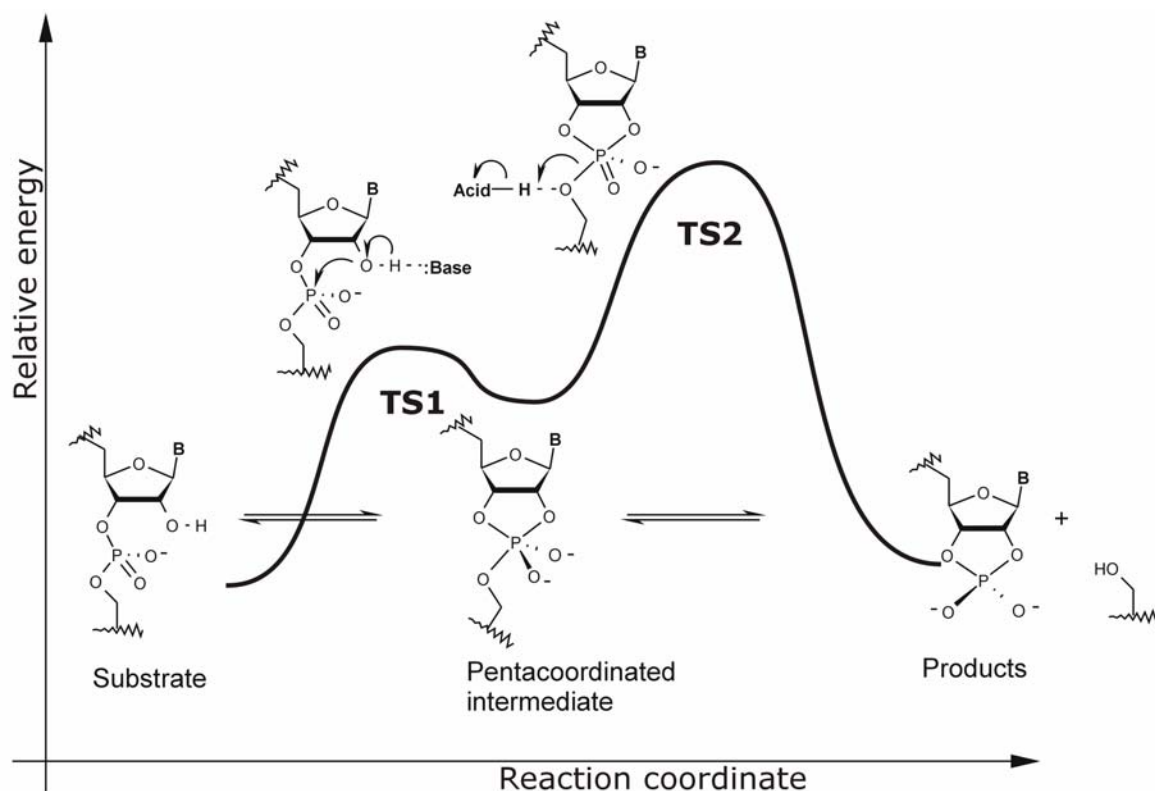


Figure 2.4 The two-step reaction scheme for the hydrolysis of a phosphodiester bond in RNA.

2.3.2 Enzymatic cleavage of phosphodiester bonds

Enzymes that hydrolyze phosphodiester and phosphomonoester bonds frequently employ multiple catalytic metal ions. If we consider the specific case of phosphodiester cleavage in RNA, the metal ions can promote this process in different ways:

- activation of the electrophile by direct coordination to the non-bridging oxygen (Figure 2.5 e) and stabilization of the intermediate with a higher concentration of the negative charge on the equatorial oxygens;
- stabilization of the negative charge development on the leaving group either by direct coordination to the 5'-oxygen (Figure 2.5 c) or by a metal bound water molecule (Figure 2.5 a);
- promotion of the deprotonation of 2'-OH by either direct coordination to the 2'-oxygen (Figure 2.5 d) or by a metal-bound hydroxide ion (general base catalysis (Figure 2.5 b));
- promotion of the in-line attack of the 2'-hydroxyl group (Figure 2.5 strategy f).

To these strategies were assigned the maximum rate acceleration factors: a and c (10^6), b and d (10^6), e (10^5), f (100).³⁷

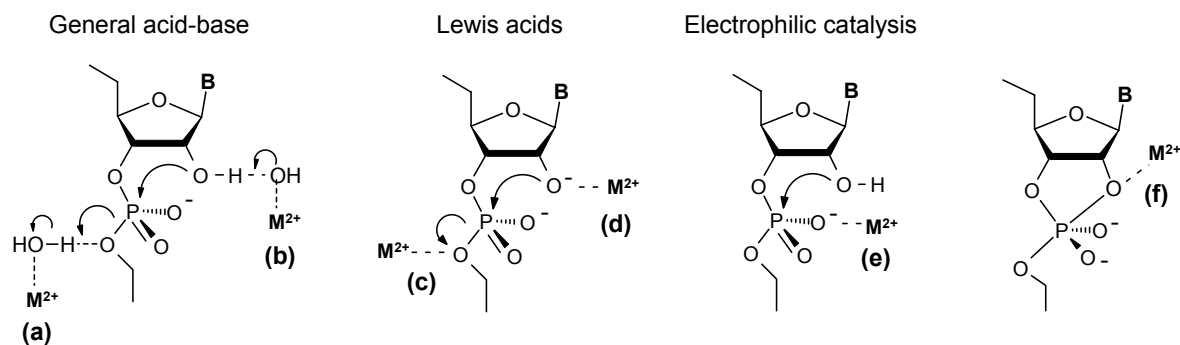


Figure 2.5 Metal ion catalysis in phosphodiester cleavage: proposed mechanism of catalysis. (a) General acid catalysis, (b) general base catalysis, (c) stabilization of the leaving group, (d) deprotonation enhancement of the attacking nucleophile, (e) electrophilicity increase of the phosphorus atom.

The metal ions most frequently employed are Mg^{2+} and Zn^{2+} , but also Mn^{2+} , Ca^{2+} and Fe^{2+} are often used. With an ionic radius of 0.6 Å, Mg^{2+} has a charge density of 3.0 \AA^{-1} (Z/r), higher than the other divalent ions. It is therefore a harder Lewis acid and can bind more strongly to the hard oxygen anions of the phosphodiester.³⁸ Zn^{2+} has a lower charge density (2.7 \AA^{-1}), but has a higher ionization potential and therefore is more effective at polarizing carbonyl bonds than Mg^{2+} .³⁹ Moreover, because of the d^{10} configuration of Zn^{2+} , the zinc complexes do not show ligand field stabilization effects and there are no energetic barriers to change their geometry, which is only dictated by ligand size and charge.⁴⁰

We have to take into account, however, that it is often difficult to investigate the presence and the actual activity *in vivo* of metal ions. Many studies and proposed mechanisms are based almost exclusively on the crystal structures of a few enzymes. Great caution should be used in obtaining these information from crystallographic data,⁴¹ because metal ion concentrations utilized in the crystallization of the enzyme often exceed the physiological concentration and often metal ions used in crystallographic analysis to identify metal binding sites are Mn^{2+} and Co^{2+} instead of Mg^{2+} .⁴² Another problem can be the distinction of functional and structural metal ions, the latter not participating in the catalytic process but contributing to the special protein conformation.

Mechanisms of hydrolysis by two-metal active centers have attracted much attention.^{42;43} Typically, two metal ions are separated by a distance of 3-4 Å and provide Lewis acid, leaving group and nucleophile activation. Although it was demonstrated and accepted that the alkaline phosphatase⁴⁴ and the purple acid phosphatase⁴⁵ (two enzymes that catalyze the removal of a phosphate group from phosphomonoesters) utilize a bimetallic active site (Zn^{2+} and Mg^{2+} the first, and Zn^{2+} and Fe^{2+} the second), two metal ions are not a general requirement for nucleases, and often these enzymes do not require metal cations at all.^{32;46;47}

If we consider RNA enzymatic hydrolysis, it can occur *via* two different mechanisms: a) intermolecular nucleophilic attack by hydroxide b) intramolecular nucleophilic attack by the 2'-hydroxyl group adjacent to the reactive phosphate (Figure 2.6).

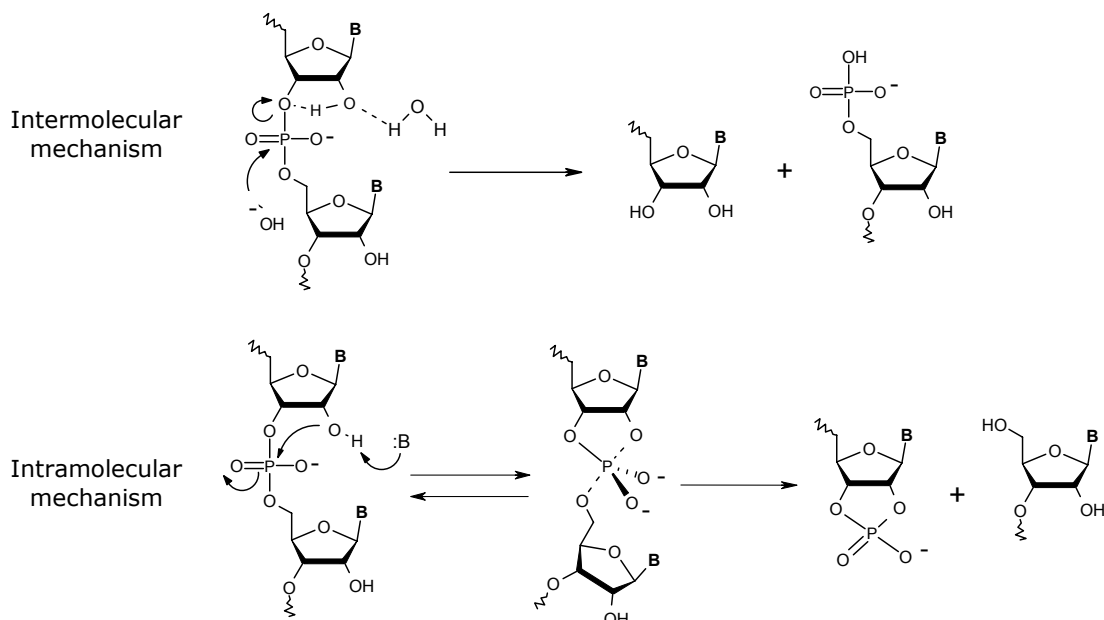


Figure 2.6 Inter- and intramolecular mechanisms of RNA phosphodiester bond cleavage.

The intermolecular mechanism involves an external nucleophile and occurs with three types of large ribozymes, such as group I and II introns and RNase P (they can also hydrolyze the DNA phosphate bonds that lack the hydroxyl group in 2' position on the ribose) and with some protein enzymes, such as DNA restriction enzymes.³¹ For these enzymes and ribozymes a mechanism with two metal ions involved has been proposed. DNA polymerase I utilizes two Mg^{2+} (or Zn^{2+}) ions;^{48;49} one ion is tightly bound to the enzyme, while the second associates upon substrate binding.⁵⁰ They activate the electrophile, stabilize the charge on the transition state, facilitate the departure of the leaving group and provide the nucleophile in the form of a metal-bound hydroxide (Figure 2.7 A). Analogous mechanisms have been proposed for the restriction endonucleases EcoRV⁵¹ and for large ribozymes,⁵² even if more recent studies have proposed that the group I intron (large ribozyme) operates via a three-metal-ion mechanism (Figure 2.7 B).^{53;54}

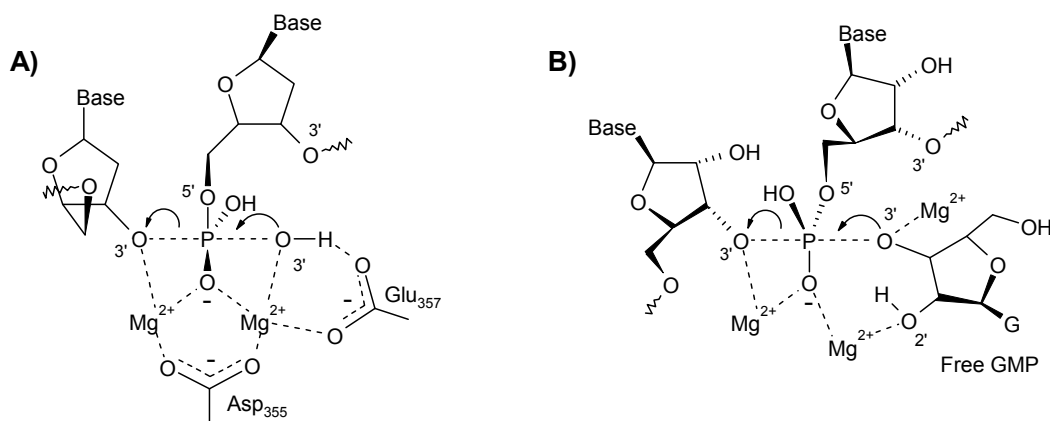


Figure 2.7 Proposed multi-metal-ion-mechanisms. A) Hydrolysis of DNA by DNA polymerase. B) Hydrolysis of RNA by group I intron ribozymes.

The intramolecular mechanism (Figure 2.6) is utilized by small ribozymes (hammerhead, hairpin, HDV and VS ribozymes) and by most of the protein ribonucleases. This mechanism is that described for the non-enzymatic hydrolysis of RNA (Chapter 2.3.1).

The hammerhead ribozymes cleave RNAs at a specific site, using Mg²⁺ as a cofactor. Even though the generally accepted mechanism of hammerhead ribozyme reactions was a single-metal-ion mechanism⁵⁵⁻⁵⁹ recent observations provided support for a double-metal-ion mechanism,^{36;60;61} where the Mg²⁺ ions act as Lewis acids by direct coordination to the 2'- and 5'-oxygens (Figure 2.8 A). The mechanism of HDV ribozymes involves one Mg²⁺ bound hydroxide, which acts as general base catalyst in the deprotonation of the 2'-oxygen, while the acid catalysis to the 5'-oxygen is provided by the N3 of a protonated cytosine (C₇₅) (Figure 2.8 B).^{62;63;63} This was the first direct proof that a nucleobase can act as an acid/base catalyst in RNA cleavage. Hairpin ribozymes do not require metal ions as cofactors and the catalysis is provided by the nucleobases.⁶⁴ The essential role is played by G₈ (Figure 2.8 C) that can work as general acid catalyst protonating the leaving group. It is also possible that a contribution is given by O6 of G₈.

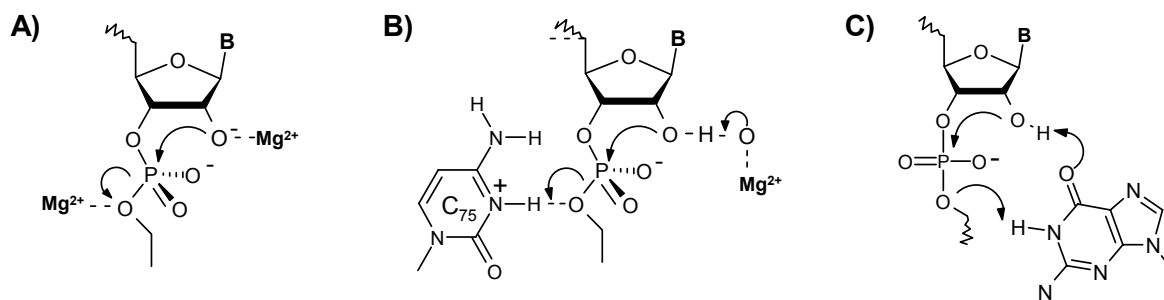


Figure 2.8 Proposed mechanisms of RNA cleavage by A) hammerhead ribozymes, B) HDV ribozymes, C) hairpin ribozymes.

Human immunodeficiency virus 1 reverse transcriptase (HIV-RT) contains, besides the polymerase active site, a ribonuclease H (RNase H) activity, acting as an endonuclease in the degradation of the viral RNA template strand during DNA synthesis. Divalent metal ions are essential for the RNase H activity and crystallographic data showed two metal ion binding sites which are 4 Å apart.⁶⁵ On the other hand, the Escherichia coli RNase H, that displays a significant sequence and structural homology to the RNase H domain of HIV-RT, seems to bind only one Mg²⁺ and to use a carboxylate side chain as a general base.⁶⁶

RNase A, a bovine pancreatic ribonuclease, is one of the most studied nucleases and it is an example of an enzyme that does not need the presence of a metal ion for its catalytic activity. It catalyzes the attack of the 2'-OH to the phosphate and the subsequent hydrolysis of the cyclic phosphate. In the first step, His 12 acts as a general base, while His 119 acts as a general acid. In the second step, the acid and base roles are reversed for H12 and H119. They exploit a water molecule for the attack at the cyclic phosphate and at the end the original histidine protonation states are restored (Figure 2.9).

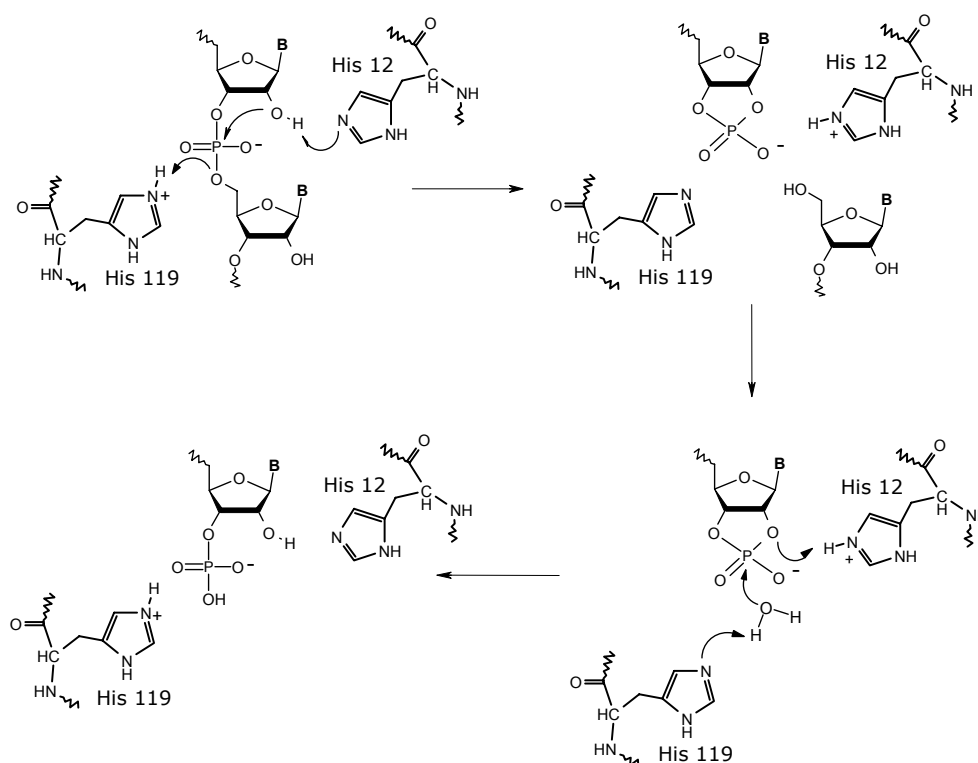


Figure 2.9 Proposed mechanisms of RNA cleavage by RNase A.

2.3.3 Mechanism of amide and ester hydrolysis

Amide and ester hydrolysis at neutral pH is known to proceed through the formation of a tetrahedral intermediate. However, several studies revealed that while

in the case of ester hydrolysis the rate-limiting step is the formation of the tetrahedral intermediate (TI),⁶⁷ i.e. the attack of the nucleophile on the electrophilic carbon, in the case of amide hydrolysis, the rate-limiting step is the breakdown of TI, i.e. the C-N bond cleavage.^{68;69} Acceleration of ester hydrolysis can therefore be provided by activation of the nucleophile or of the electrophilic carbon. The catalysis of amide hydrolysis can be achieved mainly by means of groups able to protonate the leaving nitrogen thus promoting the C-N cleavage (Figure 2.10).

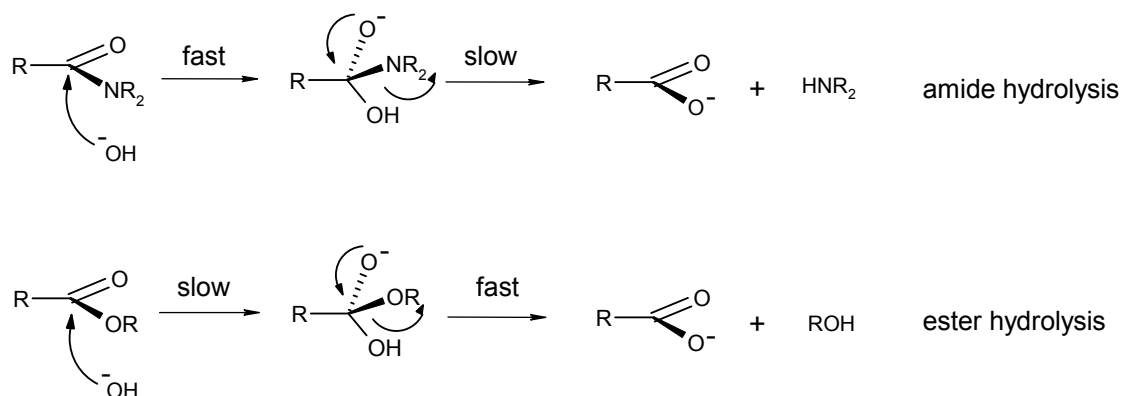


Figure 2.10 Mechanisms of amide and ester hydrolysis.

2.3.4 Enzymatic amide cleavage

Metalloproteases belong to one of the four functional classes of peptidases. They exploit one or two metal ions as cofactors in the peptide bond cleavage. The possible catalytic functions of metal ions in amide hydrolysis were illustrated by Sayre⁷⁰ who proposed five different mechanisms (we can consider the same catalytic activation for the ester hydrolysis; Figure 2.11). Some of these mechanisms resemble those proposed for phosphodiester hydrolysis, and therefore it appears clear that metal requirements for amide hydrolysis are similar to those for phosphodiester hydrolysis.

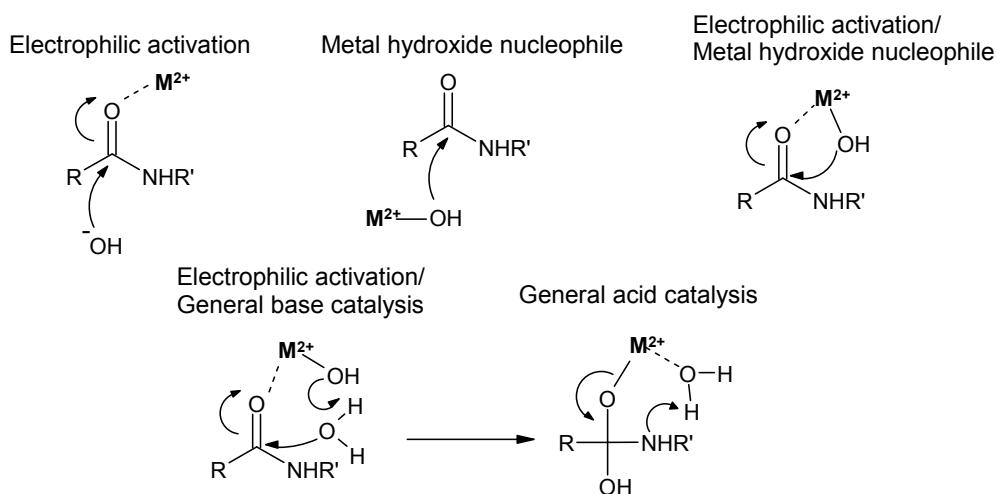


Figure 2.11 Possible catalytic functions of metal ions in peptide bond cleavage.

Metalloproteases use mainly the Zn^{2+} ion as a metal cofactor, even if the exchange of Zn^{2+} with Co^{2+} , Ni^{2+} , Cu^{2+} or Mg^{2+} produces still active enzymes and in some cases leads to hyperactivity of the enzyme.^{71;72} Carboxypeptidase A⁷³ and thermolysin⁷⁴ are the most studied metalloproteases. Their catalytic mechanisms are considered similar. They use one Zn^{2+} ion that cooperates with other protein functional groups. In both cases the Zn^{2+} is tetraordinated and binds two histidines, a glutamate and a water molecule. A Glu-carboxylate deprotonates this Zn^{2+} -coordinated water molecule, generating a zinc bound hydroxide ion that acts as a nucleophile in the reaction. Other positively charged residues, such as His231 or Arg127, provide electrostatic stabilization (Figure 2.12 A and B).

Leucine aminopeptidase (LAP) is an example of a dinuclear zinc enzyme. It is a hexameric enzyme with a molecular mass of 324kDa and catalyzes the removal of amino acids from the N-terminus of a peptide. Two Zn^{2+} ions and a Lys-ammonium are directly involved in amide bond cleavage (Figure 2.12 C). The nucleophilic attack to the carbonyl group is given by a hydroxide that bridges the two Zn^{2+} ions. The substrate is electrostatically activated by a Lys-ammonium group and by one of the Zn^{2+} ions.

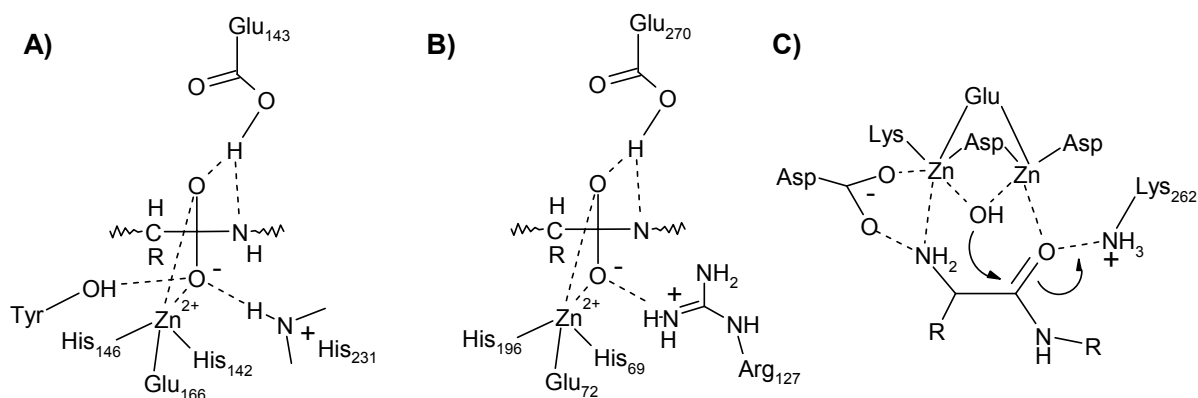


Figure 2.12 Proposed transition states for the hydrolysis of peptide bonds by: A) *thermolysin*; B) *carboxypeptidase A*; C) *leucine aminopeptidase*.

2.4 Enzyme mimics

The importance of developing simple organic systems that mimic the action of natural enzymes can be understood on the basis of two simple considerations:

- The application of enzymes in industrial production is limited due to their low stability and to their high specificity for their natural substrates. Moreover, their large scale application is sometimes prevented by their easy denaturation under abiotic conditions and their limited natural abundance;

- Only few enzymatic mechanisms have been clearly established and much has to be learnt on how a specific structure of the active site can lead to the observed rate enhancement. Enzyme models may give a better understanding of the mode of enzyme action in terms of structure, mechanism and rate acceleration.

An enzyme model^{3;75} has to provide a good binding site for the target substrate. Another important point is that the catalytic site should be preorganized and well defined with respect to substrate orientation. It appears clear⁷⁶ that it is too difficult to reach this goal by simply rigidifying the entire molecule, because the residual flexibility is often in a direction that cannot be predicted. Too rigid molecules with a slight mismatch to the transition state tend to be poor catalysts. Hereby in the search for new catalysts it is better to achieve dynamic preorganization on a molecular scaffold which displays a certain flexibility, or to combine a large number of flexible building blocks with many competing weak, non-covalent interactions. Such a structure, which combines a high grade of preorganization whilst still maintaining a certain degree of flexibility, can probably better respond to the geometric demands of substrate and transition state without excessive entropic cost.

2.5 Synthetic metallonucleases for RNA cleavage

The idea of developing synthetic nucleases that specifically cleave a target RNA and in principle inhibit the protein expression in cell culture has attracted the interest of many chemists.⁷⁷ For this reason, synthetic nucleases are the most studied class of enzyme mimics, and in the last decade several examples of catalysts able to cleave phosphodiester bonds have appeared in the literature. Although some examples of metal free nuclease mimics are known,⁷⁸⁻⁸⁰ most of the nuclease mimics employ one or more metal centers. The most used metal ions are Zn^{2+} and Cu^{2+} . They offer the advantages of being both substitutionally labile and strong Lewis acids for the activation of phosphate bonds and moreover they significantly lower the pK_a of a coordinated water molecule, thereby providing a metal-bound hydroxide at pH close to neutrality.

Before illustrating some recent examples of nuclease mimics, it is important to underline that the activity of many of them has been investigated only on model substrates, like 2-hydroxypropyl-*p*-nitrophenyl phosphate (HPNP),^{81;82} uracyl-*p*-nitrophenyl phosphate (UPNP) or dinucleotides (Figure 2.13). HPNP is considered an RNA model because of the hydroxypropyl group, which can attack the phosphate intramolecularly. However, it is more reactive as the pK_a of the nitrophenol leaving group is about eight units lower than the pK_a of an aliphatic alcohol. Anyway, the activity of a catalyst that works by stabilizing the leaving group cannot be evaluated

from this RNA model and often the trend of reactivity observed cannot be transferred to longer oligonucleotides.³² In some cases, a catalyst can efficiently cleave HPNP, but is much less active toward UPNP.⁸³ Notwithstanding these limitations, the use of activated phosphoester DNA models gives important mechanistic information on phosphate ester cleavage.⁸⁴

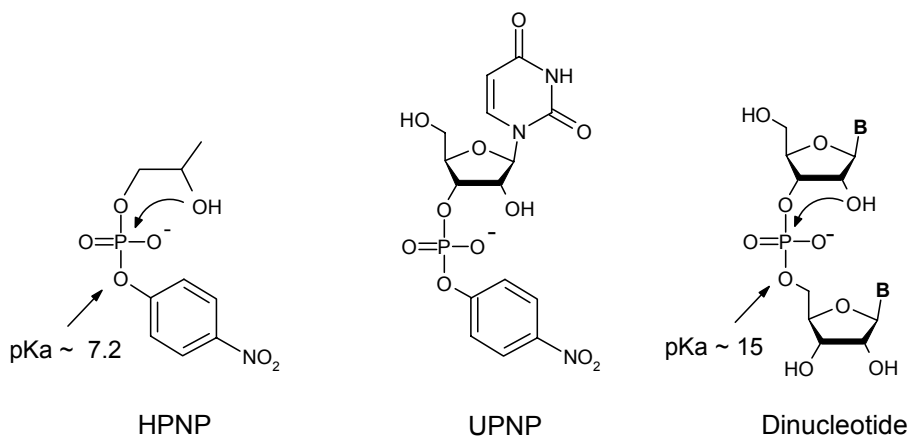
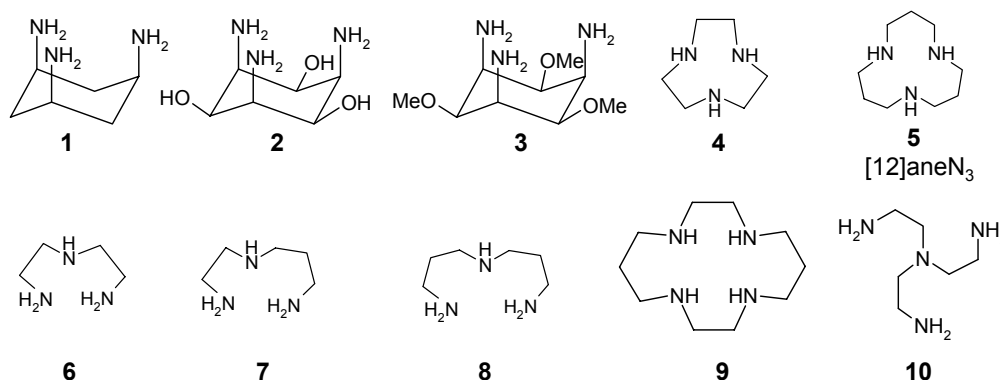


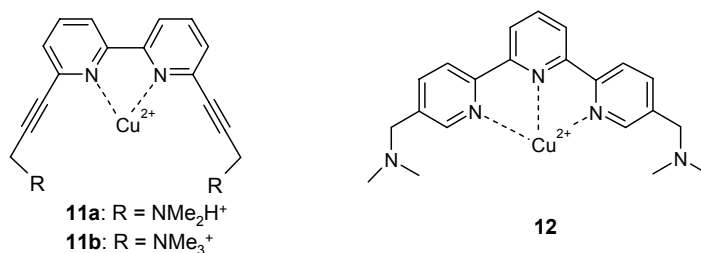
Figure 2.13 RNA models.

2.5.1 Mononuclear catalysts

Mononuclear catalysts are mainly studied to understand the factors that contribute to catalysis by metal complexes and to find the best mononuclear ligand for the development of di- and trinuclear systems. In a recent study Mancin *et al.*⁸⁴, investigating the Zn(II) complexes of the ligands **1-10** in the transesterification of HPNP, found a correlation between the pK_a of the coordinated water and the second-order rate constant. A Brønsted plot gave a slope of 0.75, suggesting that the more basic the metal hydroxide, the more active the catalyst is. The high value of this slope suggests that the basicity of the metal-complexed hydroxide is very important, perhaps because it acts as a general base catalyst. Moreover, they found that complexes of tridentate ligands, particularly if characterized by a facial coordination mode, are more reactive than those of tetradentate ligands, which can hardly supply any free binding sites for the substrate. These conclusions are in agreement with those obtained by Kimura, studying and comparing the activity of Zn^{2+} -[12]aneN₃ and Zn^{2+} -[12]aneN₄.⁸⁵

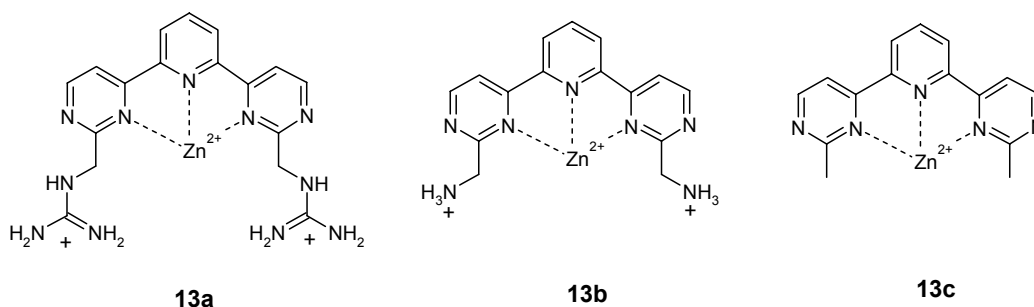


Simple nuclease mimics were designed which exploit the cooperativity of a metal ion and an organic functionality introduced on the ligand, such as an ammonium or a guanidinium group, which can participate in the catalysis according to different mechanisms. Kramer prepared compounds **11a,b**, where a 2,2'-bipyridine unit binds Cu(II) and the lateral ammonium groups in **11a** can cooperate in the transesterification of HPNP. The author found that **11a** is 1000 times more active than **11b**. The measurements were performed in acetonitrile/water 19:1 (v/v), because of the low stability of the complex in water.



Hamilton and coworkers attached tertiary amino groups to a Cu(II) terpyridine complex (**12**).⁸⁶ In water at pH 7.0, **12** cleaves HPNP seven times faster than the Cu(II) terpyridine complex devoid of the amino groups. From the pH profile they concluded that the amino groups act as auxiliary bases, probably by deprotonation of the hydroxyl group of HPNP.

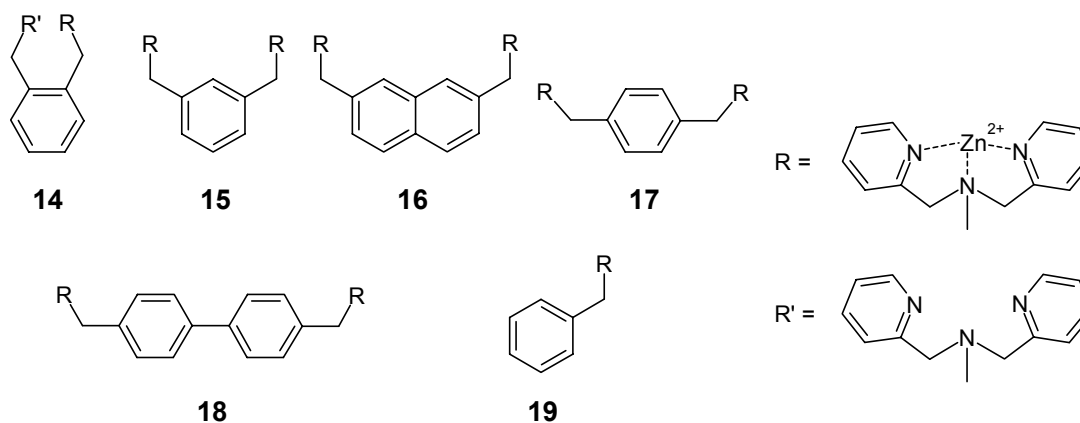
More recently, Anslyn⁸⁷ described some compounds with similar design (**13a-c**). The pseudo first order rate constants for the hydrolysis of the 0.05 mM ApA dinucleotide promoted by 5 mM **13a**, **13b** or **13c** at pH 7.4 and 37 °C, were $8.0 \times 10^{-2} \text{ h}^{-1}$, $9.0 \times 10^{-3} \text{ h}^{-1}$ and $2.4 \times 10^{-5} \text{ h}^{-1}$, respectively. **13a** is about nine times more effective than **13b**, and ca 3300 times more effective than **13c** in the hydrolysis of ApA. The difference in reactivity between **13a**, **13b** and **13c** can in part be related to the pK_a value of the water coordinated to the Zn²⁺ center in each complex, but probably the higher reactivity of **13a** is also due to a combination of the hydrogen bonding, electrostatic effects and proton-donating ability of the guanidinium groups.



2.5.2 Di- and trinuclear nuclease mimics

Di- and trinuclear systems have been developed with the aim of obtaining a cooperative action of the metallic centers, analogous to that found in different nucleases and ribozymes. Results obtained to date with metalloenzyme mimics suggest that the best catalysts are those where the distance between the metal centers is nearly the same as that found in bimetallic enzymes (in the range 3.5-6 Å).⁸⁸ Nevertheless, it is difficult to obtain cooperativity of two metal ions in synthetic catalysts and often unpredictable results are obtained.

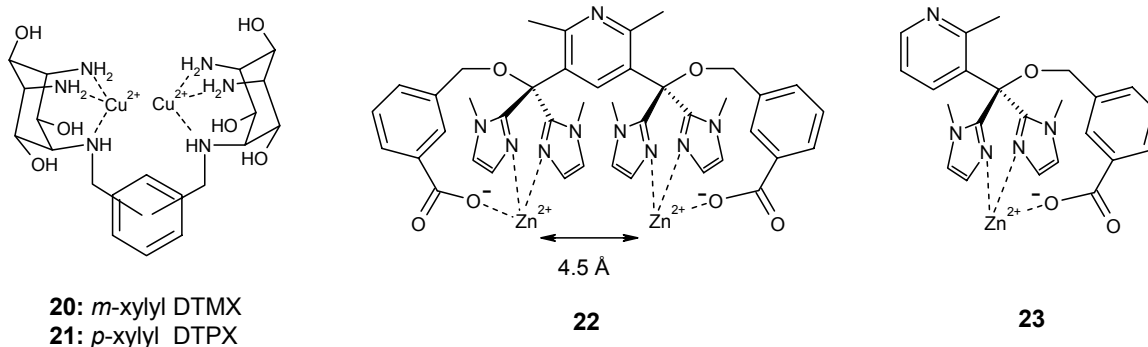
Uchimaru⁸⁹ carried out a kinetic study on the hydrolysis of UpU promoted by the dinuclear Zn(II) complexes **14-18**. The ligands have in common two di-2-pyridylmethylamino moieties separated by different spacers. Compound **14** cannot bind two zinc ions, although MC simulations suggested that the two metal ions would be more than 4 Å apart in the bimetallic complex. The order of reactivity was **15>16>17>18**, which was attributed mainly to the difference in the distance between the two Zn²⁺ ions.



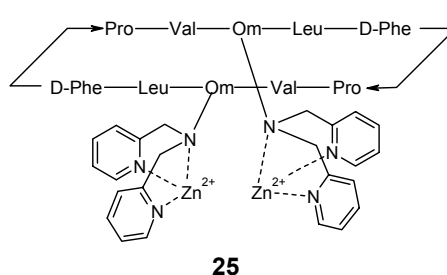
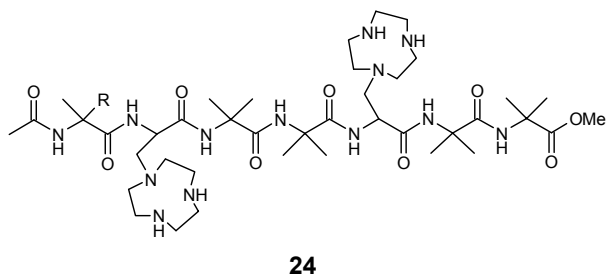
However, the metal-metal distance is not the only parameter and other factors affect the catalysis as well. Two examples of dinuclear catalysts were recently reported by Mancin and Anslyn, in which no cooperativity was observed despite the optimal distance between the metallic centers. Starting from the good results obtained with Zn and Cu complexes of *all-cis*-2,4,6-triamino-cyclohexane-1,3,5-triol (TACI), that were good catalysts in the cleavage not only of model phosphate di- and triesters,

but also of supercoiled DNA,⁹⁰ Mancin *et al.*⁹¹ prepared compounds **20** and **21** with the aim of exploiting a cooperative action of the two metals. The calculated intramolecular metal distances were 5.0 and 5.2 Å for **20** and **21**, respectively. However, **20**-[Cu]₂ and **21**-[Cu]₂ are almost two orders of magnitude less active than the mononuclear TACI-[Cu] in the cleavage of HPNP, and also the Zn complexes did not show any cooperativity of the two ions. This was explained with the formation of intracomplex μ -hydroxo bridges.

In an attempt to mimic a nuclease, Anslyn used natural ligands such as imidazole to place two Zn ions at an appropriate distance, synthesizing compound **22**.⁹² Its catalytic activity was measured for HPNP and UpU cleavage (30% methanol) and compared to that of the corresponding mononuclear catalyst **23**. Whereas in the case of HPNP, **22** was 80-fold more reactive than **23**, no difference was observed in the rate of cleavage of UpU when **22** or **23** was used. The lack of activity of **22** in this case was attributed to the fact that the complexation of the substrate (UpU) to the catalyst was not productive for catalysis.

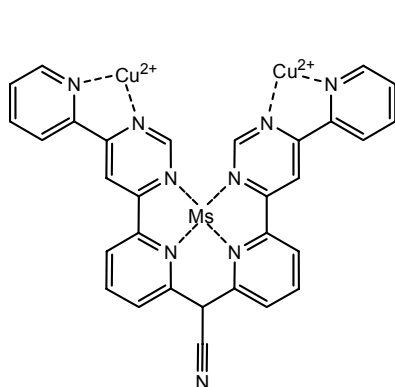


Oligopeptides have been used as scaffolds for the anchoring of metal ligands. Scrimin synthesized compound **24**, which is soluble in water.⁹³ The heptapeptide skeleton adopts a 3_{10} -helical conformation where the two aza-crown side arms face each other on the same side of the helix. The binding groups do not reciprocally interfere in the coordination process of Cu (II) and Zn(II). However, the two metallic centers show almost no cooperativity in the cleavage of HPNP. The explanation partially comes from the analysis of the HPNP binding to the catalyst. HPNP binds to **24**-[Zn]₂ with the same strength as to the mononuclear [Zn] complex. This means that the substrate can approach the peptide by inserting within the two metal centers or from either of the two lateral sides without any specific preference. As a consequence, two out of three possible modes of interaction of HPNP with **24**-[Zn]₂ do not allow the substrate to take advantage of the cooperative action of both metal centers. Surprisingly, compound **24**-[Zn]₂ showed cooperativity in the cleavage of plasmid DNA.⁹⁴



The cyclic decapeptide gramicidin S (GS) possesses a stable antiparallel β -sheet conformation, and was exploited by Kawai *et al.* as a scaffold for the introduction of one or two chelating bis(2-pyridylmethyl)amino groups.⁹⁵ In compound **25** the metal ligands are located on one side of the β -sheet, and the catalyst cleaves the HPNP (in 50% CH₃CN, pH 7.0) 300 times more efficiently than the analogous mononuclear system.

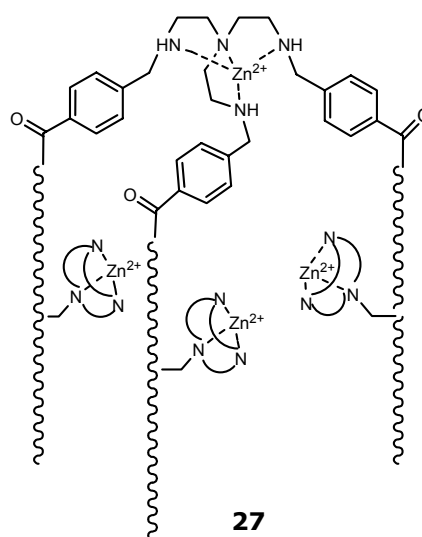
Other approaches in cooperative catalysis exploit allosteric regulation by metal ions that are not directly involved in catalysis. One example is reported by Krämer, who synthesized complexes **26a-c**, where the polyaza ligand binds one structural metal ion (Ms: Cu^{II}, Ni^{II} or Pd^{II}), and two functional (catalytic) Cu^{II} ions, which interact with the substrate.⁹⁶ An allosteric metal ions influence both the binding and the catalytic cleavage of HPNP (measurements in H₂O/DMSO 3/1). Probably, subtle differences in the ionic radius of Ms and in its tendency to distort the N₄-Ms coordination plane have an influence on the conformation of the catalyst and the orientation of the functional Cu²⁺ ions for catalysis.



26a : Ms = Cu²⁺

26b : Ms = Ni²⁺

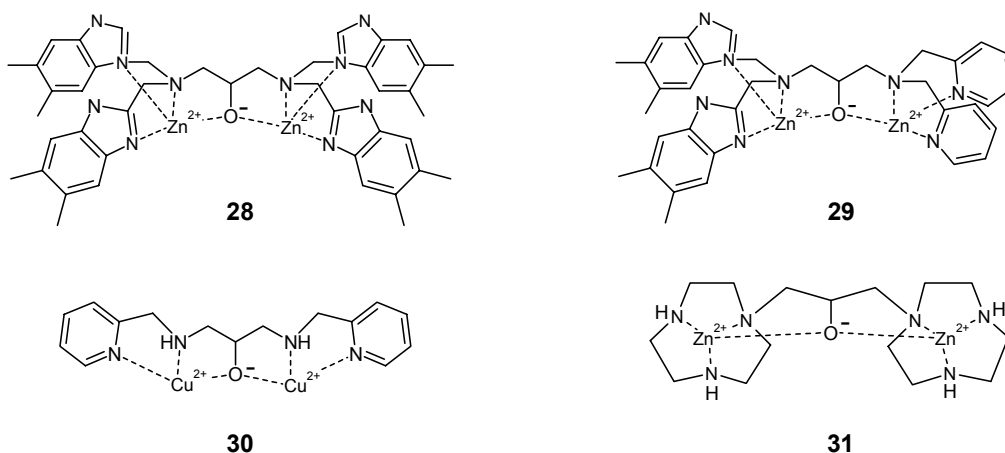
26c : Ms = Pd²⁺



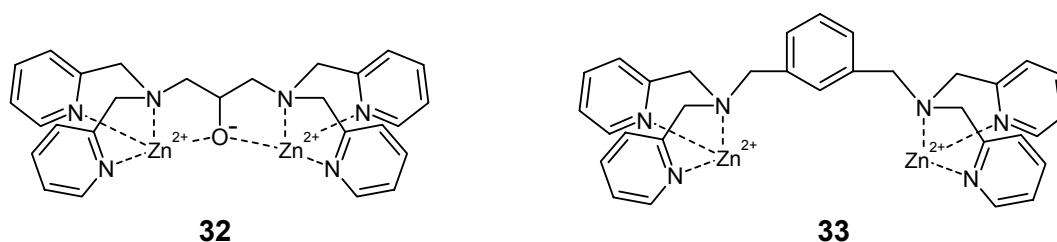
A second example (**27**) has four metal ion binding sites formed by linking three heptapeptide strands with attached macrocycles to a tris(2-aminoethylamine) (tren) unit.⁹⁷ The binding of the metal to the tren platform induces a change from an open to a closed conformation in which the three short, helical peptides are aligned in a

parallel fashion defining a pseudocavity. Upon binding to the tren unit, the three triazamacrocycle-Zn(II) units work cooperatively (50-fold increase) in the cleavage of HPNP, but not in the cleavage of a 29mer oligonucleotide, where the free ligand is more active than the corresponding zinc complex **27**.

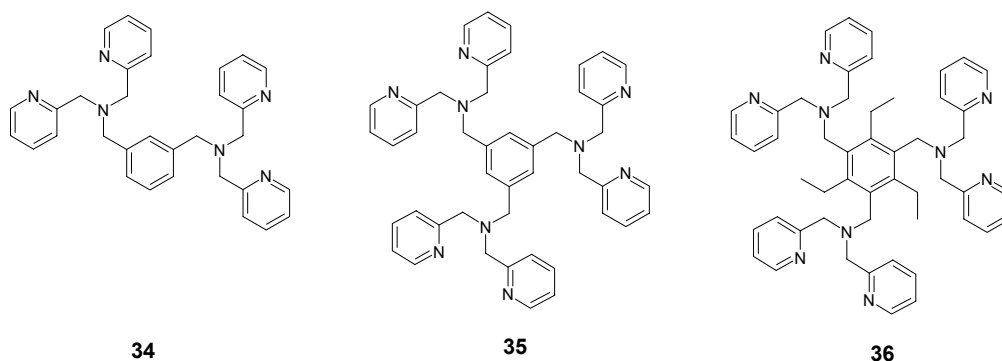
Another way of maintaining the metal ions in close proximity for a cooperative action is to use a bridging alkoxide anion. Different groups have exploited this strategy designing compounds **28**,⁹⁸ **29**,⁹⁸ **30**⁹⁹ and **31**¹⁰⁰. All four complexes have pH-rate profiles consistent with a monohydroxo-bridged complex as the active catalyst. In the case of **31**, high cooperativity of the two Zn(II) ions was found in HPNP cleavage in water. A mechanistic study demonstrated that the rate enhancement is due to the lowering of the pK_a of the complexed water molecule, to an enhancement in substrate binding and to an additional transition state stabilization. Interestingly, compound **31** cleaves oligoribonucleotides.¹⁰¹ The analogous dinuclear Cu(II) complex has very low cleavage activity, consistent with a lack of an available coordination site for catalysis.¹⁰²



Despite the fact that the use of a bridging alkoxy group in some cases resulted in rate enhancement due to metal ion cooperativity, this strategy failed in other systems. Komiyama has recently reported two catalytic systems (**32** and **33**) for dinucleotide cleavage,¹⁰³ and in each case tested complex **33** is 2 or 3-fold more effective than **32**. The superiority of **33** was explained by the fact that the active monohydroxo species of **33** has two additional coordinated water molecules that can contribute to the catalysis providing a proton in the transition state (acid-base catalysis).



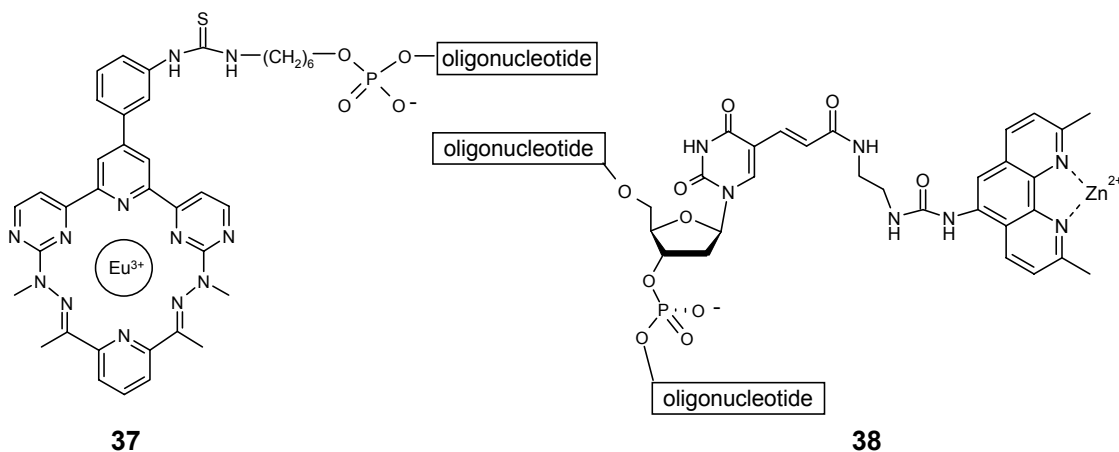
Complexes **35**-[Cu]₃ and **36**-[Cu]₃ are examples of trimetallic nuclease mimics.¹⁰⁴ **35**-[Cu]₃ demonstrated selectivity depending on the type of phosphodiester linkage. Up(2'-5')U was cleaved 50-fold faster than Up(3'-5')U, while in the case of ApA, it was the Ap(3'-5')A bond that was cleaved 50-fold faster than the corresponding Ap(2'-5')A. Neither Gp(3'-5')G nor Gp(2'-5')G were hydrolyzed to any extent. Similar studies with the more rigid **36** trinuclear Cu(II) complex showed no selectivity and lower rate constants for hydrolysis. Comparison with the dinuclear complex **34**-[Cu]₂ revealed that all three metal ions are involved in the catalysis by **35**-[Cu]₃.



2.5.3 Catalysts with an RNA recognition group

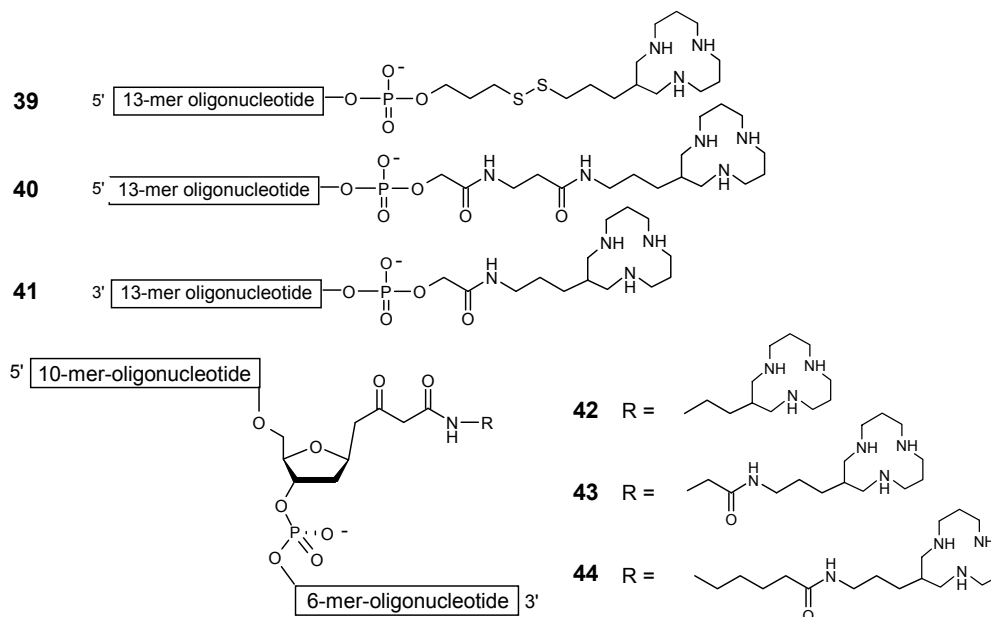
Conjugation of a metal catalyst to an RNA recognition group is exploited in order to enhance the substrate-specificity of the catalyst. Furthermore, the available binding energy that can be utilized in catalysis is increased, the most favourable situation being that binding in the transition state is selectively enhanced with respect to binding in the initial state. The most common recognition moiety used for this purpose is an antisense oligonucleotide (ASO) that base pairs with a complementary RNA strand, but examples that exploit sugars, peptides or PNA¹⁰⁵ are also reported.

Haner has reported on the synthesis and catalytic activity of a large human *c-raf-1* mRNA of a series of 2'-methoxyethoxy-modified oligonucleotides bearing a europium complex (**37**).¹⁰⁶ These compounds can cleave 60-70% of the RNA within 4 h at 37 °C, and the cleavage occurs at two or three major sites adjacent to the 3'-end of the RNA target region, preferentially after purine nucleotides.

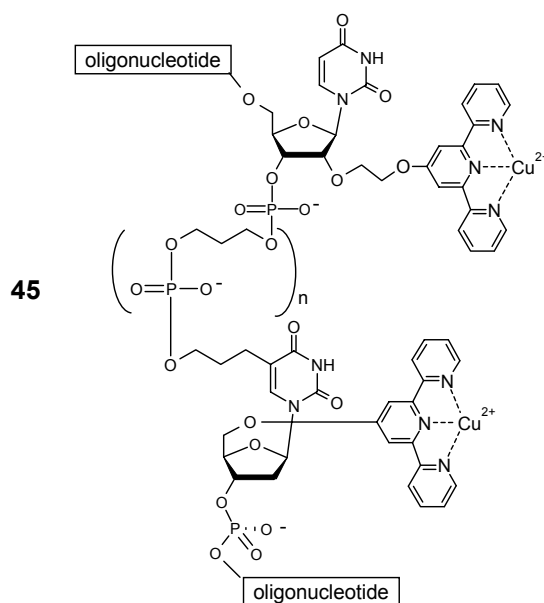


It is established that in order to achieve catalytic turnover it is more convenient to cleave the target RNA in a central part of the sequence, as the number of base pairs of both remaining fragments is thus significantly reduced and the complex with the product is weaker than that with the substrate. For this reason, Strömberg *et al.* placed a Zn(II) 2,9-dimethylphenanthroline derivative in the central part of the ASO (**38**). This compound cleaves the oligonucleotide target in a bulge that is formed upon binding to **38**.

In recent work,¹⁰⁷ Zn(II) complexes of oligonucleotides bearing a 1,5,9-triazacyclododecane ([12]aneN₃) attached at the 3'- or 5'-terminus or within the oligonucleotide (compounds **39-44**) have been studied as artificial ribonucleases. Cleavage efficiency depends not only on the site of attachment and on the length of the linker used to tether the metal complex to the oligonucleotide but also on the nature of the linker itself. The most active conjugate is **39**, bearing a disulfide-tethered [12]aneN₃ Zn(II) complex at the 3'-terminus, which cleaves 50% of the target in 20 h at 35 °C. **39** is 8 times more active than **40**, where the metal ligand is tethered to the oligonucleotide by an amide bond. The 5'-tethered conjugated **41** did not show any activity after 100 h under the same conditions. The complex **43**-[Zn] turned out to be more efficient than **44**-[Zn] and its activity is comparable to that of compound **39**.

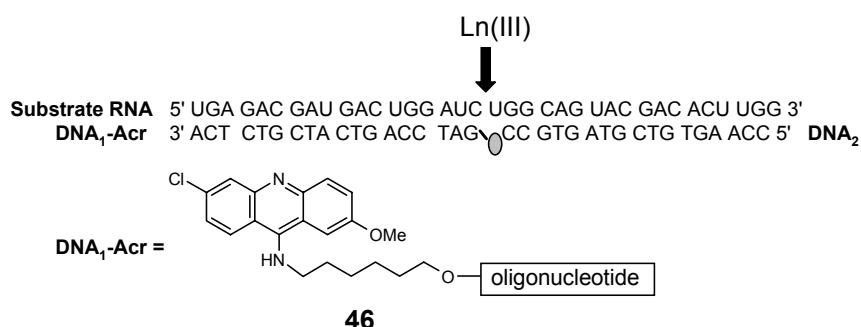


Inoue *et al.* have synthesized the most active ASO-metal complex conjugate reported so far (**45**).¹⁰⁸ It consists of two Cu(II) terpyridine complex-ASO conjugates connected by a propandiol-containing linker. Catalytic studies, conducted on the target 24-mer RNA, indicated that **45** cleaves only at the predetermined site and that it is 130-fold more effective than a single Cu(II)-ASO conjugate. By initial-rate measurements the kinetic parameters k_{cat} and K_M ($k_{\text{cat}} = 0.647 \text{ h}^{-1}$, $K_M = 5.49 \text{ nM}$), and the second order rate constant ($k_{\text{cat}}/K_M = 0.118 \text{ nM}^{-1}\text{h}^{-1}$) were obtained. An excess of RNA is also cleaved.



Kuzuya and Komiyama have used oligonucleotides bearing an acridine (**46**)¹⁰⁹ as an RNA activator.¹¹⁰⁻¹¹² The modified oligonucleotide forms a heteroduplex with the substrate RNA, the acridine intercalates into the RNA and induces a conformational

change at the bulge, selectively activating the phosphodiester linkages in front of it. As a result, these linkages are preferentially hydrolyzed over the others, by free metal ions in solution, especially lanthanides(III).



A limited number of reports use RNA recognition agents other than ASO to promote selective metal ion RNA cleavage. The cyclen unit was linked to an arginine-rich 9mer able to bind the HIV-1 TAR-RNA, with the aim of cleaving the TAR-RNA in a specific site.¹¹³ The metal free 9mer-cyclen **47** gives uridine-selective cleavage at pH 6 and 7.4, most probably through general acid-base catalysis by the deprotonated form of cyclen. The only hydrolyzed site is between U31 and G32 (Figure 2.14). Surprisingly, upon the addition of Eu^{III} or Zn^{II}, which can be complexed by cyclen and act as metal catalysts, no cleavage of the RNA target was observed after incubation for 1 h.

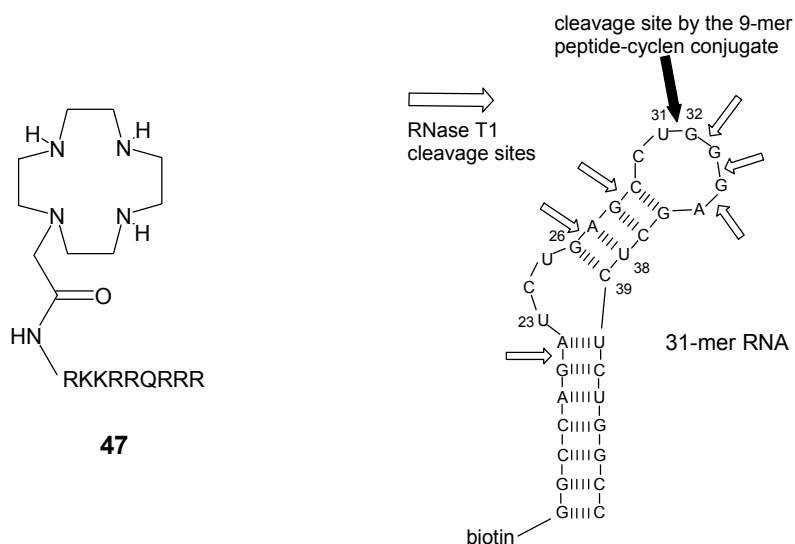
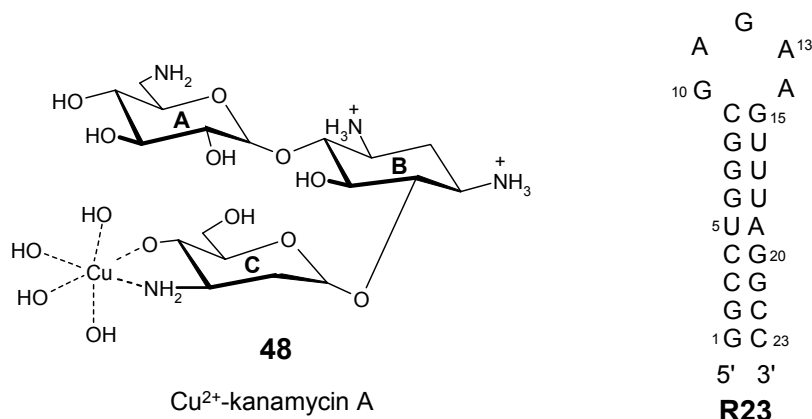


Figure 2.14

The copper complex of the aminoglycoside kanamycin A (**48**)^{114;115} exhibits efficient RNA cleavage activity at physiological pH and temperature. The catalytic properties of complex **48** were studied toward a modified 23-mer RNA aptamer (**R23**) with a high binding affinity for kanamycin A. Kanamycin A binds to the major groove of R23 through electrostatic and hydrogen bonding interactions with the amine and hydroxy groups of rings A and B, while the ring C is pendant and can chelate a metal

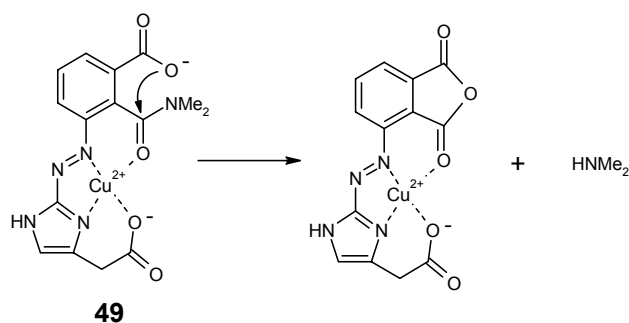
ion. The cleavage of R23 by complex **48** is not random; two sites of cleavage can be identified: one in the loop region at A¹⁴/G¹⁵ and the other in the stem region at C⁴/U⁵. The mechanism is an oxidative cleavage through reactive copper-oxo or copper-hydroxo species. Compound **48** is active also in the micromolar concentration range and in cell culture.¹¹⁶



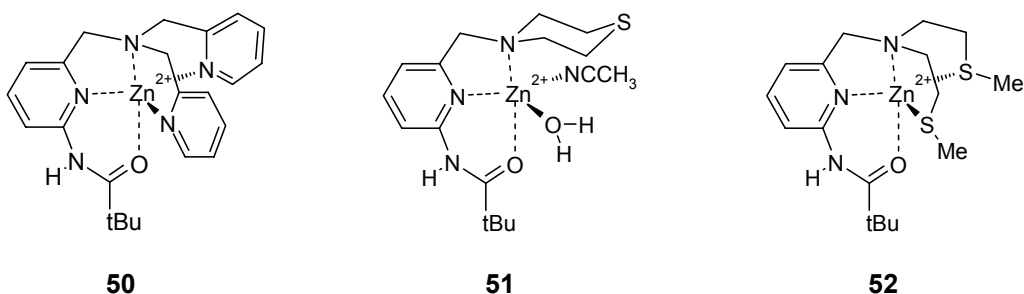
2.6 Synthetic supramolecular catalysts for amide cleavage

Although the hydrolysis of peptide bonds by metal ions is well known, in the literature there are very few examples of synthetic metallo-catalysts able to cleave amide bonds, and the reported ones have generally very low activity under mild conditions.¹¹⁷ Moreover, only a few substitutionally labile model complexes of peptidases with biologically relevant metal ions such as Cu(II) and Zn(II) are known, and as a result there is much less mechanistic information available on metal-promoted amide hydrolysis.

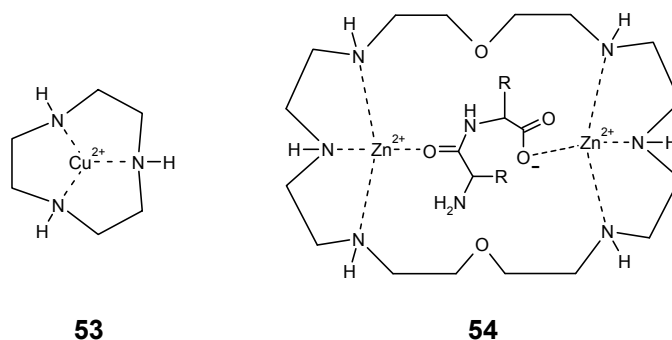
Because of the difficulties in the hydrolysis of unactivated amide bonds, nonenzymatic catalysis of amide hydrolysis has first been investigated with catalysts tethered to the substrate. The amide bond in the copper (II) complex **49** has a half-life of 10 min at 50 °C in DMSO/water (95/5), which corresponds to a ca. 300-fold rate enhancement compared to the reaction in the absence of the metal ion and the intramolecular carboxylate nucleophile.¹¹⁸



The study of the hydrolysis of the amide bond in compounds **50-52**, where the Zn ion has different coordination environments, was performed at 50 °C in methanol. All compounds undergo amide cleavage after addition of one equivalent of Me₄NOH·H₂O and the half-life was found to be 0.41 h for **50**, 3.95 h for **51** and 125 h for **52**. From these results the rate of amide cleavage appears to be correlated with the strength of amide coordination and with the Lewis acidity of the Zn center, which follows the order **50**>**51**>**52**. N₄ ligation was more efficient than the N₂S₂ coordination environment.



Metal ions are also involved in the design of most of the peptidase-like catalysts that are not covalently linked to the substrates. Hydrolysis of the dipeptide glycylglycine by (Cu²⁺)-[9]aneN₃ **53** has been reported.¹¹⁹ The reaction was studied at pH 8.1, and after 7 days of incubation with 1 mM catalyst at 50 °C, only 15% of glycylglycine was hydrolyzed. However, despite its low efficiency, **53** was only the second example reported in the literature until 1995 of protein hydrolysis by a small metal complex not tethered to the polypeptide. Bordignon *et al.* reported kinetic studies of the hydrolysis of glycylglycine catalyzed by the dinuclear Zn(II)-OBISDIEN (1,4,7,13,16,19-hexaaza-10,22-dioxacyclotetracosane) complex **54** (D₂O, pD = 8.4).¹²⁰ The authors concluded that the active form is the hydroxo species, in which the metal-bound hydroxide group is located in the OBISDIEN cavity. It was proposed that the dipeptide substrate is coordinated *via* the amide carbonyl and the carboxylate group to two Zn(II) ions at opposite ends of the macrocycle.



The dizinc model **55**-[Zn]₂ was prepared by Sakiyama *et al.*,¹²¹ and its aminopeptidase activity was tested at 25 °C in water/DMF (6/4) in *p*-nitrophenyl-L-leucine hydrolysis. A second order rate constant $k = 2.5 \times 10^{-3} \text{ M}^{-1}\text{s}^{-1}$ was measured, but also decomposition of the catalyst into a non-active species was observed.

Kostić *et al.* reported that [Pd(H₂O)₄]²⁺ selectively hydrolyzes internal X-Pro peptide bonds, and they successively developed catalyst **56** with the aim of combining the cleavage activity of the Pd(II) aquo-complex with the binding properties of a β -cyclodextrin, able to recognize aromatic side chains. They obtained the expected selectivity. Using the 9-mer substrate Arg-Pro-Pro-Gly-Phe-Ser-Pro-Phe-Arg and performing the measurements at pH 7.0 and 60 °C, after 48 h 80% of the 9-mer were consumed and the Pd(II) aquo-complex **56** cleaved only the Ser-Pro peptide bond. ROESY ¹H NMR analysis gave proof of the presence of an inclusion complex β -CD-Phe. The complex and the proposed mechanism are depicted in Figure 2.15 a.

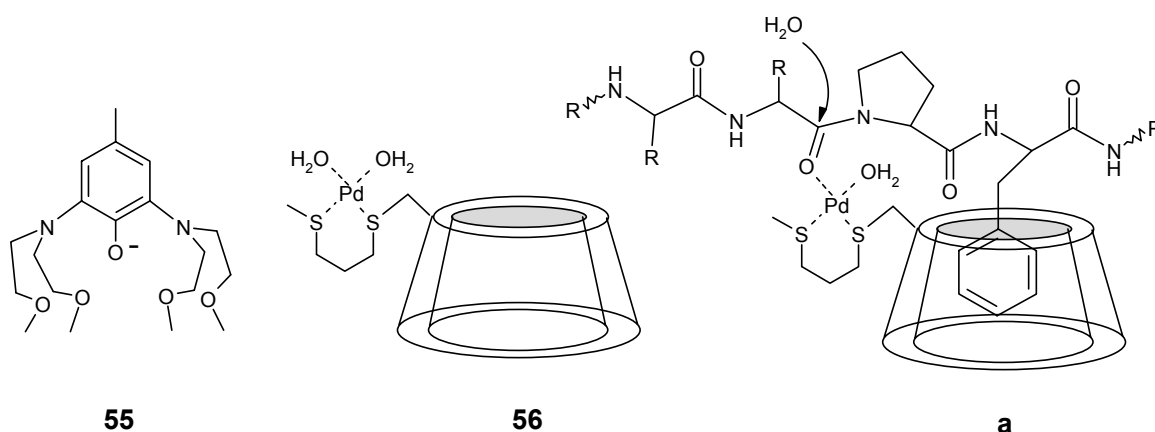


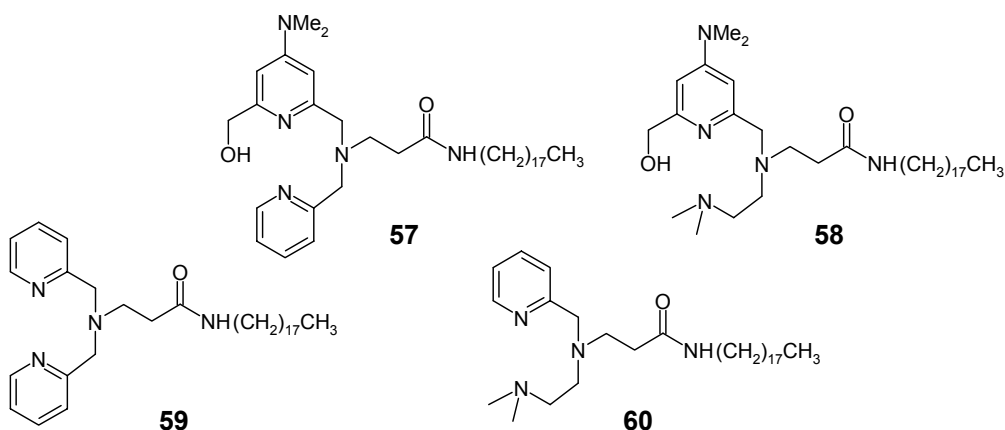
Figure 2.15 a: proposed mechanism for the hydrolysis of a 9-mer peptide by the action of **56**.

2.7 Synthetic supramolecular catalysts for ester cleavage

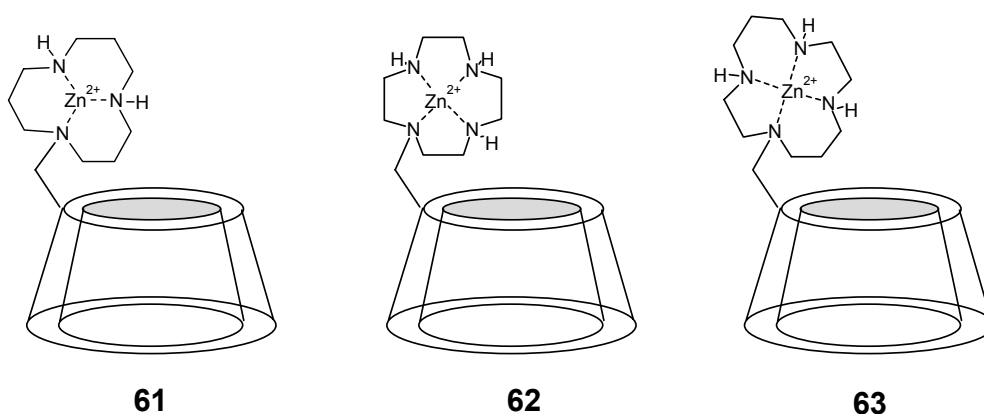
Metal complexes have been widely investigated as catalysts for ester hydrolysis and methanolysis. Also in this case, most of the studies were performed on activated substrates such as *p*-nitrophenyl acetate (PNPA) or on substrates bearing an anchoring group such as a carboxylate.

Mononuclear Cu²⁺ complexes of tetra- or tridentate ligands **57-60** were investigated in the cleavage of *p*-nitrophenyl hexanoate, in water at pH = 7.6 in the presence of cetyltrimethylammonium bromide micelles.¹²² The Cu(II) coordination in **57**-(Cu²⁺) and **58**-(Cu²⁺) has a distorted square pyramidal geometry with one coordinated water molecule, whereas **59**-(Cu²⁺) and **60**-(Cu²⁺) utilize two water molecules to complete the coordination site of the copper ion. The complexes with a pendant -CH₂OH coordinating unit **57**-(Cu²⁺) and **58**-(Cu²⁺) are more effective than

the other two, and they produce rate enhancements of 53 and 40 with respect to the uncatalyzed reaction. The authors suggest the hypothesis that the esterolysis reaction proceeds *via* the nucleophilic attack of a $-\text{CH}_2\text{OH}$ bound to the $\text{Cu}(\text{II})$ ion.

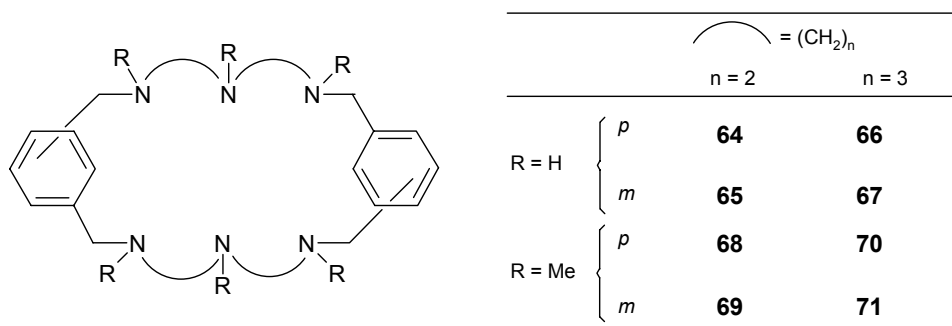


Mononuclear esterase mimics were developed by linking azacrowns to the primary face of a β -cyclodextrin (compounds **61-63**)¹²³ in order to exploit the β -CD cavity to mimic the hydrophobic pocket of carboxypeptidase A. The Zn (II) complexes **61-63** were investigated in the hydrolysis of PNPA. The reactivity of Zn(II) complexes of [12]aneN₃, [12]aneN₄, and [14]aneN₄ for hydrolyzing PNPA is raised by increasing the basicity of the zinc bound hydroxide, yielding a linear Brønsted plot. All the catalysts behave as enzyme mimics showing Michaelis-Menten kinetics. The catalytic activity of **61-63** is two orders of magnitude larger than that of the Zn triazacomplexes not bound to the β -CD, which shows that the cavity is involved in substrate binding. Unfortunately, the *p*-nitrophenolate that is formed very likely remains included in the β -CD cavity, since no catalytic turnover was observed.

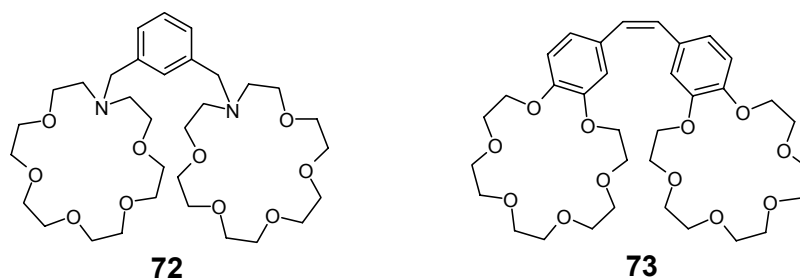


The structure and hydrolytic properties of a family of dinuclear Zn complexes containing hexaazamacrocyclic ligands (compounds **64-71**) were studied by Lobet *et al.*¹²⁴. NMR spectroscopy indicated that the structure in solution of these complexes is very different from that in the solid state. Two or more species are present in

solution in fast inter-exchange, so that the crystallographic data cannot provide a realistic picture of the position and coordination geometry of the two Zn(II) ions in solution. Only the Zn complexes of the *para*-substituted ligands (**64**, **66**, **68** and **70**) were tested for hydrolysis of PNPA in water, while the *meta* derivatives could not be used because of their low aqueous solubility. The active species were found to be LZn₂-OH. Complexes of ligands **68** and **70** bearing tertiary amines gave higher rate values compared to complexes of **64** and **66** containing secondary amines. The authors underline how small variations in the ligand can significantly influence the hydrolytic activity.



Mandolini *et al.* investigated the catalytic properties of alkaline-earth metal ions such as Ba²⁺ and Sr²⁺ in the ethanolysis of esters endowed with a carboxylate anchoring group.¹²⁵⁻¹²⁷ The crown ether moieties in **72** and **73** strongly bind Ba²⁺ or Sr²⁺ in organic solvents. Complexes **72**-[Sr]₂, **72**-[Ba]₂ or **73**-[Ba]₂ showed a synergistic action of the two metallic centers. One of the two metal ions serves as a binding unit for the carboxylate anchoring group, while the other binds to ethoxide and activates its addition to the ester carbonyl.



2.8 Calixarenes as enzyme models

Since the early times of calixarene chemistry, *cone* calix[4]arenes have been used as molecular platforms for the design and synthesis of supramolecular hosts.¹²⁸ The semirigid aromatic scaffold has the ability to preorganize the binding sites that are introduced on its *lower* and *upper* rims, while at the same time the electron rich

lipophilic cavity can be exploited as an additional binding site in receptors for polyfunctional guests.¹²⁹ Calix[4]- and calix[6]arenes have been proposed as building blocks for multifunctional enzyme models.¹³⁰ However, despite the many examples of calixarene-based supramolecular receptors, calixarene-based enzyme models are scarce.

A notable example is reported by the groups of Mandolini and Ungaro, who functionalized the calix[4]arene lower rim with a crown ether¹³¹ that can complex a Ba(II) ion.¹³² The complex **74**-[Ba] exhibits transacylase activity in the methanolysis of *p*-nitrophenyl acetate (Figure 2.16).

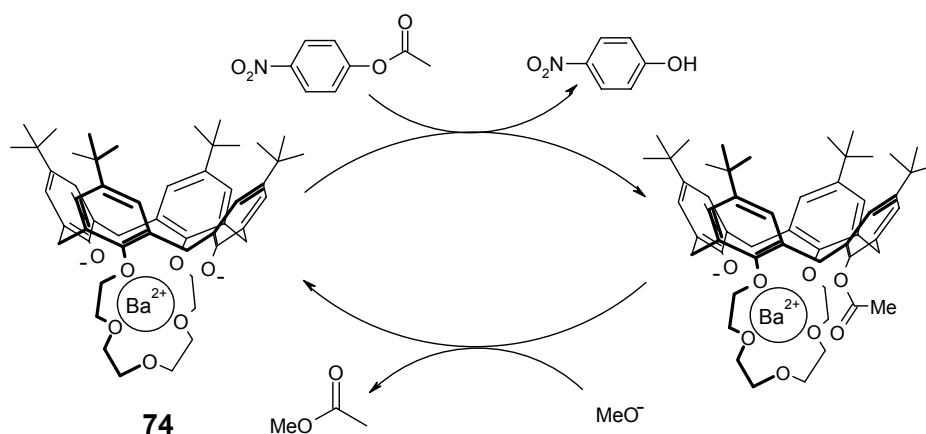


Figure 2.16

Calix[6]arenes **75** and **76** (Figure 2.17) can catalyze with turnover the methanolysis of choline *p*-nitrophenylcarbonate (PNPCC) in chloroform containing 1% methanol.¹³³ The cavity of the calixarene strongly binds the trimethylammonium head group through cation- π interactions, whereas the guanidinium moiety stabilizes, by hydrogen bonding and electrostatic interactions, the anionic tetrahedral intermediate, resulting from methoxide addition to the ester carbonyl. The synergistic action of these two functions (calixarene cavity and guanidinium moiety) affords rate accelerations that are 76 and 149 for **75** and **76**, respectively, compared to the background reaction.

2.9 Concluding remarks

Many hydrolytic enzymes, in particular nucleases and peptidases, involve metal ions present in the enzyme active center. Exploiting a combination of catalytic strategies of the metal centers (Figures 2.5 and 2.11) these enzymes provide rate enhancements larger than 10^{12} . Synthetic metallo-catalysts have been developed in attempts to mimic the hydrolytic mechanism of these enzymes. Several examples of di- and trinuclear catalysts are reported in the literature, but none of them reaches the rate accelerations of the natural enzymes, the best rate enhancements ($k_{\text{cat}}/k_{\text{uncat}}$) observed approaching 10^5 . Because of the several factors involved in the efficiency of a dinuclear catalyst (metal-metal distance and relative orientation, geometry of the metal coordination, rigidity/flexibility of the system, substrate-catalyst interaction, and so on) it is not easy to design a synthetic system and obtain cooperativity of the metal centers, and as such unpredictable results are often obtained. The calix[4]arene skeleton turned out to be an efficient and so far little explored scaffold to preorganize metal centers for cooperative catalysis.

This thesis describes the synthesis and catalytic activity in phosphate diester cleavage and ester methanolysis of di- and trinuclear metallo-catalysts based on calixarenes. *En route* to the synthesis of water soluble catalysts several calixarenes functionalized with guanidinium groups at the upper rim and with adamantyl groups at the lower rim were obtained and used to write patterns of molecules on molecular printboards (Chapter 3).

2.10 References and notes

- (1) Stryer, L. *Biochemistry*; New York, 1995.
- (2) Fersht, A. R. *Enzyme Structure and Mechanism*; W.H.Freeman: New York, 1985.
- (3) Dugas, H. *Bioorganic Chemistry*; Springer-Verlag: New York, 1988.
- (4) Trawick, B. N.; Daniher, A. T.; Bashkin, J. K. *Chem. Rev.* **1998**, *98*, 939-960.
- (5) Meunier, B. *DNA and RNA Cleavers and Chemotherapy of Cancer or Viral Diseases*; Kluwer Academic: Boston, 1996.
- (6) Parac, T. N.; Kostic, N. M. *J. Am. Chem. Soc.* **1996**, *118*, 51-58.
- (7) Pauling, L. *Chem. Eng. News* **1946**, 1375-1377.
- (8) Pauling, L. *Nature* **1948**, 707-709.
- (9) Menger, F. M. *Acc. Chem. Res.* **1985**, *18*, 128-134.
- (10) Menger, F. M. *Acc. Chem. Res.* **1993**, *26*, 206-212.
- (11) Page, M.; Jencks, W. *Proc. Natl. Acad. Sci. U. S. A.* **1971**, 1678-1683.
- (12) Villa, J.; Warshel, A. *J. Phys. Chem. B* **2001**, *105*, 7887-7907.
- (13) Khanjin, N. A.; Snyder, J. P.; Menger, F. M. *J. Am. Chem. Soc.* **1999**, *121*, 11831-11846.
- (14) Bruice, T. C.; Lightstone, F. C. *Acc. Chem. Res.* **1999**, *32*, 127-136.
- (15) Lightstone, F. C.; Bruice, T. C. *Bioorg. Chem.* **1998**, *26*, 193-199.

- (16) Illuminati, G.; Mandolini, L. *Acc. Chem. Res.* **1981**, *14*, 95-102.
- (17) Bruice, T. C.; Benkovic, S. J. *Biochemistry* **2000**, *39*, 6267-6274.
- (18) Bruice, T. C. *Acc. Chem. Res.* **2002**, *35*, 139-148.
- (19) Mesecar, A. D.; Stoddard, B. L.; Koshland, D. E. *Science* **1997**, *277*, 202-206.
- (20) Frey, P. A.; Whitt, S. A.; Tobin, J. B. *Science* **1994**, *264*, 1927-1930.
- (21) Gerlt, J. A.; Gassman, P. G. *Biochemistry* **1993**, *32*, 11943-11952.
- (22) Kollman, P. A.; Kuhn, B.; Perakyla, M. *J. Phys. Chem. B* **2002**, *106*, 1537-1542.
- (23) Kollman, P. A.; Kuhn, B.; Donini, O.; Perakyla, M.; Stanton, R.; Bakowies, D. *Acc. Chem. Res.* **2001**, *34*, 72-79.
- (24) Marti, S.; Andres, J.; Moliner, V.; Silla, E.; Tunon, I.; Bertran, J. *Chem. Eur. J.* **2003**, *9*, 984-991.
- (25) Radzicka, A.; Wolfenden, R. *Science* **1995**, *267*, 90-93.
- (26) Jarvinen, P.; Oivanen, M.; Lönnberg, H. *J. Org. Chem.* **1991**, *56*, 5396-5401.
- (27) Radzicka, A.; Wolfenden, R. *J. Am. Chem. Soc.* **1996**, *118*, 6105-6109.
- (28) Direct measurements of the hydrolysis reaction rate under neutral conditions are not possible, and the values have been obtained by extrapolating at 25 °C of measurements performed at higher temperatures and using different techniques. Different groups obtained different values, Williams and Wyman in "Williams, N. H.; Wyman, P. *Chem. Commun.* **2001**, 1268-1269" report an estimate of the half life of 100 billion of years for hydrolytic cleavage of the phosphodiester bonds in DNA. Thompson in "Thompson, J. E.; Kutateladze, T. G.; Schuster, M. C.; Venegas, F. D.; Messmore, J. M.; Raines, R. T. *Bioorganic Chemistry* **1995**, *23*, 471-481" measured 7 years for the half life of phosphodiester bonds in RNA. In "Kahne, D.; Still, W. C. *J. Am. Chem. Soc.* **1988**, *110*, 7529-7534" the half life of a peptide bond is estimated 7 years.
- (29) Grzyska, P. K.; Czyryca, P. G.; Purcell, J.; Hengge, A. C. *J. Am. Chem. Soc.* **2003**, *125*, 13106-13111.
- (30) Wang, Y. N.; Topol, I. A.; Collins, J. R.; Burt, S. K. *J. Am. Chem. Soc.* **2003**, *125*, 13265-13273.
- (31) Cassano, A. G.; Anderson, V. E.; Harris, M. E. *Biopolymers* **2004**, *73*, 110-129.
- (32) Oivanen, M.; Kuusela, S.; Lönnberg, H. *Chem. Rev.* **1998**, *98*, 961-990.
- (33) Perreault, D. M.; Anslyn, E. V. *Angew. Chem. Int. Ed* **1997**, *36*, 432-450.
- (34) Takagi, Y.; Ikeda, Y.; Taira, K. *Top. Curr. Chem.* **2004**, *232*, 213-251.
- (35) Westheimer, F. H. *Acc. Chem. Res.* **1968**, *1*, 70-78.
- (36) Zhou, D. M.; Taira, K. *Chem. Rev.* **1998**, *98*, 991-1026.
- (37) Williams, N. H.; Takasaki, B.; Wall, M.; Chin, J. *Acc. Chem. Res.* **1999**, *32*, 485-493.
- (38) Da Silva, J. J. R. F.; Williams, R. J. P. Chapter 9; In *The Biological Chemistry of the Elements: The Inorganic Chemistry of Life*; Clarendon Press: Oxford, 1994.
- (39) Bertini, I.; Gray, H. B.; Lippard, S. J.; Valentine, J. S. Chapter 2; In *Bioinorganic Chemistry*; University Science Books: Mill Valley, CA, 1994.
- (40) Parkin, G. *Chem. Rev.* **2004**, *104*, 699-767.
- (41) Cowan, J. A. *J. Biol. Inorg. Chem.* **1997**, *2*, 168-176.
- (42) Wilcox, D. E. *Chem. Rev.* **1996**, *96*, 2435-2458.
- (43) Strater, N.; Lipscomb, W. N.; Klabunde, T.; Krebs, B. *Angew. Chem. Int. Ed* **1996**, *35*, 2024-2055.
- (44) Coleman, J. E. *Ann. Rev. Biochem.* **1992**, *61*, 897-946.
- (45) Vincent, J. B.; Olivier-Lilley, G. L.; Averill, B. A. *Chem. Rev.* **1990**, *90*, 1447-1467.
- (46) Raines, R. T. *Chem. Rev.* **1998**, *98*, 1045-1065.

- (47) Kubiak, R. J.; Yue, X. J.; Hondal, R. J.; Mihai, C.; Tsai, M. D.; Bruzik, K. S. *Biochemistry* **2001**, *40*, 5422-5432.
- (48) Freemont, P. S.; Friedman, J. M.; Beese, L. S.; Sanderson, M. R.; Steitz, T. A. *Proc. Natl. Acad. Sci. U. S. A.* **1988**, *85*, 8924-8928.
- (49) Derbyshire, V.; Freemont, P. S.; Sanderson, M. R.; Beese, L.; Friedman, J. M.; Joyce, C. M.; Steitz, T. A. *Science* **1988**, *240*, 199-201.
- (50) Mullen, G. P.; Serpersu, E. H.; Ferrin, L. J.; Loeb, L. A.; Mildvan, A. S. *J. Biol. Chem.* **1990**, *265*, 14327-14334.
- (51) Vipond, I. B.; Baldwin, G. S.; HALFORD, S. E. *Biochemistry* **1995**, *34*, 697-704.
- (52) Steitz, T. A.; Steitz, J. A. *Proc. Natl. Acad. Sci. U. S. A.* **1993**, *90*, 6498-6502.
- (53) Shan, S. O.; Yoshida, A.; Sun, S. G.; Piccirilli, J. A.; Herschlag, D. *Proc. Natl. Acad. Sci. U. S. A.* **1999**, *96*, 12299-12304.
- (54) Yoshida, A.; Shan, S.; Herschlag, D.; Piccirilli, J. A. *Chem. Biol.* **2000**, *7*, 85-96.
- (55) Kuimelis, R. G.; McLaughlin, L. W. *Chem. Rev.* **1998**, *98*, 1027-1044.
- (56) Wang, S. L.; Karbstein, K.; Peracchi, A.; Beigelman, L.; Herschlag, D. *Biochemistry* **1999**, *38*, 14363-14378.
- (57) Scott, W. G.; Murray, J. B.; Arnold, J. R. P.; Stoddard, B. L.; Klug, A. *Science* **1996**, *274*, 2065-2069.
- (58) Kuimelis, R. G.; McLaughlin, L. W. *Biochemistry* **1996**, *35*, 5308-5317.
- (59) Torres, R. A.; Bruice, T. C. *J. Am. Chem. Soc.* **2000**, *122*, 781-791.
- (60) Sawata, S.; Komiyama, M.; Taira, K. *J. Am. Chem. Soc.* **1995**, *117*, 2357-2358.
- (61) Zhou, D. M.; Zhang, L. H.; Taira, K. *Proc. Natl. Acad. Sci. U. S. A.* **1997**, *94*, 14343-14348.
- (62) Ferre-D'Amare, A. R.; Zhou, K. H.; Doudna, J. A. *Nature* **1998**, *395*, 567-574.
- (63) Perrotta, A. T.; Shih, I. H.; Been, M. D. *Science* **1999**, *286*, 123-126.
- (64) Sargueil, B.; McKenna, J.; Burke, J. M. *J. Biol. Chem.* **2000**, *275*, 32157-32166.
- (65) Davies, J. F.; Hostomska, Z.; Hostomsky, Z.; Jordan, S. R.; Matthews, D. A. *Science* **1991**, *252*, 88-95.
- (66) Black, C. B.; Cowan, J. A. *Inorg. Chem.* **1994**, *33*, 5805-5808.
- (67) Fife, T. H.; Prystas, T. J. *J. Am. Chem. Soc.* **1985**, *107*, 1041-1047.
- (68) Pollack, R. M.; Bender, M. L. *J. Am. Chem. Soc.* **1970**, *92*, 7190.
- (69) Kershner, L. D.; Showen, R. L. *J. Am. Chem. Soc.* **1971**, *93*, 2014.
- (70) Sayre, L. M. *J. Am. Chem. Soc.* **1986**, *108*, 1632-1635.
- (71) Van Wart, H. E.; Lin, S. H. *Biochemistry* **1981**, *20*, 5682.
- (72) Bayliss, M. E.; Prescott, J. M. *Biochemistry* **1986**, *25*, 8113.
- (73) Christianson, D. W.; Lipscomb, W. N. *Acc. Chem. Res.* **1989**, *22*, 62-69.
- (74) Matthews, B. W. *Acc. Chem. Res.* **1988**, *21*, 333-340.
- (75) Kirby, A. J. *Angew. Chem. Int. Ed. Engl.* **1996**, *35*, 707-724.
- (76) Sanders, J. K. M. *Chem. Eur. J.* **1998**, *4*, 1378-1383.
- (77) Hegg, E. L.; Burstyn, J. N. *Coord. Chem. Rev.* **1998**, *173*, 133-165.
- (78) Anslyn, E.; Breslow, R. *J. Am. Chem. Soc.* **1989**, *111*, 4473-4482.
- (79) Komiyama, M.; Yoshinari, K. *J. Org. Chem.* **1997**, *62*, 2155-2160.
- (80) Fouace, S.; Gaudin, C.; Picard, S.; Corvaisier, S.; Renault, J.; Carboni, B.; Felden, B. *Nucleic Acids Res.* **2004**, *32*, 151-157.
- (81) Menger, F. M.; Ladika, M. *J. Am. Chem. Soc.* **1987**, *109*, 3145.
- (82) Breslow, R.; Singh, S. *Biorg. Chem.* **1988**, *16*, 408-417.
- (83) Yang, M. Y.; Richard, J. P.; Morrow, J. R. *Chem. Commun.* **2003**, 2832-2833.

- (84) Bonfa, L.; Gatos, M.; Mancin, F.; Tecilla, P.; Toneliato, U. *Inorg. Chem.* **2003**, *42*, 3943-3949.
- (85) Koike, T.; Kimura, E. *J. Am. Chem. Soc.* **1991**, *113*, 8935-8941.
- (86) Liu, S. H.; Hamilton, A. D. *Tetrahedron Lett.* **1997**, *38*, 1107-1110.
- (87) Ait-Haddou, H.; Sumaoka, J.; Wiskur, S. L.; Folmer-Andersen, J. F.; Anslyn, E. V. *Angew. Chem. Int. Ed* **2002**, *41*, 4014-4016.
- (88) Wilcox, D. E. *Chem. Rev.* **1996**, *96*, 2435-2458.
- (89) Kawahara, S.; Uchimaru, T. *Eur. J. Inorg. Chem.* **2001**, 2437-2442.
- (90) Sissi, C.; Mancin, F.; Palumbo, M.; Scrimin, P.; Tecilla, P.; Tonellato, U. *Nucleosides Nucleotides Nucleic Acids* **2000**, *19*, 1265-1271.
- (91) Mancin, F.; Rampazzo, E.; Tecilla, P.; Tonellato, U. *Eur. J. Org. Chem.* **2004**, 281-288.
- (92) Worm, K.; Chu, F. Y.; Matsumoto, K.; Best, M. D.; Lynch, V.; Anslyn, E. V. *Chem. Eur. J.* **2003**, *9*, 741-747.
- (93) Rossi, P.; Felluga, F.; Tecilla, P.; Formaggio, F.; Crisma, M.; Toniolo, C.; Scrimin, P. *Biopolymers* **2000**, *55*, 496-501.
- (94) Sissi, C.; Rossi, P.; Felluga, F.; Formaggio, F.; Palumbo, M.; Tecilla, P.; Toniolo, C.; Scrimin, P. *J. Am. Chem. Soc.* **2001**, *123*, 3169-3170.
- (95) Yamada, K.; Takahashi, Y.; Yamamura, H.; Araki, S.; Saito, K.; Kawai, M. *Chem. Commun.* **2000**, 2173.
- (96) Fritsky, I. O.; Ott, R.; Pritzkow, H.; Kramer, R. *Chem. Eur. J.* **2001**, *7*, 1221-1231.
- (97) Scarso, A.; Scheffer, U.; Gobel, M.; Broxterman, Q. B.; Kaptein, B.; Formaggio, F.; Toniolo, C.; Scrimin, P. *Proc. Natl. Acad. Sci. U. S. A.* **2002**, *99*, 5144-5149.
- (98) Albedyhl, S.; Schnieders, D.; Jancso, A.; Gajda, T.; Krebs, B. *Eur. J. Inorg. Chem.* **2002**, 1400-1409.
- (99) Gajda, T.; Jancso, A.; Mikkola, S.; Lonnberg, H.; Sirges, H. *J. Chem. Soc., Dalton Trans.* **2002**, 1757-1763.
- (100) Iranzo, O.; Kovalevsky, A. Y.; Morrow, J. R.; Richard, J. P. *J. Am. Chem. Soc.* **2003**, *125*, 1988-1993.
- (101) Iranzo, O.; Elmer, T.; Richard, J. P.; Morrow, J. R. *Inorg. Chem.* **2003**, *42*, 7737-7746.
- (102) Iranzo, O.; Richard, J. P.; Morrow, J. R. *Inorg. Chem.* **2004**, *43*, 1743-1750.
- (103) Yashiro, M.; Kaneiwa, H.; Onaka, K.; Komiyama, M. *Dalton Transactions* **2004**, 605-610.
- (104) Komiyama, M.; Kina, S.; Matsumura, K.; Sumaoka, J.; Tobey, S.; Lynch, V. M.; Anslyn, E. *J. Am. Chem. Soc.* **2002**, *124*, 13731-13736.
- (105) Verheijen, J. C.; Deiman, B. A. L. M.; Yeheskiely, E.; van der Marel, G. A.; van Boom, J. H. *Angew. Chem. Int. Ed* **2000**, *39*, 369-+.
- (106) Canaple, L.; Husken, D.; Hall, J.; Haner, R. *Bioconjugate Chem.* **2002**, *13*, 945-951.
- (107) Niittymaki, T.; Kaukinen, U.; Virta, P.; Mikkola, S.; Lönnerberg, H. *Bioconjugate Chem.* **2004**, *15*, 174-184.
- (108) Sakamoto, S.; Tamura, T.; Furukawa, T.; Komatsu, Y.; Ohtsuka, E.; Kitamura, M.; Inoue, H. *Nucleic Acids Res.* **2003**, *31*, 1416-1425.
- (109) Kuzuya, A.; Komiyama, M. *Chem. Commun.* **2000**, 2019-2020.
- (110) Kuzuya, A.; Mizoguchi, R.; Morisawa, F.; Machida, K.; Komiyama, M. *J. Am. Chem. Soc.* **2002**, *124*, 6887-6894.
- (111) Kuzuya, A.; Machida, K.; Mizoguchi, R.; Komiyama, M. *Bioconjugate Chem.* **2002**, *13*, 365-369.

- (112) Kuzuya, A.; Machida, K.; Komiyama, M. *Tetrahedron Lett.* **2002**, *43*, 8249-8252.
- (113) Michaelis, K.; Kalesse, M. *Angew. Chem. Int. Ed* **1999**, *38*, 2243-2245.
- (114) Sreedhara, A.; Patwardhan, A.; Cowan, J. A. *Chem. Commun.* **1999**, 1147-1148.
- (115) Sreedhara, A.; Cowan, J. A. *J. Biol. Inorg. Chem.* **2001**, *6*, 166-172.
- (116) Chen, C. A.; Cowan, J. A. *Chem. Commun.* **2002**, 196-197.
- (117) Kramer, R. *Coord. Chem. Rev.* **1999**, *182*, 243-261.
- (118) Suh, J. H. *Acc. Chem. Res.* **1992**, *25*, 273-279.
- (119) Hegg, E. L.; Burstyn, J. N. *J. Am. Chem. Soc.* **1995**, *117*, 7015-7016.
- (120) Bordignon Luiz, M. T.; Szpoganicz, B.; Rizzoto, M.; Basallote, M. G.; Martell, A. E. *Inorg. Chim. Acta* **1999**, *287*, 134-141.
- (121) Sakiyama, H.; Mochizuki, R.; Sugawara, A.; Sakamoto, M.; Nishida, Y.; Yamasaki, M. *J. Chem. Soc., Dalton Trans.* **1999**, 997-1000.
- (122) Bhattacharya, S.; Snehalatha, K.; Kumar, V. P. *J. Org. Chem.* **2003**, *68*, 2741-2747.
- (123) Kim, D. H.; Lee, S. S. *Bioorg. Med. Chem.* **2000**, *8*, 647-652.
- (124) Costas, M.; Anda, C.; Llobet, A.; Parella, T.; Evans, H. S.; Pinilla, E. *Eur. J. Inorg. Chem.* **2004**, 857-865.
- (125) Cacciapaglia, R.; Di Stefano, S.; Kelderman, E.; Mandolini, L. *Angew. Chem. Int. Ed* **1999**, *38*, 348-351.
- (126) Cacciapaglia, R.; Di Stefano, S.; Mandolini, L. *J. Org. Chem.* **2001**, *66*, 5926-5928.
- (127) Cacciapaglia, R.; Di Stefano, S.; Mandolini, L. *J. Org. Chem.* **2002**, *67*, 521-525.
- (128) Pochini, A.; Ungaro, R. Calixarenes and Related Hosts; In *Comprehensive Supramolecular Chemistry*; Vögtle, F., ed. Pergamon Press: New York, 1996; pp 103-142.
- (129) Arduini, A.; Casnati, A.; Dalcanale, E.; Pochini, A.; Ugozzoli, F.; Ungaro, R. *NATO ASI Ser. C* **1999**, *527*, 67-94.
- (130) Cacciapaglia, R.; Mandolini, L. Calixarene based catalytic systems; In *Calixarenes in Action*; Mandolini, L., Ungaro, R., eds. Imperial College Press: London, 2000; pp 241-264.
- (131) Baldini, L.; Bracchini, C.; Cacciapaglia, R.; Casnati, A.; Mandolini, L.; Ungaro, R. *Chem. Eur. J.* **2000**, *6*, 1322-1330.
- (132) Cacciapaglia, R.; Casnati, A.; Mandolini, L.; Ungaro, R. *J. Am. Chem. Soc.* **1992**, *114*, 10956-10958.
- (133) Cuevas, F.; Di Stefano, S.; Magrans, J. O.; Prados, P.; Mandolini, L.; de Mendoza, J. *Chem. Eur. J.* **2000**, *6*, 3228-3234.
- (134) Molenveld, P.; Engbersen, J. F. J.; Reinhoudt, D. N. *J. Org. Chem.* **1999**, *64*, 6337-6341.
- (135) Molenveld, P.; Stikvoort, W. M. G.; Kooijman, H.; Spek, A. L.; Engbersen, J. F. J.; Reinhoudt, D. N. *J. Org. Chem.* **1999**, *64*, 3896-3906.
- (136) Molenveld, P.; Engbersen, J. F. J.; Reinhoudt, D. N. *Chem. Soc. Rev.* **2000**, *29*, 75-86.
- (137) Molenveld, P.; Engbersen, J. F. J.; Reinhoudt, D. N. *Angew. Chem. Int. Ed. Engl.* **1999**, *38*, 3189-3192.

CHAPTER 3

Water soluble calix[4]arene based receptors and catalysts*

*In this chapter three different approaches will be discussed to solubilize a calix[4]arene in water with the ultimate goal of obtaining catalysts bearing three 2,6-bis[(dimethylamino)methyl]pyridine groups at the upper rim. The first method is the functionalization of the lower rim of the calixarene with OH terminating triethyleneglycol chains. The second is the introduction of adamantyl units at the calixarene lower rim which allows the exploitation of β -cyclodextrins (β -CD) as solubilizing units. β -CDs are known to form strong inclusion complexes with adamantyl groups in water solution. Several calix[4]arenes having spacers of different length and type between the macrocycle and the adamantyl units were prepared and the possibility of dissolving them in water through β -CD complexation was investigated. The synthesis of water soluble para-guanidinium di- and tetraadamantyl calix[4]arenes allowed also the study of calix[Ad]-CD interactions both in solution by microcalorimetry and on the surface of β -CD self-assembled monolayers by surface plasmon resonance. Finally, the third approach allowed the introduction of six alcohol functions on the calix[4]arene upper rim to give compound **50**. The water solubility of **50** and the catalytic activity of its Zn complex (**50**-[Zn²⁺]₃) in the transesterification of HPNP are reported.*

* Parts of the work described in this chapter have been published in: Auletta, T.; Dordi, B.; Mulder, A.; Sartori, A.; Onclin, S.; Bruinink, C. M.; Peter, M.; Nijhuis, C. A.; Beijleveld, H.; Schonherr, H.; Vancso, G. J.; Casnati, A.; Ungaro, R.; Ravoo, B. J.; Huskens, J.; Reinhoudt, D. N. *Angew.Chem.Int.Ed.* **2004**, *43*, 369-373; and in Mulder, A.; Auletta, T.; Sartori, A.; Del Ciotto, S.; Casnati, A.; Ungaro, R.; Huskens, J.; Reinhoudt, D. N. *J. Am. Chem. Soc.* **2004**, *126*, 6627-6636.

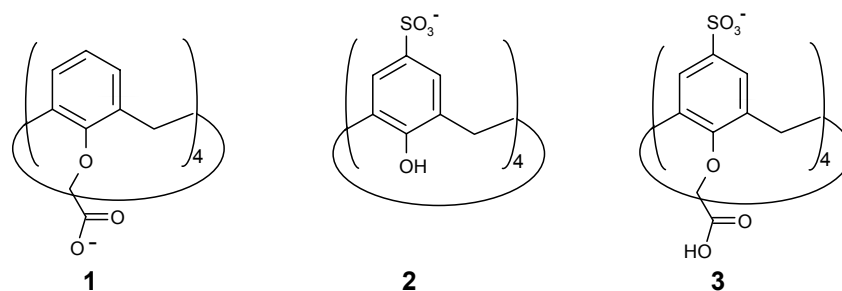
3.1 Introduction

Water solubility is an essential property of an enzyme mimic. If we consider, for example, a nuclease mimic, its activity should be tested not only on RNA models and dinucleotides, but also on oligoribonucleotides and on natural RNAs, whose conformation and reactivity can be completely different in water and in organic solvents. Moreover, one of the most ambitious goals is the *in vivo* application of these compounds (gene therapy) and water solubility is therefore an essential prerequisite.

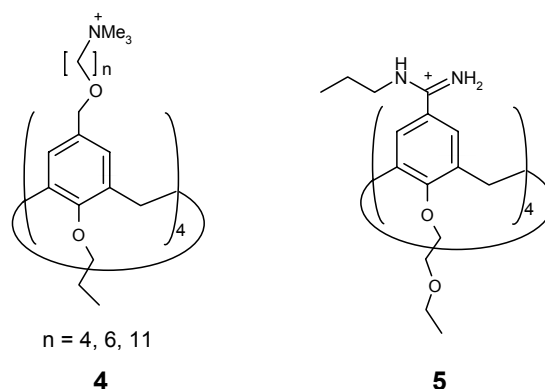
Calix[4]arenes are very promising scaffolds for the synthesis of supramolecular systems able to mimic enzymes. They offer numerous functionalization possibilities (four sites at the upper rim and four at the lower rim) with well established selective synthetic procedures. Their cone conformation is well suited for preorganization of the binding and/or catalytic groups attached to the molecule. Moreover, even when they are locked in the cone conformation, calix[4]arenes maintain a residual mobility given by the swinging of the aryl units, which can allow the catalyst to adapt to changes of the substrate as it moves into the transition state of the reaction. Finally, they offer an apolar cavity which, in water, could constitute a microenvironment similar to apolar pockets of some enzymes where the binding of the substrate and the catalysis take place. On the other hand, they have the disadvantage of having an apolar structure and they need to be functionalized with highly hydrophilic groups to make them soluble in water.¹

3.1.1 Water soluble calix[4]arenes

Most of the water soluble calix[4]arenes reported so far in the literature are compounds functionalized with negatively or positively charged groups. The alkali metal salts of *p-tert*-butylcalix[4]arene tetraacetic acid (**1**) were the first examples of water-soluble calixarenes reported in the literature (soluble only up to 5×10^{-3} M).² The solubility is provided by the formation of carboxylate anions and therefore depends on the pH of the solution. For the same reason, the introduction of phosphonate groups at the upper rim led to calixarenes soluble only under basic conditions.³ Sulfonate groups inserted at the upper rim (**2**)⁴ eventually in combination with carboxylic functions at the lower rim (**3**)⁵ ensure a remarkable solubility in water which is nearly independent of the pH of the solution.

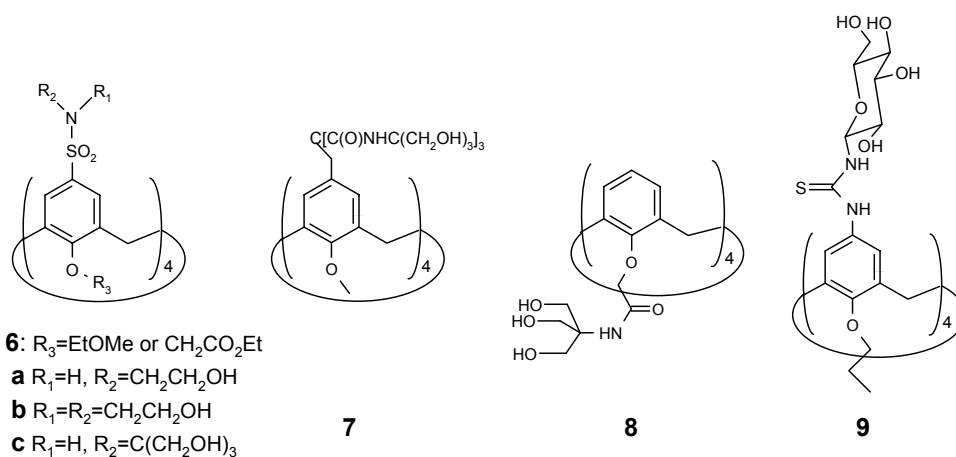


Positively charged groups were also exploited, and examples of water soluble calix[4]arenes bearing quaternary ammonium groups (**4**)⁶ and amidinium functions (**5**)⁷ are reported in the literature.



Although it is easier to solubilize calix[4]arenes in water by introducing charged groups, the use of hydrophilic neutral moieties (above all alcohols and polyols)⁸ has also been pursued in recent years. By a systematic study performed on compounds **6a-c**, Reinhoudt *et al.* found that the water solubility of a calix[4]arene increases by nearly two orders of magnitude when four additional OH groups are introduced.^{9;10} Compounds having good water solubility were obtained by introducing tris(hydroxymethyl)aminomethane (TRIS) groups either at the upper rim (**7**)¹¹ or at the lower rim (**8**) (water solubility = 0.01 M) using amide bonds.⁸ However, the TRIS group in these compounds is not stable under acidic conditions and can rearrange giving esters.¹²

Carbohydrate units have also been used to make calixarenes water soluble. These compounds, called glycolcalixarenes¹³ were designed mainly to study the cluster glycoside effect. In spite of the large number of hydroxyl groups in the molecule, the water solubility of these compounds is quite low, because the hydroxyl groups tend to form intramolecular hydrogen bonds instead of interacting with the solvent. Compound **9**, for example, is soluble in water only up to 5×10^{-5} M.¹⁴



The use of glycolic chains terminating with a methyl group, was investigated by Middel and coworkers for the water solubilization of resorcinarenes.¹⁵ Four tetraethylene glycol chains barely solubilized the cavitands in water, but when the number was increased to twelve and four hydroxyl groups were added the solubility rose to $3.5 \times 10^{-2} \text{ mol L}^{-1}$. Much longer hydroxyl terminating polyethylene glycol units were able to solubilize *p*-*tert*-butylcalix[8]arene, although the solubility limit was not reported.¹⁶

3.1.2 β -Cyclodextrins as solubilizing moieties

β -Cyclodextrins (β -CD) are cyclic oligosaccharides consisting of seven glucopyranose rings (Figure 3.1).¹⁷ The glucopyranose secondary hydroxyl groups are located on one face of the molecule (secondary face), whereas the primary OHs are located on the other face (primary face). The molecular shape is conical and quite rigid due to a belt of intramolecular hydrogen bonds. Partial substitution of the hydroxyl groups of the β -CD disrupts the network of hydrogen bonds around the rim of the β -CD, and as a result the hydroxyl groups interact much more strongly with the water molecules resulting in increased solubility compared to the β -CD. The substituents are randomly inserted onto the hydroxyl groups of the cyclodextrin and the amount of substitution is reported as Molar Substitution (MS) that is the average number of groups per anhydroglucose unit in the ring of the cyclodextrin. The hydroxypropyl β -CD (hyp- β -CD) is one of the most soluble β -CDs. Solubility of hyp- β -CDs is typically >60% at room temperature compared to β -CD. The solubility in water at r.t. of 0.8 MS hyp- β -CD, for example, is 0.428 mol L^{-1} , 25 times higher than that of the native β -CD ($0.0163 \text{ mol L}^{-1}$).

β -CDs have an apolar cavity that is well suited for the complexation of apolar guests of appropriate size in water through hydrophobic interactions. When β -CD is dissolved in water the cavity is occupied by water molecules. These molecules and the ones solvating the apolar surface of the free guest reduce cohesive interactions and are,

therefore, enthalpically higher in energy than the water molecules in the bulk solvent. During the formation of inclusion complexes, the water molecules in the cavity are released into the bulk and this energy gain is the driving force for the complexation process.¹⁸

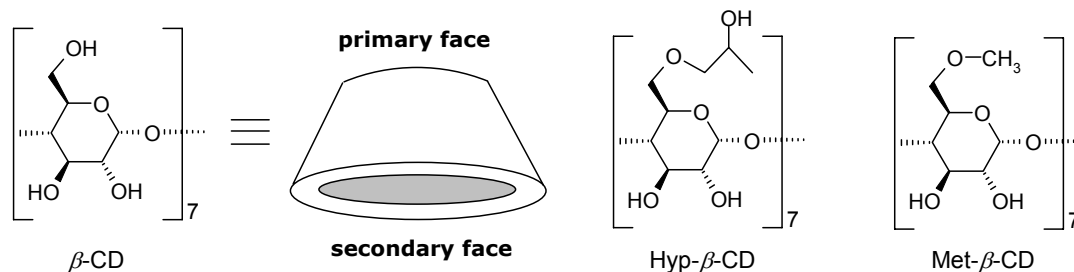


Figure 3.1 Chemical structure of β -cyclodextrins.

For this reason β -CDs have been widely studied as molecular hosts in water for different classes of apolar guests.¹⁹ Hyp- β -CDs are also commercially used for the solubilization and delivery of lipophilic drugs.^{20 21}

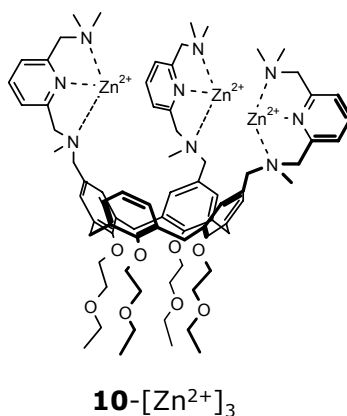
Adamantane (Ad) is one of the guests that fits very well in the β -CD cavity and forms a strong inclusion complex. The association constant of adamantane containing carboxylic acids with β -CDs is in the range 10^4 - 10^5 M^{-1} .¹⁹ By using the Ad- β -CD inclusion complex formation it was possible to solubilize dendrimers bearing several adamantane end groups in water.^{22;23} This method has never been tested in order to make calix[4]arenes soluble in water. In the literature there are only a few examples of calixarene-CD conjugates, where the β -CD is covalently bound to the calixarene.²⁴⁻²⁶

3.1.3 Aim of the work and contents of the chapter

Compound **10**- $[Zn^{2+}]_3$ has revealed very interesting catalytic activity in the transesterification both of hydroxypropyl-*p*-nitrophenyl phosphate (HPNP) and RNA dinucleotides, resulting in a promising enzyme mimic.²⁷ Nevertheless, in spite of the presence of the three Zn ions, this molecule is not completely soluble in pure water. The catalytic measurements were performed using **10**- $[Zn^{2+}]_3$ at 1 mM concentration in 35% of EtOH/buffer aqueous solution, and under these conditions the compound was highly soluble. Because of the importance of the water solubility of nuclease mimics for possible *in vivo* applications, we aimed to make an analogue of **10**- $[Zn^{2+}]_3$ soluble in water and to test its activity toward polynucleotides.

From the several possible methods to solubilize a calixarene in water, we took into consideration only those which used neutral moieties. Charged groups on the catalyst can in fact interfere in the binding of metal ions and the substrate. Oligonucleotides have a negative backbone due to the presence of phosphate anions. Because of the electrostatic repulsion, negatively charged groups on the catalyst can therefore prevent

the binding of the substrate which has the same charge. On the other hand, positively charged groups at the lower rim can decrease the stability of the metal ion complex or compete with the Zn metal centers at upper rim during the substrate binding.



Three different approaches have been explored to solubilize calix[4]arenes in water with the aim of preparing water soluble calixarene-based catalysts.

The first approach involves the introduction of polyethyleneglycol chains at the lower rim (Chapter 3.2).

The second is a supramolecular approach, which takes advantage of the high water solubility of cyclodextrins. Complexes of several lower rim adamantyl (Ad) functionalized calix[4]arenes and the β -cyclodextrin (β -CD) cavity were prepared and general studies regarding the possibilities and limitations of this water solubilizing supramolecular approach are discussed in Chapter 3.3.

The third approach consists of the introduction of six hydroxyl functions at the upper rim using diethanolamine instead of dimethylamine in the last synthetic step of the synthesis of **10** (Chapter 3.4). The water solubility and catalytic activity for the transesterification of HPNP have been studied.

3.2 Introduction of polyethyleneglycol chains at the lower rim

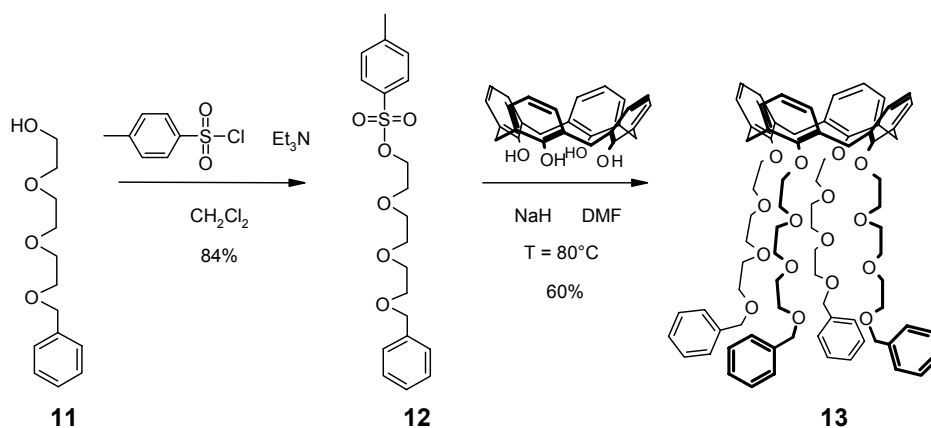
Since compound **10**-[Zn²⁺]₃ has six positive charges due to the three Zn(II) ions at the upper rim, the water solubilizing groups do not need to be highly hydrophilic. Substitution of the 2-ethoxyethoxy chains at the lower rim with hydroxyl terminating polyether chains has been the first approach undertaken to prepare a water soluble calixarene metallo catalyst. Four more OH groups in the molecule together with long glycolic chains might be enough to carry **10**-[Zn²⁺]₃ into water.

The hydroxyl functions had to be protected before the introduction at the lower rim of the macrocycles both because they react under the basic conditions used for the alkylation of the phenolic OH groups and because they can interfere during the upper rim functionalization of the calixarene. The benzyl group seemed to be an appropriate

choice, as it is stable in a wide pH range and its removal under hydrogenolytic conditions occurs in quantitative yields.

Monoprotection of triethyleneglycol was carried out according to a literature procedure²⁸ giving compound **11** in 35% yield. The other hydroxyl function was then reacted with tosyl chloride in CH_2Cl_2 to give **12** which was used as an alkylating agent to functionalize the lower rim of the tetrahydroxy-calix[4]arene²⁹ in dry DMF and in the presence of NaH. Compound **13** was obtained in the cone conformation in 60% yield (Scheme 3.1).

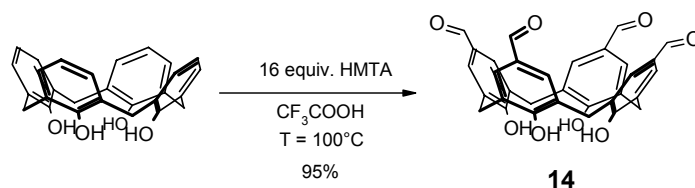
The upper rim triformylation of compound **13** was tried by two different synthetic procedures. The first used hexamethylenetetraamine (HTMA) in refluxing CF_3COOH ,³⁰ which gave, together with the formylation of the upper rim, the partial or total cleavage of the protecting benzyl groups. The second procedure was the Gross formylation ($\text{TiCl}_4/\text{Cl}_2\text{CHOCH}_3$).³¹ In this case the reaction gave several products due to the different degree of upper rim substitution and to the formylation of benzyl groups.



Scheme 3.1

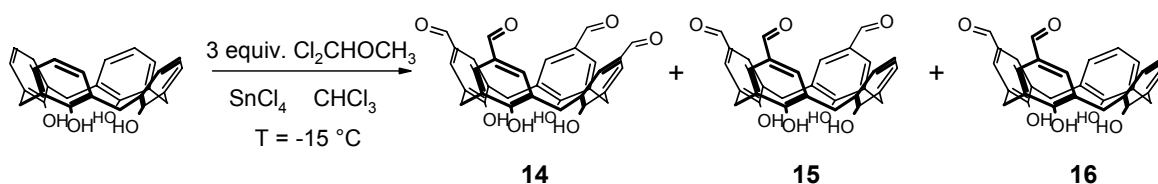
Since the triformylation of compound **13** was not successful, a different strategy was designed. First, the upper rim selective formylation of calix[4]arene was attempted with the aim of introducing the glycol chains at the lower rim in a second step. To do this, the triformyl tetrahydroxycalix[4]arene **15** had to be synthesized.

First the conditions that already allow the triformylation of tetrakis(2-ethoxyethoxy) calix[4]arene in good yields³² were used. Tetrahydroxycalix[4]arene instead of tetrakis(2-ethoxyethoxy) calix[4]arene was reacted with HMTA (16 equiv.) in TFA, but the tetraformylated calix[4]arene **14** was isolated as the only product in 95% yield (Scheme 3.2).

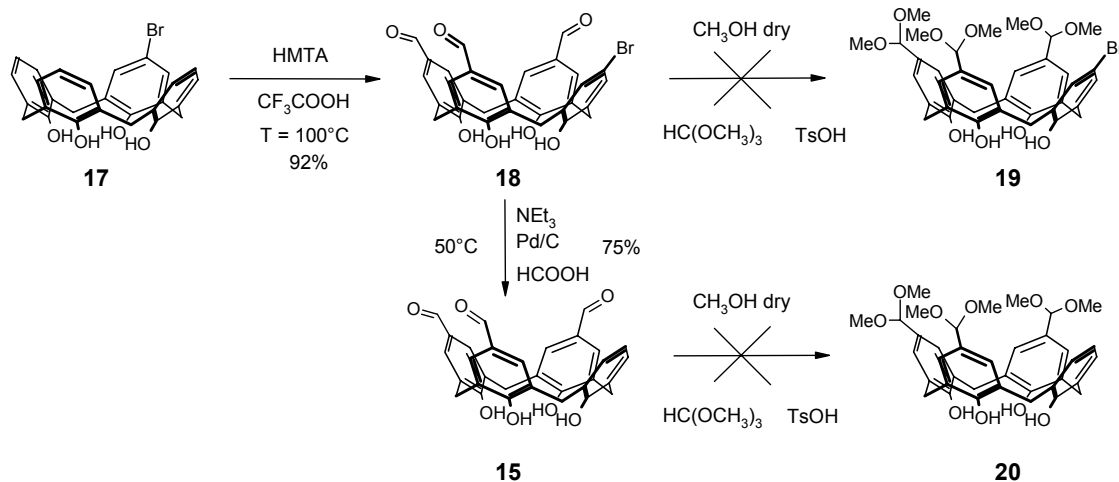
**Scheme 3.2**

Repeating the reaction with a smaller excess of HMTA (8 equiv.) still gives **14** as the only product. With only 2 equivalents of HMTA a mixture of products, that were very difficult to separate, was obtained. Nevertheless, a TLC analysis could exclude the presence of the triformylated **15** in reasonable yield. These results are explained on the basis of the known higher reactivity of the phenolic compared to alkyl ether nuclei in calixarenes.

Under the Gross formylation conditions (Scheme 3.3) no selectivity for compound **15** was observed, although it could be isolated in low yield (15%). In the reaction mixture the tetra-, 1,2-di-, 1,3-di- and mono-formylated calixarenes were present.

**Scheme 3.3**

Finally, exploiting the use of a bromine atom as protective group in one of the calixarene aromatic nuclei, a new synthetic pathway to the triformylated tetrahydroxycalix[4]arene **15** was developed. Starting from the monobromo calix[4]arene **17**³³ the formylation of the other three aromatic positions could be performed in excellent yields (Scheme 3.4).

**Scheme 3.4**

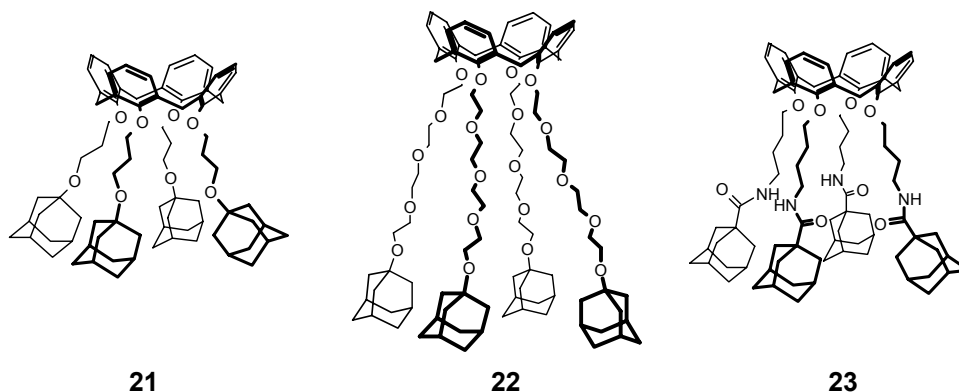
Compound **15** could be obtained by removing the bromine atom with NEt_3 , Pd/C and 10 equivalents of formic acid. Alternatively, the bromine atom can also be left in its position and removed or substituted with other functional groups in the last step.

The alkylation of the lower rim of compounds **18** and **15** needs the use of a strong base such as NaH to ensure the formation of the cone structure³⁴ and to allow complete deprotonation of phenolic OHs. For this reason, it is necessary to protect the formyl groups as acetals in order to avoid their decomposition. This protection was attempted under several conditions, but it was not possible to obtain the triacetal **19** or **20**. A possible explanation of this dramatically low reactivity could be the low solubility of calixarenes **18** and **15**, which turned out to be almost completely insoluble at 60 °C in both MeOH and CHCl_3 .

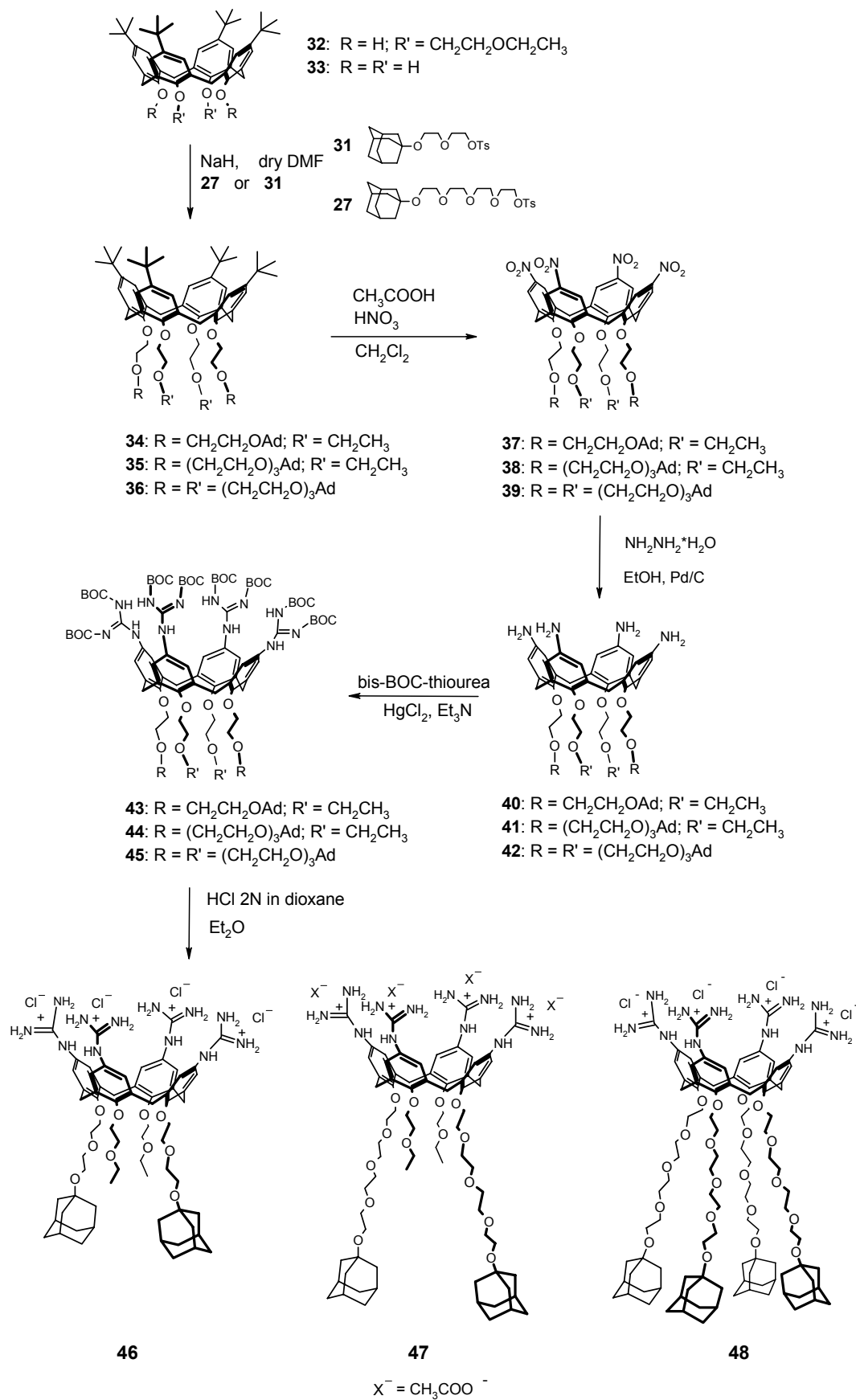
Because of the high yields and selectivity by which calix[4]arene **14**, **15** and **18** are obtained, they can be considered interesting precursors for the synthesis of more complex calixarenes. Although they can be barely be functionalized with weak electrophiles like alkoxyethyl tosylates, it is reasonable to suppose that they can easily react under less basic conditions (Na_2CO_3) with stronger electrophiles (BrCH_2COOR). Under those conditions the protection of formyl groups is probably not necessary.

3.3 Synthesis of adamantyl calix[4]arenes

The second method investigated to make calix[4]arenes soluble in water was a noncovalent approach, which exploits β -CDs as solubilizing agents. By introducing adamantanes on the calix[4]arene, we prepared molecules **21-23**, that in principle could interact with four β -CDs. In these compounds the adamantanes are linked by chains of different length and hydrophilicity in order to find the spacer necessary between the calixarene skeleton and the Ad groups to maximize the adamantane- β -CD interaction.



Tetraadamantane calix[4]arene **21** was synthesized starting from 3-(adamantan-1-yl)propan-1-ol **24**,²² which was tosylated using TsCl and triethylamine in the



Scheme 3.10

Introduction of the BOC-protected guanidinium groups using bis-BOC-thiourea³⁷ was performed under the conditions reported by the group of Qian³⁸ and led to the formation of tetraguanidinium calixarenes **43-45**. Initial attempts to deprotect the guanidinium groups using TFA led to the elimination of the adamantyl groups. The removal of the BOC groups was successfully achieved using 2 M HCl in dioxane, which gave the desired products **46-48** as tetrachloride salts. Purification of product **47** by column chromatography on SiO₂ using a *tert*-butanol/water/acetic acid mixture (6/2/1) as the eluent led to the exchange of the chloride counterions for acetate.

3.3.3 Microcalorimetric measurements

Isothermal titration calorimetry (ITC) was used to study the binding between **47** and β -CD in aqueous solution. This technique allows the direct determination of the association constant, K_i , and of the thermodynamic parameters of the complexation process (Table 3.1). The inclusion of the adamantanes in the β -CD cavity is an exothermic process (Figure 3.2). The inflection point in the titration curve indicates a 2:1 (host:guest) stoichiometry implying that **47** is bound by two CD cavities, one for each adamantyl group.

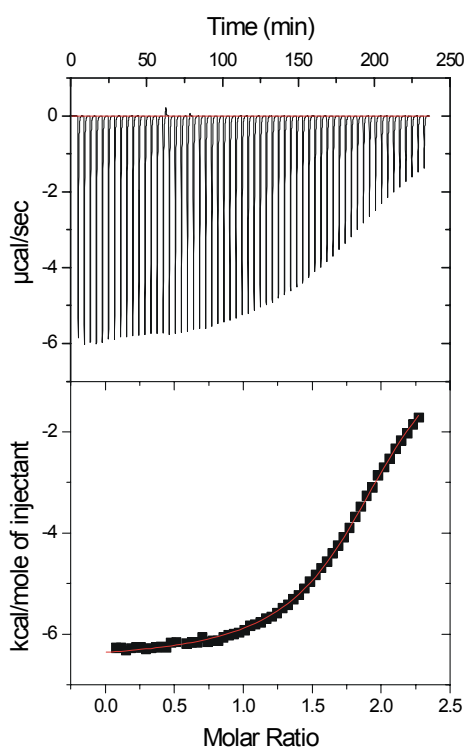


Figure 3.2 Calorimetric titration of **47** (0.5 mM) with β -CD (5 mM) in H₂O at 298 K; heat evolution per injection of β -CD (above) and plotted against the molar ratio [CD]/**47** and fit curve (below).

Table 3.1 Thermodynamic parameters of the complexation of **47** to β -CD as determined by ITC.

Guest	Stoichiometry (host:guest)	K_i (M^{-1})	ΔG° (kcal/mol)	ΔH° (kcal/mol)	$T\Delta S^\circ$ (kcal/mol)
47	2:1	$(4.6 \pm 0.3) \times 10^4$	-6.4 ± 0.1	-7.0 ± 0.5	-0.2 ± 0.6

The curve was fitted to a 2:1 binding model, considering the two adamantyl groups as two identical independent binding sites and using the intrinsic association constant, K_i , and the enthalpy of binding, ΔH_i° , as independent fitting parameters. The observed 2:1 stoichiometry and the quality of the fit using independent binding sites (Figure 3.2) indicate that both adamantyl groups bind a β -CD cavity in a similar fashion, without interference between the two binding processes. The value obtained for K_i , the intrinsic binding constant between an adamantane bound to the calixarene and a β -CD, is in the typical range (10^4 - $10^5 M^{-1}$) of β -CD-adamantane association constants.¹⁹ From this value, $K_i = 4.6 \times 10^4 M^{-1}$, it is possible to calculate the stepwise association constants $K_1 = 2 K_i$ and $K_2 = 1/2 K_i$.

Calorimetric measurements carried out in our group by Ludden³⁹ with compound **48** and β -CD showed that also in this case the binding of four adamantyl units to the β -CDs is complete and independent ($K_i = 2.9 \times 10^4 M^{-1}$). The titration with compound **46** was also performed, giving a $K_i = 5.4 \times 10^4 M^{-1}$, similar to that obtained for di-Ad calixarene **47**, revealing that a spacer chain of 7 atoms between the Ad and the calixarene skeleton is sufficient to prevent interference in the two binding processes.

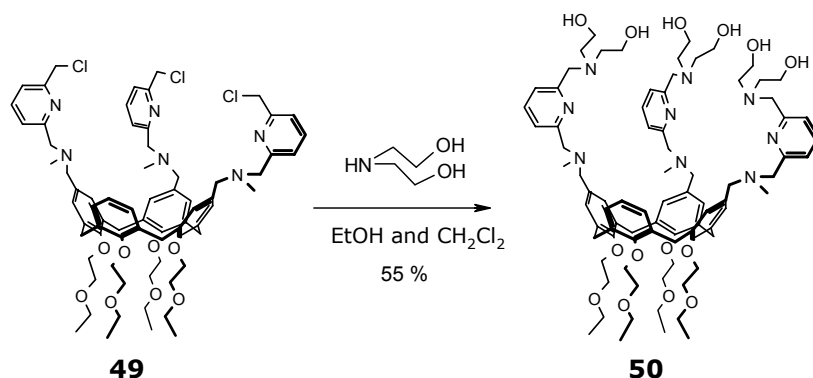
The divalent binding of compound **47** with a β -CD dimer and β -CD self-assembled monolayers (SAMs) has also been investigated in our group by Mulder.⁴⁰ The obtained binding constants for the divalent binding of **47** at CD SAMs are three orders of magnitude higher compared to the values found in solution with a β -CD dimer ($1.2 \times 10^7 M^{-1}$ with β -CD dimer, and $\sim 4 \times 10^{10} M^{-1}$ at CD SAMs). In both cases the divalent binding of **47** with β -CD dimer and CD SAMs can be considered as consistent with two independent sequential binding processes and can be explained in terms of effective concentration (C_{eff}). The intrinsic binding constant is the same for the binding in solution and at the surface, while the effective concentration is two orders of magnitude higher at CD SAMs than in solution with the β -CD dimer.

Moreover, the strong divalent binding of di-adamantyl calixarene **47** at CD SAMs surface, together with its water solubility, allowed the use of **47** as "supramolecular ink" and by microcontact printing and supramolecular dip pen nanolithography it could be selectively transferred onto a β -CD monolayer creating patterns with sub-100 nm lateral resolution stable in water solution. The patterns created on the CD SAMs could also be erased by exposing the surface to high molarity CD concentrations.⁴¹

3.4 Alternative approach to obtain water soluble calix[4]arene trinuclear catalysts

The solubilization in water of the tri-dimethylaminopyridine calix[4]arene **10** could not be achieved by either introducing benzyl protected glycolic chains at the lower rim or by exploiting the interaction of adamantyl substituents and β -CDs. The strongly acidic conditions used for the upper rim formylation gave the cleavage both of benzyl protecting groups and of adamantanes. Therefore, another way was explored, the introduction of hydroxyl functions at the upper rim. Six additional OHs on the calixarene should increase the water solubility of **10** of more than two orders of magnitude (Chapter 3.1.1).^{9;10} Since compound **10**-[Zn]₃ already showed a good solubility in EtOH/water mixtures due to the complexed Zn ions, six OHs were supposed to be sufficient.

Compound **50** was synthesized in 55% yield by reacting the tris(chloromethylpyridine) calixarene **49**³² with diethanolamine (Scheme 3.11).



Scheme 3.11

3.4.1 Water solubility and Zn(II) complexation

The water solubility of calixarene **50** was determined by UV spectrophotometry. A saturated solution of compound **50** was prepared, filtered on nylon filters (Chemtek 0.200 μ m, 4 mm) and its absorbance was measured: A (265 nm) = 0.656. Using the molar absorptivity of **50** ($\epsilon = 9,163 \text{ M}^{-1} \text{ cm}^{-1}$),⁴² its water solubility was determined to be ca. $2 \times 10^{-4} \text{ M}$.

In order to evaluate the possibility of using Zn(II) complexes of calixarene **50** as phosphodiesterase mimics in water, we investigated in more detail the binding of Zn(II) to **50**. In fact, although it had been determined by Molenveld³² that the association constant of the 2,6-bis(aminomethyl)pyridyl groups to Zn(II) in 50% CH₃CN/20 mM HEPES at pH 7.0 is higher than 10^5 M^{-1} , no values were reported for more polar solvent mixtures, such as 35% EtOH/20 mM HEPES.⁴³ In order to investigate if the formation of

the Zn(II) complex is quantitative also in 35% EtOH/20 mM HEPES, a spectrophotometric titration of the ligand **50** (0.1 mM) with Zn(ClO₄)₂ was carried out (Figure 3.3, right). For comparison, the complex formation in 50% CH₃CN/20 mM HEPES was also evaluated (Figure 3.3, left).

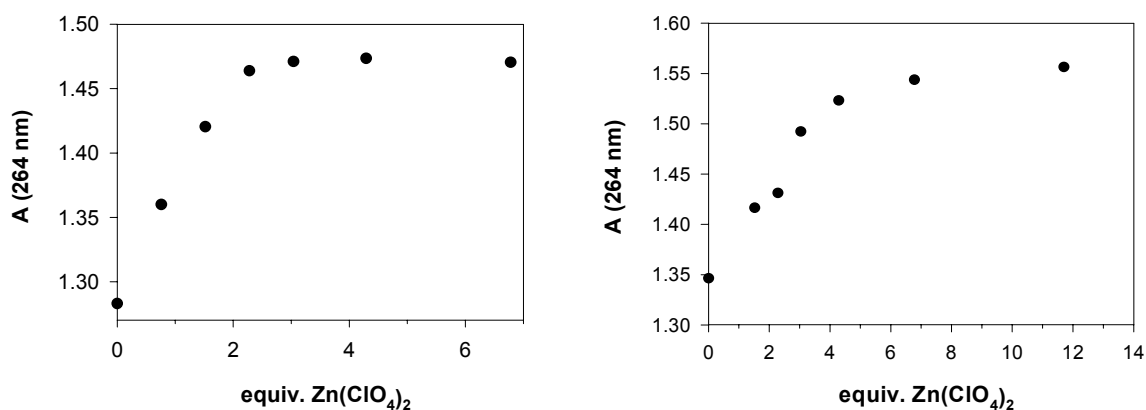


Figure 3.3 Formation of the catalytically active complex **50**-[Zn]₃ ([**50**] = 0.1 mM) in 50% CH₃CN/20 mM HEPES buffer (left) and 35% EtOH/20 mM HEPES buffer (right) pH 7.0, 25 °C.

In 50% CH₃CN the formation of the trinuclear complex is quantitative after addition of 3 equivalents of Zn(ClO₄)₂ (Figure 3.3, left). The same was not observed in 35% EtOH (Figure 3.3, right), where the complete formation of the complex occurred only after addition of 5 equivalents of Zn(ClO₄)₂. While these titrations were carried out at 0.1 mM concentration of ligand, in the catalytic measurements reported in the literature,²⁷ the concentration of **10** was 1 mM and it is reasonable to suppose that under these conditions the formation of the trinuclear calixarene complex is at least 85%. The stability constant of the complex between Zn(II) and 2,6-bis(aminomethyl)pyridine (BAMP) was measured in water (HEPES 20 mM, pH 7.0), to give a value of $K = 1.14 \times 10^3 \text{ M}^{-1}$. This means that at 1 mM concentration of ligand and Zn(II) ion the complexed and uncomplexed species are present approximately in a 1/1 ratio. As a result, this low value of association constant K precludes the use of this chelating group for systems which have to work in water at millimolar concentrations.

3.5 Catalysis

The catalytic activity of the complex **50**-[Zn]₃ was studied in the transesterification of 2-hydroxypropyl-*p*-nitrophenylphosphate (HPNP).⁴⁴ This compound is considered an RNA model because of the presence of a hydroxyl group which can give intramolecular attack on the phosphate, mimicking the action of the OH in the 2'-position on the ribose. The measurements have been carried out both in 50% CH₃CN/20 mM and in

35% EtOH/20 mM HEPES to compare the activity of **50**-[Zn]₃ to that of **10**-[Zn]₃. Moreover, a water percentage higher than 75% could not be used in the reaction medium because of the low binding constant between Zn(II) and pyridine chelating groups. The complexes were generated *in situ* by adding stoichiometric amounts of Zn(ClO₄)₂ to solutions of ligand **50**. The observed pseudo-first-order rate constants K_{obs} are reported in Table 3.2.

Table 3.2 Observed pseudo-first-order rate constants and relative rate accelerations for the transesterification of HPNP catalyzed by Zn(II) complexes at 25 °C, pH 7.0.

Catalyst	k_{obs} (s ⁻¹)	Relative rate acceleration
none ^a	1.9×10^{-8}	1
10 -[Zn] ₃ ^b	6.9×10^{-4}	36,000
50 -[Zn] ₃ ^b	1.1×10^{-4}	5800
10 -[Zn] ₃ ^c	1.5×10^{-4}	7900
50 -[Zn] ₃ ^c	4.0×10^{-5}	2100

^a Measured on a 2.0 mM HPNP solution in 50% CH₃CN/20 mM HEPES, initial rate method.

^b 1 mM, in 50% CH₃CN/20 mM HEPES (see ref. 45)

^c 1 mM, in 35% EtOH/20 mM HEPES.

Error limits = ±5%, rate constants values from full time courses

The catalyst **50**-[Zn]₃ is less active than the analogous **10**-[Zn]₃ without hydroxyl functions at the upper rim. It was demonstrated that **10**-[Zn]₃ catalyzes the transesterification of HPNP by cooperation of at least two of the metallic centers and that the active form of complex possesses one Zn(II) bound hydroxide ion.³² It is reasonable to assume that **50**-[Zn]₃ works with a mechanism analogous to that of **10**-[Zn]₃. The lower activity of **50**-[Zn]₃ compared to **10**-[Zn]₃ can be explained with a partial interference of the hydroxyl groups. They could take part in the coordination of the zinc ion hindering the binding of the substrate or partly preventing the formation of the species with a hydroxide ion at one Zn center. In spite of the improvement in the water solubility of **50**-[Zn]₃ with respect to **10**-[Zn]₃, investigations of its activity in solutions with higher percentage of water were not carried out because of the low binding constant of the 2,6-bis(aminomethyl)pyridine groups with Zn(II) in aqueous solution. For this reason we prepared new calix[4]arenes functionalizing the upper rim with 1,5,9-triazacyclododecane groups, that form very stable complexes with 3d transition metal ions (Chapter 5).

3.6 Conclusions

In this chapter the selective synthesis of tetra- and triformylated tetrahydroxy calixarenes **14** and **15** has been reported. Although the protection of the formyl groups was unsuccessful, they can be useful precursors for the synthesis of calixarenes whose lower rim can be functionalized with very reactive electrophiles.

Lipophilic tetraadamantyl calix[4]arenes **21-23** were prepared and the possibility of dissolving them in water by exploiting the interaction with β -CDs has been investigated by ^1H NMR studies. Only compound **22**, which bears long glycolic spacers could be solubilized up to a concentration of 1×10^{-4} M by hyp- β -CD. This reveals the importance of the hydrophilic character of the tetraethylene glycol chains for the success of water solubilization by this approach. Water soluble *p*-guanidinium di- and tetraadamantyl calix[4]arenes **46-48** have been synthesized and the Ad-CD interaction has been studied in aqueous solution using isothermal titration calorimetry (ITC). These measurements have shown that the 2 or 4 adamantanes present in compounds **46**, **47** and **48** respectively, can be included in the β -CD cavity without interference among binding processes. Intrinsic binding constants are, in fact, in the range $2.9\text{-}5.4 \times 10^4 \text{ M}^{-1}$, which are values typically observed for β -CD/adamantane association. Selective transfer of calixarenes **46-48** onto a β -CD monolayer could be achieved by microcontact printing and dip pen nanolithography creating patterns with sub-100 nm lateral resolution.

Finally, a calix[4]arene (**50**) equipped with three 2,6-bis[(dimethylamino)methyl]pyridine groups and six hydroxyl groups has been synthesized, which is water soluble up to 2×10^{-4} M. However, although ligand **50** is soluble in aqueous solution, the catalytic activity of its Zn^{2+} complex could only be measured in EtOH/water 35% v/v, as in pure water the Zn^{2+} complex is partially dissociated. Spectrophotometric titrations, in fact, revealed that the binding constant between the 2,6-bis(aminomethyl)pyridine group and Zn(II) in water is too low to afford the quantitative formation of the metal complex in a 1 mM aqueous solution of the ligand. The catalytic activity of **50**- $[\text{Zn}]_3$ has been evaluated in the transesterification of the RNA model HPNP, finding kinetic rate constants lower than the ones obtained with the analogous complex **10**- $[\text{Zn}]_3$.

3.7 Experimental part

General Information. All moisture sensitive reactions were carried out under nitrogen atmosphere. Most of the solvents and reagents were obtained from commercial sources and used without further purification. All dry solvents were prepared according to standard procedures and stored over molecular sieves. ^1H NMR and ^{13}C NMR spectra

were recorded on Bruker AC300 and Bruker AMX400 spectrometers. Spectra are reported in ppm downfield from TMS as an internal standard. Mass spectra by electrospray ionization (ESI) and chemical ionization (CI) methods were recorded on a Micromass ZMD and on a Finnigan Mat SSQ710 spectrometer, respectively. FAB-MS spectra were recorded with a Finnigan MAT 90 spectrometer using *m*-NBA as a matrix. MALDI-MS spectra were recorded with a PerSpective Biosystems Voyager-De-RP spectrometer. Analytical TLC was performed using Merck prepared plates (silica gel 60 F-254 on aluminium). Merck silica gel (40-63 μm) was used for flash chromatography. Spectrophotometric measurements were carried out on either a double beam Perkin Elmer Lambda 18 or on a diode array Hewlett Packard 8453 spectrophotometer.

2-(2-(2-(Phenylmethoxy)ethoxy)ethoxy)ethyl-*p*-toluenesulfonate (12)

The alcohol **11**²⁸ (14.6 g, 60.5 mmol) was dissolved in 100 mL of CH_2Cl_2 . *p*-Toluenesulfonyl chloride (11.5 g, 60.5 mmol), Et_3N (9.8 mL, 70 mmol) and DMAP (100 mg) were added and the solution was stirred overnight at room temperature. The mixture was quenched with 100 mL of 1N HCl solution. The organic phase was washed with H_2O (2 x 100 mL), dried over anhydrous Na_2SO_4 , filtered and evaporated under reduced pressure. The residue was purified by column chromatography ($\text{Et}_2\text{O}/\text{Hex}$, 4/1) to give the product **12** as a pale yellow oil. Yield 84%. ^1H NMR (300 MHz; CDCl_3): δ 7.81 (d, 2H, ArH, $J = 8.4$ Hz), 7.36-7.29 (m, 7H, ArH), 4.57 (s, 2H, ArCH₂O), 4.17 (t, 2H, RCH₂OTs, $J = 4.8$ Hz), 3.70 (t, 2H, RCH₂CH₂OTs, $J = 4.8$ Hz), 3.67-3.62 (m, 4H, BnIOCH₂CH₂O), 3.61 (s, 4H, OCH₂CH₂O), 2.45 (s, 3H, ArCH₃). ^{13}C NMR (75 MHz; CDCl_3): δ 143.9, 137.6, 132.1, 129.0, 127.3, 126.9, 126.6, 126.5, 71.9, 69.5, 69.4, 68.6, 68.5, 67.7, 20.4. MS (CI) m/z (%): 395.1 $[\text{M}+\text{H}]^+$ (100).

25,26,27,28-Tetrakis[(2-(2-(2-(phenylmethoxy)ethoxy)ethoxy)ethoxy)]calix[4]arene (13)

Calix[4]arene (0.5 g, 1.18 mmol) was dissolved in dry DMF (30 mL) and NaH (0.198 g, 8.2 mmol) was added. The solution, kept under N_2 atmosphere, was stirred for 10 min and then the benzyl-triethyleneglycol tosylate **12** (3.24 g, 8.2 mmol) was added. The mixture was heated at 75 °C for 1 day and then poured in 100 mL of 1N HCl solution. The aqueous phase was extracted with CH_2Cl_2 (2 x 100 mL). The combined organic phases were washed with water (2 x 150 mL) dried over anhydrous Na_2SO_4 , filtered and the solvent removed under vacuum. The product **13** was obtained as a pale yellow oil after purification by column chromatography ($\text{CH}_2\text{Cl}_2/\text{Et}_2\text{O}$, 4/1). Yield: 54%. ^1H NMR (300 MHz; CDCl_3): δ 7.35-7.28 (m, 20H, ArH), 6.62-5.58 (m, 12H, ArH), 4.55 (s, 8H, OCH₂Ar), 4.49 (d, 4H, ArCH₂Ar ax, $J = 13.4$ Hz), 4.13 (t, 8H, ArOCH₂, $J = 5.6$ Hz), 3.88 (t, 8H, ArOCH₂CH₂, $J = 5.6$ Hz), 3.62-3.59 (m, 32H, CH₂CH₂OCH₂CH₂OCH₂Ar), 3.15 (d, 4H, ArCH₂Ar eq, $J = 13.4$ Hz). ^{13}C NMR (75 MHz; CDCl_3): δ 156.3, 138.3, 134.9, 128.3, 128.1, 127.8, 127.7, 127.5, 122.1, 73.2, 72.9, 70.6, 70.4, 69.4, 30.9. MS (CI) m/z

(%): 1312.5 (100) [M]⁺. Anal. Calcd for C₈₀H₉₆O₁₆ (1313.64): C, 73.14; H, 7.37. Found: C, 73.51; H, 7.49.

5,11,17,23-Tetraformylcalix[4]arene (14)

Calix[4]arene (1.0 g, 2.4 mmol) and HMTA (5.0 g, 36.0 mmol) were dissolved in trifluoroacetic acid (80 mL). The solution was heated at 100 °C for 8 h and then poured into water (200 mL) and stirred for 4 h after the addition of CH₂Cl₂ (150 mL). The organic phase was separated, washed with water (2 x 150 mL) and evaporated under reduced pressure. The product **14** was obtained as white solid after trituration in CH₂Cl₂ (10 mL). TLC eluent: EtOAc/MeOH 9/1. Yield 95%. Mp >340°C. ¹H NMR (300 MHz; DMSO-d₆): δ 9.63 (s, 4H, ArCHO), 8.75 (bs, 4H, ArOH), 7.65 (s, 8H, ArH), 3.95 (bs, 8H, ArCH₂Ar). ¹³C NMR (75 MHz; DMSO-d₆): δ 190.4 (ArCHO), 160.1 (Ar ipso), 130.5 (Ar meta), 129.8 (Ar ortho), 128.1 (Ar para), 31.2 (ArCH₂Ar). MS (CI) *m/z* (%): 537 (100) [M]⁺.

5,11,17-Triformylcalix[4]arene (15)

Procedure A: Tetrahydroxycalix[4]arene (0.3 g, 0.71 mmol) was dissolved in 20 mL of dry chloroform and the solution, kept under N₂, was cooled to -15 °C. After 10 min Cl₂CHOCH₃ (0.2 mL, 2.2 mmol) and SnCl₄ (0.66 mL, 7.1 mmol) were added to the stirred solution. After 1h the reaction mixture was poured in 100 mL of 1N HCl and the solution was stirred for 2 h. After the addition of 100 mL of CH₂Cl₂, the organic phase was separated and washed twice with water, dried over anhydrous Na₂SO₄ and filtered. The solvent was evaporated under reduced pressure and column chromatography (EtOAc/Hex/MeOH 10/2/1) allowed the isolation of triformylcalixarene **15** (15% yield) and 1,2-diformylcalixarene **16** (18% yield).

Procedure B: Formic acid (66 μL, 1.7 mmol) and Pd/C (~ 10 mg) were added to the solution of monobromotriformylcalix[4]arene **18** (0.1 g, 0.17 mmol) in Et₃N (10 mL) in a Schlenk tube. The solution was heated at 50 °C for 3 h and then it was poured in 1N HCl (100 mL) and extracted with CH₂Cl₂ (100 mL). The organic phase was washed twice with water (2 x 100 mL) and evaporated under vacuum. The product was obtained pure by column chromatography (CH₂Cl₂/EtOAc/MeOH 9/2/1). Yield 70%. ¹H NMR (300 MHz; CDCl₃): δ 10.15 (bs, 4H, ArOH), 9.80 (s, 1H, ArCHO), 9.77 (s, 2H, ArCHO), 7.68 (s, 2H, ArH), 7.65 (s, 4H, ArH), 7.14 (d, 2H, ArH, J = 7.6 Hz), 6.80 (t, 1H, ArH, J = 7.6 Hz), 4.40-4.00 (bs, 4H, ArCH₂Ar), 4.00-3.60 (bs, 4H, ArCH₂Ar). ¹³C NMR (75 MHz; CDCl₃): δ 190.3 (ArCHO), 190.2 (ArCHO), 154.2, 154.0, 148.1, 131.5, 131.4, 131.0, 129.6, 129.2, 128.3, 127.8, 127.1, 31.4. MS (CI) *m/z* (%): 509.2 [M+H]⁺ (100). Anal. Calcd for C₃₁H₂₄O₇ (508.53): C, 73.23; H, 4.76. Found: C, 73.51; H, 4.90.

5,11-Diformylcalix[4]arene (16)

It was obtained as a byproduct from the preparation of compound **15** (Procedure B) ^1H NMR (300 MHz; CDCl_3): δ 10.15 (bs, 4H, ArOH), 9.77 (s, 2H, ArCHO), 7.64 (s, 4H, ArH), 7.10 (d, 2H, ArH, $J = 6.3$ Hz), 7.08 (d, 2H, ArH, $J = 6.3$ Hz), 6.76 (t, 2H, ArH, $J = 6.3$ Hz), 4.30-3.90 (bs, 4H, ArCH₂Ar), 3.90-3.50 (bs, 4H, ArCH₂Ar). MS (CI) m/z (%): 480.3 $[\text{M}+\text{H}]^+$ (100).

5-Bromo-11,17,23-triformylcalix[4]arene (18)

To a sample of monobromocalix[4]arene³³ **17** (2.5 g, 4.97 mmol) in a round bottomed flask were added CF_3COOH (200 mL) and HMTA (11.14 g, 79.45 mmol). The solution was heated at 80 °C for 5 h, or till a TLC analysis ($\text{CH}_2\text{Cl}_2/\text{EtOAc}/\text{MeOH}$, 9/2/1) of a sample, quenched in water and extracted in CH_2Cl_2 , revealed the presence of only one main spot ($R_f \sim 0.3$). The reaction mixture was poured into water (300 mL), the solution was stirred for 3 h and filtered. The solid was washed with water (200 mL) to completely remove the acid and dried under vacuum, to give **18** in 92% yield. Mp > 300 °C. ^1H NMR (300 MHz; $\text{DMSO}-d_6$): δ 9.63 (s, 2H, ArCHO), 9.61 (s, 1H, ArCHO), 7.66 (d, 2H, ArH, $J = 2.0$ Hz), 7.64-7.63 (m, 4H, ArH), 7.24 (s, 2H, ArH), 3.89 (bs, 8H, ArCH₂Ar). ^{13}C NMR (75 MHz; $\text{DMSO}-d_6$): δ 190.3 (ArCHO), 190.1 (ArCHO), 162.0, 160.7, 132.2, 130.5, 130.3, 130.2, 130.1, 129.7, 127.7, 127.0, 110.7, 31.6, 30.5. MS (CI) m/z (%): 587.2 $[\text{M}+\text{H}]^+$ (100), 507.3 $[\text{M}-\text{Br}]^+$ (80). Anal. Calcd for $\text{C}_{31}\text{H}_{23}\text{Br}_1\text{O}_7$ (587.42): C, 63.38; H, 3.95. Found: C, 63.52; H, 4.20.

3-(Adamantyl-1-oxy)propyl-*p*-toluenesulfonate (25)

3-(Adamantyl-1-oxy)-propanol **24** (4.8 g, 22.8 mmol) was dissolved in 50 mL of CH_2Cl_2 . *p*-Toluenesulfonyl chloride (4.36 g, 22.8 mmol), Et_3N (3.2 mL, 22.8 mmol) and DMAP (60 mg) were added and the solution was stirred overnight at room temperature. The mixture was quenched with 50 mL of 1N HCl solution. The organic phase was washed with H_2O (2 x 50 mL), dried over anhydrous Na_2SO_4 and evaporated under reduced pressure. The residue was purified by column chromatography (Hex/EtOAc, 16/3) to give product **25** as a colorless oil. Yield 77%. ^1H NMR (300 MHz; CDCl_3): δ 7.79 (d, 2H, ArH, $J = 8.3$ Hz), 7.34 (d, 2H, ArH, $J = 8.3$ Hz), 4.13 (t, 2H, RCH_2OTs , $J = 6$ Hz), 3.41 (t, 2H, $\text{RCH}_2\text{CH}_2\text{OTs}$, $J = 6$ Hz), 2.44 (s, 3H, ArCH₃), 2.1 (bs, 3H, Ad[CH₂CHCH₂]), 1.83 (q, 2H, AdOCH₂CH₂, $J = 6$ Hz), 1.63-1.56 (m, 6H, Ad[CHCH₂C]), 1.60 (d, 6H, Ad[CHCH₂CH], $J = 2.7$ Hz). ^{13}C NMR (75 MHz; CDCl_3): δ 144.5 (Ar para), 133.2 (Ar ipso), 129.7 (Ar meta), 127.9 (Ar ortho), 71.9 (Ad[CH₂CCH₂]), 67.9 (SOCH₂), 55.0 (AdOCH₂), 41.3 (Ad[CCH₂CH]), 36.3 (Ad[CHCH₂CH]), 30.4 (Ad[CH₂CHCH₂]), 29.9 (AdOCH₂CH₂), 21.5 (CH₃). MS (CI) m/z (%): 363.9 (20) $[\text{M}]^+$; 135 (100) $[\text{Ad}]^+$. Anal. Calcd for $\text{C}_{20}\text{H}_{28}\text{O}_4\text{S}_1$ (364.50): C, 65.90; H, 7.77; Found: C, 65.78; H, 7.64.

25,26,27,28-Tetrakis(3-(adamantyl-1-oxy)propoxy)calix[4]arene (21)

To a solution of calix[4]arene (1.0 g, 2.35 mmol) in dry DMF (25 mL) was added NaH (0.34 g, 14.1 mmol) and the mixture was stirred for 10 min before the addition of tosylate **25** (5.2 g, 14.1 mmol). The solution was refluxed overnight under nitrogen atmosphere, and then 1N HCl solution (50 mL) was poured into the solution. The white solid formed was filtered on a Buchner filter and washed with 1N HCl solution (50 mL) and water (100 mL) to completely remove DMF. The solid was kept on the Buchner filter for 1h, and then dissolved in a small amount of methanol and crystallized with acetone, obtaining **21** as a white solid. (Eluent for TLC: Hex/EtOAc, 9/1). Yield: 78%. Mp: 151.8 °C. ¹H NMR (300 MHz; CDCl₃): δ 6.60-6.53 (m, 12H, ArH), 4.44 (d, 4H, ArCH₂Ar ax, J = 13.4 Hz), 3.99 (t, 8H, ArOCH₂R, J = 7 Hz), 3.53 (t, 8H, AdOCH₂R, J = 10.1 Hz), 3.15 (d, 8H, ArCH₂Ar eq, J = 13.4 Hz), 2.19-2.12 (m, 20H, ArOCH₂CH₂R+ Ad[CH₂CHCH₂]), 1.71 (d, 6H, Ad[CHCH₂CH], J = 2.8 Hz), 1.60-1.50 (m, 6H, Ad[CHCH₂C]). ¹³C NMR (75 MHz; CDCl₃): δ 156.6 (Ar ipso), 135.0 (Ar para), 128.0 (Ar meta), 121.8 (Ar ortho), 72.6 (ArOCH₂), 71.6 (Ad[CH₂CCH₂]), 57.1 (AdOCH₂), 41.6 (Ad[CCH₂CH]), 36.6 (ArCH₂Ar), 36.4 (Ad[CHCH₂CH]), 31.1 (AdOCH₂CH₂), 30.5 (Ad[CH₂CHCH₂]). MS (CI) *m/z* (%): 1194.4 (50) [M(¹³C)+H]⁺; 1193.5 (100) [M+H]⁺. Anal. Calcd for C₈₀H₁₀₄O₈ (1193.70): C, 80.49; H, 8.78. Found: C, 80.60; H, 8.90.

(2-(2-(2-(2-(Adamantyl-1-oxy)ethoxy)ethoxy)ethoxy)ethoxy)ethanol (26)

A solution of 1-bromoadamantane (10 g, 46.5 mmol), triethylamine (1.96 mL, 139.5 mmol) and tetraethyleneglycol (200 mL) was kept at 110°C for 24 h. The mixture was allowed to cool to room temperature, 200 mL of CH₂Cl₂ were added and the solution was washed with 1N HCl (3 x 200 mL) and water (2 x 200 mL). The organic layer was dried over anhydrous Na₂SO₄ and the solvent evaporated under reduced pressure to give **26** as a light yellow oil. Yield 83%. ¹H NMR (300 MHz; CDCl₃): δ 3.71 (t, 2H, RCH₂OH, J = 4.9 Hz), 3.66-3.65 (m, 8H, ROCH₂CH₂OH), 3.61-3.56 (m, 6H, AdO(CH₂CH₂O)₃), 2.13 (bs, 3H, Ad[CH₂CHCH₂]), 1.74 (d, 6H, Ad[CHCH₂CH], J = 2.9 Hz), 1.61 (m, 6H, Ad[CHCH₂C]). ¹³C NMR (75 MHz; CDCl₃): δ 72.6 (d, RCH₂OH), 72.3 (s, Ad[CH₂CCH₂]), 71.1, 70.5, 70.4, 70.1, 61.5, 59.1 (t, AdO(CH₂CH₂O)₃CH₂), 41.3 (t, Ad[CCH₂CH]), 36.3 (t, Ad[CHCH₂CH]), 30.4 (d, Ad[CH₂CHCH₂]). MS (CI) *m/z* (%): 329.1 (100) [M+H]⁺; 327.2 (50) [M-H]⁺. Anal. Calcd for C₁₈H₃₂O₅ (328.45): C, 65.82; H, 9.82. Found: C, 65.79; H, 9.86.

2-(2-(2-(2-(Adamantyl-1-oxy)ethoxy)ethoxy)ethoxy)ethyl-*p*-toluenesulfonate (27)

Compound **26** (7 g, 21.3 mmol) was dissolved in 80 mL of CH₂Cl₂. *p*-Toluenesulfonyl chloride (4.06 g, 21.3 mmol), Et₃N (2.95 mL, 21.3 mmol) and DMAP (100 mg) were added and the solution was stirred overnight at room temperature. The mixture was

quenched with 80 mL of 1N HCl solution. The organic phase was washed with H₂O (2 x 80 mL), dried over anhydrous Na₂SO₄ and evaporated under reduced pressure. The residue was purified by column chromatography (Hex/EtOAc, 1/1) to give product **27** as a pale yellow oil. Yield 90%; ¹H NMR (300 MHz; CDCl₃): δ 7.79 (dd, 2H, ArH, J_o = 7.9 Hz, J_m = 1.0 Hz), 7.34 (dd, 2H, ArH, J_o = 7.9 Hz, J_m = 1 Hz), 4.16 (t, 2H, RCH₂OTs, J = 4.7 Hz), 3.69 (t, 2H, RCH₂CH₂OTs, J = 4.7 Hz), 3.63-3.56 (m, 12H, AdO(CH₂CH₂O)₃), 2.44 (s, 3H, ArCH₃), 2.13 (bs, 3H, Ad[CH₂CHCH₂]), 1.74 (d, 6H, Ad[CHCH₂CH], J = 2.8 Hz), 1.61 (m, 6H, Ad[CHCH₂C]). ¹³C NMR (75 MHz; CDCl₃): δ 144.7 (s, Ar[C]S), 133.0 (s, Ar[C]CH₃), 129.7 (d, Ar[C]H), 127.9 (d, Ar[C]H), 72.2 (s, Ad[CH₂CCH₂]), 71.2, 70.7, 70.6, 70.5, 69.2, 68.6, 59.2 (t, AdO(CH₂CH₂O)₄), 41.4 (t, Ad[CCH₂CH]), 36.4 (t, Ad[CHCH₂CH]), 30.5 (d, Ad[CH₂CHCH₂]), 21.6 (q, ArCH₃). MS (CI) *m/z* (%): 483.1 (100) [M+H]⁺. Anal. Calcd for C₂₅H₃₈O₇S₁ (482.63): C, 62.22; H, 7.94. Found: C, 62.17; H, 7.99.

25,26,27,28-Tetrakis[(2-(2-(2-(2-(adamantyl-1-oxy)ethoxy)ethoxy)ethoxy)ethoxy)]calix[4]arene (22)

Tetrahydroxy calix[4]arene (0.57 g, 1.35 mmol) was dissolved in dry DMF (50 mL) and NaH (0.194 g, 8.1 mmol) was added. The solution, kept under N₂ atmosphere, was stirred for 10 min and then adamantyl-tetraethyleneglycol tosylate **27** (4.56 g, 7.0 mmol) was added. The mixture was heated at 75 °C for 1 day and then poured in 150 mL of 1N HCl solution. The aqueous phase was extracted with CH₂Cl₂ (2 x 100 mL). The combined organic phases were washed with water (2 x 150 mL) dried over anhydrous Na₂SO₄, filtered and the solvent removed under vacuum. The residue was purified by column chromatography: a first column (Et₂O/EtOAc, 1/1) was necessary to purify the product (R_f 0.3) from the partially substituted calixarenes (R_f ~ 0.4), a second one (Et₂O/MeOH, 9.6/0.4) to remove the product of decomposition of the alkylating chain revealed by spraying the TLC with H₂SO₄ and heating. Compound **17** was obtained as a colorless oil. Yield: 51%. ¹H NMR (300 MHz; CDCl₃): δ 6.61-6.51 (m, 12H, ArH), 4.46 (d, 4H, ArCH₂Ar ax, J = 13.4 Hz), 4.10 (t, 8H, ArOCH₂, J = 5.6 Hz), 3.85 (t, 8H, ArOCH₂CH₂, J = 5.6 Hz), 3.62-3.55 (m, 48H, Ad(OCH₂CH₂)₃), 3.11 (d, 4H, ArCH₂Ar eq, J = 13.4 Hz), 2.12 (bs, 12H, Ad[CH₂CHCH₂]), 1.73 (d, 24H, Ad[CHCH₂C], J = 2.9 Hz), 1.65-1.55 (m, 24H, Ad[CHCH₂CH]). ¹³C NMR (75 MHz; CDCl₃): δ 156.2 (Ar ipso), 134.9 (Ar meta), 128.1 (Ar para), 122.1 (Ar ortho), 72.8 (ArOCH₂), 72.1 (Ad[CH₂CCH₂]), 71.2, 70.6, 70.5, 70.4 (ArOCH₂(CH₂OCH₂)₃R), 59.2 (AdOCH₂), 42.4 (Ad[CCH₂CH]), 36.4 (Ad[CHCH₂CH]), 30.9 (ArCH₂Ar), 30.5 (Ad[CH₂CHCH₂]). MS (CI) *m/z* (%): 1667.5 (100) [M+1+H]⁺; 1666.3 (85) [M+H]⁺; 1665.1 (75) [M]⁺; 1355 (100) [M-Ad(OCH₂CH₂)₄]⁺. Anal. Calcd for C₁₀₀H₁₄₄O₂₀ (1666.24): C, 72.08; H, 8.71. Found: C, 72.21; H, 8.80.

25,26,27,28-Tetrakis(4-N-phthalimidobutoxy)calix[4]arene (28)

NaH (0.34 g, 14.1 mmol) was added to a solution of tetrahydroxy calix[4]arene (1.0 g, 2.35 mmol) in dry DMF (25 mL), kept under nitrogen. The mixture was stirred for 10 min before the addition of N-(4-bromobutyl)phthalimide (5.3 g, 18.8 mmol). The solution was stirred for 4 days at room temperature and then it was poured in 1 N HCl solution (100 mL) and extracted with CH₂Cl₂ (3 x 70 ml). The combined organic phases were washed with water (2 x 100 mL) and then evaporated under reduced pressure. The product **28** was obtained as white solid after purification by column chromatography (Hex/EtOAc, 1/1). Yield: 56%. ¹H NMR (300 MHz; CDCl₃): δ 7.75-7.71 (m, 8H, Ar-Pht), 7.62-7.60 (m, 8H, Ar-Pht), 6.56-6.53 (m, 12H, ArH), 4.39 (d, 4H, ArCH₂Ar ax, J = 13.4 Hz), 3.93 (t, 8H, ArOCH₂, J = 7.3 Hz), 3.74 (t, CH₂NPht, J = 6 Hz), 3.12 (d, 4H, ArCH₂Ar eq, J = 13.4 Hz), 1.98 (q, 8H, ArOCH₂CH₂, J = 7.3 Hz), 1.77 (q, 8H, CH₂CH₂NPht, J = 6 Hz). ¹³C NMR (75 MHz; CDCl₃): δ 168.1 (C=O), 156.3 (Ar ipso), 134.9 (Ar ortho), 133.5 (Ar-Pht), 132.2 (Ar-Pht), 128.1 (Ar meta), 122.9 (Ar-Pht), 121.92 (Ar para), 74.3 (ArOCH₂), 37.9 (CH₂NPht), 31.0 (ArCH₂Ar), 27.6 (ArOCH₂CH₂), 25.3 (CH₂CH₂NPht). MS (CI) *m/z* (%): 1229.5 (50) [M+H]⁺; 1228.5 (100) [M]⁺. Anal. Calcd for C₇₆H₆₈O₁₂N₄ (1229.40): C, 74.25; H, 5.57; N, 4.56. Found: C, 74.13; H, 5.48; N, 4.45.

25,26,27,28-Tetrakis-(4-aminobutoxy)calix[4]arene (29)

Hydrazine monohydrate (12 mL, 364 mmol) was added to a solution of calix[4]arene **28** (1.61 g, 1.31 mmol) in abs. EtOH (50 mL) and the reaction mixture was refluxed for 15 h. The solvent was then removed under reduced pressure, the crude taken up in CH₂Cl₂ (150 mL) and the organic phase was washed with saturated aqueous NaHCO₃ solution (2 x 100 mL). The organic layer was dried over anhydrous Na₂SO₄, filtered and evaporated under vacuum giving compound **29** in 85% yield. ¹H NMR (300 MHz; CDCl₃): δ 6.60-6.56 (m, 12 H, ArH), 4.40 (d, 4H, ArCH₂Ar ax, J = 13.3 Hz), 3.90 (t, 8H, ArOCH₂, J = 7.5 Hz), 3.15 (d, 4H, ArCH₂Ar eq, J = 13.3 Hz), 2.76 (t, 8H, NH₂CH₂, J = 7.1 Hz), 1.91 (q, 8H, ArOCH₂CH₂, J = 7.5 Hz), 1.54 (q, 8H, NH₂CH₂CH₂, J = 7.1 Hz). ¹³C NMR (75 MHz; CDCl₃): δ 156.3 (Ar ipso), 134.9 (Ar ortho), 128.1 (Ar meta), 122.0 (Ar para), 74.6 (ArOCH₂), 42.1 (CH₂NH₂), 31.0 (ArCH₂Ar), 30.2 (ArOCH₂CH₂), 27.6 (CH₂CH₂NH₂). MS (CI) *m/z* (%): 709.5 (70) [M+H]⁺; 708.5 (55) [M]⁺; 637 (100) [M-CHCH₂CH₂CH₂NH₂]⁺. Anal. Calcd for C₄₄H₆₀O₄N₄ (708.99): C, 74.54; H, 8.53; N, 7.90. Found: C, 74.69; H, 8.66; N, 7.80.

25,26,27,28-Tetrakis[4-(adamantly-1-carboxylamino)butoxy]calix[4]arene (23)

To a round bottomed flask containing the 1-adamantylcarboxylic acid chloride³⁵ (0.58 g, 2.92 mmol) in dry CH₂Cl₂ (30 mL), was added a solution of tetraamino

calix[4]arene **29** (0.41 g, 0.578 mmol) in CH_2Cl_2 (20 mL) and Et_3N (0.44 mL, 3.18 mmol). The mixture was stirred at room temperature under N_2 for 2 days, or till a TLC analysis (Hex/EtOAc, 1/1) of a sample (quenched in water and extracted in CH_2Cl_2) revealed the presence of only one main spot ($R_f \sim 0.7$). The reaction was quenched pouring it into 1N HCl solution (100 mL). The organic phase was separated and the aqueous layer was extracted again with dichloromethane (100 mL). The combined organic layers were washed with water (2 x 100 mL), dried over anhydrous Na_2SO_4 , filtered and evaporated under vacuum to give **23** as white solid. This solid was triturated in methanol and filtered. Yield: 84%. Mp: 235.5 °C. ^1H NMR (300 MHz; CDCl_3): δ 6.62-6.56 (m, 12 H, ArH), 6.39 (t, 4H, NH, $J = 5.7$ Hz), 4.35 (d, 4H, ArCH₂Ar ax, $J = 13.2$ Hz), 3.84 (t, 8H, ArOCH₂, $J = 7.2$ Hz), 3.30 (dt, 8H, CH₂N, $J = 7.2$ Hz), 3.13 (d, 4H, ArCH₂Ar eq, $J = 13.2$ Hz), 2.03 (bs, 12H, Ad[CH₂CHCH₂]), 1.87 (d, 24H, Ad[CHCH₂CH], $J = 2.7$ Hz), 1.95-1.86 (m, 8H, ArOCH₂CH₂), 1.76-1.60 (m, 24H, Ad[CHCH₂C] + 8H, CH₂CH₂N). ^{13}C NMR (75 MHz; CDCl_3): δ 178.2 (C=O), 156.1 (Ar ipso), 134.9 (Ar ortho), 128.1 (Ar meta), 122.1 (Ar para), 74.6 (ArOCH₂), 40.5 (Ad[CH₂CCH₂]), 39.6 (CH₂NH), 39.2 (Ad[CCH₂CH]), 36.5 (Ad[CHCH₂CH]), 30.8 (ArCH₂Ar), 28.1 (Ad[CH₂CHCH₂]), 27.6 (ArOCH₂CH₂), 26.7 (CH₂CH₂NH). MS (CI) m/z (%): 1357.9 (100) [M+H]⁺; 1137 (50) [M-AdCONHCH₂CH₂CH₃]⁺; 1124 (90) [M-AdONHCH₂CH₂CH₂CH₂]⁺. Anal. Calcd for $\text{C}_{88}\text{H}_{116}\text{N}_4\text{O}_8$ (1357.92): C, 77.84; H, 8.61; N, 4.13. Found: C, 77.93; H, 8.71; N, 4.06.

2-(2-(Adamantyl-1-oxy)ethoxy)ethanol (**30**)

Compound **30** was obtained by the same procedure used for **26** from the diethyleneglycol. Yield 95%. ^1H NMR (300 MHz; CDCl_3): δ 3.74-3.58 (m, 8H, AdCH₂CH₂OCH₂CH₂OH), 2.16 (bs, 3H, Ad[CH₂CHCH₂]), 1.77 (d, 6H, Ad[CHCH₂CH], $J = 3.0$ Hz), 1.62 (m, 6H, Ad[CHCH₂C]). ^{13}C NMR (75 MHz; CDCl_3): δ 72.6, 71.1, 61.9, 59.5, 41.3 (Ad[CCH₂CH]), 36.3 (Ad[CHCH₂CH]), 30.4 (Ad[CH₂CHCH₂]). MS (CI) m/z (%): 241.2 (50) [M+H]⁺, 239.1 (100) [M-H]⁺. Anal. Calcd for $\text{C}_{14}\text{H}_{24}\text{O}_3$ (240.34): C, 69.96; H, 10.07. Found: C, 70.14; H, 10.23.

2-(2-(Adamantyl-1-oxy)ethoxy)ethyl-*p*-toluenesulfonate (**31**)

Compound **31** was obtained by the same procedure used for **27** from the adamantane-diethyleneglycol **30**. The residue was purified by column chromatography (Hex/EtOAc, 4/1) obtaining a colourless oil. Yield 87%; ^1H NMR (300 MHz; CDCl_3): δ 7.78 (dd, 2H, ArH, $J^3 = 8.4$ Hz, $J^4 = 1.9$ Hz), 7.32 (dd, 2H, ArH, $J = 8.4$ Hz, $J = 1.9$ Hz), 4.16-4.12 (m, 2H, RCH₂OTs), 3.70-3.66 (m, 2H, RCH₂CH₂OTs), 3.52-3.46 (m, 8H, AdOCH₂CH₂O), 2.42 (s, 3H, ArCH₃), 2.12 (bs, 3H, Ad[CH₂CHCH₂]), 1.69 (d, 6H, Ad[CHCH₂CH], $J = 2.5$ Hz), 1.65-1.54 (m, 6H, Ad[CHCH₂C]). ^{13}C NMR (75 MHz; CDCl_3): δ 144.6 (Ar[C]S), 133.1 (Ar[C]CH₃), 129.7 (Ar[C]H), 127.9 (Ar[C]H), 72.2, 71.3, 69.2, 68.6, (AdOCH₂CH₂OCH₂CH₂OTs + Ad[CH₂CCH₂]), 59.3 (CH₂OTs), 41.4 (Ad[CCH₂CH]), 36.1

(Ad[CHCH₂CH]), 30.4 (Ad[CH₂CHCH₂]), 21.5 (ArCH₃). MS (CI) *m/z* (%): 393.1 (100) [M-H]⁺. Anal. Calcd for C₂₁H₃₀O₅S₁ (394.53): C, 63.93; H, 7.67. Found: C, 63.74; H, 7.88.

25,27-Bis(2-ethoxyethoxy)-26,28-bis(2-(2-(2-(2-(adamantyl-1-oxy)ethoxy)ethoxy)ethoxy)ethoxy)-*p*-tert-butylcalix[4]arene (35)

A sample of calix[4]arene **32** (2.644 g, 3.33 mmol) was dissolved in 75 mL of dry DMF and NaH (0.4 g, 10 mmol) was added. The solution, kept under N₂ atmosphere, was stirred for 10 min before the addition of tosylate **27** (4.823 g, 10 mmol). The mixture was heated at 75°C for 2 days and then poured in 150 mL of 1N HCl solution. The aqueous phase was extracted with CH₂Cl₂ (2 x 100 mL). The combined organic phases were washed with water (2 x 100 mL), dried over anhydrous Na₂SO₄, filtered and the solvent removed under vacuum. The residue was purified by column chromatography (Hex/Et₂O/EtOAc, 1/1/1) to give **35** as a colorless oil. Yield: 90%; ¹H NMR (300 MHz; CDCl₃): δ 6.78 (s, 4H, ArH), 6.74 (s, 4H, ArH), 4.42 (d, 4H, ArCH₂Ar ax, J = 12.5 Hz), 4.10 (t, 4H, ArOCH₂, J = 5.7 Hz), 4.09 (t, 4H, ArOCH₂, J = 5.9 Hz), 3.94 (t, 4H, ArOCH₂CH₂, J = 5.7 Hz), 3.90 (t, 4H, ArOCH₂CH₂, J = 5.9 Hz), 3.68-3.56 (m, 28H, AdO(CH₂CH₂O)₃ + CH₃CH₂OR), 3.09 (d, 4H, ArCH₂Ar eq, J = 12.5 Hz), 2.13 (bs, 6H, Ad[CH₂CHCH₂]), 1.74 (d, 12H, Ad[CHCH₂C], J = 2.7 Hz), 1.60 (m, 12H, Ad[CHCH₂CH]), 1.22 (t, 6H, CH₃R, J = 6.9 Hz), 1.08 (s, 18H, ArC(CH₃)₃), 1.05 (s, 18H, ArC(CH₃)₃). ¹³C NMR (75 MHz; CDCl₃): δ 153.4 (s, Ar ipso), 153.2 (s, Ar ipso), 144.5 (s, Ar para), 144.4 (s, Ar para), 133.8 (s, Ar ortho), 133.6 (s, Ar ortho), 124.9 (d, Ar meta), 124.9 (d, Ar meta), 73.0 (t, ArOCH₂), 72.9 (t, ArOCH₂), 72.1 (s, Ad[CH₂CCH₂]), 71.2, 70.61, 70.55, 70.4, 70.3, 69.6, 66.3 (t, AdOCH₂CH₂O(CH₂CH₂O)₂CH₂ + CH₃CH₂OCH₂), 59.2 (t, AdOCH₂), 41.4 (t, Ad[CCH₂CH]), 36.4 (t, Ad[CHCH₂CH]), 33.7 (s, ArC(CH₃)₃), 31.4 (q, ArC(CH₃)₃), 31.0 (t, ArCH₂Ar), 30.5 (t, Ad[CH₂CHCH₂]), 15.4 (q, RCH₃). MS (ESI+) *m/z* (%): 1435.7 (45) [M+Na]⁺; 745.4 (90) [M+2K]²⁺; 737.2 (100) [M+Na+K]²⁺. Anal. Calcd for C₈₈H₁₃₂O₁₄ (1414.02): C, 74.75; H, 9.41. Found: C, 74.71; H, 9.46.

25,27-Bis(2-ethoxyethoxy)-26,28-bis(2-(2-(adamantyl-1-oxy)ethoxy)ethoxy)-*p*-tert-butyl-calix[4]arene (34)

Compound **34** was obtained by the same procedure used for **35** using the tosylate compound **31** as alkylating chain. The residue was purified by column chromatography (Hex/EtOAc, 8.5/1.5) obtaining a white solid. Yield 83%. Mp = 173-174 °C. ¹H NMR (300 MHz; CDCl₃): δ 6.80 (s, 4H, ArH), 6.73 (s, 4H, ArH), 4.45 (d, 4H, ArCH₂Ar ax, J = 12.6 Hz), 4.11 (t, 4H, ArOCH₂, J = 6.2 Hz), 4.10 (t, 4H, ArOCH₂, J = 5.5 Hz), 3.95 (t, 4H, ArOCH₂CH₂, J = 6.2 Hz), 3.92 (t, 4H, ArOCH₂CH₂, J = 5.5 Hz), 3.63-3.55 (m, 12H, AdOCH₂CH₂O + CH₃CH₂OR), 3.10 (d, 4H, ArCH₂Ar eq, J = 12.6 Hz), 2.13 (bs, 6H, Ad[CH₂CHCH₂]), 1.74 (d, 12H, Ad[CHCH₂C], J = 2.7 Hz), 1.63-1.59 (m, 12H, Ad[CHCH₂CH]), 1.24 (t, 6H, CH₃R, J = 6.9 Hz), 1.09 (s, 18H, ArC(CH₃)₃), 1.05 (s, 18H,

ArC(CH₃)₃). ¹³C NMR (75 MHz; CDCl₃): δ 153.4 (Ar ipso), 153.2 (Ar ipso), 144.4 (Ar para), 144.3 (Ar para), 133.9 (Ar ortho), 133.6 (Ar ortho), 124.9 (Ar meta), 124.8 (Ar meta), 73.0 (ArOCH₂), 72.0 (Ad[CH₂CCH₂]), 71.0, 70.3, 69.6, 66.3 (AdOCH₂CH₂OCH₂ + CH₃CH₂OCH₂), 59.3 (AdOCH₂), 41.5 (Ad[CCH₂CH]), 36.4 (Ad[CHCH₂CH]), 33.74 (ArC(CH₃)₃), 33.70 (ArC(CH₃)₃), 31.4 (ArC(CH₃)₃), 31.3 (ArC(CH₃)₃), 31.0 (ArCH₂Ar), 30.5 (Ad[CH₂CHCH₂]), 15.4 (RCH₃). MS (CI) *m/z* (%): 1236.1 (100) [M+H]⁺. Anal. Calcd for C₈₀H₁₁₄O₁₀ (1235.79): C, 77.76; H, 9.30. Found: C, 77.52; H, 9.51.

25,26,27,28-Tetrakis(2-(2-(2-(2-(adamantyl-1-oxy)ethoxy)ethoxy)ethoxy)ethoxy)-*p*-tert-butylcalix[4]arene (36)

Compound **36** was obtained by the same procedure used for **35** starting from *p*-tert-butyl-calix[4]arene, using a 1.75 fold excess of adamantyl-tetraethyleneglycol tosylate **27** and 1.5 fold excess of NaH for each phenolic group. The reaction time was 3 days. The residue was purified by column chromatography: a first column (Et₂O/EtOAc, 1/1) was necessary to purify the product (R_f 0.2) from the partially substituted calixarenes (R_f ~ 0.3), a second one (Et₂O/MeOH, 15/0.4) to remove the byproducts of the alkylating chain revealed by spraying with H₂SO₄ and heating. Compound **36** was obtained as a pale yellow oil. Yield: 23%. ¹H NMR (300 MHz; CDCl₃): δ 6.75 (s, 8H, ArH), 4.42 (d, 4H, ArCH₂Ar ax, J = 12.5 Hz), 4.10 (t, 8H, ArOCH₂), 3.93 (t, 8H, ArOCH₂CH₂), 3.74-3.57 (m, 48H, AdO(CH₂CH₂O)₃), 3.09 (d, 4H, ArCH₂Ar eq, J = 12.5 Hz), 2.14 (bs, 12H, Ad[CH₂CHCH₂]), 1.74 (d, 24H, Ad[CHCH₂C] J = 2.4 Hz), 1.61 (m, 24H, Ad[CHCH₂CH]), 1.07 (s, 36H, ArC(CH₃)₃). ¹³C NMR (75 MHz; CDCl₃): δ 153.3 (s, Ar ipso), 144.5 (s, Ar para), 133.7 (s, Ar ortho), 124.9 (d, Ar meta), 72.8 (t, ArOCH₂), 72.2 (s, Ad[CH₂CCH₂]), 71.3, 70.64, 70.59, 70.4, 70.3, (t, ArOCH₂(CH₂OCH₂)₃R), 59.2 (t, AdOCH₂), 41.5 (t, Ad[CCH₂CH]), 36.5 (t, Ad[CHCH₂CH]), 33.8 (s, ArC(CH₃)₃), 31.4 (q, ArC(CH₃)₃), 31.0 (t, ArCH₂Ar), 30.5 (d, Ad[CH₂CHCH₂]). MS (MALDI-TOF) *m/z* (%): 1914.5 (100) [M+1+Na]⁺, 1913.5 (85) [M+Na]⁺. Anal. Calcd. for C₁₁₆H₁₇₆O₂₀ (1890.67): C, 73.69; H, 9.38. Found: C, 73.81; H, 9.44.

5,11,17,23-Tetranitro-25,27-bis(2-ethoxyethoxy)-26,28-bis(2-(2-(2-(2-(adamantyl-1-oxy)ethoxy)ethoxy)ethoxy)ethoxy)calix[4]arene (38)

Calix[4]arene **35** (0.5 g, 0.354 mmol) was dissolved in 5 mL of dry CH₂Cl₂, the solution was kept under N₂ and cooled to 0°C. Then glacial CH₃COOH (3.24 mL, 56.58 mmol) and HNO₃ 100% (1.15 mL, 28.29 mmol) were added. The solution was stirred for 1.5 h, or till a TLC (EtOAc) analysis of a sample (quenched in water and extracted in CH₂Cl₂) indicated that the calix[4]arene starting material had disappeared. The reaction mixture was slowly poured in 80 mL of a saturated aqueous solution of NaHCO₃ and extracted with CH₂Cl₂. The organic phase was washed with water (2 x 80 mL), dried over anhydrous Na₂SO₄, filtered and evaporated under reduced pressure. The residue was purified by column chromatography (EtOAc) to give **38** as a pale yellow oil. Yield:

65%; ^1H NMR (300 MHz; CDCl_3): δ 7.63 (s, 4H, ArH), 7.52 (s, 4H, ArH), 4.66 (d, 4H, ArCH_2Ar ax, $J = 14.0$ Hz), 4.26 (t, 4H, ArOCH_2 , $J = 4.2$ Hz), 4.20 (t, 4H, ArOCH_2 , $J = 4.3$ Hz), 3.82 (t, 4H, $\text{ArOCH}_2\text{CH}_2$, $J = 4.2$ Hz), 3.75 (t, 4H, $\text{ArOCH}_2\text{CH}_2$, $J = 4.3$ Hz), 3.63-3.53 (m, 24H, $\text{AdO}(\text{CH}_2\text{CH}_2\text{O})_3$), 3.48 (q, 4H, $\text{CH}_3\text{CH}_2\text{OR}$, $J = 6.9$ Hz), 3.36 (d, 4H, ArCH_2Ar eq, $J = 14.0$ Hz), 2.12 (bs, 6H, $\text{Ad}[\text{CH}_2\text{CHCH}_2]$), 1.71 (d, 12H, $\text{Ad}[\text{CHCH}_2\text{C}]$, $J = 2.7$ Hz), 1.62 (m, 12H, $\text{Ad}[\text{CHCH}_2\text{CH}]$), 1.16 (t, 6H, $\text{CH}_3\text{CH}_2\text{OR}$, $J = 6.9$ Hz). ^{13}C NMR (75 MHz; CDCl_3): δ 161.7 (s, Ar ipso), 161.4 (s, Ar ipso), 142.9 (s, Ar para), 135.7 (s, Ar ortho), 135.4 (s, Ar ortho), 123.9 (d, Ar meta), 123.8 (d, Ar meta), 74.4 (t, ArOCH_2), 74.2 (t, ArOCH_2), 71.3 (s, $\text{Ad}[\text{CH}_2\text{CCH}_2]$), 70.6, 70.5, 70.4, 70.3, 69.4, 66.4 (t, $\text{AdOCH}_2\text{CH}_2\text{O}(\text{CH}_2\text{CH}_2\text{O})_2\text{CH}_2 + \text{CH}_3\text{CH}_2\text{OCH}_2$), 59.2 (t, AdOCH_2), 41.4 (t, $\text{Ad}[\text{CCH}_2\text{CH}]$), 36.4 (t, $\text{Ad}[\text{CHCH}_2\text{CH}]$), 31.0 (t, ArCH_2Ar), 30.4 (d, $\text{Ad}[\text{CH}_2\text{CHCH}_2]$), 15.2 (q, RCH_3). MS (ESI+) m/z (%): 1391.5 (100) $[\text{M}+\text{Na}]^+$; 707.6 (85) $[\text{M}+2\text{Na}]^{2+}$. Anal. Calcd for $\text{C}_{72}\text{H}_{96}\text{O}_{22}\text{N}_4$ (1369.57): C, 63.14; H, 7.07; N, 4.09. Found: C, 63.07; H, 7.14; N, 4.14.

5,11,17,23-Tetranitro-25,27-bis(2-ethoxyethoxy)-26,28-bis(2-(2-(adamantyl-1-oxy)ethoxy)ethoxy)calix[4]arene (37)

Compound **37** was obtained by the same procedure used for **38** from diadamantyl calix[4]arene **34**. Reaction time 4 h. The residue was purified by column chromatography (EtOAc/Hex, 7/3) obtaining a white solid. Yield 30%. Mp = 249.2 °C. ^1H NMR (300 MHz; CDCl_3): δ 7.60 (s, 4H, ArH), 7.53 (s, 4H, ArH), 4.68 (d, 4H, ArCH_2Ar ax, $J = 14.1$ Hz), 4.24 (t, 4H, ArOCH_2 , $J = 4.9$ Hz), 4.22 (t, 4H, ArOCH_2 , $J = 4.9$ Hz), 3.83 (t, 4H, $\text{ArOCH}_2\text{CH}_2$, $J = 4.9$ Hz), 3.76 (t, 4H, $\text{ArOCH}_2\text{CH}_2$, $J = 4.9$ Hz), 3.54-3.45 (m, 12H, $\text{AdOCH}_2\text{CH}_2\text{O} + \text{CH}_3\text{CH}_2\text{OR}$), 3.36 (d, 4H, ArCH_2Ar eq, $J = 14.2$ Hz), 2.11 (bs, 6H, $\text{Ad}[\text{CH}_2\text{CHCH}_2]$), 1.66 (d, 12H, $\text{Ad}[\text{CHCH}_2\text{C}]$, $J = 2.7$ Hz), 1.65-1.52 (m, 12H, $\text{Ad}[\text{CHCH}_2\text{CH}]$), 1.16 (t, 6H, $\text{CH}_3\text{CH}_2\text{OR}$, $J = 7.0$ Hz). ^{13}C NMR (75 MHz; CDCl_3): δ 161.8 (Ar ipso), 161.5 (Ar ipso), 142.9 (Ar para), 142.8 (Ar para), 135.6 (Ar ortho), 135.5 (Ar ortho), 123.8 (Ar meta), 123.7 (Ar meta), 74.4 (ArOCH_2), 74.3 (ArOCH_2), 72.1 ($\text{Ad}[\text{CH}_2\text{CCH}_2]$), 71.2, 70.3, 69.4, 66.4 ($\text{AdOCH}_2\text{CH}_2\text{OCH}_2 + \text{CH}_3\text{CH}_2\text{OCH}_2$), 59.2 (AdOCH_2), 41.5 ($\text{Ad}[\text{CCH}_2\text{CH}]$), 36.3 ($\text{Ad}[\text{CHCH}_2\text{CH}]$), 31.1 (ArCH_2Ar), 30.4 ($\text{Ad}[\text{CH}_2\text{CHCH}_2]$), 15.2 (RCH_3). MS (CI) m/z (%): 1193.5 (100) $[\text{M}+\text{H}]^+$. Anal. Calcd for $\text{C}_{64}\text{H}_{80}\text{N}_4\text{O}_{18}$ (1193.36): C, 64.41; H, 6.76; N, 4.69. Found: C, 64.27; H, 6.62; N, 4.57.

5,11,17,23-Tetranitro-25,26,27,28-tetrakis(2-(2-(2-(2-(adamantyl-1-oxy)ethoxy)ethoxy)ethoxy)ethoxy)calix[4]arene (39)

Compound **39** was obtained by the same procedure used for **38** from tetraadamantyl calix[4]arene **36**. The residue was purified by column chromatography ($\text{Et}_2\text{O}/\text{MeOH}$, 10/0.9) to give **39** as a pale yellow oil. Yield: 43%. ^1H NMR (300 MHz; CDCl_3): δ 7.58 (s, 8H, ArH), 4.66 (d, 4H, ArCH_2Ar ax, $J = 14.1$ Hz), 4.24 (t, 8H, ArOCH_2 , $J = 4$ Hz), 3.81 (t, 8H, $\text{ArOCH}_2\text{CH}_2$, $J = 4$ Hz), 3.65-3.55 (m, 48H, $\text{AdO}(\text{CH}_2\text{CH}_2\text{O})_3$), 3.38 (d, 4H,

ArCH₂Ar eq, J = 14.1 Hz), 2.12 (bs, 12H, Ad[CH₂CHCH₂]), 1.73 (d, 24H, Ad[CHCH₂C], J = 2.9 Hz), 1.60 (m, 24H, Ad[CHCH₂CH]). ¹³C NMR (75 MHz; CDCl₃): δ 161.6 (s, Ar ipso), 143.0 (s, Ar para), 135.7 (s, Ar ortho), 123.9 (d, Ar meta), 74.3 (t, ArOCH₂), 72.2 (s, Ad[CH₂CCH₂]), 71.3, 70.6, 70.5, 70.4 (t, ArOCH₂(CH₂OCH₂)₃R), 59.2 (t, AdOCH₂), 41.5 (t, Ad[CCH₂CH]), 36.4 (t, Ad[CHCH₂CH]), 31.1 (t, ArCH₂Ar), 30.5 (d, Ad[CH₂CHCH₂]). MS (ES+) *m/z* (%): 961.6 (65) [M+2K]²⁺, 953.4 (100) [M+Na+K]²⁺. Anal. Calcd for C₁₀₀H₁₄₀O₂₈N₄ (1846.23): C, 65.06; H, 7.64; N, 3.03. Found: C, 65.18; H, 7.55; N, 3.09.

5,11,17,23-Tetraamino-25,27-bis(2-ethoxyethoxy)-26,28-bis(2-(2-(2-(2-(adamantyl-1-oxy)ethoxy)ethoxy)ethoxy)ethoxy)calix[4]arene (41)

Hydrazine monohydrate (1.79 mL, 57.3 mmol) and a catalytic amount of Pd/C were added to a solution of calix[4]arene **38** (0.982 g, 0.72 mmol) in 10 mL of absolute EtOH. The solution was stirred at 80°C overnight. The mixture was cooled to room temperature, filtered and evaporated to dryness. The residue was dissolved in 50 mL of ethyl acetate and washed with a NaHCO₃ saturated aqueous solution (50 mL). The organic phase was dried with Na₂SO₄, filtered and concentrated under reduced pressure, to give calix[4]arene **41** as a pale brown oil in a quantitative yield. ¹H NMR (300 MHz; CDCl₃): δ 6.08 (s, 4H, ArH), 6.04 (s, 4H, ArH), 4.32 (d, 4H, ArCH₂Ar ax, J = 13.2 Hz), 4.00 (t, 4H, ArOCH₂, J = 5.4 Hz), 3.99 (t, 4H, ArOCH₂, J = 5.8 Hz), 3.84 (t, 4H, ArOCH₂CH₂, J = 5.4 Hz), 3.79 (t, 4H, ArOCH₂CH₂, J = 5.8 Hz), 3.62-3.58 (m, 24H, AdO(CH₂CH₂O)₃), 3.53 (q, 4H, CH₃CH₂OR, J = 6.9 Hz), 2.90 (d, 4H, ArCH₂Ar eq, J = 13.2 Hz), 2.13 (bs, 6H, Ad[CH₂CHCH₂]), 1.74 (d, 12H, Ad[CHCH₂C], J = 2.7 Hz), 1.60 (m, 12H, Ad[CHCH₂CH]), 1.20 (t, 6H, CH₃CH₂OR, J = 6.9 Hz). ¹³C NMR (75 MHz; CDCl₃): δ 149.2 (s, Ar ipso), 149.1 (s, Ar ipso), 140.1 (s, Ar para), 135.0 (s, Ar ortho), 134.9 (s, Ar ortho), 115.1 (d, Ar meta), 72.5 (t, ArOCH₂), 72.4 (t, ArOCH₂), 71.7 (s, Ad[CH₂CCH₂]), 70.7, 70.1, 69.9, 69.1, 65.8 (t, AdOCH₂CH₂O(CH₂CH₂O)₂CH₂ + CH₃CH₂OCH₂), 58.7 (t, AdOCH₂), 41.0 (t, Ad[CCH₂CH]), 35.9 (t, Ad[CHCH₂CH]), 30.5 (t, ArCH₂Ar), 30.0 (d, Ad[CH₂CHCH₂]), 15.2 (q, CH₃). MS (MALDI-TOF) *m/z* (%): 1271.5 (100) [M+Na]⁺; 1249.6 (60) [M+H]⁺. Anal. Calcd for C₇₂H₁₀₄O₁₄N₄ (1249.64): C, 69.20; H, 8.39; N, 4.48. Found: C, 69.27; H, 8.30; N, 4.40.

5,11,17,23-Tetraamino-25,27-bis(2-ethoxyethoxy)-26,28-bis(2-(2-(2-(2-(adamantyl-1-oxy)ethoxy)ethoxy)ethoxy)calix[4]arene (40)

Compound **40** was obtained as pale brown solid by the same procedure used for **41** from the tetranitrocalix[4]arene **37**. Yield > 95%. Mp = 108.3 °C. ¹H NMR (300 MHz; CDCl₃): δ 6.06 (s, 4H, ArH), 6.01 (s, 4H, ArH), 4.33 (d, 4H, ArCH₂Ar ax, J = 13.2 Hz), 3.98 (t, 8H, ArOCH₂, J = 5.5 Hz), 3.83 (t, 4H, ArOCH₂CH₂, J = 5.5 Hz), 3.78 (t, 4H, ArOCH₂CH₂, J = 5.5 Hz), 3.56-3.49 (m, 12H, AdOCH₂CH₂O + CH₃CH₂OR), 2.89 (d, 4H, ArCH₂Ar eq, J = 13.2 Hz), 2.12 (bs, 6H, Ad[CH₂CHCH₂]), 1.72 (d, 12H, Ad[CHCH₂C], J

= 2.7 Hz), 1.65-1.55 (m, 12H, Ad[CHCH₂CH]), 1.19 (t, 6H, CH₃CH₂OR, J = 7.1 Hz). ¹³C NMR (75 MHz; CDCl₃): δ 149.8 (Ar ipso), 149.5 (Ar ipso), 140.5 (Ar para), 135.5 (Ar ortho), 135.3 (Ar ortho), 115.6 (Ar meta), 73.0 (ArOCH₂), 72.9 (ArOCH₂), 72.0 (Ad[CH₂CCH₂]), 71.0, 70.3, 69.6, 66.2 (AdOCH₂CH₂OCH₂ + CH₃CH₂OCH₂), 59.2 (AdOCH₂), 41.4 (Ad[CCH₂CH]), 36.4 (Ad[CHCH₂CH]), 31.0 (ArCH₂Ar), 30.5 (Ad[CH₂CHCH₂]), 15.3 (CH₃). MS (CI) *m/z* (%): 1073.6 (100) [M+H]⁺. Anal. Calcd for C₆₄H₈₈O₁₀N₄ (1073.43): C, 71.61; H, 8.26; N, 5.22. Found: C, 71.80; H, 8.38; N, 5.14.

5,11,17,23-Tetraamino-25,26,27,28-tetrakis(2-(2-(2-(2-(adamantyl-1-oxy)ethoxy)ethoxy)ethoxy)ethoxy)calix[4]arene (42)

Compound **42** was obtained from tetranitro tetraadamantylcalix[4]arene **39** by the same procedure used for **41**. Yield > 95%. ¹H NMR (300 MHz; CDCl₃): δ 6.04 (s, 8H, ArH), 4.31 (d, 4H, ArCH₂Ar ax, J = 13.2 Hz), 3.98 (t, 8H, ArOCH₂, J = 5.8 Hz), 3.81 (t, 8H, ArOCH₂CH₂, J = 5.8 Hz), 3.66-3.57 (m, 48H, AdO(CH₂CH₂O)₃), 2.89 (d, 4H, ArCH₂Ar eq, J = 13.2 Hz), 2.13 (bs, 12H, Ad[CH₂CHCH₂]), 1.74 (d, 24H, Ad[CHCH₂C] J = 2.7 Hz), 1.58 (m, 24H, Ad[CHCH₂CH]). ¹³C NMR (75 MHz; CDCl₃): δ 150.2 (s, Ar ipso), 140.5 (s, Ar para), 135.9 (s, Ar ortho), 116.3 (d, Ar meta), 73.2 (t, ArOCH₂), 72.6 (s, Ad[CH₂CCH₂]), 71.7, 71.0, 70.8 (t, ArOCH₂(CH₂OCH₂)₃R), 59.6 (t, AdOCH₂), 41.9 (t, Ad[CCH₂CH]), 36.9 (t, Ad[CHCH₂CH]), 31.4 (t, ArCH₂Ar), 30.9 (d, Ad[CH₂CHCH₂]). MS (ES⁺) *m/z* (%): 1747.8 (25) [M+Na]⁺, 885.3 (100) [M+2Na]⁺⁺. Anal. Calcd for C₁₀₀H₁₄₈O₂₀N₄ (1726.30): C, 69.57; H, 8.64; N, 3.24. Found: C, 69.47; H, 8.47; N, 3.20.

5,11,17,23-Tetrakis[(N',N''-bis-(tert-butyloxycarbonyl)guanidyl)-25,27-bis(2-ethoxyethoxy)-26,28-bis(2-(2-(2-(2-(adamantyl-1-oxy)ethoxy)ethoxy)ethoxy)ethoxy)ethoxy)calix[4]arene (44)

To a solution of tetraamino calix[4]arene **41** (0.553 g, 0.44 mmol) in 5 mL of dry DMF, kept under N₂, were added bis-BOC-thiourea (0.538 g, 1.95 mmol) and Et₃N (0.74 mL, 5.3 mmol). The solution was cooled to 0°C with an ice bath and HgCl₂ (0.529 g, 1.95 mmol) was added. After 4 h the reaction was quenched by pouring Et₂O (30 mL) in the flask and filtering the solution to remove the mercury salts. The solvent was removed under vacuum and the residue was purified by column chromatography (Et₂O) to give **44** as a colorless oil. Yield: 45%. ¹H NMR (300 MHz; CDCl₃): δ 11.62 (s, 4H, NHBoc), 9.86 (bs, 4H, ArNH), 6.97 (s, 4H, ArH), 6.96 (s, 4H, ArH), 4.48 (d, 4H, ArCH₂Ar ax, J = 13.2 Hz), 4.13 (t, 4H, ArOCH₂, J = 5.7 Hz), 4.10 (t, 4H, ArOCH₂, J = 5.9 Hz), 3.90 (t, 4H, ArOCH₂CH₂, J = 5.7 Hz), 3.82 (t, 4H, ArOCH₂CH₂, J = 5.9 Hz), 3.67-3.54 (m, 12H, AdO(CH₂CH₂O)₃), 3.49 (q, 4H, CH₃CH₂OR, J = 6.7 Hz), 3.17 (d, 4H, ArCH₂Ar eq, J = 13.2 Hz), 2.15 (bs, 6H, Ad[CH₂CHCH₂]), 1.76 (d, 12H, Ad[CHCH₂C] J = 2.4 Hz), 1.60-1.45 (m, 12H, Ad[CHCH₂CH]), 1.51 (s, 36H, Boc), 1.47 (s, 36H, Boc), 1.23 (t, 6H, CH₃R, J = 6.7 Hz). ¹³C NMR (75 MHz; CDCl₃): δ 163.0 (s, C=O), 153.0 (s, Ar ipso),

152.5 (s, ArNHC), 134.1 (s, Ar para), 130.5 (s, Ar ortho), 122.7 (d, Ar meta), 82.5 (s, C(CH₃)₃), 78.6 (s, C(CH₃)₃), 72.7 (t, ArOCH₂), 72.6 (t, ArOCH₂), 71.6 (s, Ad[CH₂CCH₂]), 70.7, 70.1, 69.9, 69.6, 68.8, 65.8 (t, AdOCH₂CH₂O(CH₂CH₂O)₂CH₂ + CH₃CH₂OCH₂), 58.7 (t, AdOCH₂), 41.0 (t, Ad[CCH₂CH]), 35.9 (t, Ad[CHCH₂CH]), 30.7 (t, ArCH₂Ar), 30.0 (d, Ad[CH₂CHCH₂]), 27.7 (q, R(CH₃)₃), 27.6 (q, R(CH₃)₃), 14.9 (q, RCH₃). MS (FAB -VE) *m/z* (%): 2217.6 (100) [M]⁻; 2216.2 (80) [M-H]⁻. Anal. Calcd for C₁₁₆H₁₇₆O₃₀N₁₂ (2218.75): C, 62.80; H, 8.00; N, 7.58. Found: C, 62.71; H, 8.10; N, 7.63.

5,11,17,23-Tetrakis[(N',N''-bis-(tert-butyloxycarbonyl)guanidyl)-25,27-bis(2-ethoxyethoxy)-26,28-bis(2-(2-(adamantyl-1-oxy)ethoxy)ethoxy)calix[4]arene (43)

Compound **43** was obtained by the same procedure used for **44** from tetraamino calix[4]arene **40**. The residue was purified by column chromatography (Hex/EtOAc, 7/4) obtaining a white solid. Yield 65%. Mp > 320 °C dec. ¹H NMR (300 MHz; CDCl₃): δ 11.60 (s, 4H, NHBoc), 9.87 (s, 2H, ArNH), 9.79 (s, 2H, ArNH), 6.96 (s, 4H, ArH), 6.93 (s, 4H, ArH), 4.46 (d, 4H, ArCH₂Ar ax, J = 13.0 Hz), 4.11-4.07 (m, 8H, ArOCH₂), 3.88 (t, 4H, ArOCH₂CH₂, J = 5.7 Hz), 3.83 (t, 4H, ArOCH₂CH₂, J = 5.7 Hz), 3.58-3.55 (m, 8H, AdOCH₂CH₂O), 3.53 (q, 4H, CH₃CH₂OR, J = 7.0 Hz), 3.14 (d, 4H, ArCH₂Ar eq, J = 13.0 Hz), 2.12 (bs, 6H, Ad[CH₂CHCH₂]), 1.73 (d, 12H, Ad[CHCH₂C] J = 2.7 Hz), 1.63-1.55 (m, 12H, Ad[CHCH₂CH]), 1.47 (s, 36H, Boc), 1.45 (s, 36H, Boc), 1.20 (t, 6H, CH₃R, J = 7.0 Hz). ¹³C NMR (75 MHz; CDCl₃): δ 163.5 (C=O), 153.6 (Ar ipso), 153.4 (Ar ipso), 153.0 (ArNHC), 134.6 (Ar para), 134.5 (Ar para), 130.9 (Ar ortho), 123.0 (Ar meta), 82.9 (C(CH₃)₃), 79.0 (C(CH₃)₃), 73.2 (ArOCH₂), 73.1 (ArOCH₂), 72.0 (Ad[CH₂CCH₂]), 71.0, 70.1, 69.3, 66.3 (AdOCH₂CH₂OCH₂CH₂O + CH₃CH₂OCH₂), 59.2 (AdOCH₂), 41.4 (Ad[CCH₂CH]), 36.4 (Ad[CHCH₂CH]), 31.1 (ArCH₂Ar), 30.4 (Ad[CH₂CHCH₂]), 28.1 (R(CH₃)₃), 28.0 (R(CH₃)₃), 15.3 (RCH₃). MS (ESI) *m/z* (%): 1043.9 (100) [M+2Na]²⁺. Anal. Calcd for C₁₀₈H₁₆₀N₁₂O₂₆ (2042.53): C, 63.51; H, 7.90; N, 8.23. Found: C, 63.71; H, 8.01; N, 7.78.

5,11,17,23-Tetrakis[(N',N''-bis-(tert-butyloxycarbonyl)guanidyl)-25,26,27,28-tetrakis(2-(2-(2-(2-(adamantyl-1-oxy)ethoxy)ethoxy)ethoxy)ethoxy)calix[4]arene (45)

Compound **45** was obtained from tetraamino calix[4]arene **42** by the same procedure used for **44**. The residue was purified by column chromatography (Et₂O/EtOAc 1/1) to give **45** as a colorless oil. Yield: 61%. ¹H NMR (300 MHz; CDCl₃): δ 11.58 (bs, 4H, NHBoc), 9.82 (s, 4H, ArNH), 6.93 (s, 8H, ArH), 4.44 (d, 4H, ArCH₂Ar ax, J = 13 Hz), 4.09 (t, 8H, ArOCH₂, J = 5.6 Hz), 3.86 (t, 8H, ArOCH₂CH₂, J = 5.6 Hz), 3.63-3.53 (m, 48H, AdO(CH₂CH₂O)₃), 3.15 (d, 4H, ArCH₂Ar eq, J = 13 Hz), 2.13 (bs, 12H, Ad[CH₂CHCH₂]), 1.76 (d, 24H, Ad[CHCH₂C], J = 2.7 Hz), 1.60-1.45 (m, 24H,

Ad[CHCH₂CH] + 72H, Boc). ¹³C NMR (75 MHz; CDCl₃): δ 163.4 (s, C=O), 153.5 (s, Ar ipso), 152.5 (s, ArNHC), 134.6 (s, Ar para), 130.9 (s, Ar ortho), 123.1 (d, Ar meta), 79.1 (s, C(CH₃)₃), 73.0 (t, ArOCH₂), 72.1 (s, Ad[CH₂CCH₂]), 71.2, 70.6, 70.3, 70.0 (t, ArOCH₂(CH₂OCH₂)₃R), 59.2 (t, AdOCH₂), 41.4 (t, Ad[CHCH₂CH]), 36.4 (t, Ad[CHCH₂CH]), 31.2 (t, ArCH₂Ar), 30.5 (d, Ad[CH₂CHCH₂]), 30.2, 28.1 (q, R(CH₃)₃). MS (ES+) *m/z* (%): 1369.7 (100) [M+2Na]²⁺, 1358.7 (85) [M+H+Na]²⁺, 1348.7 (70) [M+2H]²⁺. Anal. Calcd for C₁₄₄H₂₂₀O₃₆N₁₂ (2695.40): C, 64.17; H, 8.22; N, 6.24. Found: C, 64.28; H, 8.16; N, 6.14.

5,11,17,23-Tetraguanidinium-25,27-bis(2-ethoxyethoxy)-26,28-bis(2-(2-(2-(2-(adamantyl-1-oxy)ethoxy)ethoxy)ethoxy)ethoxy)ethoxy)calix[4]arene, tetraacetate (47)

Calix[4]arene **44** (0.232 g, 0.1 mmol) was dissolved in the minimum volume possible of diethyl ether (3 mL) and 2M HCl solution in dioxane was added (1.83 mL, 3.66 mmol). The solution was stirred overnight at room temperature and then evaporated under reduced pressure. The residue was purified by column chromatography (BuOH/H₂O/CH₃COOH 6/2/1) to give **47** as a foam. The product was dissolved in water, filtered on microporous filters (0.2 μm) and lyophilized, obtaining a white solid. Yield: 60%. Mp > 300°C. ¹H NMR (300 MHz; CD₃OD): δ 6.67 (s, 4H, ArH), 6.61 (s, 4H, ArH), 4.62 (d, 4H, ArCH₂Ar ax, J = 13.6 Hz), 4.27 (t, 4H, ArOCH₂, J = 4.8 Hz), 4.18 (t, 4H, ArOCH₂, J = 4.9 Hz), 3.98 (t, 4H, ArOCH₂CH₂, J = 4.8 Hz), 3.92 (t, 4H, ArOCH₂CH₂, J = 4.9 Hz), 3.56-3.48 (m, 28H, AdO(CH₂CH₂O)₃ + CH₃CH₂OR), 3.27 (d, 4H, ArCH₂Ar eq, J = 13.6 Hz), 2.13 (bs, 6H, Ad[CH₂CHCH₂]), 1.94 (s, 12H, CH₃COO⁻), 1.76 (d, 12H, Ad[CHCH₂C] J = 2.7 Hz), 1.67-1.60 (m, 12H, Ad[CHCH₂CH]), 1.15 (t, 6H, CH₃CH₂OR, J = 6.9 Hz). ¹H NMR (300 MHz; D₂O): δ 6.67 (s, 4H, ArH), 6.63 (s, 4H, ArH), 4.44 (d, 4H, ArCH₂Ar ax, J = 13.6 Hz), 4.19 (bs, 4H, ArOCH₂), 4.13 (bs, 4H, ArOCH₂), 3.88 (bs, 4H, ArOCH₂CH₂), 3.61 (bs, 4H, ArOCH₂CH₂), 3.56-3.51 (m, 28H, AdO(CH₂CH₂O)₃ + CH₃CH₂OR), 3.26 (d, 4H, ArCH₂Ar eq, J = 13.6 Hz), 2.01 (bs, 6H, Ad[CH₂CHCH₂]), 1.79 (s, 12H, CH₃COO⁻), 1.62 (bs, 12H, Ad[CHCH₂C]), 1.57-1.42 (m, 12H, Ad[CHCH₂CH]), 1.01 (t, 6H, CH₃CH₂OR, J = 6.9 Hz). ¹³C NMR (75 MHz; CD₃OD): δ 156.1 (s, C=N), 155.9 (s, C=N), 155.2 (s, Ar ipso), 154.7 (s, Ar ipso), 136.0 (s, Ar para), 135.5 (s, Ar para), 128.6 (s, Ar ortho), 124.4 (d, Ar meta), 124.1 (d, Ar meta), 73.4 (t, ArOCH₂), 71.7 (s, Ad[CH₂CCH₂]), 70.3, 70.1, 69.8, 69.6, 69.2 (t, AdOCH₂CH₂O(CH₂CH₂O)₂CH₂ + CH₃CH₂OCH₂), 58.5 (t, AdOCH₂), 40.7 (t, Ad[CCH₂CH]), 35.5 (t, Ad[CHCH₂CH]), 30.0 (d, Ad[CH₂CHCH₂]), 29.9 (t, ArCH₂Ar), 13.9 (q, RCH₃). MS (MALDI-TOF) *m/z* (%): 1418.7 (100) [M-4CH₃COO⁻-3H]⁺. Anal. Calcd for C₈₄H₁₂₈O₂₂N₁₂ (1658.02): C, 60.85; H, 7.78; N, 10.14. Found: C, 60.93; H, 7.71; N, 10.06.

5,11,17,23-Tetraguanidinium-25,27-bis(2-ethoxyethoxy)-26,28-bis(2-(2-(adamantyl-1-oxy)ethoxy)ethoxy)ethoxy)calix[4]arene, tetrachloride (46)

Compound **46** was obtained from Boc-protected tetraguanidiniumcalix[4]arene **43** by the same procedure used for **47**. Yield > 95%. Mp > 300 °C. ^1H NMR (300 MHz; CD_3OD): δ 6.75 (s, 4H, ArH), 6.67 (s, 4H, ArH), 4.65 (d, 4H, ArCH_2Ar ax, $J = 13.4$ Hz), 4.28 (t, 4H, ArOCH_2 , $J = 4.8$ Hz), 4.22 (t, 4H, ArOCH_2 , $J = 4.9$ Hz), 3.98 (t, 4H, $\text{ArOCH}_2\text{CH}_2$, $J = 4.8$ Hz), 3.94 (t, 4H, $\text{ArOCH}_2\text{CH}_2$, $J = 4.9$ Hz), 3.67-3.60 (m, 12H, $\text{AdOCH}_2\text{CH}_2\text{O} + \text{CH}_3\text{CH}_2\text{OR}$), 3.31 (d, 4H, ArCH_2Ar eq, $J = 13.6$ Hz), 2.15 (bs, 6H, $\text{Ad}[\text{CH}_2\text{CHCH}_2]$), 1.78 (d, 12H, $\text{Ad}[\text{CHCH}_2\text{C}]$ $J = 2.7$ Hz), 1.74-1.62 (m, 12H, $\text{Ad}[\text{CHCH}_2\text{CH}]$), 1.23 (t, 6H, $\text{CH}_3\text{CH}_2\text{OR}$, $J = 7.0$ Hz). ^1H NMR (300 MHz; D_2O): δ 6.84 (s, 4H, ArH), 6.69 (s, 4H, ArH), 4.56 (d, 4H, ArCH_2Ar ax, $J = 13.5$ Hz), 4.26 (bs, 8H, ArOCH_2), 4.01-4.96 (m, 8H, $\text{ArOCH}_2\text{CH}_2$), 3.69-3.64 (m, 12H, $\text{AdOCH}_2\text{CH}_2\text{O} + \text{CH}_3\text{CH}_2\text{OR}$), 3.37 (d, 4H, ArCH_2Ar eq, $J = 13.5$ Hz), 2.10 (bs, 6H, $\text{Ad}[\text{CH}_2\text{CHCH}_2]$), 1.70 (bs, 12H, $\text{Ad}[\text{CHCH}_2\text{C}]$), 1.67-1.52 (m, 12H, $\text{Ad}[\text{CHCH}_2\text{CH}]$), 1.20 (t, 6H, $\text{CH}_3\text{CH}_2\text{OR}$, $J = 7.2$ Hz). ^{13}C NMR (75 MHz; CD_3OD): δ 158.3 (C=N), 157.7 (Ar ipso), 157.4 (Ar ipso), 138.2 (Ar para), 137.9 (Ar para), 130.2 (Ar ortho), 127.1 (Ar meta), 126.9 (Ar meta), 75.6 (ArOCH_2), 75.4 (ArOCH_2), 73.9, 72.6, 72.3, 71.5, 68.4, 67.9, 60.9 (AdOCH_2), 43.0 ($\text{Ad}[\text{CCH}_2\text{CH}]$), 37.8 ($\text{Ad}[\text{CHCH}_2\text{CH}]$), 32.3 ($\text{Ad}[\text{CH}_2\text{CHCH}_2]$), 32.3 (ArCH_2Ar), 16.1 (RCH_3). MS (ESI) m/z (%): 621.6 (100) $[\text{M}-4\text{Cl}-2\text{H}]^{2+}$. Anal. Calcd for $\text{C}_{68}\text{H}_{100}\text{O}_{10}\text{N}_{12}\text{Cl}_4$ (1245.62): C, 65.57; H, 8.09; N, 13.49. Found: C, 65.39; H, 8.17; N, 13.61.

5,11,17,23-Tetraguanidinium-25,26,27,28-tetrakis(2-(2-(2-(2-(adamantyl-1-oxy)ethoxy)ethoxy)ethoxy)ethoxy)calix[4]arene, tetrachloride (48)

Compound **48** was obtained from Boc-protected tetraguanidiniumcalix[4]arene **45** by the same procedure used for **47**. It was possible to obtain **48** as a white solid dissolving it in CH_2Cl_2 and adding hexane to the solution. Yield > 95%. Mp > 300 °C. ^1H NMR (300 MHz; CD_3OD): δ 6.72 (s, 8H, ArH), 4.66 (d, 4H, ArCH_2Ar ax, $J = 13.4$ Hz), 4.26 (t, 8H, ArOCH_2 , $J = 4.5$ Hz), 3.99 (t, 8H, $\text{ArOCH}_2\text{CH}_2$, $J = 4.5$ Hz), 3.70-3.57 (m, 48H, $\text{AdO}(\text{CH}_2\text{CH}_2\text{O})_3$), 3.32 (d, 4H, ArCH_2Ar eq, $J = 13.4$ Hz), 2.04 (bs, 12H, $\text{Ad}[\text{CH}_2\text{CHCH}_2]$), 1.67 (d, 24H, $\text{Ad}[\text{CHCH}_2\text{C}]$, $J = 2.7$ Hz), 1.55 (m, 24H, $\text{Ad}[\text{CHCH}_2\text{CH}]$). ^{13}C NMR (75 MHz; CD_3OD): δ 158.2 (s, C=N), 157.6 (s, Ar ipso), 138.1 (s, Ar ortho), 130.2 (s, Ar para), 127.1 (d, Ar meta), 75.5 (t, ArOCH_2), 74.0 (s, $\text{Ad}[\text{CH}_2\text{CCH}_2]$), 72.6, 72.3, 72.1, 72.0, 71.9 (t, $\text{ArOCH}_2(\text{CH}_2\text{OCH}_2)_3$), 60.8 (t, AdOCH_2), 42.3 (t, $\text{Ad}[\text{CHCH}_2\text{CH}]$), 37.8 (t, $\text{Ad}[\text{CCH}_2\text{CH}]$), 32.3 (d, $\text{Ad}[\text{CH}_2\text{CHCH}_2]$), 32.2 (t, ArCH_2Ar). MS (ES+) m/z (%): 632.8 (100) $[\text{M}-\text{H}-4\text{Cl}]^{3+}$. Anal. Calcd for $\text{C}_{104}\text{H}_{160}\text{O}_{20}\text{N}_{12}\text{Cl}_4$ (2040.30): C, 61.22; H, 7.90; N, 8.24. Found: C, 61.33; H, 7.87; N, 8.15.

5,11,17-Tris[N-((6-N,N-dihydroxyethylaminomethyl)pyridin-2-yl-methyl)-N-methylaminomethyl]-25,26,27,28-tetrakis(2-ethoxyethoxy)calix[4]arene (50)

Tris(2-chloromethylpyridine)calixarene **49**³² (200 mg, 0.16 mmol) in CH₂Cl₂ (5 mL) was added dropwise to a solution of diethanolamine (3 g, 28.5 mmol) in absolute EtOH (2 mL). The mixture was stirred under nitrogen at RT for 2 days. The solvent was evaporated and the crude product dissolved in EtOAc (70 mL). The organic phase was washed with NaHCO₃ aqueous saturated solution (2 x 70 mL) and water (70 mL), dried over anhydrous Na₂SO₄, filtered and the solvent evaporated under reduced pressure. The product was obtained as a pale yellow oil after purification by column chromatography on basic Al₂O₃ (CH₂Cl₂/Et₂O/MeOH/Et₃N 7/2/0.9/0.1). Yield 55%. ¹H NMR (300 MHz; CDCl₃): δ 7.63 (t, 2H, PyH, J = 7.6 Hz), 7.54 (t, 1H, PyH, J = 7.6 Hz), 7.42 (d, 2H, PyH, J = 7.6 Hz), 7.12 (d, 3H, PyH, J = 7.6 Hz), 7.06 (d, 1H, PyH, J = 7.6 Hz), 6.91 (d, 2H, ArH, J = 1.8 Hz), 6.87 (d, 2H, ArH, J = 1.8 Hz), 6.42 (s, 2H, ArH), 6.34 (d, 2H, ArH, J = 7.5 Hz), 6.14 (t, 1H, ArH, J = 7.5 Hz), 4.46 (d, 4H, ArCH₂Ar ax, J = 13.1 Hz), 4.20 (t, 4H, ArOCH₂, J = 6.1 Hz), 4.01 (t, 2H, ArOCH₂, J = 5.5 Hz), 4.00 (t, 2H, ArOCH₂, J = 5.4 Hz), 3.86 (t, 4H, ArOCH₂CH₂, J = 6.1 Hz), 3.84 (s, 4H, NCH₂Py), 3.82 (t, 2H, ArOCH₂CH₂, J = 5.5 Hz), 3.81 (t, 2H, ArOCH₂CH₂, J = 5.4 Hz), 3.78 (s, 2H, NCH₂Py), 3.57-3.52 (m, 18H, CH₂OH + PyCH₂N), 3.51 (q, 8H, OCH₂CH₃, J = 7.0 Hz), 3.29 (s, 4H, ArCH₂N), 3.21 (s, 2H, ArCH₂N), 3.11 (d, 2H, ArCH₂Ar eq, J = 13.1 Hz), 3.09 (d, 2H, ArCH₂Ar eq, J = 13.1 Hz), 2.81 (t, 8H, CH₂CH₂OH, J = 5.1 Hz), 2.76 (t, 4H, CH₂CH₂OH, J = 5.1 Hz), 2.10 (s, 6H, NCH₃), 1.66 (s, 3H, NCH₃), 1.22 (t, 6H, CH₂CH₃, J = 7.0 Hz), 1.16 (t, 6H, CH₂CH₃, J = 7.0 Hz). ¹³C NMR (75 MHz; CDCl₃): δ 159.7, 158.8, 158.3, 156.1, 155.3, 154.5, 137.4, 137.3, 135.5, 134.0, 133.7, 132.1, 129.2, 128.3, 127.7, 122.1, 121.5, 121.1, 120.9, 73.5, 72.7, 69.6, 66.4, 66.2, 62.7, 62.4, 61.8, 61.1, 59.7, 59.5, 57.8, 57.7, 42.3, 42.0, 30.8, 15.3, 15.2. MS (ES+) *m/z* (%): 1488.7 [M+Na]⁺ (80), 745.0 [M+H+Na]²⁺ (95), 755.9 [M+2Na]²⁺ (100). Anal. Calcd for C₈₃H₁₁₉N₉O₁₄ (1466.92): C, 67.96; H, 8.17; N, 8.59. Found: C, 67.78; H, 8.26; N, 8.42.

Determination of the water solubility of 21-23 by interaction with β-CD

The water solubility of β-CD complexes with calixarenes **21-23** was measured using ¹H-NMR spectroscopy. The calixarene and the CD (native β-CD, met-β-CD or hyp-β-CD) were weighted in a test tube and 1 mL of D₂O, containing an internal standard (potassium salt of phtalic acid) at known concentration, was added. The weights were calculated in order to have a solution 10⁻² M of CD and 0.25 equiv. of calixarene. The solutions were stirred for 3 hours at room temperature, sonicated for 15 min, filtered over millipore filters (0.45 μM) and the NMR spectra were registered on a Bruker AC300 device. The integration of the signals of the standard and of the calixarene allowed us to calculate the concentration of the calixarene in solution. Every experiment was repeated twice.

Equilibrium and Rate Measurements

UV titrations were carried out on a double beam spectrophotometer. Data obtained in the titration of DMAP with $\text{Zn}(\text{ClO}_4)_2$ were treated according to a standard binding isotherm for the case of 1:1 association. Transesterification of 0.2 mM HPNP (in 50% (v/v) CH_3CN - 20 mM aqueous HEPES buffer, and 35% (v/v) EtOH - 20 mM aqueous HEPES buffer, 25 °C, pH = 7) carried out in the presence of 1 mM **50**-[Zn]₃ was monitored by UV-Vis following the *p*-nitrophenol release at 400 nm.

Calorimetric Titrations

Calorimetric measurements were carried out using a Microcal VP-ITC instrument with a cell volume of 1.4115 mL. For studying the complexation of **47** with native β -cyclodextrin (CD), 5 μL aliquots of a 5 mM solution of CD were added to a 0.5 mM solution of **47** in the calorimetric cell, monitoring the heat change after each addition. All thermodynamic parameters given in the text are based on three independent calorimetric titrations.

3.8 References and notes

- (1) Casnati, A.; Sciotto, D.; Arena, G. Water-soluble calixarenes; In *Calixarenes 2001*; Asfari, Z., Böhmer, V., Harrowfield, J., Vicens, J., eds. Kluwer Academic Publishers: Dordrecht, 2001; pp 440-456.
- (2) Arduini, A.; Pochini, A.; Reverberi, S.; Ungaro, R. *J. Chem. Soc. , Chem. Commun* **1984**, 981-982.
- (3) Almi, M.; Arduini, A.; Casnati, A.; Pochini, A.; Ungaro, R. *Tetrahedron* **1989**, *45*, 2177-2182.
- (4) Shinkai, S.; Tsubaki, T.; Sone, T.; Manabe, O. *Tetrahedron Lett.* **1984**, *25*, 5315-5318.
- (5) Casnati, A.; Ting, Y. H.; Berti, D.; Fabbi, M.; Pochini, A.; Ungaro, R.; Sciotto, D.; Lombardo, G. G. *Tetrahedron* **1993**, *49*, 9815-9822.
- (6) Arimori, S.; Nagasaki, T.; Shinkai, S. *J. Chem. Soc. , Perkin Trans. 2* **1995**, 679-683.
- (7) Corbellini, F.; Fiammengo, R.; Timmerman, P.; Crego, C. M.; Versluis, K.; Heck, A. J. R.; Luyten, I.; Reinhoudt, D. N. *J. Am. Chem. Soc.* **2002**, *124*, 6569-6575.
- (8) Segura, M.; Sansone, F.; Casnati, A.; Ungaro, R. *Synthesis* **2001**, 2105-2112.
- (9) Grote Gansey, M. H. B.; Verboom, W.; Reinhoudt, D. N. *Tetrahedron Lett.* **1994**, *35*, 7127-7130.
- (10) Grote Gansey, M. H. B.; Steemers, F. J.; Verboom, W.; Reinhoudt, D. N. *Synthesis* **1997**, 643-648.
- (11) Newkome, G. R.; Hu, Y. F.; Saunders, M. J.; Fronczek, F. R. *Tetrahedron Lett.* **1991**, *32*, 1133-1136.

- (12) Anelli, P. L.; Brocchetta, M.; Canipari, S.; Losi, P.; Manfredi, G.; Tomba, C.; Zecchi, G. *Gazz. Chim. Ital.* **1997**, *127*, 135-142.
- (13) Marra, A.; Scherrmann, M. C.; Dondoni, A.; Casnati, A.; Minari, P.; Ungaro, R. *Angew. Chem. Int. Ed. Engl.* **1994**, *33*, 2479-2481.
- (14) Sansone, F.; Chierici, E.; Casnati, A.; Ungaro, R. *Org. Biomol. Chem.* **2003**, *1*, 1802-1809.
- (15) Middel, O.; Verboom, W.; Reinhoudt, D. N. *Eur. J. Org. Chem.* **2002**, 2587-2597.
- (16) Shi, Y. H.; Zhang, Z. H. *J. Chem. Soc., Chem. Commun* **1994**, 375-376.
- (17) For reviews on CD chemistry see *Chem. Rev.* **1998**, *98*, Issue 5.
- (18) Diederich, F. *Cyclophanes*; Royal Society of Chemistry: Cambridge, 1991.
- (19) Rekharsky, M. V.; Inoue, Y. *Chem. Rev.* **1998**, *98*, 1875-1917.
- (20) Uekama, K.; Hirayama, F.; Irie, T. *Chem. Rev.* **1998**, *98*, 2045-2076.
- (21) Hirayama, F.; Uekama, K. *Advanced Drug Delivery Reviews* **1999**, *36*, 125-141.
- (22) van Bommel, K. J. C.; Metseelaar, G. A.; Verboom, W.; Reinhoudt, D. N. *J. Org. Chem.* **2001**, *66*, 5405-5412.
- (23) Michels, J. J.; Baars, M. W. P. L.; Meijer, E. W.; Huskens, J.; Reinhoudt, D. N. *J. Chem. Soc., Perkin Trans. 2* **2000**, 1914-1918.
- (24) Dalessandro, F.; Gulino, F. G.; Impellizzeri, G.; Pappalardo, G.; Rizzarelli, E.; Sciotto, D.; Vecchio, G. *Tetrahedron Lett.* **1994**, *35*, 629-632.
- (25) Vandienst, E.; Snellink, B. H. M.; Vonpiekartz, I.; Engbersen, J. F. J.; Reinhoudt, D. N. *J. Chem. Soc., Chem. Commun* **1995**, 1151-1152.
- (26) Bügler, J.; Sommerdijk, N. A. J. M.; Visser, A. J. W. G.; van Hoek, A.; Nolte, R. J. M.; Engbersen, J. F. J.; Reinhoudt, D. N. *J. Am. Chem. Soc.* **1999**, *121*, 28-33.
- (27) Molenveld, P.; Engbersen, J. F. J.; Reinhoudt, D. N. *Chem. Soc. Rev.* **2000**, *29*, 75-86.
- (28) Allan, C. B.; Spreer, L. O. *J. Org. Chem.* **1994**, *59*, 7695-7700.
- (29) Gutsche, C. D.; Levine, J. A.; Sujeeth, P. K. *J. Org. Chem.* **1985**, *50*, 5802-5806.
- (30) Komori, T.; Shinkai, S. *Chem. Lett.* **1992**, 901-904.
- (31) Arduini, A.; Manfredi, G.; Pochini, A.; Sicuri, A. R.; Ungaro, R. *J. Chem. Soc., Chem. Commun* **1991**, 936-937.
- (32) Molenveld, P.; Stikvoort, W. M. G.; Kooijman, H.; Spek, A. L.; Engbersen, J. F. J.; Reinhoudt, D. N. *J. Org. Chem.* **1999**, *64*, 3896-3906.
- (33) Casnati, A.; Fochi, M.; Minari, P.; Pochini, A.; Reggiani, M.; Ungaro, R.; Reinhoudt, D. N. *Gazz. Chim. Ital.* **1996**, *126*, 99-106.
- (34) Groenen, L. C.; Ruel, B. H. M.; Casnati, A.; Timmerman, P.; Verboom, W.; Harkema, S.; Pochini, A.; Ungaro, R.; Reinhoudt, D. N. *Tetrahedron Lett.* **1991**, *32*, 2675-2678.
- (35) Corey, E. J.; Noe, M. C. *J. Am. Chem. Soc.* **1996**, *118*, 319-329.
- (36) Arduini, A.; Fanni, S.; Manfredi, G.; Pochini, A.; Ungaro, R.; Sicuri, A. R.; Ugozzoli, F. *J. Org. Chem.* **1995**, *60*, 1448-1453.
- (37) Iwanowicz, E. J.; Poss, M. A.; Lin, J. *Synth. Commun.* **1993**, *23*, 1443-1445.

- (38) Kim, K. S.; Qian, L. G. *Tetrahedron Lett.* **1993**, *34*, 7677-7680.
- (39) Ludden, M., unpublished results.
- (40) Mulder, A.; Auletta, T.; Sartori, A.; Del Ciotto, S.; Casnati, A.; Ungaro, R.; Huskens, J.; Reinhoudt, D. N. *J. Am. Chem. Soc.* **2004**, *126*, 6627-6636.
- (41) Auletta, T.; Dordi, B.; Mulder, A.; Sartori, A.; Onclin, S.; Bruinink, C. M.; Peter, M.; Nijhuis, C. A.; Beijleveld, H.; Schonherr, H.; Vancso, G. J.; Casnati, A.; Ungaro, R.; Ravoo, B. J.; Huskens, J.; Reinhoudt, D. N. *Angew. Chem. Int. Ed* **2004**, *43*, 369-373.
- (42) A stock solution of the calixarene in doubly distilled water was prepared at 25 °C. Known volumes of this stock solution were diluted with known amounts of water to give a maximal absorbance between 0.2 and 0.5, and the absorbance maximum was plotted versus concentration. The slope of the straight line is ϵ .
- (43) Molenveld, P.; Engbersen, J. F. J.; Reinhoudt, D. N. *Angew. Chem. Int. Ed. Engl.* **1999**, *38*, 3189-3192.
- (44) The catalytic measurements were performed by Riccardo Salvio at the University of Rome.
- (45) We repeated the measurement of the transesterification of HPNP in the presence of **10**-[Zn]₃ in CH₃CN/H₂O (1:1) already performed by Molenveld in "Molenveld, P.; Stikvoort, W. M. G.; Kooijman, H.; Spek, A. L.; Engbersen, J. F. J.; Reinhoudt, D. N. *J. Org. Chem.* **1999**, *64*, 3896-3906", and substantially confirmed it. The measured rate enhancement resulted slightly lower (K_{rel} of 36,000 instead of 64,000).

CHAPTER 4

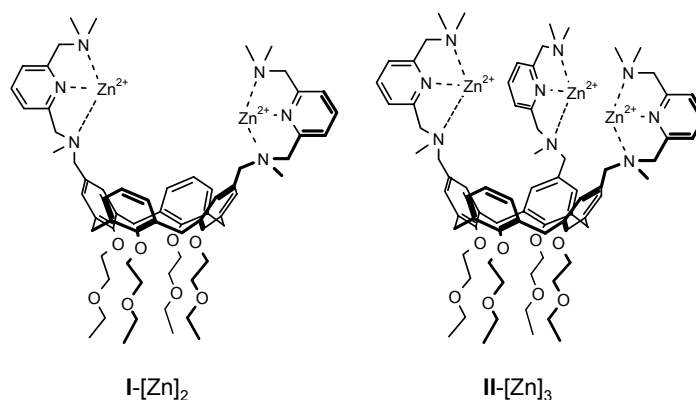
Synthesis and catalytic activity of upper rim proximal calix[4]arene dinuclear metal complexes*

*In this chapter the synthesis and characterization of tetraalkoxycalix[4]arenes in the cone conformation bearing two hydroxymethyl groups in proximal (1,2) positions at the upper rim is described. The oxidation of these compounds allowed the isolation of 1,2-diformyl and 1,2-diacid tetraalkoxycalix[4]arenes, which can be considered useful intermediates for the synthesis of calixarene-based molecular receptors having proximal binding groups. By functionalizing 1,2- and 1,3-hydroxymethyl tetrapropoxycalix[4]arenes with monoaza-18-crown-6, we obtained two novel regioisomeric calixarene derivatives **8** and **9**. The catalytic activity of their dinuclear Ba^{2+} complexes was investigated in the ethanolysis of esters **11-14**, endowed with a carboxylate anchoring group. For the first time, a direct comparison between diametral and proximal calix[4]arene supramolecular catalysts has been performed, revealing that the proximal calix[4]arene catalyst **8** is by far superior to its diametral regioisomer **9** in the reactions of all the investigated esters. The studies revealed the importance of a good match between the ester size and the metal-to-metal distance, although the superiority of **8** compared to **9** with all of the esters investigated cannot be ascribed only to a more suitable intramolecular distance in the former.*

* The work described in this chapter has been published in: Sartori, A.; Casnati, A.; Mandolini, L.; Sansone, F.; Reinhoudt, D. N.; Ungaro, R. *Tetrahedron* **2003**, 59, 5539-5534; Cacciapaglia, R.; Casnati, A.; Di Stefano, S.; Mandolini, L.; Paolemili, D.; Reinhoudt, D. N.; Sartori, A.; Ungaro, R. *Chemistry* **2004**, 10, 4436-4442.

4.1 Introduction

An important requirement in the design of selective receptors for molecular recognition and efficient supramolecular catalysts is the optimal spatial distribution of the recognition and catalytic groups. This requirement is crucial in biomimetic catalysis, since the productive (Michaelis) complex has to be selectively obtained and the preferential binding of the transition state over reactants (and products) must occur. Considering these requirements it becomes clear how the calix[4]arene scaffold can be very suitable in the design of supramolecular catalysts; in fact it has four phenolic rings whose *para* positions (upper rim) can be easily and selectively functionalized with catalytic groups precisely located in space. The functionalization of the lower rim with alkyl groups of different length and size allows the control of the conformational flexibility of the entire macrocycle. Reinhoudt and co-workers have exploited this peculiarity of the calix[4]arene scaffold and synthesized dinuclear and trinuclear metal complexes (**I** and **II**) able to mimic phosphodiesterase enzymes.^{1;2} The calix[4]arene was functionalized at the upper rim with 2,6-bis[(dimethylamino)methyl]pyridine units which complex Zn(II) ions. It was demonstrated that the two metal centers in 1,3-diametral positions of compound **I**-[Zn]₂ can cooperate in the catalysis of phosphate diester cleavage of the HPNP, providing a Lewis acid activation of the substrate phosphoryl group and, at the same time, a general base catalysis by means of a metal bound hydroxide ion.



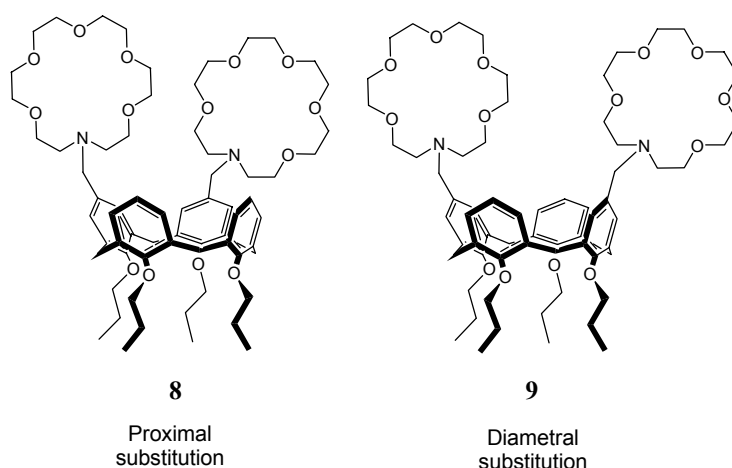
Compound **II**-[Zn]₃ showed a catalytic activity comparable to that of **I**-[Zn]₂ in HPNP transesterification, but a much higher one in dinucleotide cleavage. During these studies it was not possible to clarify if the observed higher efficiency of the trinuclear catalyst was due to the cooperation of all three metal centres or to the fact that in **II**-[Zn]₃ two catalytic groups are present in the 1,2-proximal positions at the upper rim of the calix[4]arene scaffold, whereas in the dinuclear catalyst **I**-[Zn]₂ the metal centers are in the 1,3-diametral positions.

Calix[4]arene-based supramolecular catalysts bearing catalytic groups only at the upper rim proximal positions are not reported in the literature, and therefore nothing is known about their catalytic efficiency in comparison with their diametral analogues. Quite remarkably there are also no examples of studies on the molecular recognition properties of 1,3-diametral difunctionalized calix[4]arene receptors compared with the corresponding 1,2-proximal regioisomers. It seemed therefore important to develop a synthetic procedure for upper rim 1,2-difunctionalized calix[4]arene derivatives, which eventually would allow the synthesis of novel receptors and catalysts having recognition or catalytic groups in proximal positions.

In this chapter the synthesis of 1,2-diformyl-tetraalkoxycalix[4]arenes is reported. These are key intermediates for the synthesis of more complex calix[4]arenes, substituted in proximal positions.

Moreover, recently it has been shown that dinuclear Ba^{2+} complexes of bis-crown homoditopic ligands can catalyze with turnover the ethanolysis of esters equipped with a carboxylate function.³⁻⁵ It seemed of interest to investigate the catalytic activity of similar dinuclear Ba^{2+} complexes built on a calix[4]arene platform.

The synthesis of novel homodinuclear calix[4]arene ligands **8** and **9**, where the azacrowns are respectively located in proximal or diametral positions are reported, together with the catalytic activity of their Ba^{2+} complexes in the ethanolysis of esters endowed with a carboxylate function. This is the first example of a direct comparison between diametral and proximal calix[4]arene supramolecular catalysts.



4.2 Upper rim 1,2-difunctionalization of calix[4]arenes

The (selective) formylation of calix[4]arenes is one of the most useful methods of upper rim functionalization^{6;7} and has allowed the synthesis of a large variety of host molecules.⁸⁻¹⁰ Nevertheless, the 1,2-diformyl tetraalkoxycalix[4]arene derivatives in

the cone conformation are a class of compounds practically unknown, in line with the general difficulties encountered in calix[4]arene chemistry in obtaining proximal upper rim difunctionalized derivatives. Among these compounds, in fact, only the 1,2-dibromo,^{11;12} 1,2-dinitro¹³⁻¹⁷ and 1,2-bis(chloromethyl)⁷ derivatives have been described. A very recent report on the Gross formylation of calix[4]arene tetraethers using different reaction conditions¹⁸ confirmed the earlier observations¹⁹ of a preference in the diametral over the proximal diformylation. The formylation of calixarenes is usually carried out using hexamethylenetetramine (HMTA) in trifluoroacetic acid (TFA),²⁰ if exhaustive functionalization is required. On the other hand, the Gross formylation (TiCl_4 or $\text{SnCl}_4/\text{Cl}_2\text{CHOCH}_3$)²¹ allows us to obtain, in some cases, a remarkable control on the partial functionalization. The selective diametral (1,3) diformylation of calix[4]arene 1,3-diethers can be easily achieved using the Gross method²² since the phenolic aromatic nuclei are more reactive than the corresponding ethers (transfer of selectivity from the lower to the upper rim). Much more difficult is the control in the upper rim formylation of calix[4]arene tetraethers, although in some cases good yields of upper rim 1,3-diformylated calix[4]arene tetraethers have been obtained.^{18;19;23}

The synthesis of upper rim 1,2-difunctionalized calix[4]arenes could potentially be carried out through the transfer of selectivity from the lower rim of 1,2-dialkoxy calix[4]arenes or by the direct selective upper rim functionalization of calix[4]arene tetraethers (Figure 4.1).

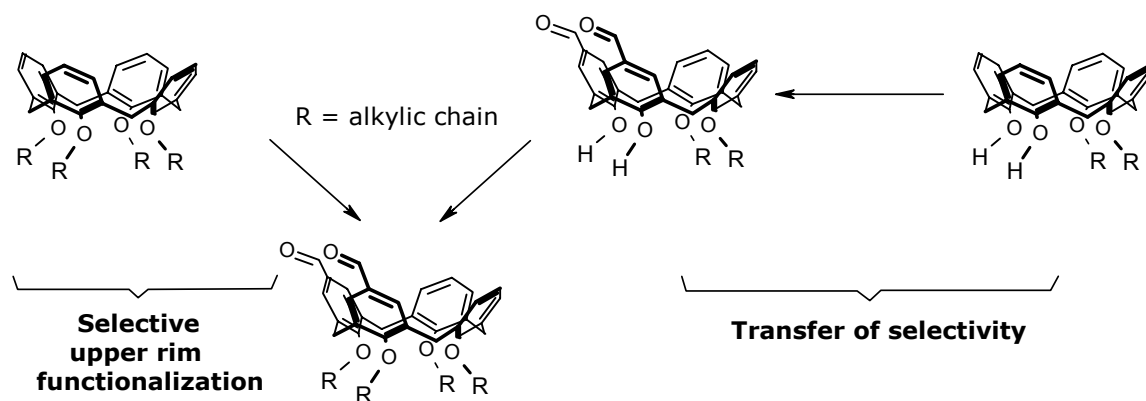
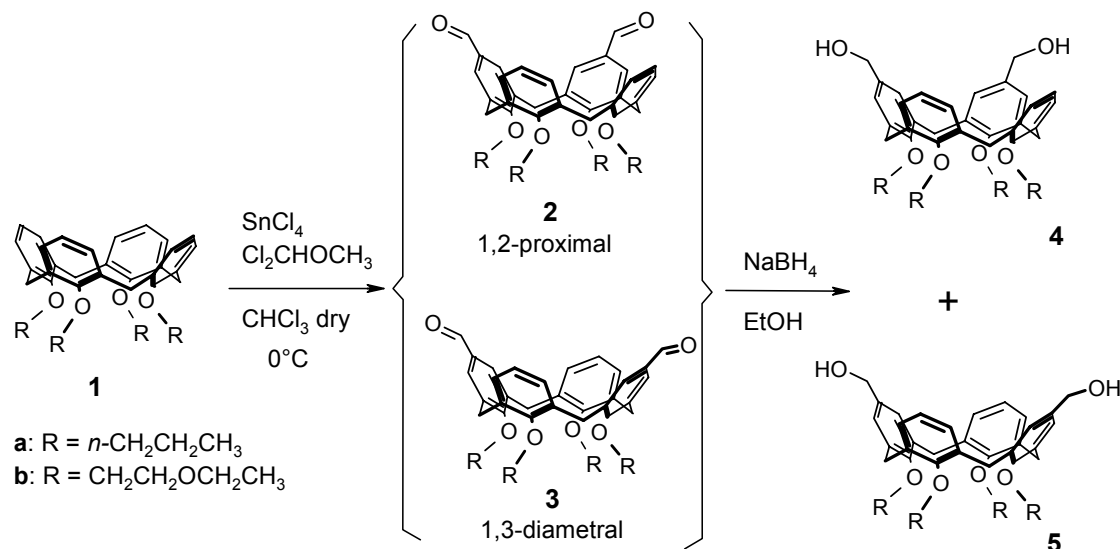


Figure 4.1

The first method requires the synthesis of calix[4]arenes 1,2-dialkylated at the lower rim which can be obtained only in moderate yields.²⁴ Moreover, the subsequent O-alkylation of the phenolic nuclei substituted in the *para*-positions with groups, such as formyl, may be hampered by stability and stereochemical problems. In fact, the strongly basic conditions (NaH, DMF) used in the alkylation and required to obtain the cone conformation may give partial decomposition of the -CHO groups. Moreover, it

has been observed that the presence of electron-withdrawing groups in *para*-position of the phenolic nuclei^{25;26} tends to favour the formation of non-cone isomers. We therefore decided to reinvestigate the direct formylation of selected tetraalkoxycalix[4]arenes **1a,b** in the cone structure, in order to find the best conditions to obtain 1,2-diformylated derivatives **2**.



Scheme 4.1

We have conducted the formylation reaction of **1b** under different conditions (temperature, equivalents of Lewis acid and Cl₂CHOCH₃) and found that by reacting **1b** at 0°C with 15 equiv. of SnCl₄ and Cl₂CHOCH₃ (Scheme 4.1) the more common 1,3-diformylation reaction is somewhat decreased and the 1,2-diformylated derivative **2b** is formed in significant amounts. By integration in the ¹H NMR spectrum of the –CHO signals of compounds **2b** (δ 9.65) and **3b** (δ 9.59) it was possible to calculate the ratio of 40/60 between the two isomers (Entry 1, Table 4.1). The reaction of tetrapropoxycalix[4]arene **1a** under the same conditions (Entry 2, Table 4.1) afforded a large amount of tri- and tetraformylated calixarene. A substantial decrease of the equivalents of SnCl₄ and Cl₂CHOCH₃ (Entry 3, Table 4.1) gave a statistical mixture of diametral and proximal diformyl derivatives **2a/3a** (65/35) in 30% yield. A similar reduction of the amount of formylating agents with respect to **1b** (Entry 4, Table 4.1) caused a drop in reactivity, since only 40% of reagent was converted to monoformyl calixarene. This seems to indicate that the Lewis acid is bound to the more coordinating ethoxy-ethoxy chains at the lower rim of calixarene **1b**, thus decreasing the reactivity and influencing the regiochemistry of the reaction.¹⁹ On the other hand, the propoxy groups of **1a** do not coordinate SnCl₄ to the same extent and a nearly statistical ratio **2a/3a** is thus obtained. Increases in the reaction temperature or

changing for Duff formylation conditions (Entry 5, Table 4.1) gave only an increase of polysubstituted (tri- and tetraformylated) compounds and a decrease in the **2/3** ratio.

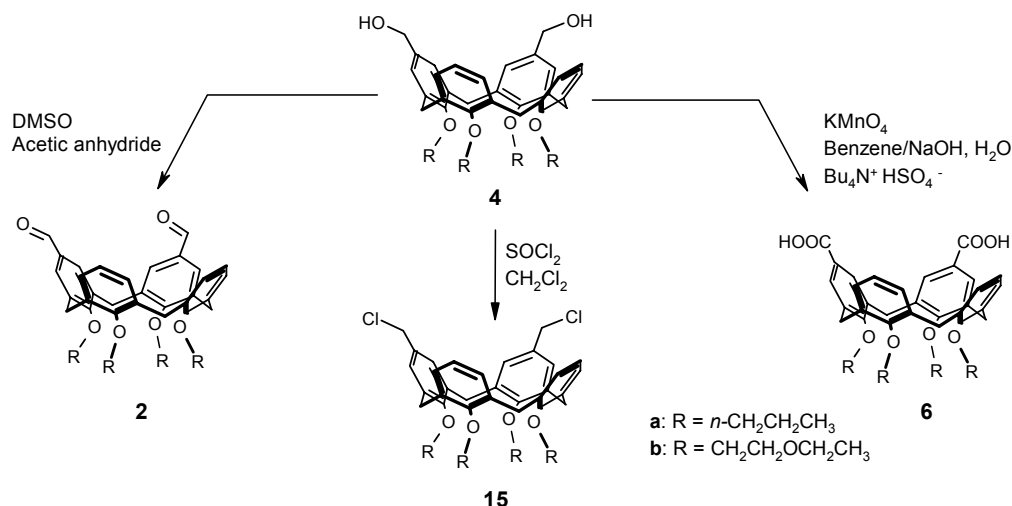
Table 4.1 Formylation of tetraalkoxycalix[4]arenes **1** with SnCl_4 and $\text{Cl}_2\text{HCOCH}_3$ at 0°C in dry CHCl_3 .

Entry	Calix[4]arene	eq. SnCl_4 / eq. $\text{Cl}_2\text{HCOCH}_3^\ddagger$	Yield %				Relative ratio % 2/3
			mono ^{19;27}	tri ^{19;28}	tetra ^{19;29}	(2+3)	
1	1b	15/15	30	5	0	48	40/60
2	1a	15/15	0	30	65	5	§
3	1a	3/3	40	15	0	30	65/35
4	1b	3/3	40 [†]	0	0	0	n.a.
5	1b	#	0	70	5	20	15/85

10 eq. of HMTA in CF_3COOH at 50°C for 15h; [†] 60% of **1b** was also recovered;

§ not determined; [‡] with respect to 1 equiv. of **1a,b**;

n.a. = not applicable.



Scheme 4.2

All attempts to separate **2** from **3** by chromatography failed. However, reduction of the mixture with NaBH_4 in ethanol quantitatively afforded the dialcohols **4** and **5**, which could be separated by column chromatography. Swern oxidation of the isolated dialcohols **4a** and **4b** gave the 1,2-diformylated derivatives **2a,b** in 85-88% yield. Oxidation with KMnO_4 under phase transfer conditions gave the carboxylic acids **6a,b** in 85-90% yield (Scheme 4.2).

The NMR spectra of dialcohols **4a** and **4b** do not clearly reveal the 1,2 substitution pattern of the calixarenes. In both **4a** and **4b** we observe only one doublet for each of the protons of the methylene bridges, instead of expected three signals. The main difference with their 1,3-regioisomeric compounds is in the aromatic region of the ^1H NMR spectra. As observed for similar compounds,³⁰ the diametral alcoholic functions in

5 can form intramolecular hydrogen bonds in apolar solvents such as CDCl_3 , forcing the calixarene skeleton to assume a closed flattened cone conformation. In this structure the substituted aromatic rings are almost parallel and their protons are in the shielding cone of the two flattened unsubstituted aromatic rings. Therefore, there are two groups of signals for the aromatic protons of **5a** and **5b**. A singlet for the substituted ring at higher field ($\delta = 6.4$) and a doublet and a triplet at lower field ($\delta \approx 6.9$ and 6.8). In the case of the 1,2-difunctionalized calix[4]arenes the distance between the two alcoholic groups does not allow the formation of intramolecular hydrogen bonds and the calix[4]arene assumes a more regular cone conformation. As a result, the aromatic protons have similar chemical shifts giving a multiplet between 6.65 and 6.55 ppm. The more regular cone conformation of **4** compared to **5** is also confirmed by the chemical shift of the ArCH_2OH methylene groups. In the case of the proximal 1,2-disubstituted dialcohols **4**, this signal is 0.15 ppm downfield compared to the corresponding diametral 1,3-disubstituted compounds **5**. On the contrary, the proximal substitution pattern is very clear in the ^1H NMR spectra of the two diformyl derivatives **2a,b**. This is especially true for the signals of the methylene bridges that are diagnostic of the calix[4]arene symmetry. As a result of the plane of symmetry present in the molecule, three doublets for the axial and three doublets for the equatorial protons of the methylene bridges are present. Moreover, in the case of **2a**, the aromatic protons of the substituted rings at 7.14 and 7.12 ppm show a *meta* coupling ($J = 1.8$ Hz) (Figure 4.2). A similar ^1H NMR pattern is also exhibited by the 1,2-diacids **6a,b**.

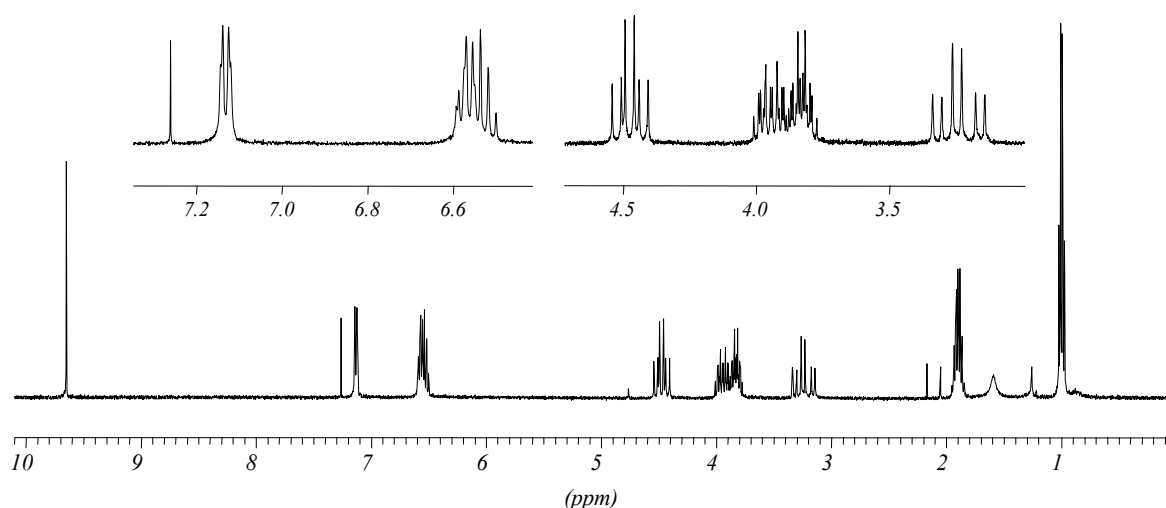
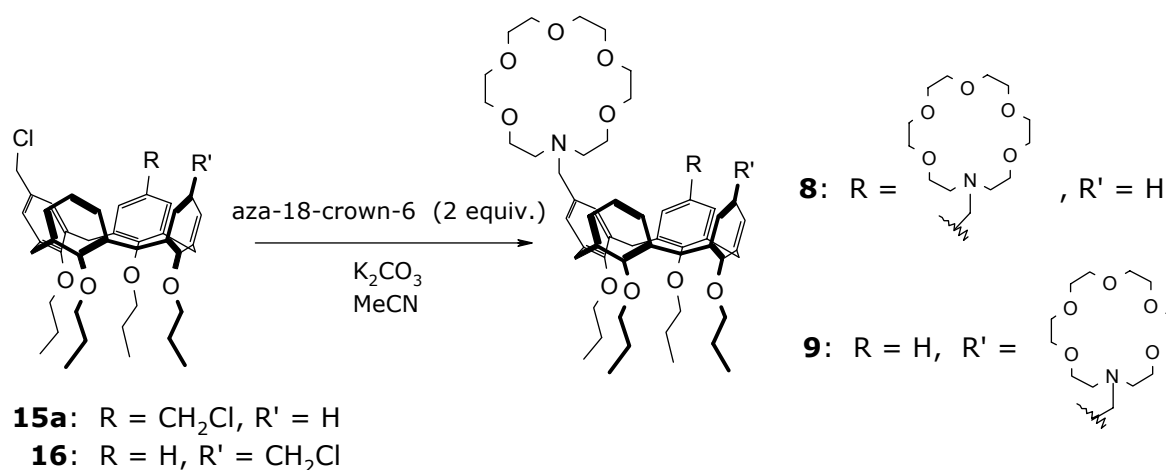


Figure 4.2 ^1H NMR spectrum of compound **2a** in CDCl_3 (400 MHz, 298 K), with expanded aromatic and methylene proton regions.

4.3 Synthesis of bis(monoaza-18-crown-6)calix[4]arenes

The isolation of 1,2-hydroxymethyl calix[4]arenes **4a,b** allowed the synthesis of calixarene based catalysts bearing the ligands in proximal positions. As depicted in Scheme 4.3, two monoaza-18-crown-6 were attached to the calixarene platform in proximal (1,2) and diametral (1,3) positions, giving the regioisomeric ligands **8** and **9** respectively. The synthesis of these two isomeric homoditopic calix[4]arenes was carried out with the aim of studying and comparing the catalytic activity of their Ba^{2+} complexes in the basic ethanolysis of esters **11-14**, in which the distance between the carboxylate anchoring group and the reaction site increases in the given order. A comparison with the activity of the dinuclear Ba^{2+} complex of the closely related ligand **10**³ should give information about the usefulness of the calixarene scaffold in the preorganization of the catalytic groups, while the comparison with the monometallic ligand **7**-[Ba] should furnish an assessment of the synergism of the two metals in the corresponding bimetallic complexes.

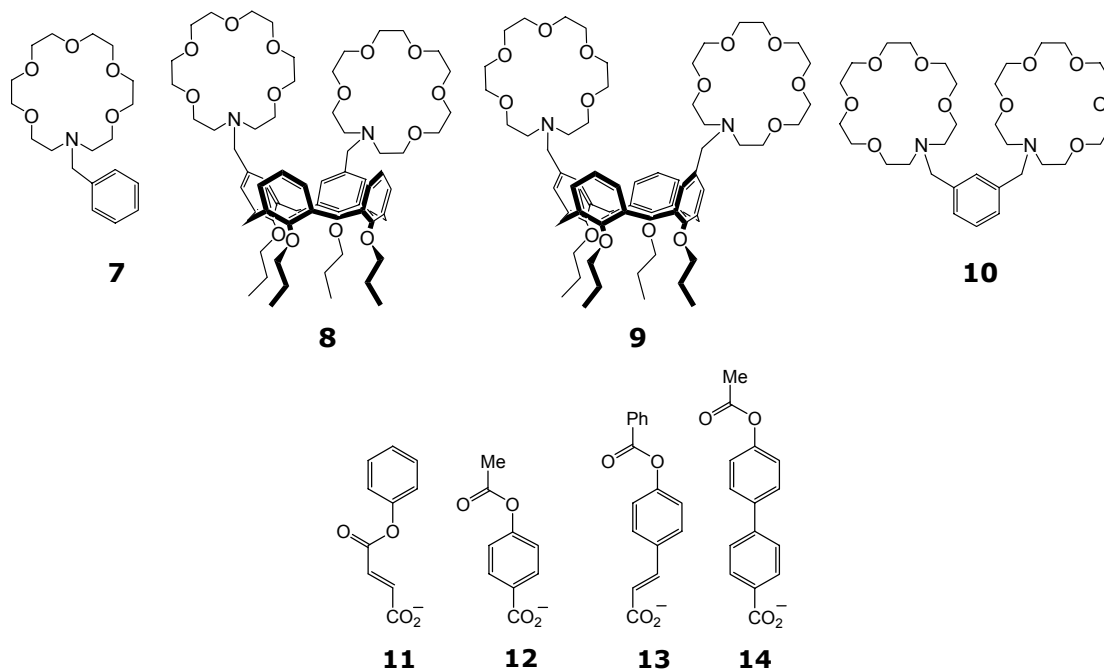
The reaction of dialcohols **4a** and **5a** with thionyl chloride in dichloromethane for 2 h gave the corresponding bis(chloromethyl)calix[4]arenes **15a** and **16** in quantitative yield. Reaction of these compounds **15a** and **16** with 2 equiv. of 1-aza-18-crown-6 in the presence of K_2CO_3 in MeCN gave ligands **8** and **9**, respectively, in good yields (Scheme 4.3).



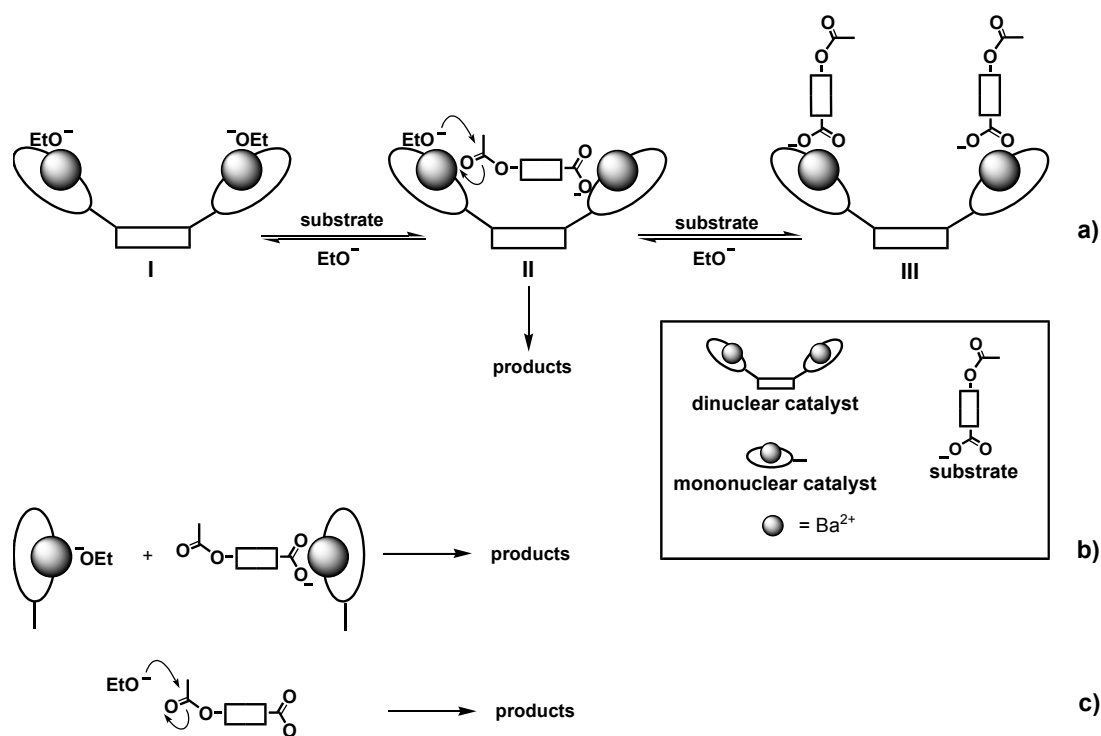
Scheme 4.3 Synthesis of ligands **8** and **9**.

4.4 Catalysis

The catalytic activity of the Ba^{2+} complexes of compounds **7-10** was investigated in the basic ethanolysis of esters **11-14**.³¹



Barium complexes were prepared *in situ* by mixing equivalent amounts of the ligands **7-10** and $\text{Ba}(\text{SCN})_2$. The solutions of these complexes used for rate measurements were 0.20 mM for the monotopic ligand **7** or 0.10 mM for the ditopic ligands **8-10**, 0.20 mM $\text{Ba}(\text{SCN})_2$ and 1.00 mM EtONMe_4 . As shown by Mandolini and coworkers,^{3,4} using similar systems devoid of the calix[4]arene unit, under the given conditions complexation of Ba^{2+} to the crown ether moieties is virtually complete, and EtO^- forms a tight ion pair with the complexed cation (structure **I** in Scheme 4.4). Addition of a substrate endowed with a carboxylate anchoring group converts **I** into the productive (Michaelis) complex **II**, with an equilibrium constant of 65.³ Since in all of the kinetic experiments the substrate concentration was 0.025 mM, the conditions of the kinetic runs were close to saturation, with no less than 90% of the substrate bound to the catalyst, and with a negligible formation of the 2:1 substrate-catalyst unproductive complex **III**.



Scheme 4.4 a) Mechanism of ester ethanolysis catalyzed by dinuclear barium complexes, showing productive (**II**) and non-productive (**I** and **III**) species, b) the corresponding intermolecular model reaction based on mononuclear complexes, and c) background reaction.

4.4.1 Rate accelerations and synergism factors

The kinetics was monitored spectrophotometrically at 25 °C following the increase of phenoxide concentration with time (a typical kinetic run is plotted in Figure 4.3); they show in all cases good adherence to first-order time dependence. The low substrate/catalyst ratio avoids important product inhibition effects in the reaction.

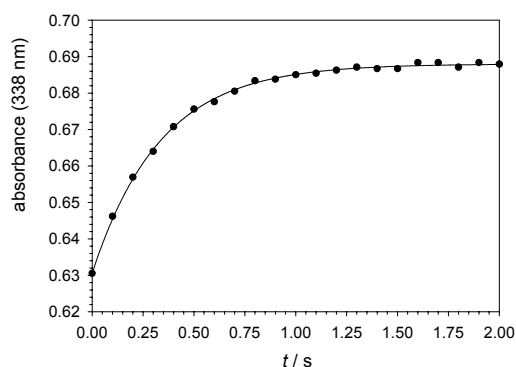


Figure 4.3 UV-Vis monitored product formation in the basic ethanolysis of **13** in the presence of $\mathbf{8} \cdot [\text{Ba}]_2$.

Catalytic rate constants (k_{obs}) for the ethanolysis of esters **11-14** obtained in the presence of catalysts based on aza-18-crown-6 are listed in Table 4.2. The other quantities listed in Table 4.2 are different ways to express the catalytic efficiency:

k_{obs}/k_0 is the rate acceleration over the background ethanolysis brought about by the various catalysts;

$k_{\text{obs}}^{\text{di}}/k_{\text{obs}}^{\text{mono}}$ is the degree of synergism between metal centers in the dinuclear catalysts.

Table 4.2 Basic ethanolysis of esters **11-14** catalyzed by the Ba^{2+} complexes of ligands **7-10**.^[a]

Entry	Substrate	Catalyst	k_{obs} (s^{-1})	k_{obs}/k_0 ^[b]	$k_{\text{obs}}^{\text{di}}/k_{\text{obs}}^{\text{mono}}$	EM ^[c] (M)
1	11	7 -[Ba]	0.040	300		
2		8 -[Ba] ₂	4.7	35100	120	0.036
3		9 -[Ba] ₂	0.18	1340	4.5	0.0014
4		10 -[Ba] ₂	0.37	2760	9.2	0.0028
5	12	7 -[Ba]	0.018	20		
6		8 -[Ba] ₂	20	22000	1100	0.51
7		9 -[Ba] ₂	0.38	420	21	0.010
8		10 -[Ba] ₂	1.08	1220	61	0.028
9	13	7 -[Ba]	0.0078	52		
10		8 -[Ba] ₂	3.0	20000	385	0.22
11		9 -[Ba] ₂	0.086	570	11	0.006
12		10 -[Ba] ₂	0.64	4240	82	0.046
13	14	7 -[Ba]	0.016	12		
14		8 -[Ba] ₂	0.22	170	14	0.0026
15		9 -[Ba] ₂	0.032	24	2	0.0004
16		10 -[Ba] ₂	0.40	300	25	0.0047

[a] Runs carried out in EtOH at 25°C on 0.025 mM substrate in the presence of 1.00 mM EtONMe₄, 0.20 mM monotopic or 0.10 mM ditopic ligand, and 0.20 mM Ba(SCN)₂. [b] k_0 is the pseudo-first-order rate constant observed in the presence of 1.00 mM EtONMe₄ alone. Ester **11**, $k_0 = 1.34 \times 10^{-4} \text{ s}^{-1}$; ester **12**, $k_0 = 9.1 \times 10^{-4} \text{ s}^{-1}$; ester **13**, $k_0 = 1.51 \times 10^{-4} \text{ s}^{-1}$; ester **14**, $k_0 = 1.32 \times 10^{-3} \text{ s}^{-1}$. [c] Calculated as $k_{\text{obs}}/k_{\text{inter}}$. The k_{inter} values ($\text{M}^{-1} \text{ s}^{-1}$) listed below for the various substrates were measured under the set of conditions given in reference [34]: **11**, 130; **12**, 39; **13**, 14; **14**, 85.

In line with previous observations,³⁻⁵ solutions containing the metal complexes showed in all cases enhanced rates of ethanolysis compared with solutions containing EtONMe₄ alone (background ethanolysis). Rate-enhancing factors ranged from one to more than four orders of magnitude, with a marked dependence on the individual substrate-catalyst combinations.

The mononuclear complex caused rate accelerations on the order of 10- to 50-fold (entries 5, 9, and 13 in Table 4.2), with the exception of ester **11**, whose ethanolysis rate increased 300-fold in the presence of **7**-[Ba] (entry 1 in Table 4.2). As previously noted,³ binding of the metal ion to carboxylate transforms a moderately electron-releasing (rate-retarding) substituent into an electron-withdrawing (rate-enhancing) one. In accordance with this idea, the much higher sensitivity of the reaction of **11** to the electron-withdrawing influence of the Ba²⁺-paired carboxylate can be attributed to the fact that in **11** the carboxylate-carbonyl distance is the shortest in the series of the investigated esters.

The superiority of dinuclear catalysts compared with their mononuclear counterpart shows that in all cases the two metal ions work together in a cooperative fashion, in accordance with the catalytic mechanism depicted in Scheme 4.4. The $k_{obs}^{di}/k_{obs}^{mono}$ ratios range from the very low value of 2 observed in the cleavage of **14** by **9**-[Ba]₂ (Table 4.2, entry 15), to the remarkably high values of 1100 (Table 4.2, entry 6) for the reaction of **12**, catalyzed by **8**-[Ba]₂.

4.4.2 Effective Molarities

Since the dinuclear catalysts transform an otherwise intermolecular reaction between ester and ethoxide into an intramolecular (intracomplex) reaction, the Effective Molarity (*EM*) concept^{32;33} strictly applies to the catalytic process at hand.

The effective molarity, defined as the ratio k_{intra}/k_{inter} , can then be easily calculated from the ratio of the pseudo-first-order rate constant k_{cat} of the intracomplex process and the second order rate constant k_2^{inter} of the analogous intermolecular model reaction [Equation (1)]. The value of k_2^{inter} is given by the ratio of the pseudo-first-order rate constant obtained in the presence of the mononuclear complex (k_{obs}^{mono}) and the concentration of the reactant (**7**-Ba²⁺·EtO⁻).³⁴

$$EM = \frac{k_{cat}}{k_2^{inter}} = \frac{k_{cat}}{\frac{k_{obs}^{mono}}{(\mathbf{7}\text{-[Ba]}\cdot\text{EtO}^-)}} \quad (1)$$

Under the reaction conditions for the data reported in Table 4.2, at least 90% of the substrate is bound to the catalyst, therefore k_{cat} equals almost $k_{\text{obs}}^{\text{di}}$ and thus, in first approximation, EM values can be calculated from Equation (2).

$$EM \sim \frac{k_{\text{obs}}^{\text{di}}}{\frac{k_{\text{obs}}^{\text{mono}}}{(7\text{-[Ba]}\cdot\text{EtO}^-)}} \quad (2)$$

While the degree of synergism $k_{\text{obs}}^{\text{di}}/k_{\text{obs}}^{\text{mono}}$ is a function of the reaction conditions (it depends, *inter alia*, on the concentration), the EM value is an intrinsic property of the system that does not depend on the experimental conditions, but only on the molarity in concentration units.

A graphical illustration of the requirements of catalysis in terms of substrate size and catalyst structure, as well as a panoramic view of the varying catalytic efficiency observed for the different substrate-catalyst pairs is given by plots of EM vs. the carboxylate-carbonyl distance in the ester substrate, taken between the carbon atoms of the two functions (Figure 4.4).

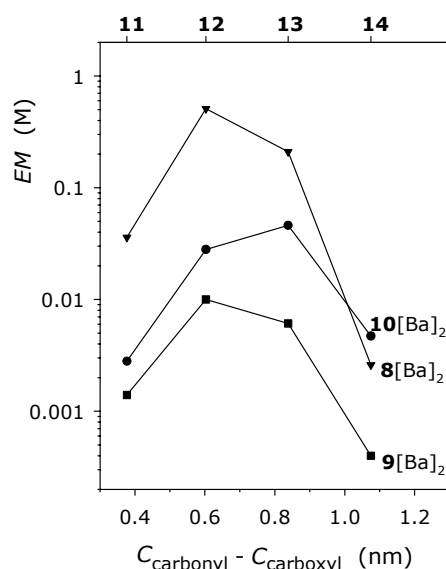


Figure 4.4 EM profiles for reaction of substrates **11-14** in the presence of dinuclear catalysts based on aza-crown ligands.

The first observation is that the proximal dinuclear catalyst **8**-[Ba]₂ is in all cases superior to its diametral regioisomer **9**-[Ba]₂. The EM profile shows that the catalytic efficiency of **8**-[Ba]₂ reaches its maximum value in the reaction of ester **12**, and drops dramatically to a very low value in the reaction of the "longest" ester **14**, which would

indicate that catalyst **8**-[Ba]₂ cannot expand its intermetal distance to fit the long carboxylate-carbonyl distance in **14**.

Thus, a good match of the ester's carboxylate-carbonyl distance to the catalyst intermetal distance plays a key role in determining catalytic efficiency. Moreover, the dependence of the *EM* on the carboxylate-carbonyl distance is similar for the two calixarene based catalysts. Ester **12** is the best substrate for both catalysts, yet the reaction catalyzed by the proximal regioisomer **8**-[Ba]₂ is 53 times faster than the reaction catalyzed by the diametral regioisomer **9**-[Ba]₂. A careful inspection of molecular models of the complexes between the catalysts and the tetrahedral intermediate involved in the methanolysis of **12** fails to reveal the reasons for the catalytic superiority of the proximal regioisomer. Clearly, in addition to the purely geometrical match of ester size to intermetal distance, there are other factors, but their origin defies a simple explanation. They are possibly related to conformational effects in the catalysts and/or steric repulsions in the host-guest complexes between catalyst and transition state.

The *EM* values in Table 4.2 are much lower than the remarkably high values, amounting to several orders of magnitude, usually reported for intramolecular processes involving small and medium sized cyclic species.^{32;33;35} The number of skeletal single bonds in the bifunctional chain molecules undergoing cyclization has an important influence on the efficiency of intramolecular processes because a part of the torsional entropy is lost upon cyclization. A general treatment proposed by Mandolini some years ago relates the entropy loss upon cyclization and hence the entropic component of the *EM* to the number of rotatable bonds in the open chain reactant.³³ Such a treatment was recently extended to the reactions of supramolecular ternary complexes³⁶ and is applied to the catalytic processes described here.

If one regards the carboxylate-metal-(crown ether) and ethoxide-metal-(crown ether) moieties as pseudo-single-bonds, there are 9 rotatable bonds in the productive complex involved in the ethanolysis of **12** catalyzed by **8**-[Ba]₂ and 10 rotatable bonds in the reaction of **13** catalyzed by **8**-[Ba]₂. Based on the admittedly rough assumption that the torsional entropy associated to such pseudo-bonds is comparable to that of a covalent bond, the above numbers of rotatable bonds translate into an *EM* value of 0.67 M for the reaction of the **12**-**8**-[Ba]₂ pair and one of 0.47 M for the reaction of the **13**-**8**-[Ba]₂ pair. These values compare remarkably well with the experimental values of 0.51 M and 0.22 M (Table 4.2).

The close adherence of experimental and predicted values strongly suggests that a virtually ideal match between bimetallic catalyst and transition state is achieved in the given catalytic processes, whose efficiency is solely determined by the relatively large entropy losses due to the involvement of several rotatable bonds. In all the other

cases, the lower-than-predicted *EM* values may be taken as a strong indication of the existence of a more or less pronounced mismatch between catalyst and transition state.

4.4 Conclusions

By varying the reaction temperature and the ratio of reagents and catalyst in the Gross formylation, conditions have been found which give reasonable amount of 1,2-diformylated tetraalkoxycalix[4]arenes. They were, for the first time, isolated in a pure form and characterized together with the corresponding 1,2-dialcohols, 1,2-diacids and 1,2-dichlorides, that can be considered important calix[4]arene intermediates for the synthesis of more complex receptors and catalysts bearing functions in proximal positions.

Starting from the 1,2- and 1,3-dihydroxymethyl calix[4]arenes **4a** and **5a**, two novel regioisomeric calix[4]arene derivatives **8** and **9**, bearing two aza-18-crown-6 units at proximal or respectively diametral positions of the upper rim, were synthesized. The catalytic activities of their dinuclear Ba²⁺ complexes were investigated in the ethanolysis of esters **11-14**, endowed with a carboxylate anchoring group, revealing that: (i) the two metal ions in the dinuclear catalysts work together in a cooperative fashion;^{37;38} (ii) the proximal calix[4]arene catalyst **8** is by far superior to its diametral regioisomer **9** in the ethanolysis of all the investigated esters; (iii) the distance between the carboxylate and ester carbonyl groups influences the reactivity of the catalytic ester cleavage in a way that is decidedly suggestive of the importance of a good match between substrate size and metal-to-metal distance.

However, other factors, whose origin is still poorly understood, may come into play. This is most likely the case with the calixarene-based catalysts **8** and **9**. The superiority of **8** relative to **9** with all of the esters **11-14** can hardly be ascribed to more suitable intramolecular distances in the former, providing an indication that additional, still poorly understood effects, may contribute significantly to catalytic efficiency.

The number of rotatable bonds in the productive complexes of catalysts and reactants sets upper limits to catalytic efficiency, to be reached under conditions in which strain effects are unimportant. Interestingly, such upper limits imposed by entropic restrictions were practically reached in a number of cases, namely, the reactions of the **12 8**-[Ba]₂ and **13 8**-[Ba]₂ pairs. The lower *EMs* recorded for the remaining substrate-catalyst combinations would probably indicate the existence of more or less pronounced distortions from ideal geometry in the productive complexes.

However, considering the best substrate-catalyst complexes **12-8**·[Ba]₂ and **13-8**·[Ba]₂ the calculated EM values, 0.51 and 0.22 mol/L respectively, are those typical for the cyclization of 10-12 membered chains. This means that, even showing very high synergy factors, the catalyst **8**·[Ba]₂ is still far from the enzyme systems that work with EM values typical of a cyclization of 3 or 5-6 membered chains (10³-10⁸ mol/L).

The obtained synthetic results allowed, for the first time, a comparison of the catalytic activity of diametral (1,3) calix[4]arene catalysts with their proximal (1,2) analogues.

4.5 Experimental part

General Information: Electrospray ionization (ESI) and chemical ionization (CI) mass spectra were recorded on a Micromass ZMD and on a Finnigan Mat SSQ710 spectrometer, respectively. FAB-MS spectra were recorded with a Finnigan MAT 90 spectrometer using *m*-NBA as a matrix. ¹H NMR and ¹³C NMR spectra were recorded on Bruker AC300 and Bruker AMX400 spectrometers at 300 K. Chemical shifts (δ) are reported in ppm downfield from TMS used as internal standard. Analytical TLC was performed using Merck prepared plates (silica gel 60 F-254 on aluminium). Merck silica gel (40-63 μm) was used for flash chromatography. Melting points were determined on an electrothermal apparatus in capillaries sealed under nitrogen.

Materials: All moisture sensitive reactions were carried out under nitrogen atmosphere. Most of the solvents and all reagents were commercial and used without further purification. All dry solvents were prepared according to standard procedures and stored over molecular sieves. Bis(chloromethyl)calix[4]arene **16**³⁹ and acid **14**·H⁺⁴⁰ were prepared as described in the literature. Ligands **10**,³ and **7**³ and acids **11**·H⁺,⁴ **12**·H⁺,³ **13**·H⁺,⁴ were available from previous investigations.

Formylation of calix[4]arenes **1a,b** and isolation of the mixture of **5,11-(2)** and **5,17-diformyl calix[4]arenes (3)**

The tetraalkylated calix[4]arene **1a,b** (2 g) were dissolved in 100 mL of dry chloroform and the solution, kept under N₂, was cooled to 0 °C with an ice bath. After 15 min Cl₂CHOCH₃ and SnCl₄ (3 eq. for **1a**; 15 eq. for **1b**) were added to the vigorously stirred solution. After 1.5 h the reaction mixture was poured in 300 mL of 1N HCl and the solution was stirred for 2 h. After the addition of 150 mL of CH₂Cl₂, the organic phase was separated and washed twice with water, dried over Na₂SO₄ and filtered. The solvent was evaporated under reduced pressure and the mixture of **2** and **3** was obtained after purification by column chromatography (eluent: Hex/EtOAc

8.8/1.2 for the tetrapropoxy derivatives; Hex/EtOAc 7/3 for the tetraethoxyethoxy derivatives). For yields see Table 4.1.

5,11-Bis(hydroxymethyl)-25,26,27,28-tetrapropoxycalix[4]arene (4a)

A 0.45 g (0.691 mmol) sample of the 1,3-(**3a**) and 1,2-(**2a**) diformyl tetrapropoxycalix[4]arene mixture was dissolved in absolute EtOH. NaBH₄ (79 mg, 2.07 mmol) was added and the solution was stirred for 3h. The solvent was evaporated under reduced pressure, the solid was dissolved in CH₂Cl₂ (100 mL) and the resulting solution washed with water (2×100 mL). The organic layer was separated and the solvent removed under vacuum. The residue was submitted to column chromatography (CH₂Cl₂/EtOAc/Hex, 2/2/3) obtaining the 1,3-dialcohol **5a** (151 mg) and the 1,2-dialcohol **4a** (257 mg) derivatives. **4a**: Mp = 139.8 °C. ¹H NMR (300 MHz; CDCl₃): δ 6.65-6.56 (m, 10H, ArH), 4.45 (d, 4H, ArCH₂Ar ax, J = 13.4 Hz), 4.33 (s, 4H, ArCH₂OH), 3.85 (t, 4H, ArOCH₂, J = 7.6 Hz), 3.84 (t, 4H, ArOCH₂, J = 7.4 Hz), 3.14 (d, 4H, ArCH₂Ar eq, J = 13.4 Hz), 1.95-1.87 (m, 8H, ArOCH₂CH₂), 1.00 (t, 6H, CH₂CH₃, J = 7.5 Hz), 0.99 (t, 6H, CH₂CH₃, J = 7.4 Hz). ¹³C NMR (75 MHz; CDCl₃): δ 156.7, 156.3, 135.2, 135.1, 134.4, 128.2, 127.4, 127.3, 121.6, 76.7, 65.2, 31.0, 23.3, 10.3. MS (CI) *m/z* (%): 652.3 (100) [M]⁺. Anal. Calcd for C₄₂H₅₂O₆ (652.87): C, 77.27; H, 8.03. Found: C, 77.15; H, 8.19.

5,11-Bis(hydroxymethyl)-25,26,27,28-tetrakis(2-ethoxyethoxy)calix[4]arene (4b)

Compound **4b** was obtained using the same procedure reported for **4a**, starting from the mixture of the two diformyl tetraethoxyethyl derivatives (**2b+3b**). The residue was submitted to column chromatography (CH₂Cl₂/EtOAc/Hex, 5/5/1) obtaining the 1,3-dialcohol **5b** (448 mg) and the 1,2-dialcohol **4b** (290 mg) derivatives. Compound **4b** is a colourless oil. ¹H NMR (300 MHz; CDCl₃): δ 6.58-6.47 (m, 10H, ArH), 4.43 (d, 4H, ArCH₂Ar ax, J = 13.5 Hz), 4.24 (s, 4H, ArCH₂OH), 4.04 (t, 8H, ArOCH₂, J = 6.0 Hz), 3.76 (t, 8H, ArOCH₂CH₂, J = 6.0 Hz), 3.47 (q, 8H, ROCH₂CH₃, J = 6.9 Hz), 3.07 (d, 4H, ArCH₂Ar eq, J = 13.5 Hz), 1.12 (t, 12H, ROCH₂CH₃, J = 6.9 Hz). ¹³C NMR (75 MHz; CDCl₃): δ 156.4, 156.1, 135.2, 135.1, 135.0, 134.5, 128.2, 127.3, 121.9, 73.2, 69.6, 66.3, 65.2, 30.8, 29.7, 15.3. MS (FAB+VE) *m/z* (%): 773.0 (100) [M+H]⁺. Anal. Calcd for C₄₆H₆₀O₁₀ (772.98): C, 71.48; H, 7.82. Found: C, 71.34; H, 7.94.

5,11-Diformyl-25,26,27,28-tetrapropoxycalix[4]arene (2a)

Acetic anhydride (65 μL, 0.68 mmol) was added to a stirred solution of 1,2-bis(hydroxymethyl)-calix[4]arene **4a** (21 mg, 0.0327 mmol) in 1mL of dry DMSO. The reaction mixture was stirred for 20 h at room temperature and then poured in 15 mL

of 1N NaOH aqueous solution. The aqueous phase was extracted with CH_2Cl_2 (3×15 mL) and the combined organic phases were dried over anhydrous Na_2SO_4 and filtered. The solvent was evaporated under reduced pressure and the residue was purified by column chromatography (Hex/EtOAc, 9/1). Yield 88%. ^1H NMR (400 MHz; CDCl_3): δ 9.65 (s, 2H, ArCHO), 7.14 (d, 2H, ArHCHO, $J_m = 1.8$ Hz), 7.12 (d, 2H, ArHCHO, $J_m = 1.8$ Hz), 6.60-6.50 (m, 6H, ArH), 4.52 (d, 1H, ArCH₂Ar ax, $J = 13.7$ Hz), 4.47 (d, 2H, ArCH₂Ar ax, $J = 13.4$ Hz), 4.42 (d, 1H, ArCH₂Ar ax, $J = 13.4$ Hz), 3.98 (dt, 1H, ArOCH_AH_B, $J^2 = 10.2$ Hz, $J^3 = 7.6$ Hz), 3.91 (dt, 1H, ArOCH_AH_B, $J^2 = 10.2$ Hz, $J^3 = 7.3$ Hz), 3.86 (dt, 1H, ArOCH_CH_D, $J^2 = 10.2$ Hz, $J^3 = 7.3$ Hz), 3.804 (dt, 1H, ArOCH_CH_D, $J^2 = 10.2$ Hz, $J^3 = 7.3$ Hz), 3.32 (d, 1H, ArCH₂Ar eq, $J = 13.7$ Hz), 3.24 (d, 2H, ArCH₂Ar eq, $J = 13.4$ Hz), 3.16 (d, 1H, ArCH₂Ar eq, $J = 13.4$ Hz), 1.93-1.86 (m, 8H, ArOCH₂CH₂), 1.07 (t, 6H, CH₂CH₃, $J = 7.6$ Hz), 0.99 (t, 6H, CH₂CH₃, $J = 7.6$ Hz). ^{13}C NMR (75 MHz; CDCl_3): δ 191.4, 162.2, 156.4, 136.5, 135.4, 135.2, 134.1, 131.0, 130.5, 129.8, 128.5, 128.0, 122.1, 76.7, 30.9, 23.3, 23.2, 10.2, 10.1. MS (ESI+) m/z (%): 671.3 (100) $[\text{M}+\text{Na}]^+$. Anal. Calcd for $\text{C}_{42}\text{H}_{48}\text{O}_6$ (648.84): C, 77.75; H, 7.46. Found: C, 77.63; H, 7.59.

5,11-Diformyl-25,26,27,28-tetrakis(2-ethoxyethoxy)calix[4]arene (2b)

Compound **2b** was obtained using the same procedure reported for **2a** and starting from the dialcohol **4b**. The residue was purified by column chromatography (Hex/EtOAc, 7/3). Yield 85%. ^1H NMR (300 MHz; CDCl_3): δ 9.65 (s, 2H, ArCHO), 7.17-7.13 (m, 4H, ArH), 6.61-6.50 (m, 6H, ArH), 4.64 (d, 1H, ArCH₂Ar ax, $J = 13.8$ Hz), 4.55 (d, 2H, ArCH₂Ar ax, $J = 13.7$ Hz), 4.46 (d, 1H, ArCH₂Ar ax, $J = 13.6$ Hz), 4.24-4.07 (m, 8H, ArOCH₂), 3.84-3.77 (m, 8H, ArOCH₂CH₂), 3.56-3.48 (m, 8H, ROCH₂CH₃), 3.30 (d, 1H, ArCH₂Ar eq, $J = 13.8$ Hz), 3.24 (d, 2H, ArCH₂Ar eq, $J = 13.7$ Hz), 3.15 (d, 1H, ArCH₂Ar eq, $J = 13.6$ Hz), 1.26-1.15 (m, 12H, CH₃R). ^{13}C NMR (75 MHz; CDCl_3): δ 191.5, 162.1, 156.2, 136.5, 135.6, 135.2, 134.2, 131.2, 130.6, 129.9, 128.6, 128.2, 122.5, 73.6, 73.2, 69.8, 69.6, 66.4, 30.8, 15.3, 15.2. MS (CI) m/z (%): 768.8 (100) $[\text{M}]^+$. Anal. Calcd for $\text{C}_{46}\text{H}_{56}\text{O}_{10}$ (768.95): C, 71.85; H, 7.34. Found: C, 71.97; H, 7.45.

5,11-Dicarboxy-25,26,27,28-tetrapropoxycalix[4]arene (6a)

To a solution of 1,2-dialcohol **4a** (30 mg 0.037 mmol) in benzene (4 mL) were added potassium permanganate (58 mg, 0.37 mmol), 8 mL of 6% NaOH aqueous solution and a catalytic amount of tetrabutylammonium hydrogen sulphate (2 mg, 0.006 mmol). The mixture was vigorously stirred at room temperature overnight. EtOAc (80 mL) and 1N HCl (80 mL) were added. The organic layer was separated, washed with water (80 mL) and dried over anhydrous Na_2SO_4 . Then the solvent was evaporated under reduced pressure obtaining a white solid. Yield: 85%; Mp > 300°C.

^1H NMR (300 MHz; CD_3COCD_3): δ 7.41 (d, 2H, ArH, $J_m = 2.3$ Hz), 7.40 (d, 2H, ArH, $J_m = 2.3$ Hz), 6.67-6.62 (m, 4H, ArH), 6.55 (dd, 2H, ArH, $J_1 = 7.6$ Hz, $J_2 = 6.8$ Hz), 4.58 (d, 1H, ArCH_2Ar ax, $J = 13.6$ Hz), 4.55 (d, 2H, ArCH_2Ar ax, $J = 13.5$ Hz), 4.52 (d, 1H, ArCH_2Ar ax, $J = 13.5$ Hz), 4.05-3.99 (m, 4H, ArOCH_2), 3.95-3.90 (m, 4H, ArOCH_2), 3.42 (d, 1H, ArCH_2Ar eq, $J = 13.6$ Hz), 3.32 (d, 2H, ArCH_2Ar eq, $J = 13.5$ Hz), 3.23 (d, 1H, ArCH_2Ar eq, $J = 13.5$ Hz), 2.05-1.95 (m, 8H, $\text{ArOCH}_2\text{CH}_2$), 1.09 (t, 6H, CH_2CH_3 , $J = 7.3$ Hz), 1.08 (t, 6H, CH_2CH_3 , $J = 7.3$ Hz). ^{13}C NMR (75 MHz; CD_3COCD_3): δ 166.8, 160.9, 156.7, 135.7, 135.4, 135.1, 134.7, 130.4, 130.1, 128.5, 128.1, 124.3, 122.1, 76.9, 76.7, 30.7, 23.4, 23.3, 9.9. MS (ESI-) m/z (%): 679.5 (100) $[\text{M-H}]^-$; 339 (50) $[\text{M-2H}]^{2-}$. Anal. Calcd for $\text{C}_{42}\text{H}_{48}\text{O}_8$ (680.84): C, 74.09; H, 7.11. Found: C, 73.95; H, 7.24.

5,11-Dicarboxy-25,26,27,28-tetrakis(2-ethoxyethoxy)calix[4]arene (6b)

Compound **6b** was obtained using the same procedure reported for **6a** and starting from the 1,2-dialcohol **4b**. Yield: 90%; Mp = 178°C; ^1H NMR (300 MHz; CD_3OD): δ 7.34 (s, 4H, ArH), 6.62-6.50 (m, 6H, ArH), 4.64 (d, 1H, ArCH_2Ar ax, $J = 13.8$ Hz), 4.60 (d, 2H, ArCH_2Ar ax, $J = 14.0$ Hz), 4.55 (d, 1H, ArCH_2Ar ax, $J = 14.1$ Hz), 4.25-4.17 (m, 4H, ArOCH_2), 4.15-4.08 (m, 4H, ArOCH_2), 3.90-3.86 (m, 8H, $\text{ArOCH}_2\text{CH}_2$), 3.62-3.53 (m, 8H, ROCH_2CH_3), 3.29 (d, 1H, ArCH_2Ar eq, $J = 13.8$ Hz), 3.23 (d, 2H, ArCH_2Ar eq, $J = 14.0$ Hz), 3.16 (d, 1H, ArCH_2Ar eq, $J = 14.1$ Hz), 1.24-1.17 (m, 12H, ROCH_2CH_3); ^{13}C NMR (75 MHz; CD_3OD): δ 162.6, 158.0, 137.2, 136.7, 136.6, 136.1, 131.9, 131.5, 129.9, 129.6, 123.7, 75.1, 74.8, 71.5, 71.4, 67.7, 32.2, 16.0; MS (CI) m/z (%): 800.8 (100) $[\text{M}]^+$. Anal. Calcd for $\text{C}_{46}\text{H}_{56}\text{O}_{12}$ (800.95): C, 68.98; H, 7.05. Found: C, 68.86; H, 7.20.

5,11-Bis(chloromethyl)-25,26,27,28-tetrapropoxycalix[4]arene (15a)

Thionyl chloride (2.2 mL, 3.0 mmol) was added to a solution of calix[4]arene **4a** (100 mg, 0.153 mmol) in CH_2Cl_2 (8 mL) and the reaction mixture was stirred for 2h. The solvent was removed under reduced pressure to give the dichloromethyl derivative **15a** (105 mg, 0.152 mmol, quantitative yield), which was pure enough for further modification. An analytically pure sample was obtained by extraction of a CH_2Cl_2 solution of **15a** with saturated NaHCO_3 aqueous solution, subsequently followed by drying the organic layer over anhydrous Na_2SO_4 , and removal of the solvent under vacuum.

^1H NMR (300 MHz, CDCl_3): δ 6.65-6.58 (m, 10H, ArH), 4.48 (d, 1H, ArCH_2Ar ax, $J = 13.3$ Hz), 4.47 (d, 2H, ArCH_2Ar ax, $J = 13.4$ Hz), 4.46 (d, 1H, ArCH_2Ar ax, $J = 13.4$ Hz), 4.33 (s, 4H, ArCH_2Cl), 3.89 (t, 4H, ArOCH_2 , $J = 7.1$ Hz), 3.87 (t, 4H, ArOCH_2 , $J = 7.4$ Hz), 3.18 (d, 4H, ArCH_2Ar eq, $J = 13.4$ Hz), 2.00-1.88 (m, 8H, $\text{ArOCH}_2\text{CH}_2$), 1.03

(t, 6H, CH_2CH_3 , $J = 7.6$ Hz), 1.02 (t, 6H, CH_2CH_3 , $J = 7.5$ Hz). ^{13}C NMR (75 MHz, CDCl_3): δ 156.6 (Ar ipso), 156.3 (Ar ipso), 135.6 (Ar ortho), 135.2 (Ar ortho), 135.1 (Ar ortho), 134.7 (Ar ortho), 130.6 (Ar para), 128.6 (Ar meta), 128.4 (Ar meta), 128.1 (Ar meta), 128.0 (Ar meta), 121.6 (Ar para), 76.6 (ArOCH_2), 46.7 (ArCH_2), 30.9 (ArCH_2Ar), 23.1 (OCH_2CH_2), 10.2 (CH_3). MS (CI) m/z (%): 688.3 (100) $[\text{M}]^+$, 690.3 (65) $[\text{M}+2]^+$. Anal. Calcd for $\text{C}_{42}\text{H}_{52}\text{O}_4\text{Cl}_2$ (691.78): C, 72.92; H, 7.57; Cl, 10.25. Found: C, 72.88; H, 7.53; Cl, 10.30.

5,11-Bis(chloromethyl)-25,26,27,28-tetrakis(2-ethoxyethoxy)calix[4]arene (15b)

Compound **15b** was obtained using the same procedure reported for **15a** and starting from 1,2-dialcohol **4b**. Colorless oil. Yield > 95%. ^1H NMR (300 MHz; CDCl_3): δ 6.62-6.56 (m, 10H, ArH), 4.49 (d, 4H, ArCH_2Ar ax, $J = 13.5$ Hz), 4.29 (s, 4H, ArCH_2Cl), 4.11 (t, 4H, ArOCH_2 , $J = 5.6$ Hz), 4.10 (t, 4H, ArOCH_2 , $J = 5.6$ Hz), 3.82 (t, 8H, $\text{ArOCH}_2\text{CH}_2$, $J = 5.6$ Hz), 3.54 (q, 8H, OCH_2CH_3 , $J = 7.0$ Hz), 3.14 (d, 4H, ArCH_2Ar eq, $J = 13.5$ Hz), 1.20 (t, 12H, CH_2CH_3 , $J = 7.0$ Hz). ^{13}C NMR (75 MHz; CDCl_3): δ 156.6, 156.3, 135.5, 135.2, 135.1, 134.7, 131.0, 128.6, 128.4, 128.2, 128.1, 122.0, 73.2, 73.1, 69.6, 66.3, 46.6, 30.8, 29.6, 15.2. MS (ES) m/z (%): 831.6 $[\text{M}+\text{Na}]^+$ (100). Anal. Calcd for $\text{C}_{46}\text{H}_{58}\text{Cl}_2\text{O}_8$ (809.87): C, 68.22; H, 7.22. Found: C, 68.31; H, 7.33.

5,11-Bis[N-(monoaza-18-crown-6)methyl]-25,26,27,28-tetrapropoxycalix[4]arene (8)

Potassium carbonate (53 mg, 0.383 mmol) and 1-aza-18-crown-6 (100 mg, 0.380 mmol) were added to a solution of the dichloro derivative **15a** (80 mg, 0.116 mmol) in dry MeCN (5 mL). The reaction mixture was heated at 60°C for three days under nitrogen atmosphere. The solvent was evaporated under reduced pressure and the crude product dissolved in CH_2Cl_2 (50 mL). The organic layer was washed with 0.1 M LiOH and the aqueous layer was extracted with an additional portion of CH_2Cl_2 (50 mL). The combined organic layers were evaporated under vacuum and the residue was purified by column chromatography on silica gel (eluent: $\text{CH}_2\text{Cl}_2/\text{MeOH}/\text{NET}_3$ 8.4/1.6/0.1). The fractions containing the product were combined, the solvent evaporated and the residue dissolved in CH_2Cl_2 and washed with 0.1 M LiOH. After evaporation of the organic solvent under vacuum the ditopic ligand **8** was obtained as a colorless oil (75 mg, 0.066 mmol, 57% yield). ^1H NMR (300 MHz, CDCl_3): δ 6.63-6.50 (m, 10H, ArH), 4.44 (d, 1H, ArCH_2Ar ax, $J = 13.1$ Hz), 4.41 (d, 2H, ArCH_2Ar ax, $J = 13.1$ Hz), 4.38 (d, 1H, ArCH_2Ar ax, $J = 13.1$ Hz), 3.83 (t, 4H, ArOCH_2 , $J = 7.3$ Hz), 3.81 (t, 4H, ArOCH_2 , $J = 7.3$ Hz), 3.68-3.60 (m, 32H, $\text{OCH}_2\text{CH}_2\text{O}$), 3.52 (t, 8H, $\text{NCH}_2\text{CH}_2\text{O}$, $J = 5.8$ Hz), 3.38 (d, 2H, $\text{ArCH}_A\text{H}_B\text{N}$, $J_{AB} = 13.9$ Hz), 3.33 (d, 2H,

ArCH_AH_BN, J_{AB} = 13.9 Hz), 3.12 (d, 1H, ArCH₂Ar eq, J = 13.1 Hz), 3.10 (d, 2H, ArCH₂Ar eq, J = 13.1 Hz), 3.06 (d, 1H, ArCH₂Ar eq, J = 13.1 Hz), 2.59 (t, 8H, NCH₂CH₂O, J = 5.8 Hz), 1.98-1.85 (m, 8H, ArOCH₂CH₂), 0.98 (t, 12H, CH₂CH₃, J = 7.4 Hz). ¹³C NMR (75 MHz, CDCl₃): δ 156.4, 155.4, 135.1, 134.9, 134.4, 128.6, 128.5, 128.0, 127.9, 121.7, 76.7, 70.7, 70.3, 70.2, 69.9, 59.3, 53.3, 30.9, 23.1, 10.2. MS (CI) *m/z* (%): 1143.8 (100) [M+H⁺]. Anal. Calcd for C₆₆H₉₈N₂O₁₄ (1143.52): C, 69.32; H, 8.64; N, 2.45. Found: C, 69.27; H, 8.70, N, 2.40.

5,17-Bis[N-(monoaza-18-crown-6)methyl]-25,26,27,28-tetrapropoxycalix[4]arene (9)

Potassium carbonate (85 mg, 0.615 mmol) and 1-aza-18-crown-6 (0.21 g, 0.794 mmol) were added to a solution of the dichloro derivative **16**³⁹ (0.2 g, 0.290 mmol) in dry MeCN (6 mL). The reaction mixture was heated at 60°C overnight under nitrogen atmosphere. The solvent was evaporated under reduced pressure and the crude product dissolved in CH₂Cl₂ (100 mL). The organic layer was washed with 0.1 M LiOH and the aqueous layer was extracted with additional CH₂Cl₂ (100 mL). The combined organic phases were evaporated under vacuum and the product was obtained as a pale yellow oil (232 mg, 0.203 mmol, 70% yield) upon column chromatography (neutral Al₂O₃, eluent: CH₂Cl₂/MeOH 9.2/0.8). An analytical sample was obtained as a white solid by crystallization from cold methanol; (Mp = 99.6-100°C). ¹H NMR (300 MHz, CDCl₃): δ 6.92 (s, 4H, ArH), 6.26-6.17 (m, 6H, ArH), 4.40 (d, 4H, ArCH₂Ar ax, J = 3.2 Hz), 3.93 (t, 4H, ArOCH₂, J = 7.9 Hz), 3.72-3.59 (m, 48H, ArOCH₂ + ArCH₂N + NCH₂(CH₂OCH₂)₅), 3.09 (d, 4H, ArCH₂Ar eq, J = 13.2 Hz), 2.81 (bs, 8H, OCH₂CH₂NCH₂CH₂O), 1.94 (q, 4H, ArOCH₂CH₂, J = 7.9 Hz), 1.86 (q, 4H, ArOCH₂CH₂, J = 7.5 Hz), 1.06 (t, 6H, ArOCH₂CH₂CH₃, J = 7.5 Hz). ¹³C NMR (75 MHz, CDCl₃): δ 156.6, 155.3, 136.0, 133.6, 129.4, 127.3, 121.9, 76.7, 76.4, 70.8, 70.7, 70.3, 69.9, 59.8, 53.7, 30.8, 23.3, 22.9, 10.6, 9.9. MS (ESI) *m/z*: 602.3 (40) [M+Na+K]²⁺, 594.4 (60) [M+2Na]²⁺, 583.4 (100) [M+Na+H]²⁺, 572.4 (35) [M+2H]²⁺. Anal. Calcd for C₆₆H₉₈N₂O₁₄ (1143.52): C, 69.32; H, 8.64; N, 2.45. Found: C, 69.26; H, 8.72; N, 2.40.

4.6 References and notes

- (1) Molenveld, P.; Stikvoort, W. M. G.; Kooijman, H.; Spek, A. L.; Engbersen, J. F. J.; Reinhoudt, D. N. *J. Org. Chem.* **1999**, *64*, 3896-3906.
- (2) Molenveld, P.; Engbersen, J. F. J.; Reinhoudt, D. N. *Chem. Soc. Rev.* **2000**, *29*, 75-86.
- (3) Cacciapaglia, R.; Di Stefano, S.; Kelderman, E.; Mandolini, L. *Angew. Chem. Int. Ed* **1999**, *38*, 348-351.

- (4) Cacciapaglia, R.; Di Stefano, S.; Mandolini, L. *J. Org. Chem.* **2002**, *67*, 521-525.
- (5) Cacciapaglia, R.; Di Stefano, S.; Mandolini, L. *J. Am. Chem. Soc.* **2003**, *125*, 2224-2227.
- (6) Bohmer, V.; Vysotsky, M. O. *Aust. J. Chem.* **2001**, *54*, 671-677.
- (7) van Loon, J.-D.; Arduini, A.; Coppi, L.; Verboom, W.; Ungaro, R.; Pochini, A.; Harkema, S.; Reinhoudt, D. N. *J. Org. Chem.* **1990**, *55*, 5639-5646.
- (8) Casnati, A.; Sansone, F.; Ungaro, R. *Acc. Chem. Res.* **2003**, *36*, 246-254.
- (9) Harvey, P. D. *Coord. Chem. Rev.* **2002**, *233*, 289-309.
- (10) Arduini, A.; Pochini, A.; Secchi, A.; Ugozzoli, F. Recognition of neutral molecules; In *Calixarenes 2001*; Asfari, Z., Böhmer, V., Harrowfield, J., Vicens, J., eds. Kluwer Academic Publishers: Dordrecht, 2001; pp 457-475.
- (11) Gagnon, J.; Vezina, M.; Drouin, M.; Harvey, P. D. *Can. J. Chem.* **2001**, *79*, 1439-1446.
- (12) Ohseto, F.; Yamamoto, H.; Matsumoto, H.; Shinkai, S. *Tetrahedron Lett.* **1995**, *36*, 6911-6914.
- (13) Hesek, D.; Inoue, Y.; Drew, M. G. B.; Beer, P. D.; Hembury, G. A.; Ishida, H.; Aoki, F. *Org. Lett.* **2000**, *2*, 2237-2240.
- (14) Jankowski, C. K.; Dozol, J. F.; Allain, F.; Tabet, J. C.; Ungaro, R.; Casnati, A.; Vicens, J.; Asfari, A.; Boivin, J. *Pol. J. Chem.* **2002**, *76*, 701-711.
- (15) Kelderman, E.; Derhaeg, L.; Heesink, G. J. T.; Verboom, W.; Engbersen, J. F. J.; vanHulst, N. F.; Persoons, A.; Reinhoudt, D. N. *Angew. Chem. Int. Ed. Engl.* **1992**, *31*, 1075-1077.
- (16) Timmerman, P.; Boerrigter, H.; Verboom, W.; Reinhoudt, D. N. *Recl. Trav. Chim. Pays-Bas* **1995**, *114*, 103-111.
- (17) Verboom, W.; Durie, A.; Egberink, R. J. M.; Asfari, Z.; Reinhoudt, D. N. *J. Org. Chem.* **1992**, *57*, 1313-1316.
- (18) Arora, V.; Chawla, H. M.; Santra, A. *Tetrahedron* **2002**, *58*, 5591-5597.
- (19) Arduini, A.; Fanni, S.; Manfredi, G.; Pochini, A.; Ungaro, R.; Sicuri, A. R.; Ugozzoli, F. *J. Org. Chem.* **1995**, *60*, 1448-1453.
- (20) Komori, T.; Shinkai, S. *Chem. Lett.* **1992**, 901-904.
- (21) Arduini, A.; Manfredi, G.; Pochini, A.; Sicuri, A. R.; Ungaro, R. *J. Chem. Soc., Chem. Commun* **1991**, 936-937.
- (22) Arduini, A.; Fabbi, M.; Mantovani, M.; Mirone, L.; Pochini, A.; Secchi, A.; Ungaro, R. *J. Org. Chem.* **1995**, *60*, 1454-1457.
- (23) Molenveld, P.; Engbersen, J. F. J.; Kooijman, H.; Spek, A. L.; Reinhoudt, D. N. *J. Am. Chem. Soc.* **1998**, *120*, 6726-6737.
- (24) Groenen, L. C.; Ruel, B. H. M.; Casnati, A.; Timmerman, P.; Verboom, W.; Harkema, S.; Pochini, A.; Ungaro, R.; Reinhoudt, D. N. *Tetrahedron Lett.* **1991**, *32*, 2675-2678.
- (25) Casnati, A.; Bonetti, F.; Sansone, F.; Ugozzoli, F.; Ungaro, R. *Collect. Czech. Chem. Commun.* **2004**, *69*, 1063-1079.
- (26) Bogdan A.; Vysotsky, M. A.; Bohmer, V. *Collect. Czech. Chem. Commun.* **2004**, *69*, 1009-1026.

- (27) Kelderman, E.; Derhaeg, L.; Verboom, W.; Engbersen, J. F. J.; Harkema, S.; Persoons, A.; Reinhoudt, D. N. *Supramol. Chem.* **1993**, *2*, 183-190.
- (28) Batelaan, J. G., Engbersen, J. F., Kelderman, E., Reinhoudt, D. N., and Verboom, W. EP 93-202029, January 12, **1994**; *Chem. Abstr.*, 121, 121358.
- (29) Dondoni, A.; Marra, A.; Scherrmann, M. C.; Casnati, A.; Sansone, F.; Ungaro, R. *Chem. Eur. J.* **1997**, *3*, 1774-1782.
- (30) Pelizzi, N.; Casnati, A.; Ungaro, R. *Chem. Commun.* **1998**, 2607-2608.
- (31) The catalytic measurements were performed by Stefano Di Stefano at the University of Rome.
- (32) Kirby, A. J. *Adv. Phys. Org. Chem.* **1980**, *17*, 183-278.
- (33) Mandolini, L. *Adv. Phys. Org. Chem.* **1986**, *22*, 1-111.
- (34) The intermolecular model is the second-order reaction between the ester substrate bound *via* its diametral carboxylate to a crown-complexed Ba²⁺ ion and an ethoxide ion paired to a crown-complexed Ba²⁺ ion, as shown in Scheme 4.4b. Since under the conditions of excess EtO⁻ adopted for the measurement of *k*_{obs} values possible contributions to the overall rate from the reaction of the substrate-containing ternary complex with free EtO⁻ ion cannot be ruled out, a new set of kinetic runs was carried out with the following reactant concentrations: **7**, 1.00 mM; Ba(SCN)₂, 1.00 mM; EtONMe₄, 1.00 mM; ester substrate, 0.025 mM. Under this new set of reaction conditions any contribution from free EtO⁻ can be ruled out.
- (35) Galli, C.; Mandolini, L. *Eur. J. Org. Chem.* **2000**, 3117-3125.
- (36) Cacciapaglia, R.; Di Stefano, S.; Mandolini, L. *Acc. Chem. Res.* **2004**, *37*, 113-122.
- (37) Worm, K.; Chu, F. Y.; Matsumoto, K.; Best, M. D.; Lynch, V.; Anslyn, E. V. *Chem. Eur. J.* **2003**, *9*, 741-747.
- (38) Mancin, F.; Rampazzo, E.; Tecilla, P.; Tonellato, U. *Eur. J. Org. Chem.* **2004**, 281-288.
- (39) Casnati, A.; Fochi, M.; Minari, P.; Pochini, A.; Reggiani, M.; Ungaro, R.; Reinhoudt, D. N. *Gazz. Chim. Ital.* **1996**, *126*, 99-106.
- (40) Gray, G. W.; Hartley, J. B.; Brynmor, J. *J. Chem. Soc.* **1955**, 1412-1420.

Synthesis and catalytic activity of Zn(II) calix[4]arene complexes in aryl ester methanolysis*

*In the previous chapter the comparison between the activity of 1,2- and 1,3-dinuclear calix[4]arenes revealed a large superiority of the proximal regioisomer in the ethanolysis of aryl esters. In this chapter the synthesis of the calix[4]arene **5** equipped with two 2,6-bis[(dimethylamino)methyl]pyridine ligating groups in proximal positions is reported. The catalytic activity of its Zn(II) complex was investigated in the methanolysis of aryl esters and compared to that of the other calixarene Zn complexes having 2,6-bis[(dimethylamino)methyl]pyridine groups in different positions. The synthesis of a new series of ligands **8-11**, obtained by the introduction at the calix[4]arene upper rim of one, two (in diametral or proximal positions) and three triazacyclododecane ([12]aneN₃) macrocycles is also described. The catalytic activity of Zn(II) complexes of [12]aneN₃-calixarenes (**8-11**) was investigated in the methanolysis of aryl esters. The presence of a carboxylic anchoring group on the substrate is necessary to obtain high rate enhancements. The 1,2-proximal calix[4]arene complexes **5**-[Zn]₂ and **10**-[Zn]₂ are much more effective than their regioisomers with metal ions in diametral positions. The slightly higher activity of the trinuclear catalysts can be simply explained by a statistical advantage over the dinuclear ones, although in the case of **6**-[Zn]₃ and *p*-carboxyphenyl acetate **33**, the involvement of the third metal ion in the catalytic mechanism is possible.*

* Cacciapaglia, R.; Casnati, A.; Mandolini, L.; Reinhoudt, D. N.; Salvio, S.; Sartori, A.; Ungaro, R., submitted to *J. Org. Chem.*

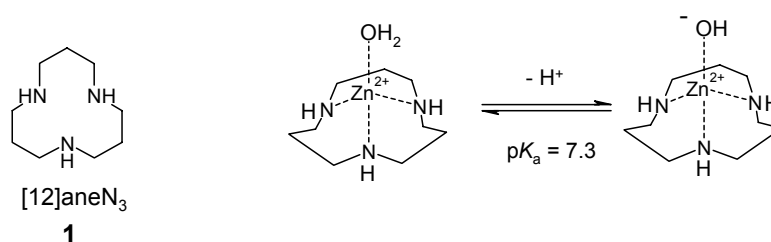
5.1 Introduction

As described in Chapter 2, metal ions can accelerate the hydrolysis of phosphate, amide and ester bonds in many different ways, i.e. by the activation of the electrophile, stabilization of the leaving group and of the negative charges in the transition state or activation of the nucleophile by lowering its pK_a .^{1;2} However, only a combination of these strategies³ might provide the rate enhancement, even larger than 10^{12} , observed in several hydrolytic enzymes.^{4;5} This enhancement is obtained thanks to the proper disposition of the metal centers in the active site of the enzymes. Supramolecular chemists dealing with catalysis are therefore trying to mimic enzyme activity preorganizing metal centers on proper molecular scaffolds. However, a high preorganization of the catalytic groups is not easily achieved in a synthetic system and the largest rate enhancements (k_{cat}/k_{uncat}) observed with di- and trinuclear hydrolytic enzyme mimics⁶ only reach 10^5 . Therefore, the understanding of the best spatial disposition of the groups entrusted to bind the metal ions is the first step towards the design of a catalyst with high cooperativity of metal centers.

The calix[4]arene skeleton was shown to be a useful scaffold to preorganize metal centers able to show cooperativity in catalytic processes.⁷ Zn(II) ions coordinated to 2,6-bis[(dimethylamino)methyl]pyridine units at the upper rim of the calix[4]arene can cooperate in the phosphate diester cleavage.^{8;9} With some substrates, the trinuclear catalyst **6**-[Zn]₃ showed a much higher activity than **4**-[Zn]₂ bearing two metal centers in the 1,3-positions on the calixarene. However, it was not possible to clarify if the observed higher efficiency of **6**-[Zn]₃ was due to the cooperation of all the three metal centers or to the fact that, in contrast to the dinuclear catalyst, **6**-[Zn]₃ bears catalytic groups in 1,2-proximal positions.

In Chapter 4 we have described the synthesis of 1,2-diformyltetraalkoxy calix[4]arenes, which are useful intermediates for the synthesis of derivatives with metal binding groups in 1,2-proximal positions. It was also shown for the first time that the proximal dinuclear calix[4]arene catalyst is superior to the diametral regioisomer in ester ethanolysis. The metal centers in the 1,2-positions can better cooperate in the binding of the substrate and the activation of the nucleophile with respect to the metal centers in the 1,3-positions. For this reason, it was interesting to compare the activity of the calixarene **5**-[Zn]₂ bearing the 2,6-bis(dimethylamino)-pyridine units in 1,2-proximal positions with that of its diametral regioisomer **4**-[Zn]₂ and of the trinuclear calix[4]arene **6**-[Zn]₃. The synthesis of **5** will be reported in the first part of this chapter.

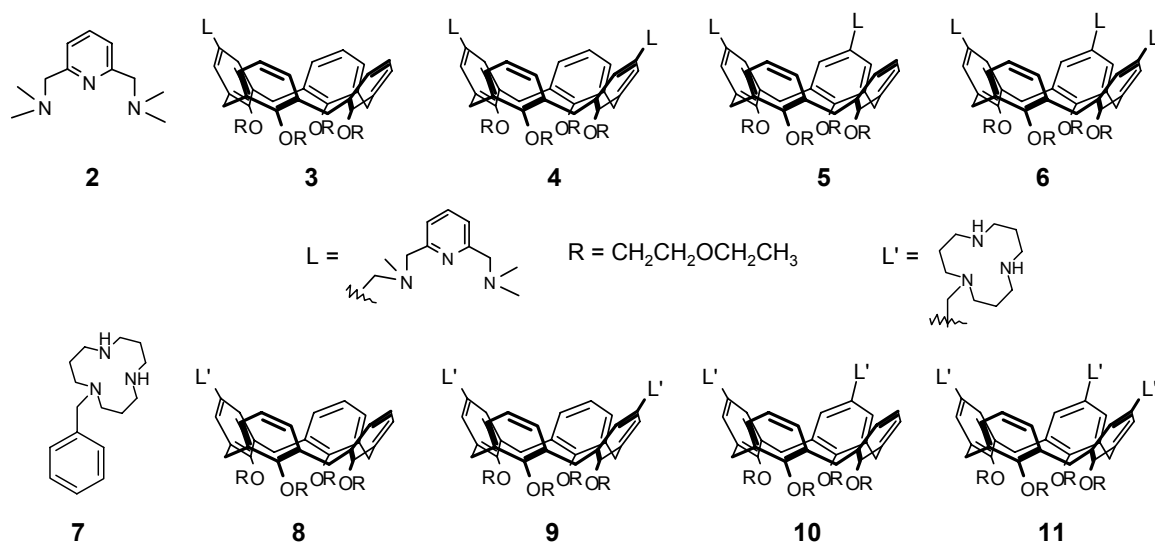
Another crucial point in the development of a supramolecular metallo-catalyst is the choice of the ligands. In Chapter 3 we concluded that the binding of Zn(II) to the 2,6-bis(dimethylamino)pyridine units in water is too low to assure quantitative formation of the complex at millimolar concentration. Stronger coordinating units have therefore to be used to develop polynuclear catalytic systems able to act in pure water. The azacrowns are macrocyclic polyamines known to form very stable complexes with 3d transition metal ions showing $\log K$ values ranging from 8 to $16^{10;11}$ in water. These metal complexes have therefore been studied as artificial enzymes.¹² In particular, the complexes of 1,5,9-triazacyclododecane ([12]aneN₃) **1** cleave phosphodiester bonds^{13;14} more effectively than the complexes of the tetradentate [12]aneN₄ and [14]aneN₄ ligands.^{15;16} Moreover, besides the higher binding ability, [12]aneN₃ offers other interesting advantages compared to the 2,6-bis(dimethylamino)pyridine **2**. First of all, **1** is relatively hydrophilic and possibly the presence of two or three [12]aneN₃ groups on a calixarene might afford better water solubility. Moreover, **1** can considerably lower the pK_a value of the metal-bound water molecule (Scheme 5.1). In the case of the complex **1**-[Zn], for instance, the pK_a value of the metal-bound water molecule is 7.3,¹⁷ a value comparable to that of ~ 7 found for the (His)₃-Zn²⁺-OH₂ at the active center of carbonic anhydrase. This property is very important since recently a direct dependence of the activity of hydrolytic enzyme mimics with the basicity of the metal bound hydroxide was found,¹⁵ suggesting that OH⁻ acts as a general base catalyst.



Scheme 5.1

In this chapter, we also report on the synthesis of new calixarene ligands **8-11**, obtained by the introduction of one, two (in diametral or proximal positions) and three [12]aneN₃ macrocycles, respectively, at the upper rim. Moreover, a procedure is described for the synthesis of calix[4]arenes bearing three metal ligating groups and a functional group (formyl or carboxylic acid, **29** and **31** respectively) at the upper rim, to which a moiety for the substrate recognition can be linked.

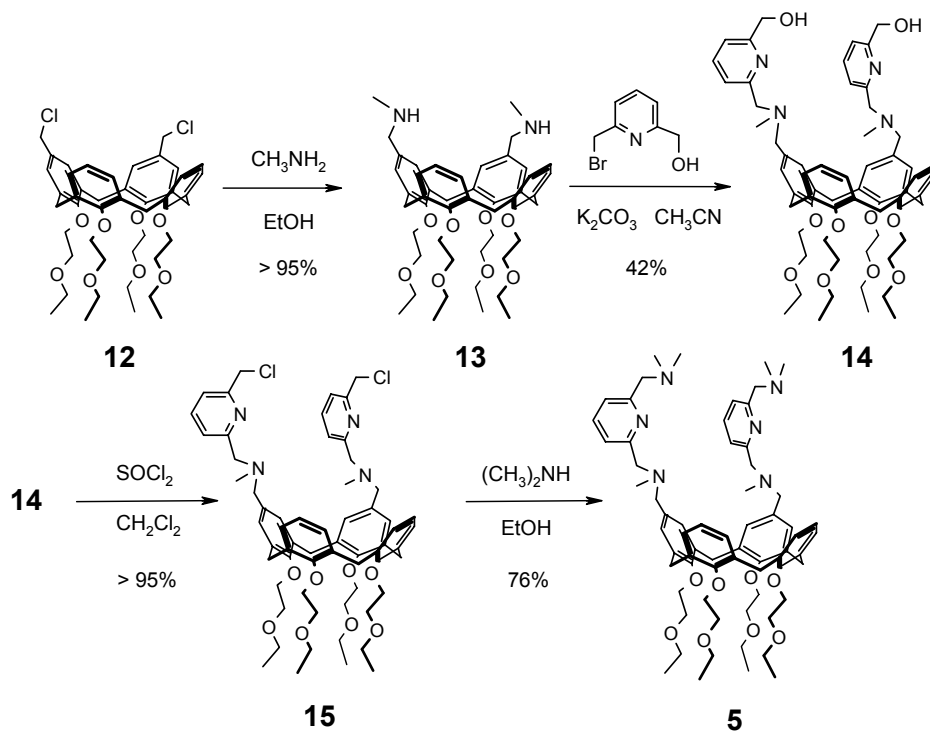
The catalytic activity of pyridine-calix[4]arene (**3-6**) and [12]aneN₃-calixarene (**8-11**) Zn(II) complexes in the methanolysis of aryl esters reveals the cooperative role of the metal centers in proximal positions in catalysis.



5.2 Synthesis

5.2.1 Synthesis of 1,2-bisdiaminopyridine-calix[4]arene

The synthesis of the difunctionalized receptor **5** (Scheme 5.2) was carried out starting from 1,2-dichloromethylcalix[4]arene **12**, obtained through the procedure reported in the previous chapter. The dichloromethyl derivative **12** was reacted with a large excess of methylamine in EtOH solution to give compound **13** in quantitative yield. The pyridine group was then introduced by reacting **13** with exactly two equivalents of 2-bromomethyl-6-hydroxymethylpyridine¹⁸ in acetonitrile (yield 42%), in order to avoid the quaternization of the nitrogen center.



Scheme 5.2

The hydroxyl groups of **14** were then quantitatively converted to chlorides using SOCl_2 in CH_2Cl_2 , and calixarene **15** was reacted with a large excess of dimethylamine in EtOH, obtaining compound **5** with the two chelating arms in proximal positions.

The ^1H NMR spectrum of compound **5** (Figure 5.1) confirms the symmetry due to the 1,2-proximal substitution of the calix[4]arene upper rim. Three doublets for the equatorial protons of the methylene bridges are present as a consequence of the plane of symmetry of the molecule. The protons H_a and H_b of methylene groups attached to *para*-position of the aromatic ring of the calixarene are diastereotopic and give rise to two doublets at 3.25 and 3.19 ppm with a geminal coupling constant of 12.9 Hz.

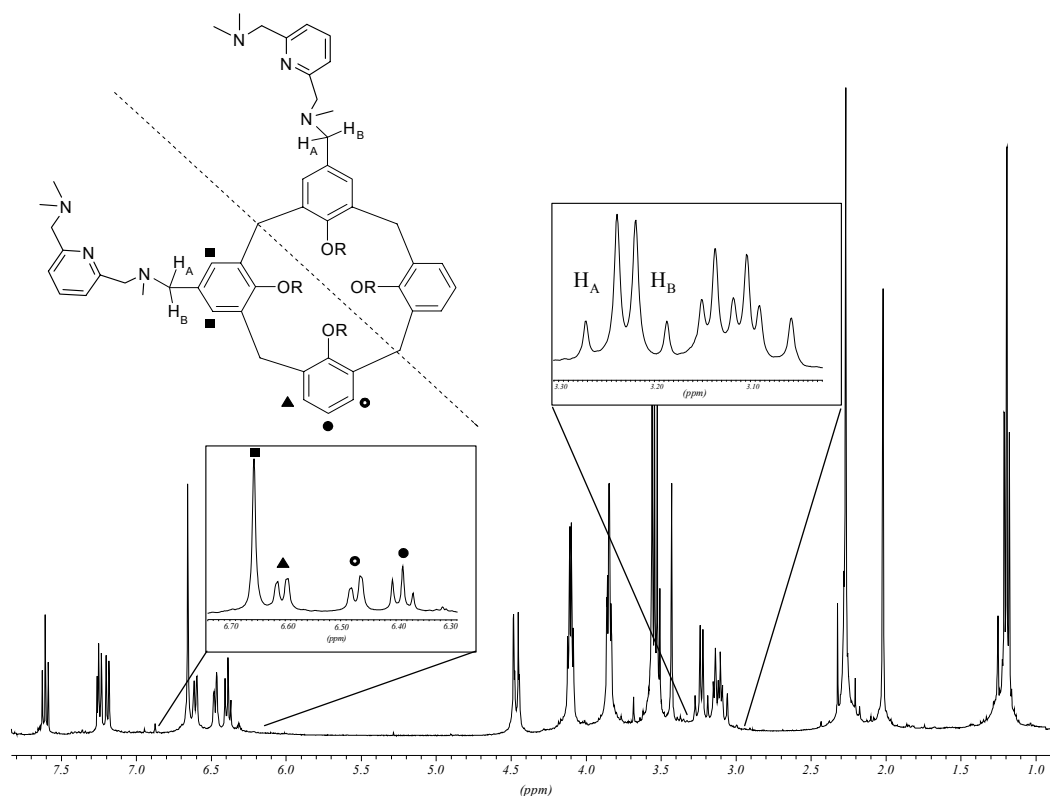
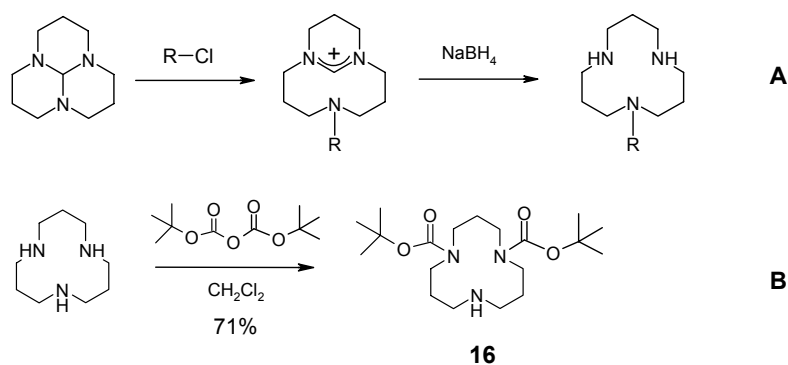


Figure 5.1 ^1H NMR spectrum of compound **5** in CDCl_3 (300 MHz, 300K), with expanded aromatic and methylene proton regions.

5.2.2 Synthesis of [12]ane N_3 -calix[4]arenes

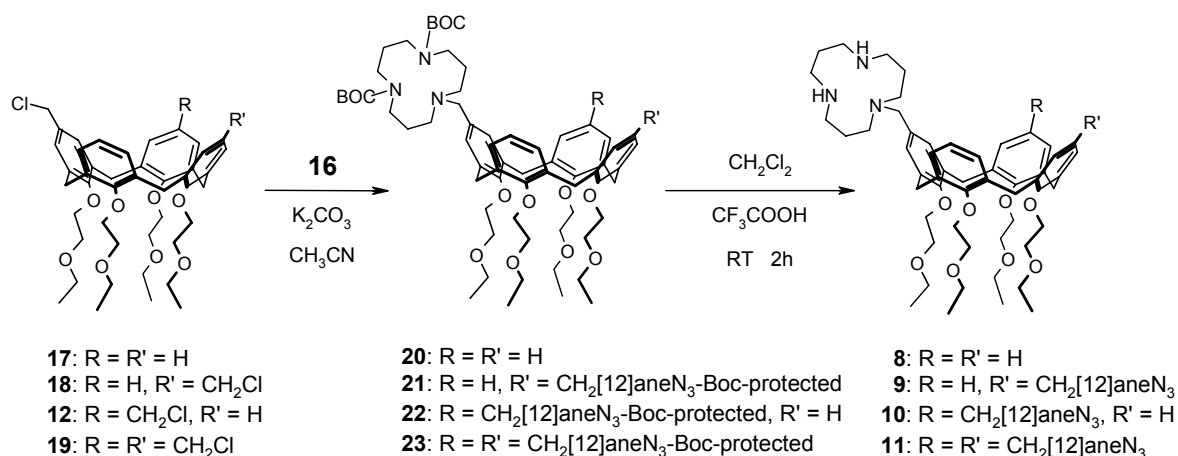
Besides the problem of quaternization, the monoalkylation of a polyazacrown competes also with polysubstitution, due to the possible alkylation of different *N*-atoms of the macrocycle. In some cases good yields were obtained performing the reactions under high dilution conditions. The alkylating agent is added to a solution containing an excess of the polyazacrown, without the necessity of protecting the other amino groups. This procedure has also been successfully applied to the monofunctionalization of the calix[4]arene upper rim with cyclen.¹⁹ Another strategy,

developed to avoid polysubstitution, takes advantage of the possible partial protection of some nitrogen atoms in polyazacrown ethers, like cyclen (1,4,7,10-tetraazacyclododecane) and 1,4,7-triazacyclononane.²⁰ For the [12]aneN₃, Weisman used a central carbon fragment to protect the nitrogen atoms from subsequent electrophilic attacks (Scheme 5.3 A) thus preventing polysubstitution. After the first alkylation step an amidinium species forms, that prevents the alkylation of the two nitrogen atoms sharing a positive charge. Reduction of the amidinium species with NaBH₄ gives the product. Alternatively, [12]aneN₃ can also be selectively protected at two positions with Boc groups in good yield²¹ (Scheme 5.3 B) and it was decided to use bisBoc-[12]aneN₃ **16** for the synthesis of polynuclear calixarenes because of the easier purification of the protected [12]aneN₃ intermediate.



Scheme 5.3

The introduction of [12]aneN₃ at the upper rim of calix[4]arenes has been carried out reacting the bisBoc-protected [12]aneN₃ with the proper chloromethylcalix[4]arene and K₂CO₃ as a base in dry acetonitrile (Scheme 5.4). The reaction rates are quite low, probably because of the steric hindrance of the nucleophile. This is probably also the reason why polyalkylation (quaternization) of **16** has never been observed as a serious side reaction. The yield of the monofunctionalized compound **20** is good (70%) after two reaction days, while 5 days are necessary to obtain good yields of the di- and tri-functionalized compounds **21-23**. The presence of Boc on the amino groups allowed an easy purification of these compounds by flash chromatography on silica gel. Deprotection of Boc groups with trifluoroacetic acid in dichloromethane was quantitative, giving pure products **8-11**.



Scheme 5.4

Compounds **8-11** are more soluble in water than the corresponding calixarenes with pyridine units at the upper rim. In fact, a ¹H NMR spectrum of **11** in D₂O could be recorded (Figure 5.2), indicating a solubility in water of at least 10⁻⁴ M.

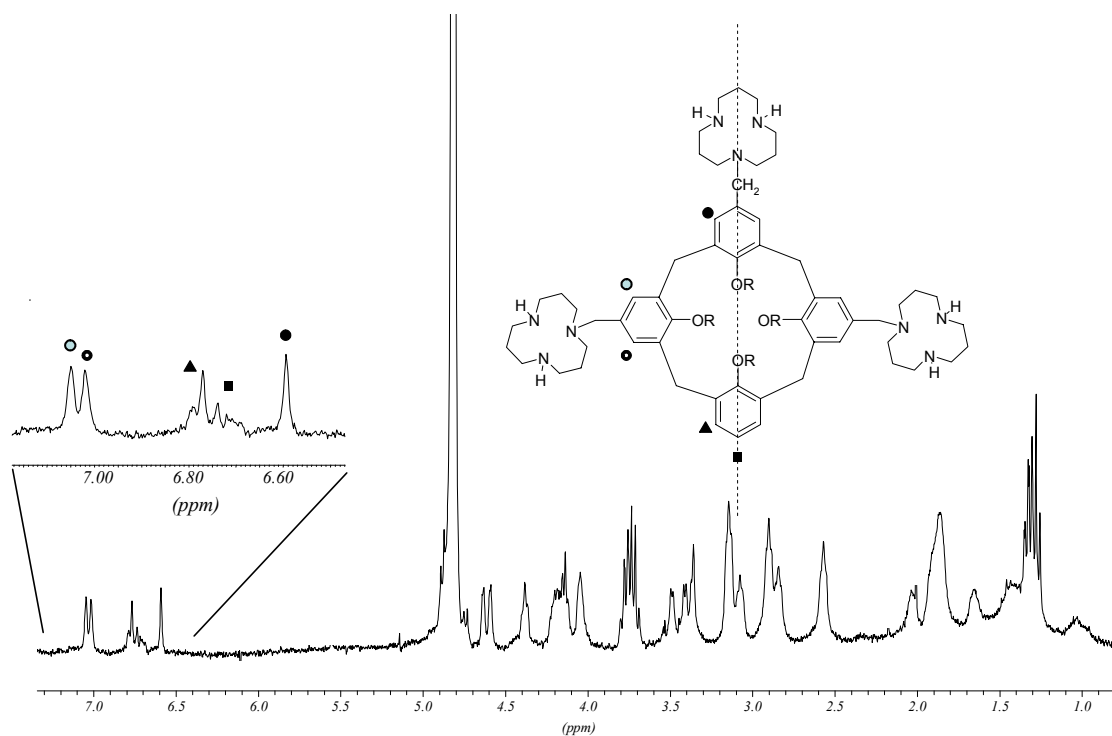
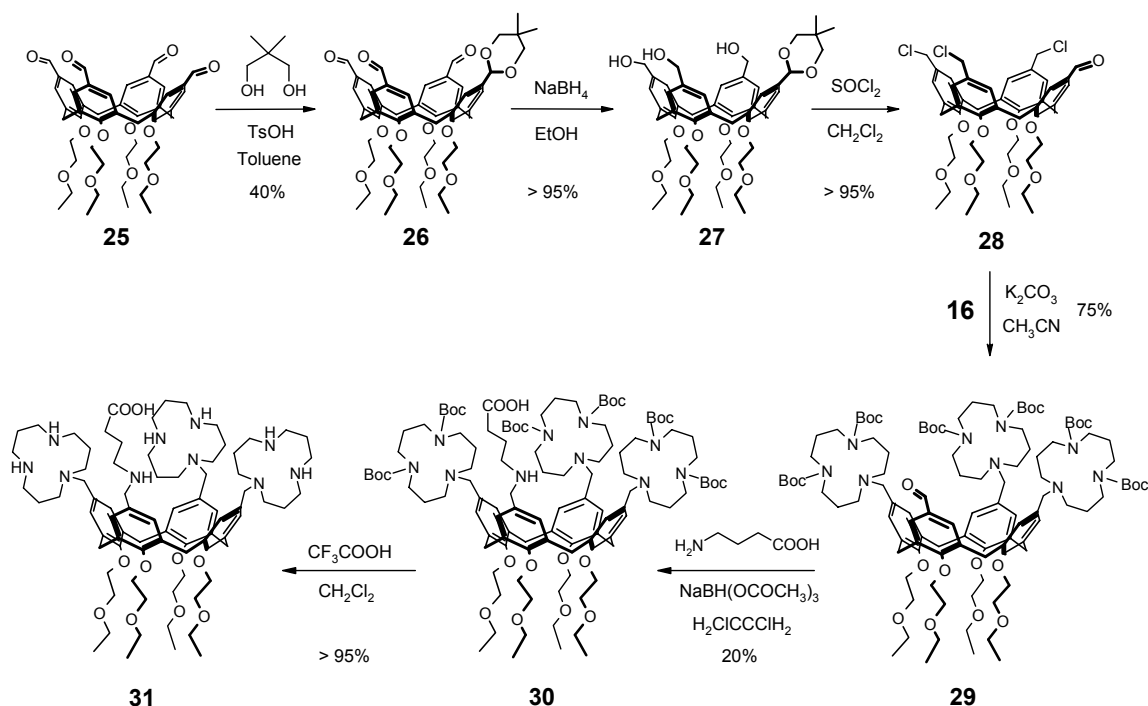


Figure 5.2 ¹H NMR spectrum of compound **11** in D₂O (300 MHz, 298K), with expanded aromatic proton region.

The introduction of a recognition group for substrates can remarkably improve the efficiency of a catalyst both by favoring the formation of the Michaelis catalyst-substrate complex, and by directing the cleavage in a targeted position. The latter point is important in the case of substrates (e.g. oligonucleotides) that offer several

different cleavage positions, and site-specificity is the main goal of the catalyst, as it is required for *in vivo* applications.

The calix[4]arene scaffold has four different positions at the upper rim which may be functionalized. On three of them, the ligand groups for catalysis can be introduced, while on the fourth a recognition function can be linked. A synthetic pathway was established that allows the selective functionalization of the calix[4]arene with three [12]aneN₃ macrocycles and a functional group on the fourth aromatic ring (Scheme 5.5). Starting from the tetraformyl compound **25**, which can be obtained in very good yield, it was possible to selectively protect only one formyl group as cyclic acetal. The reduction of **26** with NaBH₄ quantitatively gave trialcohol **27** with the protected formyl function. Substitution of the hydroxyl groups with chlorides and deprotection of the formyl group could be achieved in a single step stirring **27** in the presence of a large excess of thionyl chloride. Compound **28** has three chloromethyl groups that can undergo nucleophilic substitution and a formyl group which can be subsequently functionalized. Compound **28** was reacted with bisBoc-[12]aneN₃ (**16**) and K₂CO₃ in acetonitrile to give **29**, that might be functionalized with a recognition group by reductive amination.



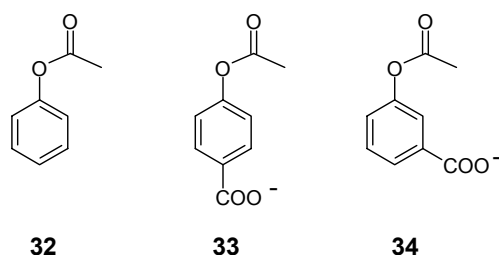
Scheme 5.5

Alternatively, a spacer such as 4-aminobutyric acid can be introduced by reductive amination to give compound **30**, although in low yield (20%). The spacer has the function of increasing the distance between the active center and the recognition site, allowing the attachment of a recognition group through the formation of an amide

bond. The deprotection of **30** was achieved by treatment with trifluoroacetic acid that gives compound **31** in quantitative yield.

5.3 Binding and catalysis

Zn(II) complexes of compounds **2-6** and **7-11** were tested as catalysts of the methanolysis of aryl esters **32-34**.²² Complexation studies and catalytic measurements were carried out at 25 °C, in methanol at pH 10.4 with *N,N*-diisopropyl-*N*-(2-methoxyethyl)amine/perchlorate salt buffer ($pK_a = 10.4$ in methanol; $[B]=[BH^+ClO_4^-]=10$ mM).



The UV-Vis titration of 2,6-bis[*N,N'*-(dimethyl)aminomethyl]pyridine (**2**) with $Zn(ClO_4)_2$ in MeOH indicates a strong binding ($K = 6 \times 10^4 \pm 20\% M^{-1}$) of Zn^{II} . If this value is maintained also in the case of the calixarene-based ligands **3-6** then one can reasonably assume that in MeOH, at $[ligand] = 1$ mM, the formation of monometallic (**2**-[Zn], **3**-[Zn]), bimetallic (**4**-[Zn]₂, **5**-[Zn]₂) and trimetallic (**6**-[Zn]₃) complexes is quantitative upon addition of one, two or three molar equivalents of $Zn(ClO_4)_2$, respectively, to the ligand solution. This was indeed proven by UV titration of **6** with $Zn(ClO_4)_2$ (Figure 5.3).

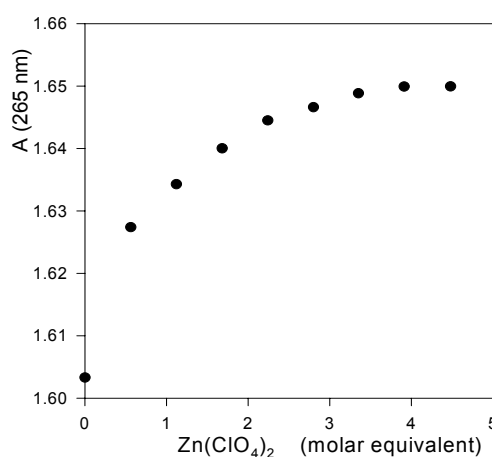


Figure 5.3 UV titration of 0.104 mM **6** with $Zn(ClO_4)_2$ in MeOH (25 °C).

The titration of ligand **2**-[Zn] with tetramethylammonium benzoate was also carried out, in order to evaluate the association between complexed Zn(II) ion and the carboxylate anion. A very high association constant ($K = 1.8 \times 10^4 M^{-1}$) was found,

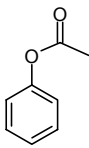
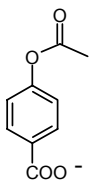
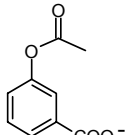
which implies that an almost quantitative binding occurs under the conditions of the catalytic measurements between the carboxylate anchoring group, whenever present in the substrate, and the metal center of the catalyst.²⁴

UV-Vis measurements of the association constant of Zn(II) to [12]aneN₃ could not be carried out, because of the absence of a chromophore. On the other side in the case of triazacalixarenes the complexation of the metal ion did not affect the UV spectrum of the ligand. Nevertheless, on the basis of the high values reported in the literature for the complexation of Zn(II) to [12]aneN₃ ($K = 8.5 \times 10^8 \text{ M}^{-1}$ in 50% aqueous ethanol v/v, 25 °C)²³ the formation of the Zn-complexes of ligands **7-11** was assumed to be quantitative after addition of one equivalent of Zn(ClO₄)₂ per triaza unit.

5.3.1 Methanolysis catalyzed by pyridine-calixarene Zn^{II} complexes

Kinetic data for the methanolysis of esters **32-34** catalyzed by Zn(II) complexes of compounds **2-6** are reported in Table 5.1. All metal complexes cause a small rate enhancement of the methanolysis of phenyl acetate (**32**). Interestingly, the fact that the mononuclear calix[4]arene complex **3**-[Zn] is three times more active than the reference complex **2**-[Zn] indicates that hydrophobic interactions with the calixarene skeleton might play a role in the catalytic process. The polynuclear calix[4]arene complexes are in this case less active than the monosubstituted **3**-[Zn], indicating that the presence of more than one ligand moiety at the upper rim probably decreases the interaction between the calixarene and the substrate. The efficiency of these calixarene catalysts is strongly enhanced by the presence of a distal anchoring group on the substrate (**33** and **34**). Zn(II) complexes show indeed a good catalytic activity in the methanolysis of esters **33** and **34**. With no exception, complexes **5**-[Zn]₂ and **6**-[Zn]₃ are the most effective catalysts in the series, and rate enhancements up to four orders of magnitude were observed. The ditopic catalyst **5**-[Zn]₂, bearing the two pyridine ligands in 1,2-proximal positions, is much more effective than the 1,3-isomer **3**-[Zn]₂ having the two pyridine ligands in 1,3-diametral positions. Thus we can infer that two metal ions complexed by two ligands on vicinal aromatic rings can act cooperatively and produce a synergistic action that results in considerable rate enhancements. The ratio of k_{obs} values in the presence of 1,2-disubstituted and 1,3-disubstituted catalysts ($k_{\text{obs}(1,2)}/k_{\text{obs}(1,3)}$) is always > 1 and can be used as an indication of the superiority of the 1,2-dinuclear complex **5**-[Zn]₂ over its isomer, the 1,3-dinuclear complex **4**-[Zn]₂. The highest ratio was observed with ester **33** ($k_{\text{obs}(1,2)}/k_{\text{obs}(1,3)} = 26$), where the carboxylate group is in the *para* position with respect to the ester, but it is also significant with ester **34** ($k_{\text{obs}(1,2)}/k_{\text{obs}(1,3)} = 15$).

Table 5.1 Pseudo first-order rate constants and relative rate accelerations for the basic methanolysis of esters **32-34** catalyzed by the Zn²⁺ complexes of ligands **2-6**.^{a,b}

Substrate	Catalyst	k_{obs} (s ⁻¹)	k_{rel}
 32	–	$9.4 \times 10^{-7}{}^d$	1.0
	2 –[Zn]	$5.3 \times 10^{-6}{}^c$	5.6
	3 –[Zn]	$1.5 \times 10^{-5}{}^c$	16
	4 –[Zn] ₂	$4.1 \times 10^{-6}{}^c$	4.4
	5 –[Zn] ₂	$9.7 \times 10^{-6}{}^c$	10
	6 –[Zn] ₃	$1.2 \times 10^{-5}{}^c$	13
 33	–	$5.5 \times 10^{-7}{}^d$	1.0
	2 –[Zn]	$2.1 \times 10^{-5}{}^c$	38
	3 –[Zn]	$2.9 \times 10^{-5}{}^c$	53
	4 –[Zn] ₂	$1.3 \times 10^{-4}{}^c$	240
	5 –[Zn] ₂	3.4×10^{-3}	6200
	6 –[Zn] ₃	1.3×10^{-2}	24000
 34	–	$2.2 \times 10^{-7}{}^d$	1.0
	2 –[Zn]	$2.6 \times 10^{-5}{}^c$	120
	3 –[Zn]	$9.1 \times 10^{-5}{}^c$	410
	4 –[Zn] ₂	$2.2 \times 10^{-4}{}^c$	1000
	5 –[Zn] ₂	3.3×10^{-3}	15000
	6 –[Zn] ₃	2.9×10^{-3}	13000

^a Reaction conditions: *N,N*-diisopropyl-*N*-(2-methoxyethyl)amine/perchlorate salt buffer ([B] = [BH⁺] = 10 mM, pH = 10.4), 0.1 mM substrate, 1 mM catalyst. ^b HPLC monitoring (reaction of substrates **32-34** were carried out in the presence of metal complexes) or UV monitoring (reaction of **32-34** were carried out in the presence of tetramethylammonium methoxide). Error limits = ±5%. ^c Initial rate measurements, 0.5 mM substrate. ^d Values calculated at pH = 10.4, from experimental first order rate constant k_{obs} obtained at 5 mM tetramethylammonium methoxide: $k = (k_{\text{obs}} / 0.005) \times 10^{-(\text{p}K_{\text{MeOH}} - \text{pH})}$, with the molar autoprotolysis constant of methanol $K_{\text{MeOH}} = 10^{-16.77}$ (see ref. 25).

The effect of the introduction of a third metal center on the catalytic efficiency strictly depends on the substrate structure but, in general, is not dramatic. With substrate **34** the efficiency of the two catalysts **5**–[Zn]₂ and **6**–[Zn]₃ is almost the same. Although the statistical advantage of **6**–Zn₃ over **5**–[Zn]₂ has to be taken into account, a possible contribution of the third Zn^{II} ion becomes clear in the methanolysis of **33**, where the trimetallic complex **6**–[Zn]₃ is approximately 4 times more efficient than the bimetallic complex **5**–[Zn]₂. For **33** it has been suggested that each of the three Zn^{II} ions plays a different role: one binds the substrate, the second one activates the electrophilic site by coordination to the carbonyl oxygen and the third one delivers the nucleophile.

5.3.2 Methanolysis catalyzed by [12]aneN₃-calixarene Zn^{II} complexes

The methanolysis of esters **32–34** was also investigated in the presence of Zn(II) complexes of compounds **7–11** where the metal ligands are the [12]aneN₃ macrocycles. The kinetic data are reported in Table 5.2. The measurements were carried out at a much lower concentration of catalyst ([cat] = 0.2 mM) compared to the **2–6** Zn^{II} complexes ([cat] = 1 mM) and this should be considered when comparing the k_{obs} values for the two classes of catalysts. All metal complexes are poor catalysts in the methanolysis of the substrate **32**, lacking a carboxylate anchoring group. This is in line with what was observed with the pyridine based catalysts. In this case, the calixarene cavity does not seem to play a significant role in the substrate binding; **7**-[Zn] and **8**-[Zn] can in fact provide the same rate enhancement for the methanolysis of **32**, and the activity of the most crowded **11**-[Zn]₃ is exactly 3-fold that of the monosubstituted calixarene Zn^{II} complex **8**-[Zn]. When the substrate possesses a carboxylate group that can be strongly bound by a Zn^{II} ion, a much higher catalytic efficiency was observed. The picture is similar to that shown by **2–6** Zn^{II} complexes. The 1,2-dinuclear complex **10**-Zn₂ is more effective than its distal regioisomer **9**-[Zn]₂ with both substrates **33** and **34**. The largest difference was observed with ester **34** ($k_{obs(1,2)}/k_{obs(1,3)} = 41$), where the carboxylate group is in the *meta* position, and much less with esters **33** ($k_{obs(1,2)}/k_{obs(1,3)} = 7.1$). The third metal center in **11**-[Zn]₃ does not seem to play a relevant role in the catalytic mechanism. The k_{rel} values obtained in the presence of **11**-[Zn]₃ are the highest observed for these systems. However, since they are only twice as large as the values obtained with the dinuclear catalyst **10**-[Zn]₂, the superiority of **11**-[Zn]₃ is likely due to the statistical advantage offered by this trinuclear system. In this case no experimental evidences of the trinuclear catalysis depicted in Figure 5.4 have been obtained, although the lack of such evidences might be due to concurrent factors with opposite effects in the investigated system.

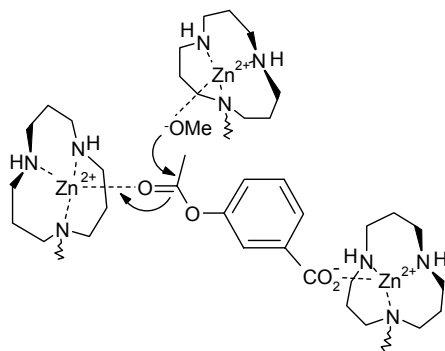
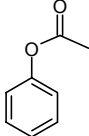
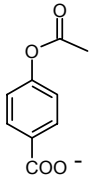
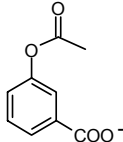


Figure 5.4 The proposed trimetallic catalysis in the methanolysis of **34** catalyzed by **11**-[Zn]₃.

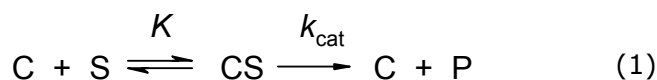
Table 5.2 Pseudo first-order rate constants and relative rate accelerations for the basic methanolysis of esters **32-34** catalyzed by the Zn²⁺ complexes of ligands **7-11**.^{a,b}

Substrate	Catalyst	k_{obs} (s ⁻¹)	k_{rel}
 <p>32</p>	–	$9.4 \times 10^{-7}{}^d$	1.0
	7 -[Zn]	$9.2 \times 10^{-6}{}^c$	9.8
	8 -[Zn]	$7.1 \times 10^{-6}{}^c$	7.5
	9 -[Zn] ₂	$1.4 \times 10^{-5}{}^c$	15
	10 -[Zn] ₂	$1.9 \times 10^{-5}{}^c$	20
	11 -[Zn] ₃	$2.2 \times 10^{-5}{}^c$	23
 <p>33</p>	–	$5.5 \times 10^{-7}{}^d$	1.0
	7 -[Zn]	$3.0 \times 10^{-5}{}^c$	54
	8 -[Zn]	$2.3 \times 10^{-5}{}^c$	42
	9 -[Zn] ₂	5.6×10^{-5}	100
	10 -[Zn] ₂	3.9×10^{-4}	710
	11 -[Zn] ₃	5.6×10^{-4}	1000
 <p>34</p>	–	$2.2 \times 10^{-7}{}^d$	1.0
	7 -[Zn]	$3.9 \times 10^{-5}{}^c$	180
	8 -[Zn]	$2.4 \times 10^{-5}{}^c$	110
	9 -[Zn] ₂	6.4×10^{-5}	290
	10 -[Zn] ₂	2.7×10^{-3}	12000
	11 -[Zn] ₃	6.3×10^{-3}	29000

^a Reaction conditions: *N,N*-diisopropyl-*N*-(2-methoxyethyl)amine/perchlorate salt buffer ([B] = [BH⁺] = 10 mM, pH = 10.4), 0.1 mM substrate, 0.2 mM catalyst. ^b UV monitoring, error limits = ±5%. ^c Initial rate measurements. ^d Values calculated at pH = 10.4, from experimental first order rate constant k_{obs} obtained at 5 mM tetramethylammonium methoxide: $k = (k_{\text{obs}}/0.005) \times 10^{-(pK_{\text{MeOH}} - \text{pH})}$, with the molar autoprotolysis constant of methanol $K_{\text{MeOH}} = 10^{-16.77}$ (see ref.25).

Finally, an interesting property of the systems **10**-[Zn]₂ and **11**-[Zn]₃ which was not shown by the corresponding pyridine systems, is the significant shape selectivity for the *m*-carboxyphenyl acetate **34**. In the presence of **10**-Zn₂, the ratio is $k_{\text{rel}(\mathbf{34})}/k_{\text{rel}(\mathbf{33})} = 17$ and in the presence of **11**-[Zn]₃ the selectivity is even higher ($k_{\text{rel}(\mathbf{34})}/k_{\text{rel}(\mathbf{33})} = 29$). We have to consider that the complexation by a metal ion of the carboxylate group in *meta* position, closer to the reactive center, exerts an inductive electronwithdrawing effect thus enhancing the reactivity of the carbonyl center. But only a 3-fold increase in k_{rel} can be ascribed to this activation (*i.e.* $k_{\text{rel}(\mathbf{34})}/k_{\text{rel}(\mathbf{33})}$ found with the mononuclear catalysts). The major effect on selectivity found with **10**-[Zn]₂ and **11**-[Zn]₃ is therefore due to a better match of **34** with the catalyst which ends up (translates?) into a higher cooperativity of the two metal centers in the 1,2-positions.

An careful kinetic investigation was carried out on the methanolysis of *m*-carboxyphenyl acetate **34** in the presence of catalyst **10**-[Zn]₂. The study of variation of k_{obs} on catalyst concentration at constant substrate (9×10^{-5} M) was preferred to the classical Michaelis investigation (reaction rate vs. substrate concentration) in order to avoid the formation of 2:1 substrate:catalyst complexes at high concentrations of **34**. The agreement between the experimental points and the plot of eq. (2), calculated with nonlinear least squares parameters, shows that the reaction follows a Michaelis-Menten kinetics (1) with formation of an intermediate catalyst-substrate complex, which subsequently converts into the product. The K and k_{cat} values obtained are $K = 4.51 \times 10^3 \pm 13\% \text{ M}^{-1}$ and $k_{\text{cat}} = 6.34 \times 10^{-3} \pm 4\% \text{ s}^{-1}$, respectively.



$$k_{\text{obs}} = \frac{K k_{\text{cat}} [\text{C}]}{K[\text{C}] + 1} \quad (2)$$

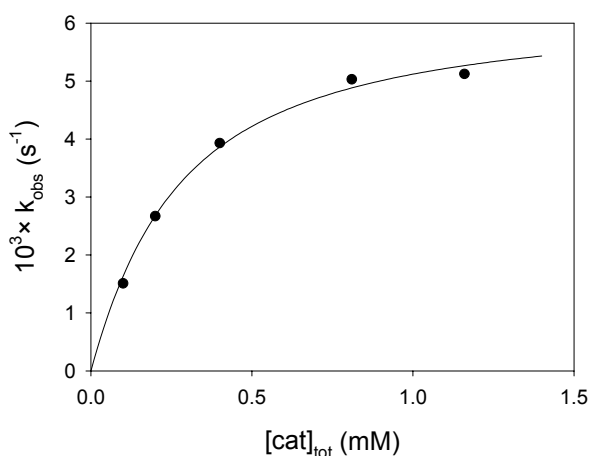


Figure 5.5 Rate as a function of the catalyst concentration for the methanolysis of **34** (9×10^{-5} M) catalyzed by **10**-Zn₂ in MeOH at pH = 10.4 (*N,N*-diisopropyl-*N*-(2-methoxyethyl)amine/bromide salt buffer ($[B] = [BH^+] = 10 \text{ mM}$, pH = 10.4)).

Turnover catalysis was observed in the methanolysis of *m*-carboxyphenyl acetate **34** carried out in the presence of **10**-[Zn]₂. One molar equivalent of substrate is added at time zero. A second molar equivalent is added after complete conversion into products of the first substrate aliquot, and so on for at least four catalytic cycles. Only a 10% increase in the half-life time of the reaction is found after each catalytic cycle, which indicates turnover with a modest product-inhibition.

5.4 Conclusions

In this chapter the synthesis and catalytic activity in aryl ester methanolysis of several new metallo catalysts based on calix[4]arenes are reported. Calix[4]arene **5**, bearing two 2,6-bis[(dimethylamino)methyl]pyridine groups in proximal positions, has been obtained starting from the 1,2-dichloromethylcalix[4]arene **12**. A new class of mono- and polynuclear calix[4]arenes (**8-11**) has been synthesized by attaching one, two (in diametral and proximal positions) or three [12]aneN₃ macrocycles at the upper rim of the calixarene platform. In addition, a synthetic strategy aimed at selectively functionalizing three *p*-positions of the calix[4]arene with metal chelating groups and introducing a functional group (CHO or COOH) on the fourth aromatic ring, has been established. Starting from **25** we prepared compound **31**, which has three triazamacrocycle ligands and an additional carboxylic function to which a recognition group can be attached.

The k_{obs} values obtained in the methanolysis of aryl esters **32-34** catalyzed by the Zn(II) complexes of compounds **2-6** and **7-11** revealed the superiority of the 1,2-dinuclear calix[4]arene complexes with respect to the corresponding 1,3-dinuclear regioisomers. The two metal centers in proximal positions can cooperate in the catalytic process, one by coordinating the carboxylate group of the substrate and the other by delivering the active nucleophile. Very low degree of cooperativity is observed when the metal centers are in diametral positions. The higher rate enhancements obtained with the trinuclear catalysts can be explained simply taking into account the statistical advantage of these compounds over the corresponding 1,2-dinuclear ones. Only in the case of **6**-[Zn]₃ with the ester **33**, a significant contribution of the third Zn(II) ion in the activation of the ester carbonyl group can be envisaged.

The Zn(II) complexes **10**-[Zn]₂ and **11**-[Zn]₃, based on [12]aneN₃-calixarenes, showed a remarkable shape-selectivity for the *m*-carboxyphenyl acetate **34** over its isomer *p*-carboxyphenyl acetate **33**. Studies carried out on the ester **34** with **10**-Zn₂ showed that the reaction follows a Michaelis-Menten kinetics with the formation of an intermediate catalyst-substrate complex (association constant $K = 4.51 \times 10^3 \text{ M}^{-1}$), which subsequently reacts with a first-order rate constant $k_{\text{cat}} = 6.34 \times 10^{-3} \text{ s}^{-1}$.

5.5 Experimental part

General information. For general information on instruments and chemicals see Chapter 3. The synthesis of compound **12** is described in Chapter 4. Compounds **3**, **4**, **6**, 2-bromomethyl-6-hydroxymethylpyridine¹⁸ and *N*-benzyl-1,5,9-triazacyclododecane **7**²⁶ were synthesized according to literature procedures.

5,11-Bis[(*N*-methyl)aminomethyl]-25,26,27,28-tetrakis(2-ethoxyethoxy)calix[4]arene (13)

A 33% methylamine solution in EtOH (10 mL) was added to a round bottomed flask containing the bischloromethylcalix[4]arene **12** (260 mg, 0.32 mmol). The solution was stirred at room temperature until a sample, checked on TLC (Al₂O₃, CH₂Cl₂/MeOH 9/1), revealed the presence of only one spot (~48 h). The EtOH was evaporated under vacuum; the crude product was dissolved in CH₂Cl₂ (30 mL) and washed with a 10% NaHCO₃ solution (30 mL). The organic phase was dried over anhydrous Na₂SO₄, filtered and evaporated under vacuum to give compound **13** (252 mg, 0.32 mmol) as a colorless oil. Yield 97%. ¹H NMR (300 MHz; CDCl₃): δ 7.18 (d, 2H, ArH, J = 1.6 Hz), 6.86 (dd, 2H, ArH, J = 7.4 Hz, J = 1.2 Hz), 6.73 (d, 2H, ArH, J = 1.6 Hz), 6.68 (d, 2H, ArH, J = 7.4 Hz), 6.58 (t, 2H, ArH, J = 7.4 Hz), 4.51 (d, 1H, ArCH₂Ar ax, J = 13.1 Hz), 4.50 (d, 2H, ArCH₂Ar ax, J = 13.1 Hz), 4.47 (d, 1H, ArCH₂Ar ax, J = 13.1 Hz), 4.16-4.07 (m, 8H, ArOCH₂), 3.94 (d, 2H, ArCH_AH_BN, J = 13.4 Hz), 3.82 (t, 8H, ArOCH₂CH₂, J = 5.5 Hz), 3.62 (d, 2H, ArCH_AH_BN, J = 13.4 Hz), 3.53 (q, 4H, OCH₂CH₃, J = 7.0 Hz), 3.51 (q, 4H, OCH₂CH₃, J = 7.0 Hz), 3.24 (d, 1H, ArCH₂Ar eq, J = 13.1 Hz), 3.14 (d, 3H, ArCH₂Ar eq, J = 13.1 Hz), 2.28 (s, 6H, NCH₃), 1.19 (t, 12H, CH₂CH₃, J = 7.0 Hz). ¹³C NMR (75 MHz; CDCl₃): δ 156.7, 155.9, 135.8, 135.6, 134.9, 134.3, 130.4, 129.6, 128.5, 128.3, 124.4, 122.6, 73.5, 73.2, 69.6, 69.5, 66.3, 51.6, 30.8, 30.7, 30.5, 15.2. MS (CI) *m/z* (%): 799.4 [M+H]⁺ (75), 767.5 [M-NHCH₃]⁺ (100). Anal. Calcd for C₄₈H₆₆N₂O₈ (799.06): C, 72.15; H, 8.33; N, 3.51. Found: C, 72.32; H, 8.41; N, 3.44.

5,11-Bis[*N*-((6-hydroxymethylpyridin-2-yl)-methyl)-*N*-methylaminomethyl]-25,26,27,28-tetrakis(2-ethoxyethoxy)calix[4]arene (14)

To a solution of diaminocalix[4]arene **13** (250 mg, 0.315 mmol) in dry CH₃CN were added K₂CO₃ (88 mg, 0.64 mmol) and 2-bromomethyl-6-hydroxymethylpyridine¹⁸ (130 mg, 0.64 mmol). The solution was stirred under N₂ atmosphere for 2 days. The solvent was removed under reduced pressure and the residue dissolved again in CH₂Cl₂ (70 mL). The organic layer was washed with a Na₂CO₃ saturated solution (70 mL) and the aqueous phase extracted with CH₂Cl₂ (70 mL). The combined organic layers were evaporated under vacuum and the product **14** was obtained as a colorless oil (138 mg, 0.132 mmol) after purification by column chromatography (SiO₂; CH₂Cl₂/MeOH, 9/1). Yield 42%. ¹H NMR (400 MHz; CDCl₃): δ 7.62 (t, 2H, PyH, J = 7.4 Hz), 7.19 (d, 2H, PyH, J = 7.4 Hz), 7.13 (d, 2H, PyH, J = 7.4 Hz), 6.68 (d, 2H, ArH, J = 1.6 Hz), 6.63 (bs, 4H, ArH), 6.47 (d, 2H, ArH, J = 7.4 Hz), 6.34 (t, 2H, ArH, J = 7.4 Hz), 4.72 (s, 4H, PyCH₂OH), 4.49 (d, 1H, ArCH₂Ar ax, J = 12.9 Hz), 4.48 (d, 2H, ArCH₂Ar ax, J = 12.9 Hz), 4.46 (d, 1H, ArCH₂Ar ax, J = 13.3 Hz), 4.12 (t, 4H, ArOCH₂,

$J = 5.8$ Hz), 4.10 (t, 4H, ArOCH_2 , $J = 5.8$ Hz), 3.86 (t, 4H, $\text{ArOCH}_2\text{CH}_2$, $J = 5.8$ Hz), 3.85 (t, 4H, $\text{ArOCH}_2\text{CH}_2$, $J = 5.8$ Hz), 3.55 (q, 4H, OCH_2CH_3 , $J = 7.0$ Hz), 3.53 (q, 4H, OCH_2CH_3 , $J = 7.0$ Hz), 3.35 (d, 2H, $\text{ArCH}_A\text{H}_B\text{N}$, $J = 14.0$ Hz), 3.28 (d, 2H, $\text{ArCH}_A\text{H}_B\text{N}$, $J = 14.0$ Hz), 3.25 (d, 2H, $\text{NCH}_A\text{H}_B\text{Py}$, $J = 14.4$ Hz), 3.12 (d, 2H, $\text{NCH}_A\text{H}_B\text{Py}$, $J = 14.4$ Hz), 3.12 (d, 3H, $\text{ArCH}_2\text{Ar eq}$, $J = 12.9$ Hz), 3.07 (d, 1H, $\text{ArCH}_2\text{Ar eq}$, $J = 13.3$ Hz), 1.97 (s, 6H, $\text{ArCH}_2\text{NCH}_3$), 1.21 (t, 6H, CH_2CH_3 , $J = 7.0$ Hz), 1.20 (t, 6H, CH_2CH_3 , $J = 7.0$ Hz). ^{13}C NMR (75 MHz; CDCl_3): δ 159.1, 159.0, 156.5, 155.8, 137.6, 135.4, 135.2, 135.0, 132.1, 129.5, 129.2, 128.5, 128.4, 122.5, 121.8, 119.2, 73.6, 73.5, 70.0, 66.8, 64.8, 62.2, 61.8, 42.8, 32.6, 31.2, 15.7. MS (CI) m/z (%): 1041.6 $[\text{M}+\text{H}]^+$ (100). Anal. Calcd for $\text{C}_{62}\text{H}_{80}\text{N}_4\text{O}_{10}$ (1041.34): C, 71.51; H, 7.74; N, 5.38. Found: C, 71.64; H, 7.84; N, 5.46.

5,11-Bis[*N*-((6-chloromethylpyridin-2-yl)-methyl)-*N*-methyl-aminomethyl]-25,26,27,28-tetrakis(2-ethoxyethoxy)calix[4]arene (15)

Thionyl chloride (0.14 mL, 1.9 mmol) was added to a solution of calix[4]arene **14** (100 mg, 0.096 mmol) in CH_2Cl_2 (15 mL) and the mixture was stirred for 3 h. The solvent was removed under reduced pressure to give in quantitative yield bis(2-chloromethylpyridine) **15** (102 mg, 0.096 mmol), which was pure enough for further reactions. An analytical sample of **15** was dissolved in CH_2Cl_2 , washed with a saturated NaHCO_3 solution and dried over anhydrous Na_2SO_4 . Dichloromethane was removed under vacuum to give compound **15**. ^1H NMR (400 MHz; CDCl_3): δ 7.67 (t, 2H, PyH , $J = 7.4$ Hz), 7.33 (d, 2H, PyH , $J = 7.4$ Hz), 7.25 (d, 2H, PyH , $J = 7.4$ Hz), 6.67 (s, 2H, ArH), 6.65 (s, 2H, ArH), 6.62 (d, 2H, ArH , $J = 7.4$ Hz), 6.47 (d, 2H, ArH , $J = 7.4$ Hz), 6.39 (t, 2H, ArH , $J = 7.4$ Hz), 4.65 (s, 4H, PyCH_2Cl), 4.47 (d, 3H, $\text{ArCH}_2\text{Ar ax}$, $J = 13.3$ Hz), 4.45 (d, 1H, $\text{ArCH}_2\text{Ar ax}$, $J = 13.3$ Hz), 4.12 (t, 4H, ArOCH_2 , $J = 5.8$ Hz), 4.10 (t, 4H, ArOCH_2 , $J = 5.5$ Hz), 3.85 (t, 4H, $\text{ArOCH}_2\text{CH}_2$, $J = 5.5$ Hz), 3.84 (t, 4H, $\text{ArOCH}_2\text{CH}_2$, $J = 5.8$ Hz), 3.54 (q, 4H, OCH_2CH_3 , $J = 7.0$ Hz), 3.53 (q, 4H, OCH_2CH_3 , $J = 7.0$ Hz), 3.39 (s, 4H, NCH_2Py), 3.27 (d, 2H, $\text{ArCH}_A\text{H}_B\text{N}$, $J = 12.9$ Hz), 3.24 (d, 2H, $\text{NCH}_A\text{H}_B\text{Py}$, $J = 12.9$ Hz), 3.14 (d, 1H, $\text{ArCH}_2\text{Ar eq}$, $J = 12.9$ Hz), 3.13 (d, 2H, $\text{ArCH}_2\text{Ar eq}$, $J = 12.9$ Hz), 3.08 (d, 1H, $\text{ArCH}_2\text{Ar eq}$, $J = 13.3$ Hz), 2.03 (s, 6H, $\text{ArCH}_2\text{NCH}_3$), 1.20 (t, 12H, CH_2CH_3 , $J = 7.0$ Hz). ^{13}C NMR (75 MHz; CDCl_3): δ 160.2, 156.5, 156.0, 155.8, 137.7, 135.3, 135.1, 135.0, 132.2, 129.2, 129.0, 128.5, 128.4, 122.8, 122.5, 121.2, 73.6, 70.1, 66.7, 62.9, 62.0, 47.2, 42.9, 31.2, 15.7. MS (CI) m/z (%): 1077.7 $[\text{M}+\text{H}]^+$ (100). Anal. Calcd for $\text{C}_{62}\text{H}_{78}\text{N}_4\text{O}_8\text{Cl}_2$ (1079.23): C, 69.06; H, 7.29; N, 5.20. Found: C, 69.21; H, 7.16; N, 5.29.

5,11-Bis[*N*-((6-*N,N*-dimethylaminomethylpyridin-2-yl)-methyl)-*N*-methylaminomethyl]-25,26,27,28-tetrakis(2-ethoxyethoxy)calix[4]arene (5**)**

Dimethylamine 33% in EtOH (10 mL) was added to a round bottomed flask containing the calix[4]arene **15** (98 mg, 0.09 mmol). The solution was stirred overnight and then evaporated. The product was purified by column chromatography (neutral Al₂O₃, CH₂Cl₂/MeOH 99/1) to give **5** as a pale yellow oil (75 mg, 0.068 mmol). Yield 76%. ¹H NMR (400 MHz; CDCl₃): δ 7.61 (t, 2H, PyH, J = 7.4 Hz), 7.25 (d, 2H, PyH, J = 7.4 Hz), 7.19 (d, 2H, PyH, J = 7.4 Hz), 6.66 (s, 4H, ArH), 6.60 (d, 2H, ArH, J = 7.4 Hz), 6.47 (d, 2H, ArH, J = 7.4 Hz), 6.38 (t, 2H, ArH, J = 7.4 Hz), 4.46 (d, 3H, ArCH₂Ar ax, J = 12.9 Hz), 4.45 (d, 1H, ArCH₂Ar ax, J = 13.3 Hz), 4.09 (t, 4H, ArOCH₂, J = 5.8 Hz), 4.08 (t, 4H, ArOCH₂, J = 5.4 Hz), 3.84 (t, 4H, ArOCH₂CH₂, J = 5.4 Hz), 3.83 (t, 4H, ArOCH₂CH₂, J = 5.8 Hz), 3.56 (s, 4H, NCH₂Py), 3.53 (q, 8H, OCH₂CH₃, J = 7.0 Hz), 3.43 (s, 4H, PyCH₂N(CH₃)₂), 3.25 (d, 2H, ArCH_AH_BN, J = 12.9 Hz), 3.19 (d, 2H, ArCH_AH_BN, J = 12.9 Hz), 3.13 (d, 1H, ArCH₂Ar eq, J = 13.3 Hz), 3.12 (d, 2H, ArCH₂Ar eq, J = 12.9 Hz), 3.07 (d, 1H, ArCH₂Ar eq, J = 12.9 Hz), 2.27 (s, 12H, N(CH₃)₂), 2.02 (s, 6H, ArCH₂NCH₃), 1.194 (t, 6H, CH₂CH₃, J = 7.0 Hz), 1.192 (t, 6H, CH₂CH₃, J = 7.0 Hz). ¹³C NMR (75 MHz; CDCl₃): δ 159.8, 158.5, 156.6, 155.7, 137.0, 135.4, 135.0, 132.7, 129.2, 129.0, 128.6, 128.5, 122.5, 121.6, 121.4, 73.5, 70.1, 66.7, 66.3, 63.5, 62.1, 46.1, 42.8, 31.2, 30.1, 15.7. MS (CI) *m/z* (%): 1095.6 [M+H]⁺ (100). Anal. Calcd for C₆₆H₉₀N₆O₈ (1095.48): C, 72.36; H, 8.28; N, 7.67. Found: C, 72.48; H, 8.19; N, 7.78.

5-[(*N,N'*-Bis-(*tert*-butyloxycarbonyl)-1,5,9-triazacyclododec-1-yl-methyl]-25,26,27,28-tetrakis(2-ethoxyethoxy)calix[4]arene (20**)**

To a solution of chloromethylcalix[4]arene **17** (115 mg, 0.152 mmol) in dry acetonitrile (4 mL) were added K₂CO₃ (23 mg, 0.17 mmol) and bis-Boc-protected [12]aneN₃ **16** (85 mg, 0.229 mmol) and the reaction mixture was stirred under nitrogen for 2 days. The solvent was evaporated and the residue was dissolved in CH₂Cl₂ (40 mL) and washed with a saturated NaHCO₃ aqueous solution (40 mL). The aqueous phase was extracted again with dichloromethane (40 mL) and the combined organic layers were evaporated under vacuum. The crude was purified by column chromatography (SiO₂; Et₂O/hexane, 1/1), giving calix[4]arene **20** (118 mg) as colorless oil. Yield 70%. ¹H NMR (300 MHz; CDCl₃): δ 6.73-6.70 (m, 4H, ArH), 6.62 (d, 2H, ArH, J = 7.4 Hz), 6.58 (d, 2H, ArH, J = 7.0 Hz), 6.48 (t, 1H, ArH, J = 7.0 Hz), 6.43 (s, 2H, ArH), 4.50 (d, 2H, ArCH₂Ar ax, J = 13.2 Hz), 4.49 (d, 2H, ArCH₂Ar ax, J = 13.2 Hz), 4.19 (t, 4H, ArOCH₂, J = 6.0 Hz), 4.07 (t, 4H, ArOCH₂, J = 5.6 Hz), 3.88 (t, 4H, ArOCH₂CH₂, J = 6.0 Hz), 3.83 (t, 4H, ArOCH₂CH₂, J = 5.6 Hz), 3.54 (q, 4H, OCH₂CH₃, J = 7.0 Hz), 3.53 (q, 4H, OCH₂CH₃, J = 7.0 Hz), 3.36 (t, 4H,

BocNCH₂CH₂CH₂NBoc, J = 6.8 Hz), 3.21(t, 4H, NHCH₂CH₂CH₂NBoc, J = 5.9 Hz), 3.16 (s, 2H, ArCH₂N), 3.14 (d, 2H, ArCH₂Ar eq, J = 13.2 Hz), 3.11 (d, 2H, ArCH₂Ar eq, J = 13.2 Hz), 2.09 (t, 4H, ArCH₂NHCH₂, J = 5.7 Hz), 1.90 (quin, 2H, BocNCH₂CH₂CH₂NBoc, J = 6.8 Hz), 1.67 (quin, 4H, NHCH₂CH₂CH₂NBoc, J = 5.9 Hz), 1.47 (s, 18H, C(CH₃)₃), 1.21 (t, 6H, OCH₂CH₃, J = 7.0 Hz), 1.20 (t, 6H, OCH₂CH₃, J = 7.0 Hz). ¹³C NMR (75 MHz; CDCl₃): δ 156.5, 156.2, 155.9, 154.8, 135.3, 134.6, 134.1, 131.5, 128.6, 128.2, 128.1, 128.0, 122.2, 122.0, 79.1, 73.3, 72.9, 69.6, 66.3, 66.2, 56.4, 49.8, 45.3, 43.4, 30.9, 30.8, 28.5, 26.9, 26.5, 15.2; MS (ES+) *m/z* (%): 1096.3 (30) [M+H]⁺, 1118.0 (100) [M+Na]⁺, 570.6 (80) [M+2Na]²⁺. Anal. Calcd for C₆₄H₉₃N₃O₁₂ (1096.46): C, 70.18; H, 8.55; N, 3.83. Found: C, 70.04; H, 8.68; N, 3.77.

5,17-Bis[(N',N''-bis-(tert-butyloxycarbonyl)-1,5,9-triazacyclododec-1-yl-methyl]-25,26,27,28-tetrakis(2-ethoxyethoxy)calix[4]arene (21)

Compound **21** was synthesized according to the preparation of **20**, starting from 1,3-dichloromethylcalix[4]arene **18** and using a 1.2 fold excess of K₂CO₃ and 1.35 excess of bisBoc-protected [12]aneN₃ **16** per chloromethyl group. Reaction time 4 days. The crude product was purified by column chromatography (Et₂O/Hex, 4/1), giving calix[4]arene **21** as a colorless oil. Yield 54%. ¹H NMR (300 MHz; CDCl₃): δ 6.85 (s, 4H, ArH), 6.34-6.22 (m, 6H, ArH), 4.48 (d, 4H, ArCH₂Ar ax, J = 13.2 Hz), 4.22 (t, 4H, ArOCH₂, J = 5.4 Hz), 3.98 (t, 4H, ArOCH₂, J = 5.7 Hz), 3.87 (t, 4H, ArOCH₂CH₂, J = 5.4 Hz), 3.80 (t, 4H, ArOCH₂CH₂, J = 5.7 Hz), 3.57 (q, 4H, OCH₂CH₃, J = 6.9 Hz), 3.50 (q, 4H, OCH₂CH₃, J = 7.2 Hz), 3.39 (s, 4H, ArCH₂N), 3.38-3.29 (m, 16H, BocNCH₂CH₂CH₂NBoc + NHCH₂CH₂CH₂NBoc), 3.10 (d, 4H, ArCH₂Ar eq, J = 13.2 Hz), 2.41 (t, 8H, ArCH₂NHCH₂, J = 6.0 Hz), 1.93 (quin, 4H, BocNCH₂CH₂CH₂NBoc, J = 6.0 Hz), 1.80 (quin, 8H, NHCH₂CH₂CH₂NBoc, J = 6.0 Hz), 1.45 (s, 36H, C(CH₃)₃), 1.23 (t, 6H, OCH₂CH₃, J = 6.9 Hz), 1.17 (t, 6H, OCH₂CH₃, J = 7.2 Hz). ¹³C NMR (75 MHz; CDCl₃): δ 156.5, 156.2, 155.1, 135.8, 133.8, 132.2, 129.4, 127.6, 122.2, 79.2, 73.6, 72.6, 69.7, 69.6, 66.4, 66.2, 57.9, 50.2, 45.1, 43.6, 30.9, 28.5, 27.1, 26.8, 15.3, 15.2. MS (MALDI-TOF) *m/z* (%): 1480.5 (100) [M+H]⁺. Anal. Calcd for C₈₄H₁₃₀N₆O₁₆ (1479.99): C, 68.17; H, 8.85; N, 5.68. Found: C, 68.29; H, 9.01; N, 5.50.

5,11-Bis[(N',N''-bis-(tert-butyloxycarbonyl)-1,5,9-triazacyclododec-1-yl-methyl]-25,26,27,28-tetrakis(2-ethoxyethoxy)calix[4]arene (22)

Compound **22** was synthesized according to the preparation of **20**, starting from 1,2-dichloromethyl calix[4]arene **12** and using a 1.2 fold excess of K₂CO₃ and 1.35 fold excess of bisBoc-protected [12]aneN₃ **16** per chloromethyl group. Reaction time 3 days. The crude was purified by column chromatography (Hex/EtOAc/Et₂O, 6/4/1), giving calix[4]arene **22** as a colorless oil. Yield 45%. ¹H NMR (300 MHz; CDCl₃): δ

6.67 (dd, 2H, ArH, $J^3 = 7.6$ Hz, $J^4 = 1.3$ Hz), 6.63 (dd, 2H, ArH, $J^3 = 7.6$ Hz, $J^4 = 1.3$ Hz), 6.55 (d, 2H, ArH, $J = 1.0$ Hz), 6.53 (t, 2H, ArH, $J = 7.6$ Hz), 6.46 (d, 2H, ArH, $J = 1.0$ Hz), 4.50 (d, 1H, ArCH₂Ar ax, $J = 13.0$ Hz), 4.48 (d, 2H, ArCH₂Ar ax, $J = 13.2$ Hz), 4.45 (d, 1H, ArCH₂Ar ax, $J = 13.0$ Hz), 4.11 (t, 8H, ArOCH₂, $J = 5.6$ Hz), 3.85 (t, 8H, ArOCH₂CH₂, $J = 5.6$ Hz), 3.54 (q, 4H, OCH₂CH₃, $J = 7.1$ Hz), 3.53 (q, 4H, OCH₂CH₃, $J = 7.1$ Hz), 3.35 (bs, 8H, BocNCH₂CH₂CH₂NBoc), 3.24 (t, 8H, NCH₂CH₂CH₂NBoc, $J = 6.7$ Hz), 3.20 (s, 4H, ArCH₂N), 3.15 (d, 1H, ArCH₂Ar eq, $J = 13.0$ Hz), 3.11 (d, 2H, ArCH₂Ar eq, $J = 13.2$ Hz), 3.07 (d, 1H, ArCH₂Ar eq, $J = 13.0$ Hz), 2.15 (bs, 8H, ArCH₂NCH₂), 1.90 (quin, 4H, BocNCH₂CH₂CH₂NBoc, $J = 6.7$ Hz), 1.69 (bs, 8H, ArCH₂NCH₂CH₂), 1.45 (s, 36H, C(CH₃)₃), 1.20 (t, 6H, OCH₂CH₃, $J = 7.1$ Hz), 1.19 (t, 6H, OCH₂CH₃, $J = 7.1$ Hz). ¹³C NMR (75 MHz; CDCl₃): δ 156.2, 155.2, 135.0, 134.6, 134.4, 131.7, 128.7, 128.6, 128.5, 128.1, 128.0, 127.7, 122.1, 79.1, 73.1, 69.7, 66.3, 49.8, 45.3, 43.5, 30.9, 29.7, 28.5, 26.5, 15.3. MS (ES+) m/z (%): 1479.9 (10) [M+H]⁺, 1502.4 (35) [M+Na]⁺, 762.4 (100) [M+2Na]²⁺. Anal. Calcd for C₈₄H₁₃₀N₆O₁₆ (1479.99): C, 68.17; H, 8.85; N, 5.68. Found: C, 68.05; H, 8.99; N, 5.51.

5,11,17-Tris[(*N',N''*-bis-(*tert*-butyloxycarbonyl)-1,5,9-triazacyclododec-1-yl-methyl]-25,26,27,28-tetrakis(2-ethoxyethoxy)calix[4]arene (23)

Compound **23** was synthesized according to the preparation of **20**, starting from trichloromethylcalix[4]arene **19** and using a 1.15 fold excess of K₂CO₃ and bisBoc-protected [12]aneN₃ **16** per chloromethyl group. Reaction time 5 days. The crude was purified by column chromatography using Et₂O as eluent, giving calix[4]arene **23** as a colorless oil. Yield 60%. ¹H NMR (300 MHz; CDCl₃): δ 6.82 (d, 2H, ArH, $J = 1.0$ Hz), 6.74 (d, 2H, ArH, $J = 1.0$ Hz), 6.25 (s, 3H, ArH), 6.09 (s, 2H, ArH), 4.45 (d, 2H, ArCH₂Ar ax, $J = 13.2$ Hz), 4.42 (d, 2H, ArCH₂Ar ax, $J = 13.2$ Hz), 4.21 (t, 4H, ArOCH₂, $J = 6.2$ Hz), 3.92 (t, 4H, ArOCH₂, $J = 5.2$ Hz), 3.84 (t, 4H, ArOCH₂CH₂, $J = 6.2$ Hz), 3.75 (t, 4H, ArOCH₂CH₂, $J = 5.2$ Hz), 3.52 (q, 4H, OCH₂CH₃, $J = 7.0$ Hz), 3.44 (q, 4H, OCH₂CH₃, $J = 7.0$ Hz), 3.35 (s, 4H, ArCH₂N), 3.33-3.26 (m, 20H, CH₂NBocCH₂), 3.08 (bs, 4H, NCH₂CH₂CH₂NBoc), 3.06 (d, 2H, ArCH₂Ar eq, $J = 13.2$ Hz), 3.02 (d, 2H, ArCH₂Ar eq, $J = 13.2$ Hz), 2.94 (s, 2H, ArCH₂N), 2.35 (bs, 8H, ArCH₂NCH₂), 1.94-1.78 (bs, 10H, ArCH₂NCH₂ + BocNCH₂CH₂CH₂NBoc), 1.75 (m, 8H, ArCH₂NCH₂CH₂), 1.52 (bs, 4H, ArCH₂NCH₂CH₂), 1.40 (s, 54H, C(CH₃)₃), 1.27 (t, 6H, OCH₂CH₃, $J = 7.0$ Hz), 1.19 (t, 6H, OCH₂CH₃, $J = 7.0$ Hz). ¹³C NMR (75 MHz; CDCl₃): δ 156.4, 156.2, 156.1, 155.1, 154.0, 135.8, 135.7, 133.7, 133.2, 132.1, 131.4, 129.3, 128.1, 127.5, 125.4, 122.0, 79.2, 79.1, 73.7, 72.4, 69.7, 69.6, 66.4, 66.1, 57.9, 49.9, 49.5, 45.4, 45.1, 43.5, 43.4, 30.9, 30.3, 29.6, 28.5, 27.2, 27.1, 26.7, 26.4, 15.3, 15.2. MS (FAB+) m/z

(%): 1863.3 (100) $[M+H]^+$. Anal. Calcd for $C_{104}H_{167}N_9O_{20}$ (1863.53): C, 67.03; H, 9.03; N, 6.76. Found: C, 67.20; H, 9.19; N, 6.67.

General procedure for the Boc deprotection

Boc protecting groups were removed from compounds **20**, **21**, **22** and **23** by the following procedure: the Boc-protected calix[4]arene was dissolved in CH_2Cl_2 (2 mL) and trifluoroacetic acid (1 mL) was added. The solution was stirred for 2 h and then evaporated under reduced pressure. The residue was taken up with dichloromethane (20 mL) and Li_2CO_3 aqueous saturated solution (20 mL). The organic phase was separated and the aqueous one was extracted again with CH_2Cl_2 (2 x 20 mL), the organic fractions were combined and evaporated under vacuum, obtaining the corresponding deprotected products **8**, **9**, **10** and **11**, respectively, in quantitative yield.

5-[*N*-(1,5,9-Triazacyclododecyl)-methyl]-25,26,27,28-tetrakis(2-ethoxyethoxy)calix[4]arene (**8**)

1H NMR (300 MHz; $CDCl_3$): δ 7.05-7.01 (m, 4H, ArH), 6.82 (t, 2H, ArH, $J = 7.5$ Hz), 6.56 (t, 1H, ArH, $J = 7.5$ Hz), 6.41 (d, 2H, ArH, $J = 7.5$ Hz), 6.25 (s, 2H, ArH), 4.56 (d, 2H, $ArCH_2Ar$ ax, $J = 13.1$ Hz), 4.49 (d, 2H, $ArCH_2Ar$ ax, $J = 12.8$ Hz), 4.40 (dt, 2H, $ArOCH_AH_B$, $J^2 = 11.0$ Hz, $J^3 = 6.3$ Hz), 4.31 (dt, 2H, $ArOCH_AH_B$, $J^2 = 11.0$ Hz, $J^3 = 6.3$ Hz), 3.99-3.90 (m, 12H, $ArOCH_2 + ArOCH_2CH_2$), 3.80-3.73 (m, 4H, $ArOCH_2CH_2$), 3.70 (s, 2H, $ArCH_2N$), 3.57 (q, 2H, OCH_2CH_3 , $J = 7.0$ Hz), 3.55 (q, 2H, OCH_2CH_3 , $J = 6.9$ Hz), 3.52 (q, 4H, OCH_2CH_3 , $J = 6.9$ Hz), 3.15 (d, 2H, $ArCH_2Ar$ eq, $J = 12.8$ Hz), 3.14 (d, 2H, $ArCH_2Ar$ eq, $J = 13.1$ Hz), 3.08 (bs, 4H, $HNCH_2CH_2CH_2NH$), 2.95 (bs, 4H, $NCH_2CH_2CH_2NH$), 2.12 (bs, 2H, $ArCH_2NCH_2$), 1.90 (bs, 2H, $ArCH_2NCH_2$), 1.66 (bs, 4H, $NCH_2CH_2CH_2NH$), 1.51 (bs, 2H, $NHCH_2CH_2CH_2NH$), 1.24 (t, 3H, OCH_2CH_3 , $J = 7.0$ Hz), 1.23 (t, 3H, OCH_2CH_3 , $J = 6.9$ Hz), 1.18 (t, 6H, OCH_2CH_3 , $J = 6.9$ Hz). ^{13}C NMR (75 MHz; $CDCl_3$): δ 156.9, 155.7, 154.7, 136.7, 136.4, 134.5, 133.6, 131.5, 128.8, 128.2, 127.4, 122.9, 122.4, 119.9, 74.4, 74.3, 72.3, 69.6, 69.4, 66.4, 66.3, 66.1, 52.1, 48.0, 47.4, 44.0, 30.7, 23.2, 21.9, 15.3, 15.1. MS (ES+) m/z (%): 896.7 (30) $[M+H]^+$, 918.5 (100) $[M+Na]^+$. Anal. Calcd for $C_{54}H_{77}N_3O_8$ (896.23): C, 72.37; H, 8.66; N, 4.69. Found: C, 72.21; H, 8.76; N, 4.78.

5,17-Bis[*N*-(1,5,9-triazacyclododecyl)-methyl]-25,26,27,28-tetrakis(2-ethoxyethoxy)calix[4]arene (**9**)

1H NMR (300 MHz; $CDCl_3$): δ 6.75 (s, 4H, ArH), 6.32-6.22 (m, 6H, ArH), 4.45 (d, 4H, $ArCH_2Ar$ ax, $J = 13.5$ Hz), 4.15 (t, 4H, $ArOCH_2$, $J = 6.0$ Hz), 3.95 (t, 4H, $ArOCH_2$, $J = 5.1$ Hz), 3.80 (t, 4H, $ArOCH_2CH_2$, $J = 6.0$ Hz), 3.76 (t, 4H, $ArOCH_2CH_2$, $J = 5.1$ Hz), 3.50 (q, 4H, OCH_2CH_3 , $J = 6.9$ Hz), 3.45 (q, 4H, OCH_2CH_3 , $J = 7.2$ Hz), 3.33 (s, 4H,

ArCH₂N), 3.04 (d, 4H, ArCH₂Ar eq, J = 13.5 Hz), 2.97 (bs, 8H, HNCH₂CH₂CH₂NH), 2.73 (bs, 8H, CH₂NHCH₂CH₂CH₂NHCH₂), 2.42 (bs, 8H, ArCH₂NCH₂), 1.85 (bs, 4H, NHCH₂CH₂CH₂NH), 1.75 (bs, 8H, ArCH₂NCH₂CH₂), 1.16 (t, 6H, OCH₂CH₃, J = 6.9 Hz), 1.10 (t, 6H, OCH₂CH₃, J = 7.2 Hz). ¹³C NMR (75 MHz; CDCl₃): δ 156.7, 155.3, 135.9, 133.9, 130.6, 129.4, 127.6, 122.3, 73.6, 72.9, 69.8, 69.6, 66.4, 66.2, 55.2, 51.9, 50.0, 46.8, 31.0, 23.9, 15.3, 15.2. MS (FAB+) *m/z* (%): 1079.6 (100) [M+H]⁺. Anal. Calcd for C₆₄H₉₈N₆O₈ (1079.52): C, 71.21; H, 9.15; N, 7.78. Found: C, 71.39; H, 9.27; N, 7.68.

5,11-Bis[*N*-(1,5,9-triazacyclododecyl)-methyl]-25,26,27,28-tetrakis(2-ethoxyethoxy)calix[4]arene (10)

¹H NMR (300 MHz; CDCl₃): δ 6.66-6.63 (m, 4H, ArH), 6.56-6.52 (m, 4H, ArH), 6.46 (s, 2H, ArH), 4.51 (d, 2H, ArCH₂Ar ax, J = 13.1 Hz), 4.49 (d, 2H, ArCH₂Ar ax, J = 13.1 Hz), 4.15 (t, 4H, ArOCH₂, J = 5.5 Hz), 4.13 (t, 4H, ArOCH₂, J = 5.5 Hz), 3.86 (t, 4H, ArOCH₂CH₂, J = 5.5 Hz), 3.85 (t, 4H, ArOCH₂CH₂, J = 5.5 Hz), 3.54 (q, 4H, OCH₂CH₃, J = 6.9 Hz), 3.53 (q, 4H, OCH₂CH₃, J = 6.9 Hz), 3.30 (d, 2H, ArCH_AH_BN, J = 14.0 Hz), 3.24 (d, 2H, ArCH_AH_BN, J = 14.0 Hz), 3.15 (d, 1H, ArCH₂Ar eq, J = 13.1 Hz), 3.12 (d, 2H, ArCH₂Ar eq, J = 13.1 Hz), 3.08 (d, 1H, ArCH₂Ar eq, J = 13.1 Hz), 2.97 (t, 8H, HNCH₂CH₂CH₂NH, J = 4.8 Hz), 2.72 (t, 8H, NCH₂CH₂CH₂NH, J = 4.8 Hz), 2.18 (bs, 8H, ArCH₂NCH₂), 1.88 (bs, 4H, HNCH₂CH₂CH₂NH), 1.67 (bs, 8H, NCH₂CH₂CH₂NH), 1.22 (t, 6H, OCH₂CH₃, J = 6.9 Hz), 1.20 (t, 6H, OCH₂CH₃, J = 6.9 Hz). ¹³C NMR (75 MHz; CDCl₃): δ 156.2, 155.2, 135.1, 134.7, 134.5, 130.9, 129.2, 128.9, 128.1, 122.2, 73.2, 69.7, 69.6, 66.3, 55.2, 51.8, 49.9, 49.5, 47.1, 31.0, 30.8, 29.7, 27.7, 25.2, 15.3. MS (ES+) *m/z* (%): 540.2 (100) [M+2H]²⁺. Anal. Calcd for C₆₄H₉₈N₆O₈ (1079.52): C, 71.21; H, 9.15; N, 7.78. Found: C, 71.38; H, 9.29; N, 7.59.

5,11,17-Tris[*N*-(1,5,9-triazacyclododecyl)-methyl]-25,26,27,28-tetrakis(2-ethoxyethoxy)calix[4]arene (11)

¹H NMR (300 MHz; CDCl₃): δ 6.86 (d, 2H, ArH, J = 1.1 Hz), 6.82 (d, 2H, ArH, J = 1.1 Hz), 6.29 (s, 3H, ArH), 6.14 (s, 2H, ArH), 4.43 (d, 2H, ArCH₂Ar ax, J = 12.8 Hz), 4.41 (d, 2H, ArCH₂Ar ax, J = 13.2 Hz), 4.20 (t, 4H, ArOCH₂, J = 6.2 Hz), 3.92 (t, 4H, ArOCH₂, J = 5.1 Hz), 3.84 (t, 4H, ArOCH₂CH₂, J = 6.2 Hz), 3.74 (t, 4H, ArOCH₂CH₂, J = 5.1 Hz), 3.50 (q, 4H, OCH₂CH₃, J = 6.9 Hz), 3.40 (q, 4H, OCH₂CH₃, J = 6.9 Hz), 3.34 (d, 2H, ArCH_AH_BN, J = 13.2 Hz), 3.26 (d, 2H, ArCH_AH_BN, J = 13.2 Hz), 3.07 (d, 2H, ArCH₂Ar eq, J = 12.8 Hz), 3.05 (d, 2H, ArCH₂Ar eq, J = 13.2 Hz), 3.00 (s, 2H, ArCH₂N), 2.76 (t, 8H, HNCH₂CH₂CH₂NH, J = 4.8 Hz), 2.69 (t, 4H, HNCH₂CH₂CH₂NH, J = 4.8 Hz), 2.63 (t, 8H, NCH₂CH₂CH₂NH, J = 5.1 Hz), 2.48 (t, 4H, NCH₂CH₂CH₂NH, J = 5.2 Hz), 2.41 (bs, 8H, ArCH₂NCH₂), 1.92 (bs, 4H, ArCH₂NCH₂), 1.61 (bs, 14H,

NCH₂CH₂CH₂NHCH₂CH₂, 1.37 (bs, 4H, NCH₂CH₂CH₂NH), 1.17 (t, 3H, OCH₂CH₃, J = 7.0 Hz), 1.14 (t, 3H, OCH₂CH₃, J = 7.0 Hz), 1.10 (t, 6H, OCH₂CH₃, J = 7.0 Hz). ¹³C NMR (75 MHz; CDCl₃): δ 156.4, 155.1, 154.2, 135.7, 133.9, 133.3, 131.6, 129.9, 129.4, 129.3, 127.6, 122.3, 73.7, 72.6, 69.7, 69.6, 66.4, 66.2, 55.9, 52.3, 51.2, 49.9, 49.5, 47.1, 47.0, 31.0, 30.3, 29.7, 25.6, 25.2, 25.1, 24.9, 15.3, 15.2. MS (ES+) *m/z* (%): 1262.8 (30) [M+H]⁺, 632.0 (100) [M+2H]²⁺. Anal. Calcd for C₇₄H₁₁₉N₉O₈ (1262.82): C, 70.38; H, 9.50; N, 9.98. Found: C, 70.25; H, 9.41; N, 9.83.

5,11,17,23-tetraformyl-25,26,27,28-tetrakis(2-ethoxyethoxy)calix[4]arene (25)

To a solution of 25,26,27,28-tetrakis(2-ethoxyethoxy)calix[4]arene (2.5 g, 3.5 mmol) in trifluoroacetic acid (70 mL) was added hexamethylenetetramine (15.7 g, 112 mmol). The reaction mixture was heated at 140 °C for 36 h, cooled to room temperature and poured into water (150 mL). CH₂Cl₂ (30 mL) was added to this solution, which was vigorously stirred for 3 h. The aqueous phase was extracted with CH₂Cl₂ (2 x 150 mL), after which the combined organic phases were washed with saturated NaHCO₃ solution (100 mL) and water (200 mL). The solvent was evaporated under reduced pressure and the residue purified by column chromatography (EtOAc/Hex, 6/4) to give product **25** in 76% yield. The analytical data were the same as reported in the literature.²⁷

5-(5,5-Dimethyl-1,3-dioxane-2-yl)-11,17,23-triformyl-25,26,27,28-tetrakis(2-ethoxyethoxy)calix[4]arene (26)

Tetraformylcalix[4]arene **25** (3 g, 3.63 mmol), 2,2-dimethyl-1,3-propanediol (0.379 g, 3.63 mmol) and a catalytic amount of *p*-toluenesulfonic acid were dissolved in dry toluene (160 mL). The solution was kept under N₂. Above the round bottomed flask was put a dropping funnel half filled with 4 Å molecular sieves, and a refrigerator. The solution was refluxed for 20 h, after which it was filtered over anhydrous Na₂CO₃ and the toluene evaporated under vacuum. The product **26** (R_f = 0.29) was purified by column chromatography (Hex/EtOAc 1/1; column pretreated with Hex/EtOAc 1/1 + NEt₃ 2% v/v) obtaining a white foaming solid (1.56 g) in 47% yield. Mp = 67 °C. ¹H NMR (300 MHz; CDCl₃): δ 9.63 (s, 2H, ArCHO), 9.51 (s, 1H, ArCHO), 7.22 (s, 4H, ArH), 7.05 (s, 2H, ArH), 6.64 (s, 2H, ArH), 4.90 (s, 1H, ArCHO₂), 4.61 (d, 2H, ArCH₂Ar ax, J = 13.8 Hz), 4.52 (d, 2H, ArCH₂Ar ax, J = 13.7 Hz), 4.24-4.15 (m, 6H, ArOCH₂), 4.00 (t, 2H, ArOCH₂, J = 5.4 Hz), 3.80-3.75 (m, 6H, ArOCH₂CH₂), 3.72 (t, 2H, ArOCH₂CH₂, J = 5.4 Hz), 3.60 (d, 2H, OCH_AH_BC(CH₃)₂, J = 11.0 Hz), 3.51 (d, 2H, OCH_BH_AC(CH₃)₂, J = 11.0 Hz), 3.52-3.43 (m, 8H, ROCH₂CH₃), 3.28 (d, 2H, ArCH₂Ar eq, J = 13.8 Hz), 3.24 (d, 2H, ArCH₂Ar eq, J = 13.7 Hz), 1.18 (t,

6H, ROCH₂CH₃, J = 7.2 Hz), 1.15 (s, 3H, CCH₃), 1.13 (t, 6H, ROCH₂CH₃, J = 6.9 Hz), 0.71 (s, 3H, CCH₃). ¹³C NMR (75 MHz; CDCl₃): δ 191.5, 191.3, 162.2, 161.5, 156.1, 136.4, 135.7, 135.3, 133.7, 133.1, 131.3, 131.2, 130.6, 130.0, 129.7, 126.0, 100.8, 77.2, 73.8, 73.6, 73.3, 69.6, 69.2, 66.3, 66.2, 30.7, 29.9, 23.0, 21.7, 15.1. MS (CI) *m/z* (%): 911.4 (100) [M+H]⁺. Anal. Calcd for C₅₃H₆₆O₁₃ (911.10): C, 69.87; H, 7.30. Found: C, 69.80; H, 7.38.

5-(5,5-Dimethyl-1,3-dioxane-2-yl)-11,17,23-trishydroxymethyl-25,26,27,28-tetrakis(2-ethoxyethoxy)calix[4]arene (27)

The solution of triformylmonoprotected calix[4]arene **26** (1 g, 1.0 mmol) and NaBH₄ (190 mg, 5.0 mmol) in absolute EtOH (40 mL) was stirred for 4 h. The solvent was evaporated and the crude dissolved in CH₂Cl₂ (50 mL) and saturated NaHCO₃ solution (50 mL). The aqueous phase was extracted again with CH₂Cl₂ (50 mL); the organic fractions were combined and the solvent was evaporated under reduced pressure, obtaining the product **27** in quantitative yield. Mp = 74.3 °C. ¹H NMR (300 MHz; CDCl₃): δ 7.00 (s, 2H, ArH), 6.84 (s, 2H, ArH), 6.41 (d, 2H, ArH, J = 1.7 Hz), 6.33 (d, 2H, ArH, J = 1.7 Hz), 5.22 (s, 1H, ArCHO₂), 4.49 (d, 2H, ArCH₂Ar ax, J = 13.3 Hz), 4.48 (d, 2H, ArCH₂Ar ax, J = 13.3 Hz), 4.39 (s, 2H, ArCH₂OH), 4.24-4.13 (m, 8H, ArCH₂OH + ArOCH₂), 4.04 (t, 4H, ArOCH₂, J = 5.4 Hz), 3.86 (t, 2H, ArOCH₂CH₂, J = 5.9 Hz), 3.83 (t, 2H, ArOCH₂CH₂, J = 6.2 Hz), 3.80 (t, 4H, ArOCH₂CH₂, J = 5.4 Hz), 3.72 (d, 2H, OCH_AH_BC(CH₃)₂, J = 10.9 Hz), 3.58 (d, 2H, OCH_BH_AC(CH₃)₂, J = 11.0 Hz), 3.57-3.47 (m, 8H, ROCH₂CH₃), 3.15 (d, 2H, ArCH₂Ar eq, J = 13.3 Hz), 3.14 (d, 2H, ArCH₂Ar eq, J = 13.3 Hz), 1.27 (s, 3H, CCH₃), 1.21 (t, 6H, ROCH₂CH₃, J = 7.0), 1.17 (t, 6H, ROCH₂CH₃, J = 7.0), 0.76 (s, 3H, CCH₃). ¹³C NMR (75 MHz; CDCl₃): δ 157.5, 156.4, 155.8, 135.6, 135.4, 135.0, 134.9, 133.9, 133.6, 132.0, 127.5, 126.5, 126.3, 126.2, 101.9, 77.5, 73.6, 72.8, 72.6, 69.6, 69.5, 69.2, 66.3, 66.2, 64.5, 64.2, 30.8, 30.1, 23.0, 21.8, 15.3, 15.2. MS (CI) *m/z* (%): 917.8 (100) [M+H]⁺. Anal. Calcd for C₅₃H₇₂O₁₃ (917.15): C, 69.41; H, 7.91. Found: C, 69.56; H, 8.05.

5-Formyl-11,17,23-trischloromethyl-25,26,27,28-tetrakis(2-ethoxyethoxy)calix[4]arene (28)

Thionyl chloride (1 mL, 13.6 mmol) was added to a solution of trishydroxymethyl monoprotected calix[4]arene **27** (500 mg, 0.545 mmol) in CH₂Cl₂ (20 mL) and the solution was stirred for 2h. Water (2 mL) was then added to the reaction mixture that was vigorously stirred for 2 days. 20 mL of 0.5 N NaOH aqueous solution were added and the extracted organic phase was washed with water (2 x 20 mL). The organic layers were combined and the solvent evaporated under vacuum, obtaining a colourless oil pure enough for further modification. Yield > 95%. ¹H NMR (300 MHz;

CDCl₃): δ 9.63 (s, 1H, ArCHO), 7.14 (s, 2H, ArH), 6.71 (s, 4H, ArH), 6.57 (s, 2H, ArH), 4.56 (d, 2H, ArCH₂Ar ax, J = 13.5 Hz), 4.48 (d, 2H, ArCH₂Ar ax, J = 13.5 Hz), 4.32 (s, 4H, ArCH₂Cl), 4.18 (s, 2H, ArCH₂Cl), 4.20-4.08 (m, 8H, ArOCH₂), 3.83-3.78 (m, 8H, ArOCH₂CH₂), 3.55-3.47 (m, 8H, ROCH₂CH₃), 3.22 (d, 2H, ArCH₂Ar eq, J = 13.5 Hz), 3.13 (d, 2H, ArCH₂Ar eq, J = 13.5 Hz), 1.19 (t, 12H, ROCH₂CH₃, J = 6.9 Hz). ¹³C NMR (75 MHz; CDCl₃): δ 191.4, 162.0, 156.5, 156.3, 135.9, 135.3, 134.9, 134.7, 131.4, 131.1, 130.0, 128.9, 128.52, 128.48, 73.6, 73.3, 69.6, 69.5, 66.33, 66.28, 46.4, 46.3, 30.8, 30.7, 15.2, 15.1. MS (CI) *m/z* (%): 885.2 (55) [M+H]⁺, 849.8 (100) [M-Cl]⁺. Anal. Calcd for C₄₈H₅₉Cl₃O₉ (886.35): C, 65.04; H, 6.71. Found: C, 64.89; H, 6.60.

5-Formyl-11,17,23-tris[(N',N''-bis-(tert-butyloxycarbonyl)-1,5,9-triazacyclododec-1-yl-methyl]-25,26,27,28-tetrakis(2-ethoxyethoxy)calix[4]arene (29)

Trichloromethyl monoformylcalix[4]arene **28** (95 mg, 0.107 mmol) was dissolved in dry acetonitrile (3 mL). K₂CO₃ (63 mg, 0.45 mmol) and bis-Boc-protected [12]aneN₃ **16** (185 mg, 0.50 mmol) were added and the solution was stirred under nitrogen for 10 days. The solvent was evaporated and the residue was dissolved in CH₂Cl₂ (40 mL) and washed with saturated NaHCO₃ solution (40 mL). The aqueous phase was extracted again with dichloromethane (40 mL) and the combined organic layers were evaporated under vacuum. The crude product was purified by column chromatography using Et₂O as eluent, giving calix[4]arene **29** (154 mg) as white foaming solid. Yield 74%. Mp = 65.5 °C. ¹H NMR (300 MHz; CDCl₃): δ 9.41 (s, 1H, ArCHO), 6.86 (s, 2H, ArH), 6.83 (s, 2H, ArH), 6.75 (s, 2H, ArH), 6.13 (s, 2H, ArH), 4.53 (d, 2H, ArCH₂Ar ax, J = 13.4 Hz), 4.42 (d, 2H, ArCH₂Ar ax, J = 13.3 Hz), 4.25-4.13 (m, 4H, ArOCH₂), 4.06 (t, 2H, ArOCH₂, J = 5.0 Hz), 3.96 (t, 2H, ArOCH₂, J = 4.9 Hz), 3.86-3.75 (m, 8H, ArOCH₂CH₂), 3.52 (q, 4H, OCH₂CH₃, J = 7.0 Hz), 3.46 (q, 4H, OCH₂CH₃, J = 6.9 Hz), 3.36-3.28 (m, 24H, CH₂N-BOC-CH₂), 3.15 (d, 2H, ArCH₂Ar eq, J = 13.3 Hz), 3.12 (s, 4H, ArCH₂N), 3.05 (d, 2H, ArCH₂Ar eq, J = 13.4 Hz), 2.79 (s, 2H, ArCH₂N), 2.37 (bs, 8H, ArCH₂NCH₂), 2.07 (bs, 4H, ArCH₂NCH₂), 1.95-1.70 (m, 6H, BOCNCH₂CH₂CH₂NBOC), 1.77 (bs, 8H, ArCH₂NCH₂CH₂), 1.57 (bs, 4H, ArCH₂NCH₂CH₂), 1.43 (s, 54H, C(CH₃)₃), 1.19 (t, 3H, OCH₂CH₃, J = 6.9 Hz), 1.18 (t, 3H, OCH₂CH₃, J = 6.9 Hz), 1.14 (t, 6H, OCH₂CH₃, J = 7.0 Hz). ¹³C NMR (75 MHz; CDCl₃): δ 190.9, 161.1, 156.1, 156.0, 154.2, 135.6, 135.4, 134.8, 133.2, 132.4, 132.2, 131.1, 129.6, 128.4, 79.1, 79.0, 73.9, 73.5, 72.5, 69.6, 66.4, 66.3, 66.0, 57.9, 57.0, 49.9, 49.7, 45.2, 45.1, 43.6, 43.4, 31.0, 29.5, 28.4, 27.3, 27.1, 26.7, 26.3, 15.22, 15.17, 15.10. MS (ES⁺) *m/z* (%): 1913.5 (10) [M+Na]⁺, 968.3 (100) [M+2Na]²⁺. Anal. Calcd for

C₁₀₅H₁₆₈N₉O₂₁ (1892.54): C, 66.64; H, 8.95; N, 6.66. Found: C, 66.43; H, 8.84; N, 6.78.

5-[*N*-(3-Carboxypropyl)-aminomethyl]-11,17,23-tris[(*N'*,*N''*-bis-(*tert*-butyloxycarbonyl)-1,5,9-triazacyclododec-1-yl-methyl)]-25,26,27,28-tetrakis(2-ethoxyethoxy)calix[4]arene (30)

The tristriaza monoformylcalix[4]arene **29** (50 mg, 0.026 mmol) was dissolved in dry dichloroethylene (10 mL). 4-aminobutyric acid (5 mg, 0.048 mmol), previously kept under vacuum for 5 h, and NaBH(CH₃COO)₃ (12 mg, 0.056 mmol) were added and the solution was vigorously stirred under nitrogen for 1 day. The solution was poured in HCl 0.1 N (10 mL), and the organic phase was extracted. The aqueous phase was extracted again with dichloromethane (10 mL) and the combined organic layers were evaporated under vacuum. The crude was purified by column chromatography (SiO₂, eluent CH₂Cl₂/MeOH 9.2/0.8 then changed to CH₂Cl₂/MeOH 8.2/1.8) obtaining **30** as a pale yellow oil. Yield 20%. ¹H NMR (300 MHz; CD₃OD): δ 6.84 (s, 2H, ArH), 6.73 (s, 2H, ArH), 6.68 (s, 2H, ArH), 6.65 (s, 2H, ArH), 4.61 (d, 2H, ArCH₂Ar ax, J = 13.2 Hz), 4.59 (d, 2H, ArCH₂Ar ax, J = 13.1 Hz), 4.19-4.13 (m, 8H, ArOCH₂), 3.91-3.83 (m, 8H, ArOCH₂CH₂), 3.58-3.51 (m, 8H, OCH₂CH₃), 3.42-3.29 (m, 32H, CH₂N-BOC-CH₂ + ArCH₂N), 3.21 (d, 2H, ArCH₂Ar eq, J = 13.2 Hz), 3.17 (d, 2H, ArCH₂Ar eq, J = 13.1 Hz), 3.01 (t, 2H, NHCH₂CH₂CH₂COOH, J = 5.3 Hz), 2.53 (bs, 8H, ArCH₂NCH₂), 2.40 (bs, 6H, ArCH₂NCH₂ + CH₂COOH), 1.95 (bs, 6H, BOCNCH₂CH₂CH₂NBOC), 1.87-1.82 (m, 2H, CH₂CH₂COOH), 1.76 (bs, 12H, NCH₂CH₂CH₂NBOC), 1.46 (s, 54H, C(CH₃)₃), 1.19 (t, 6H, OCH₂CH₃, J = 6.9 Hz), 1.18 (t, 6H, OCH₂CH₃, J = 6.9 Hz). MS (ES+) *m/z* (%): 2001.4 (20) [M+Na]⁺, 1012.3 (100) [M+2Na]²⁺. Anal. Calcd for C₁₀₉H₁₇₇N₁₀O₂₂ (1979.67): C, 66.13; H, 9.01; N, 7.07. Found: C, 66.29; H, 9.13; N, 6.98.

5-[*N*-(3-Carboxypropyl)-aminomethyl]-11,17,23-tris[1,5,9-triazacyclododec-1-yl-methyl]-25,26,27,28-tetrakis(2-ethoxyethoxy)calix[4]arene (31)

The Boc-protected calix[4]arene **30** (10 mg, 0.005 mmol) was dissolved in 2 mL of CH₂Cl₂ and 0.3 mL of trifluoroacetic acid was added. The solution was stirred for 2 h and then evaporated under reduced pressure. The residue was taken up with dichloromethane (20 mL) and saturated Li₂CO₃ solution (20 mL). The aqueous phase was extracted again with CH₂Cl₂ (2 x 20 mL), the organic fractions were collected and evaporated under vacuum, obtaining the deprotected product (6.7 mg) in almost quantitative yield. ¹H NMR (300 MHz; CDCl₃/CD₃OD 2/1): δ 6.81 (s, 2H, ArH), 6.75 (s, 2H, ArH), 6.41 (s, 2H, ArH), 6.34 (s, 2H, ArH), 4.56 (d, 2H, ArCH₂Ar ax, J = 13.1 Hz), 4.54 (d, 2H, ArCH₂Ar ax, J = 13.1 Hz), 4.26 (t, 4H, ArOCH₂, J = 5.8 Hz), 4.02 (t, 4H, ArOCH₂, J = 5.1 Hz), 3.93 (t, 4H, ArOCH₂CH₂, J = 5.8 Hz), 3.84 (t, 4H, ArOCH₂CH₂, J

= 5.1 Hz), 3.61-3.43 (m, 12H, OCH₂CH₃ + ArCH₂N), 3.24 (s, 2H, ArCH₂NH), 3.21 (s, 2H, ArCH₂N), 3.15 (d, 2H, ArCH₂Ar eq, J = 13.1 Hz), 3.13 (d, 2H, ArCH₂Ar eq, J = 13.1 Hz), 2.98 (t, 8H, HNCH₂CH₂CH₂NH, J = 4.4 Hz), 2.92 (t, 4H, HNCH₂CH₂CH₂NH, J = 4.4 Hz), 2.83 (bs, 8H, NCH₂CH₂CH₂NH, J = 4.4 Hz), 2.74 (t, 4H, NCH₂CH₂CH₂NH, J = 4.8 Hz), 2.53 (bs, 8H, ArCH₂NCH₂), 2.37 (t, 2H, NHCH₂CH₂CH₂COOH, J = 7.3 Hz), 2.29 (t, 4H, ArCH₂NCH₂, J = 4.8 Hz), 2.12 (t, 2H, CH₂COOH, J = 6.8 Hz), 1.79 (bs, 14H, NCH₂CH₂CH₂NH + HNCH₂CH₂CH₂NH), 1.72-1.69 (m, 2H, CH₂CH₂COOH), 1.61 (bs, 4H, NCH₂CH₂CH₂NH), 1.21-1.13 (m, 12H, OCH₂CH₃). ¹³C NMR (75 MHz; CDCl₃/CD₃OD 2/1): δ 165.7, 157.0, 155.6, 150.5, 136.3, 136.0, 134.6, 134.2, 133.1, 130.7, 130.4, 130.2, 130.0, 128.5, 128.2, 74.3, 73.3, 70.5, 70.3, 70.2, 66.8, 66.7, 53.6, 52.8, 53.3, 51.9, 50.0, 36.1, 32.3, 31.4, 31.3, 30.6, 29.7, 26.4, 24.5, 24.3, 24.2, 15.2, 15.1. MS (ES+) *m/z* (%): 689.9 (100) [M+2H]²⁺, 700.8 (95) [M+H+Na]²⁺. Anal. Calcd for C₇₉H₁₂₈N₁₀O₁₀ (1377.95): C, 68.86; H, 9.36; N, 10.16. Found: C, 68.67; H, 9.23; N, 10.29.

5.6 References and notes

- (1) Takagi, Y.; Ikeda, Y.; Taira, K. *Top. Curr. Chem.* **2004**, *232*, 213-251.
- (2) Sayre, L. M. *J. Am. Chem. Soc.* **1986**, *108*, 1632-1635.
- (3) Williams, N. H.; Takasaki, B.; Wall, M.; Chin, J. *Acc. Chem. Res.* **1999**, *32*, 485-493.
- (4) Wilcox, D. E. *Chem. Rev.* **1996**, *96*, 2435-2458.
- (5) Strater, N.; Lipscomb, W. N.; Klabunde, T.; Krebs, B. *Angew. Chem. Int. Ed* **1996**, *35*, 2024-2055.
- (6) Morrow, J. R.; Iranzo, O. *Curr. Opin. Chem. Biol.* **2004**, *8*, 192-200.
- (7) Cacciapaglia, R.; Mandolini, L. Calixarene based catalytic systems; In *Calixarenes in Action*; Mandolini, L., Ungaro, R., eds. Imperial College Press: London, 2000; pp 241-264.
- (8) Molenveld, P.; Stikvoort, W. M. G.; Kooijman, H.; Spek, A. L.; Engbersen, J. F. J.; Reinhoudt, D. N. *J. Org. Chem.* **1999**, *64*, 3896-3906.
- (9) Molenveld, P.; Engbersen, J. F. J.; Reinhoudt, D. N. *Chem. Soc. Rev.* **2000**, *29*, 75-86.
- (10) Zompa, L. J. *Inorg. Chem.* **1978**, *17*, 2531-2536.
- (11) Kodama, M.; Kimura, E. *J. Chem. Soc., Dalton Trans.* **1977**, 2269-2276.
- (12) Kimura, E. *Acc. Chem. Res.* **2001**, *34*, 171-179.
- (13) Kuusela, S.; Lönnberg, H. *J. Chem. Soc., Perkin Trans. 2* **1994**, *2*, 2301-2306.
- (14) Niittymäki, T.; Kaukinen, U.; Virta, P.; Mikkola, S.; Lönnberg, H. *Bioconjugate Chem.* **2004**, *15*, 174-184.
- (15) Bonfa, L.; Gatos, M.; Mancin, F.; Tecilla, P.; Toneliato, U. *Inorg. Chem.* **2003**, *42*, 3943-3949.
- (16) Koike, T.; Kimura, E. *J. Am. Chem. Soc.* **1991**, *113*, 8935-8941.

- (17) Kimura, E.; Shiota, T.; Koike, T.; Shiro, M.; Kodama, M. *J. Am. Chem. Soc.* **1990**, *112*, 5805-5811.
- (18) Newcomb, M.; Timko, J. M.; Walba, D. M.; Cram, D. J. *J. Am. Chem. Soc.* **1977**, *99*, 6392-6398.
- (19) Molenveld, P. *Ph. D. Thesis* **1999**, *Enschede*, ISBN 90 365 1282 4.
- (20) Weisman, G. R.; Reed, D. P. *J. Org. Chem.* **1996**, *61*, 5186-5187.
- (21) Brandes, S.; Gros, C.; Denat, F.; Pullumbi, P.; Guillard, R. *Bull. Soc. Chim. Fr.* **1996**, *133*, 65-73.
- (22) The catalytic measurements were performed by Riccardo Salvio at the University of Rome.
- (23) Hendrickson, K. M.; Geue, J. P.; Wyness, O.; Lincoln, S. F.; Ward, A. D. *J. Am. Chem. Soc.* **2003**, *125*, 3889-3895.
- (24) For more details see: Cacciapaglia, R.; Casnati, A.; Mandolini, L.; Reinhoudt, D. N.; Salvio, S.; Sartori, A.; Ungaro, R., manuscript in preparation.
- (25) Bosch, E.; Bou, P.; Allemann, H.; Roses, M. *Anal. Chem.* **1996**, *68*, 3651-3657.
- (26) HubschWeber, P.; Youinou, M. T. *Tetrahedron Lett.* **1997**, *38*, 1911-1914.
- (27) Arduini, A.; Fanni, S.; Manfredi, G.; Pochini, A.; Ungaro, R.; Sicuri, A. R.; Ugozzoli, F. *J. Org. Chem.* **1995**, *60*, 1448-1453.

CHAPTER 6

Cleavage of phosphate diester RNA models and dinucleotides by metallo(II) complexes of calix[4]arenes functionalized with nitrogen ligands

*In this chapter the catalytic activity of 1,2-bis(dimethylamino)methylpyridine-calix[4]arene Zn(II) complex (**7**-[Zn]₂) in the 2-hydroxypropyl-*p*-nitrophenyl phosphate (HPNP) transesterification is reported and compared to that of Zn(II) complexes of 1,3-bis- and tris- diaminopyridine-calixarenes already reported in the literature. The catalytic activity in the HPNP transesterification of the metal complexes of [12]aneN₃-calixarenes (**11-14**), whose synthesis is described in Chapter 5, is also reported. The Zn(II) complexes of **11-14** exhibit in the HPNP transesterification in CH₃CN/water (1:1) an unexpected lack of cooperativity of the metal centers. The catalytic activity of the Cu(II) complexes **9**-[Cu], **12**-[Cu]₂, **13**-[Cu]₂ and **14**-[Cu]₃ was investigated in pure water both in the HPNP and the dinucleotide cleavage. The metal centers in **13**-[Cu]₂ and **14**-[Cu]₃ show a synergistic action in the catalysis with a good selectivity for UpU and UpG. The different behavior of the Cu(II) in comparison with Zn(II) complexes might be due to the different coordination geometry of the copper(II) ions.*

6.1 Introduction

The ribonuclease activity of synthetic catalysts is commonly tested on RNA model compounds. One of the most used is the 2-hydroxypropyl *p*-nitrophenyl phosphate (HPNP),^{1;2} which has a hydroxyl function that can attack intramolecularly the phosphorous atom, mimicking the hydroxyl function in 2'-position of ribose. The use of HPNP instead of true RNA substrates has several advantages. First of all the simplicity of the experimental measurements; the release of *p*-nitrophenol upon transesterification allows indeed the reaction to be followed by UV-Vis spectrophotometry. Secondly, HPNP has only one metal binding site and one site for hydrolytic cleavage making mechanistic studies simpler. Finally, it usually exhibits enhanced cleavage rates with respect to di- and oligonucleotides because of the good leaving group, (*p*-nitrophenol), which makes easy the monitoring of the reaction even with inefficient catalysts. However, there are also some drawbacks associated with the use of HPNP. The stability of the phosphorane intermediate is dramatically changed by the presence of an electron-withdrawing group, as *p*-nitrophenyl, and this may have a significant effect on the reaction mechanism. Moreover, RNA possesses additional metal ion binding sites on its nitrogenous bases and phosphates, which may be important from a mechanistic standpoint. For these reasons the data obtained using activated RNA models, as HPNP, often do not directly correlate to those found with RNA substrates,^{3;4} and therefore the use of a model should be considered only as the first step in the investigation of the activity of a nuclease mimic.

Dinucleoside monophosphates (3',5'-NpN) resemble normal RNA polymers more closely than phosphodiester with good leaving group (for an in-depth discussion see chapter 7.1). RNA dimers have only one cleavage site and the products can be analyzed by HPLC methods.

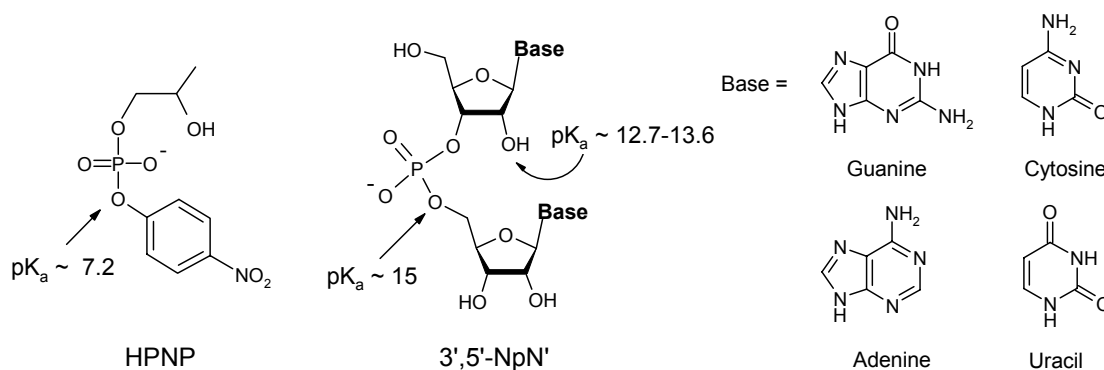


Figure 6.1

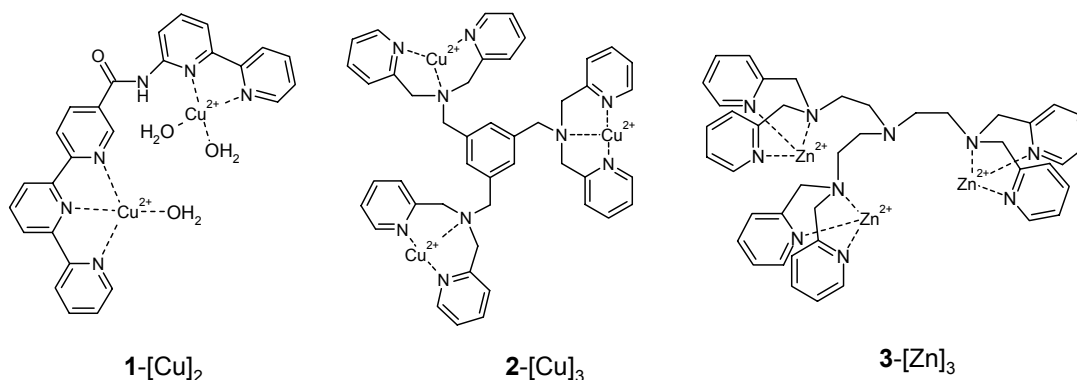
The nature of the base has an effect on the reactivity of the dinucleotide phosphate bond, although this effect is quite modest. Among the values measured by Witzel⁵ for

the dinucleotide hydroxide ion catalyzed cleavage (Table 6.1) the most reactive dinucleotide, UpC, reacts only 4 times faster than the least reactive ApC. A common pattern observed is a slightly higher reactivity of pyrimidine nucleoside 3'-phosphodiester compared to their purine counterparts. The nature of the base affects the pK_a of the nucleophilic 2'-hydroxyl group, influencing in this way the rate of the phosphate bond cleavage. Beside this effect, the nature of the base can play a more important role in the phosphate cleavage when the reaction is catalyzed by supramolecular metal complexes. Metal-nitrogen (or oxygen) interactions between the catalyst and substrate, together with π -interactions and/or unfavorable repulsive forces can provide selectivity in the dinucleotide cleavage. These factors are hardly predictable *a priori*, and often it is not easy to find satisfactory explanations, even when a remarkable dinucleotide selectivity is found.

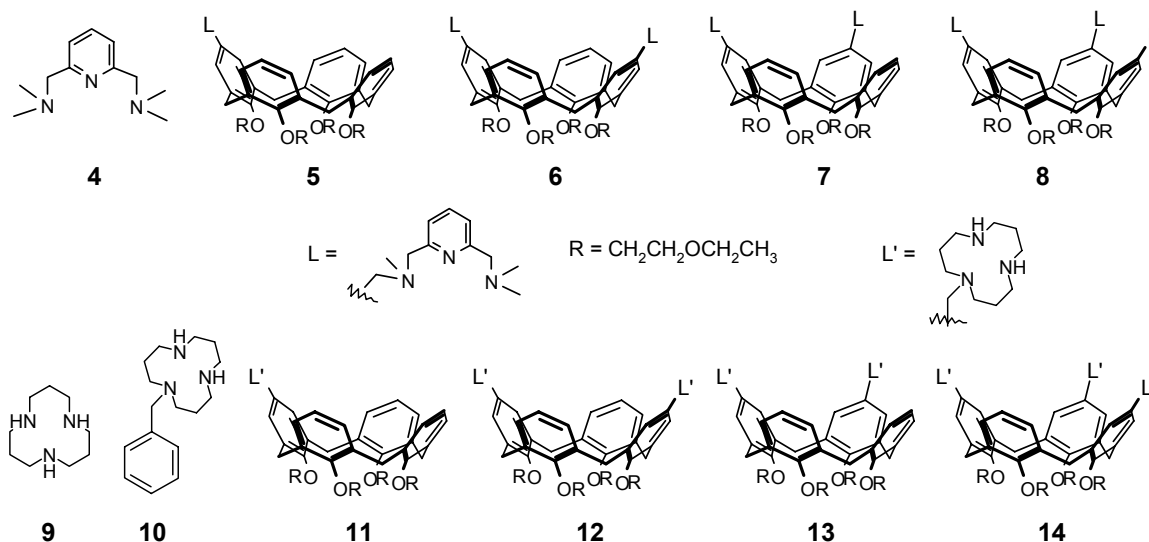
Table 6.1 Observed pseudo-first-order rate constants for the hydroxide ion catalyzed cleavage of 3',5'-dinucleotides (NpN), in 0.5 M NaOH (aq) 28 °C.⁵

3',5'-NpN	$k, 10^{-5} \text{ s}^{-1}$
UpA	15.7
ApA	5.3
GpA	7.3
CpA	12.5
ApC	4.8
GpC	8.9
CpC	12.6
UpC	22

Among the complexes reported in the literature that have dinucleotide selectivity, complex **1**-[Cu]₂ shows a remarkable base preference for adenine,⁶ hydrolyzing ApA 12, 17 and 87 times faster than CpC, UpU and GpG, respectively. The reason was attributed to a strong π - π stacking interaction between adenine and the bipyridine-Cu(II) unit. The catalyst **2**-[Cu]₃ cleaves ApA almost 50 times more efficiently than the UpU dimer and the selectivity was attributed, in this case, to a better geometrical complementarity between the metal centers.⁷ Compound **3**-[Zn]₃ reported by Komiyama *et al.*⁸ shows rate enhancements depending on the structure of the substrate. They gave no reason for the reactivity order CpA > ApA > GpA > UpA \approx ApG > GpC, with CpA being about 10 times more reactive than GpC. The calix[4]arene based catalyst **8**-[Zn]₃ was found to catalyze GpG cleavage 160 times more effectively than ApA cleavage. This high selectivity was attributed to a possible favorable binding between a Zn(II) ion and the anionic nitrogen of the guanine, resulting from deprotonation by a Zn(II) bound hydroxide anion.



In Chapter 5 the synthesis of the calix[4]arene **7**, functionalized in the 1,2-proximal positions with 2,6-bis(dimethylaminomethyl)pyridine ligating groups, and of calix[4]arenes **11-14**, functionalized with 1,5,9-triazacyclododecane ([12]aneN₃), was reported. The Zn(II) complexes of these compounds were studied as catalysts in the methanolysis of aryl esters revealing the superiority of the 1,2-disubstituted compounds (**7**-[Zn]₂ and **13**-[Zn]₂) over their corresponding 1,3-disubstituted (**6**-[Zn]₂ and **12**-[Zn]₂) counterparts. In this chapter the activity of **7**-[Zn]₂ in the HPNP transesterification will be reported. These studies were performed in order to verify if the cooperative catalysis by the metal ions in proximal positions, observed in acyl transfer reactions (Chapter 5), is also found in the phosphodiester cleavage.



The catalytic activity of Zn(II) complexes of compounds **9-10** and **12-14** is included for comparison. It is very important that the water solubility of the copper(II) complexes of ligands **9-10** and **12-14** allowed to investigate their catalytic activity in the transesterification of HPNP and/or dinucleotides in pure water, under conditions similar to the physiological ones.⁹

6.2 Catalytic activity of Zn(II) complexes in HPNP transesterification

In order to compare the phosphodiesterase activity of the 1,2-dinuclear calix[4]arene **7**-[Zn]₂ with that of its regioisomer 1,3-dinuclear **6**-[Zn]₂, their efficiency in HPNP transesterification was evaluated. The reaction was carried out in 50% CH₃CN/20 mM HEPES, in the presence of 1 mM metal complex, generated *in situ* by adding a stoichiometric amount of Zn(ClO₄)₂ to the solution of the ligand. The k_{obs} and k_{rel} are reported in Table 6.2.¹⁰ The k_{rel} values clearly show that in HPNP transesterification the highest cooperation is observed when the metal centers are in the 1,3-diametral positions as in **6**-[Zn]₂. Comparing the activity of the dinuclear ligand **7**-[Zn]₂ with that of the mononuclear **5**-[Zn], the former is one order of magnitude more efficient than the latter, indicating that the metal centers in 1,2 positions can still cooperate in catalysis. However, **7**-[Zn]₂ is 6.5 times less efficient than the diametral isomer **6**-[Zn]₂. The trinuclear catalyst **8**-[Zn]₃ does not seem to exploit all three metal centers in the catalysis of HPNP cleavage, since it shows a lower rate enhancement than the dinuclear **6**-[Zn]₂. Therefore the third metal center does not play any catalytic role in HPNP transesterification.

Table 6.2 Observed pseudo-first-order rate constants and relative rate accelerations for the transesterification of HPNP catalyzed by Zn(II) complexes of ligands **4-8** at 25 °C, pH 7.0.^a

Catalyst	k_{obs} (s ⁻¹)	Relative rate acceleration
none	1.9 × 10 ⁻⁸ ^b	1
4 -[Zn]	3.4 × 10 ⁻⁶	180
5 -[Zn]	1.7 × 10 ⁻⁵	900
6 -[Zn] ₂	1.3 × 10 ⁻³	68,000
7 -[Zn] ₂	2.0 × 10 ⁻⁴	11,000
8 -[Zn] ₃	6.9 × 10 ⁻⁴	36,000

^a [Cat] = 1 mM, [HPNP] = 0.2 mM, in 50% CH₃CN/20 mM HEPES, rate constants values from full time courses unless otherwise statement. Error limits = ±5%.

^b Measured in a 2.0 mM HPNP solution, in 50% CH₃CN/20 mM HEPES, initial rate method.

Zn(II) complexes of ligands **9**, **10**, **12**, **13** and **14** were investigated in the HPNP transesterification as well. The mononuclear calix[4]arene complex **11**-[Zn] could not be tested because of its low solubility in the solvent mixture used for catalytic measurements.

The kinetic studies were carried out in 50% CH₃CN/20 mM HEPES, on a 0.2 mM metal complex solution, generated *in situ* by adding the proper number of equivalents of ZnBr₂ to the ligand solution.

The Zn complex of [12]aneN₃ **9**-[Zn] (Table 6.3) is a catalyst more efficient than the Zn complex of 2,6-bis[(dimethylamino)methyl]pyridine **4**-[Zn] (Table 6.2), and taking into account that the k_{obs} values reported in Tables 6.2 and 6.3 are obtained at a different concentration of catalyst, the efficiency of **9**-[Zn] is about 12 times higher than that of **4**-[Zn].¹¹ The presence of a benzyl group on [12]aneN₃ in **10**-[Zn] causes a slight decrease of the activity of the Zn(II) complex with respect to **9**-[Zn], nevertheless it is still 5 times more active than **4**-[Zn]. Despite the good efficiency of the mononuclear triaza Zn(II) complex, the dinuclear catalysts **12**-[Zn]₂ and **13**-[Zn]₂, having two [12]aneN₃ ligands on the calixarene upper rim show no cooperativity of the Zn(II) metal centers. The trinuclear complex **14**-[Zn]₃ exhibits only a very low degree of cooperation. There is practically no difference in the activity between the 1,3-diametral (**12**-[Zn]₂) and the 1,2-proximal (**13**-[Zn]₂) disubstituted calixarenes. The two metal centers act independently providing only a modest rate enhancement. These results contrast with those found in the methanolysis of aryl esters (Chapter 5) where the metal centers in dinuclear (**13**-[Zn]₂) and trinuclear (**14**-[Zn]₃) complexes strongly cooperate in the catalysis. It is difficult to find a reasonable explanation for this different behavior, which must be due to the different structures of the productive complexes in the various cases.

Table 6.3 Observed pseudo-first-order rate constants and relative rate accelerations for the transesterification of HPNP catalyzed by Zn(II) complexes of **9**, **10**, **12**, **13** and **14** at 25 °C, pH 7.0.^a

Catalyst	k_{obs} (s ⁻¹)	Relative rate acceleration
none	1.9×10^{-8} ^b	1
9 -[Zn]	8.6×10^{-6}	450
10 -[Zn]	3.7×10^{-6}	190
12 -[Zn] ₂	6.0×10^{-6}	320
13 -[Zn] ₂	6.3×10^{-6}	330
14 -[Zn] ₃	2.1×10^{-5}	1100

^a [Cat] = 0.2 mM, [HPNP] = 0.15 mM, in 50% CH₃CN/20 mM HEPES, initial rate method. Error limits = ±5%.

^b Measured on a 2.0 mM HPNP solution, in 50% CH₃CN/20 mM HEPES.

6.3 Catalytic activity of Cu(II) triazacalix[4]arene complexes in HPNP transesterification

In spite of the low catalytic efficiency obtained with Zn(II) complexes of [12]aneN₃-calixarene **12**, **13** and **14**, the corresponding Cu(II) complexes were also investigated in HPNP transesterification. Copper(II) has been largely used in the design of nuclease mimics,¹²⁻¹⁴ because analogously to zinc(II) it is a strong Lewis acid and forms substitutionally labile complexes. Cu(II) ion binds strongly to [12]aneN₃ (**9**) in water; the binding constant reported for the complex **9**-Cu(II) ($\log K_{\text{CuL}} = 12.7$, at 25 °C) is much higher than the one reported for **9**-Zn(II) ($\log K_{\text{Zn}} = 8.8$).^{15;16} The high value of K_{Cu} assures the quantitative formation of di- and trinuclear complexes **12**-[Cu]₂, **13**-[Cu]₂ and **14**-[Cu]₃ under the conditions of the catalytic measurements, using one equivalent of CuBr₂ per triaza unit.¹⁷

The copper(II) complexes of the [12]aneN₃-calixarene ligands showed a water solubility higher than the analogous zinc(II) complexes, and the catalytic measurements could be carried out in water (20 mM HEPES) without observing any precipitation. The water solubility of **14**-[Cu]₃, measured by UV-Vis measurements is 5.35 mM at 25 °C.

The catalytic activity of complexes **10**-[Cu], **12**-[Cu]₂, **13**-[Cu]₂ and **14**-[Cu]₃ in the HPNP transesterification in water is reported in Table 6.4. Surprisingly the k_{uncat} measured for HPNP cleavage in water is higher than the k_{uncat} in 50% CH₃CN/H₂O mixture (Table 6.3). It is known that the rate of uncatalyzed hydrolysis both of monophosphate esters and bis(*p*-nitrophenyl) phosphate (BNPP) in organic solvent/water mixtures decreases with increasing the amount of water,¹⁸⁻²⁰ except in the case of DMSO²¹. However, the measured k_{obs} value for the HPNP uncatalyzed reaction is in accordance with that reported by Scrimin *et al.*²². Comparing the rate enhancements, it is possible to point out that the mononuclear copper(II) complex **10**-[Cu] is less efficient than the analogous Zn(II) complex **10**-[Zn] (Table 6.3). This can be explained because the water molecule bound to the copper ion in **10**-[Cu] is less acidic than the water bound to the zinc ion in **10**-[Zn]. The $\text{p}K_{\text{a}}$ value reported in the literature for a bound water molecule in the complex **9**-Cu(II) is 8.4,¹⁵ while 7.3 is the $\text{p}K_{\text{a}}$ reported for the triaza Zn(II) complex (**9**-Zn).²³ As a consequence, the concentration of metal-bound OH⁻ at neutral pH is lower in the case of copper complexes, reducing a possible contribution of acid-base catalysis.

A more interesting result is the high degree of cooperativity observed in complexes **13**-[Cu]₂ and **14**-[Cu]₃. A measure of the degree of synergism between metal centers in di- and trinuclear catalysts is the ratio $k_{\text{obs}}^{\text{di}}/k_{\text{obs}}^{\text{mono}}$ and $k_{\text{obs}}^{\text{tri}}/k_{\text{obs}}^{\text{mono}}$, where $k_{\text{obs}}^{\text{mono}}$ is the observed pseudo-first-order rate constant found with mononuclear complex

10-[Cu]. In the case of 1,2-dinuclear calixarene complex **13**-[Cu]₂ this ratio is 40, and in the case of the trinuclear complex **14**-[Cu]₃ it is 22.5. Therefore the different coordination geometry of Cu(II) with respect to Zn(II), can favor a cooperative action of the metal centers. The highest synergism in HPNP cleavage is shown by the metal centers in proximal positions, whereas the diametral **12**-[Cu]₂ complex gives rate acceleration only twice of that of the mononuclear catalyst **10**-[Cu].

Table 6.4 Observed pseudo-first-order rate constants and relative rate accelerations for the transesterification of HPNP catalyzed by Cu(II) complexes **10**, **12**, **13** and **14** at 25 °C, in 20 mM HEPES, pH 7.0.

Catalyst	k_{obs} (s ⁻¹)	Relative rate acceleration
none	2.8×10^{-7} ^b	1
10 -[Cu]	7.6×10^{-6}	27
12 -[Cu] ₂	1.1×10^{-5}	39
13 -[Cu] ₂	3.0×10^{-4}	1100
14 -[Cu] ₃	1.7×10^{-4}	610

^a [Cat] = 0.2 mM, [HPNP] = 0.15 mM, in 20 mM HEPES, initial rate method. Error limits = ±5%.

^b Measured on a 2.0 mM HPNP solution.

The HPNP transesterification rate in the presence of **14**-[Cu]₃ was measured as a function of the substrate concentration at pH 7.0. The catalyst **14**-[Cu]₃ shows a saturation kinetics (Michaelis-Menten profiles) (Figure 6.2). The kinetic data are reported in Table 6.5.

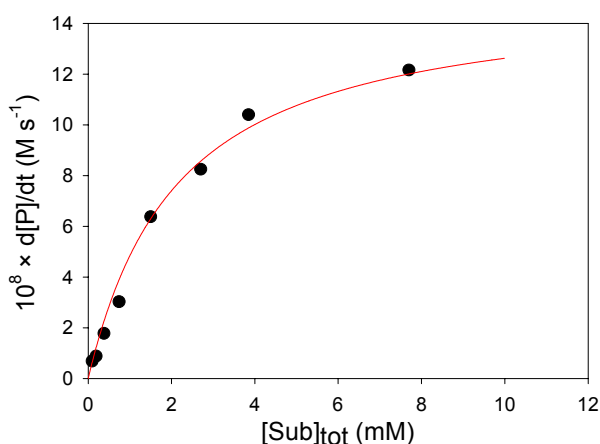


Figure 6.2 Saturation kinetics for **14**-[Cu]₃ (0.2 mM) in the transesterification of HPNP in 20 mM HEPES pH 7.0, 25 °C.

Table 6.5 Kinetic data for the transesterification of HPNP catalyzed by **14**-[Cu]₃ in 20 mM HEPES, pH 7, at 25 °C.

Catalyst	k_2 ($M^{-1}s^{-1}$)	k_{cat} (s^{-1})	K_M (M)	K_{ass} (M^{-1})
14 -[Cu] ₃	0.38	7.6×10^{-4}	2.0×10^{-3}	5.0×10^2

The K_{ass} between the **9**-Cu(II) complex and 2,4-dinitrophenylethyl phosphate (analogous to HPNP) in water, at 25 °C, pH 8.1, was reported to be $30 M^{-1}$.¹⁵ The higher value of K_{ass} found for the trinuclear complex **14**-[Cu]₃ indicates a possible cooperative action of the metal centers in substrate binding.

6.4 Catalytic activity of Cu(II) complexes in dinucleotide cleavage

The catalytic activity of the trinuclear complex **14**-[Cu]₃ was investigated in the cleavage of several dinucleotides 3',5'-NpN (for dinucleotide structures see Figure 6.1). The reactions were carried out in water (20 mM HEPES buffer, pH 7.0) at 50 °C, and the product formation was monitored by HPLC analysis of aliquots of the reaction mixture. The reaction products were the cyclic ribonucleotide monophosphate 2',3'-cNMP and the corresponding nucleosides, demonstrating that the RNA dinucleotides are cleaved by intramolecular transesterification *via* the 2'-OH. The values of k_{obs} , calculated by the initial rate method, are listed in Table 6.6, together with the relative rate accelerations with respect to GpA cleavage.

The trinuclear complex **14**-[Cu]₃ is an efficient catalyst in the cleavage of UpU and UpG. The k_{uncat} value $6.9 \times 10^{-9} s^{-1}$ for the uncatalyzed reactions at 50 °C and pH 7.0 was calculated using the empirical equation reported by Breaker and co-workers corrected for temperature, pH and $[K^+]$.²⁴ The rate accelerations in the presence of **14**-[Cu]₃ for UpU and UpG cleavage over the uncatalyzed reactions (k_{cat}/k_{uncat}) are ca. 7600 and 6800, respectively. The other dinucleotides are cleaved less efficiently and the rate enhancements are close. Catalyst **14**-[Cu]₃ is selective for UpU and UpG, which are cleaved respectively 39 and 30 times faster than the less reactive dinucleotide GpA. In the case of CpA no cleavage was observed after one day of incubation.

The reason of the selectivity is not clear, also because it was not possible to determine the K_M and k_{cat} values. The rate of UpU cleavage was measured as a function of the concentration of the catalyst, but the experimental data do not fit well to a Michaelis-Menten kinetic curve, probably because of precipitation at high catalyst

concentration. To explain the observed selectivity one might assume an interaction between a Cu(II) ion and the acidic NH of the uracyl, that can be deprotonated by a metal-bound hydroxide anion. Most probably it is a combination of factors (steric hindrance, electrostatic interactions, hydrophobic interactions, etc.) that makes UpU and UpG more reactive substrates in the presence of **14**-[Cu]₃.

When the $k_{\text{cat}}/k_{\text{uncat}}$ ratios are compared, the complex **14**-[Cu]₃ is more efficient in the cleavage of UpU and UpG than in the cleavage of HPNP. This can indicate an interaction between the bases and the metal centers which increases the substrate binding and/or leaving group stabilization by catalysis of **14**-[Cu]₃. If present, the latter is more effective in the dinucleotide cleavage, where the leaving group has a pK_a 8 orders of magnitude higher than the *p*-nitrophenol of HPNP.

Table 6.6 Observed pseudo-first-order rate constants for the cleavage of RNA dinucleotides catalyzed by **14**-[Cu]₃, and relative rate accelerations with respect to GpA cleavage.^a

Substrate	k_{obs} (s ⁻¹)	Relative rate acceleration
CpA	-	-
GpA	1.4 x 10 ⁻⁶	1
CpG	2.1 x 10 ⁻⁶	1.5
CpC	2.5 x 10 ⁻⁶	1.8
ApG	2.7 x 10 ⁻⁶	1.9
GpG	2.8 x 10 ⁻⁶	2.0
GpU	3.7 x 10 ⁻⁶	2.7
UpG	4.2 x 10 ⁻⁵	30
UpU	5.5 x 10 ⁻⁵	39

^a In 20 mM HEPES buffer, pH 7.0, 50 °C; [Cat] = 1 mM, [Dinucleotide] = 0.1 mM. HPLC analysis. Error limits = ± 10%.

The transesterification rate of UpU and CpA, the two dinucleotides most and least efficiently cleaved by **14**-[Cu]₃ respectively, was also investigated in the presence of the mono- (**9**-[Cu]) and dinuclear complexes (**12**-[Cu]₂ and **13**-[Cu]₂). The observed pseudo first-order rate constants are listed in Table 6.7. Surprisingly in the case of CpA cleavage, we found that both the mononuclear (**9**-[Cu]) and dinuclear (**12**-[Cu]₂, **13**-[Cu]₂) complexes can catalyze the reaction. The fact that the 1,3-dinuclear

complex **12**-[Cu]₂ is only twice more efficient than the mononuclear reveals the absence of cooperation between the metal centers. Although quite low, a synergistic action of the metal centers is on the other side observed for the 1,2-dinuclear complex **13**-[Cu]₂ ($k_{\text{obs}}^{\text{di}}/k_{\text{obs}}^{\text{mono}} = 5.5$). The complete inactivity of the trinuclear complex **14**-[Cu]₃ could be explained *via* the formation of a strong non-productive catalyst-substrate complex (selective stabilization of the initial state with respect to the transition state).

In the case of UpU cleavage we observed the order of reactivity shown by most of the calixarene catalysts. The efficiency of 1,2-dinuclear (**13**-[Cu]₂) and trinuclear (**14**-[Cu]₃) complexes is very similar, with a slight superiority of **14**-[Cu]₃. As already observed in HPNP and CpA cleavage, the metal centers in 1,3 positions do not cooperate in the catalysis of UpU transesterification. The rate enhancement found with **12**-[Cu]₂ is indeed very close to the value found for the mononuclear catalyst **9**-[Cu].

Table 6.7 Observed pseudo-first-order rate constants for the cleavage of CpA and UpU dinucleotides and relative rate accelerations with respect to the reaction catalyzed by the mononuclear catalyst **9**-[Cu].^a

Catalyst	CpA		UpU	
	$k_{\text{obs}} (s^{-1})$	$k_{\text{obs}}/k_{\text{obs}}(\mathbf{9}\text{-[Cu]})$	$k_{\text{obs}} (s^{-1})$	$k_{\text{obs}}/k_{\text{obs}}(\mathbf{9}\text{-[Cu]})$
9 -[Cu]	6.6×10^{-7}	1	2.7×10^{-7}	1
12 -[Cu] ₂	1.3×10^{-6}	2.0	3.8×10^{-7}	1.4
13 -[Cu] ₂	3.7×10^{-6}	5.6	4.2×10^{-5}	160
14 -[Cu] ₃	-	-	5.5×10^{-5}	200

^a In 20 mM HEPES buffer, pH 7.0, 50 °C; [Cat] = 1 mM, [Dinucleotide] = 0.1 mM. HPLC analysis. Error limits = ± 10%.

6.5 Conclusions

In this chapter the phosphodiesterase activity of several metallo catalysts based on calix[4]arenes is reported. The HPNP transesterification rates in the presence of Zn(II) complexes of calix[4]arenes **4-8** provided with dimethylaminomethylpyridine ligand moieties reveal that there is a synergistic action of the metal centers in diametral positions, differently from what observed in the methanolysis of aryl esters (Chapter 5). Surprisingly, the metal centers of the zinc(II) complexes of di- and trinuclear [12]aneN₃-calix[4]arenes **12**, **13** and **14** do not cooperate in the activation of the phosphate bond of HPNP. On the other hand a synergistic action of the metal centers in proximal positions has been found with copper(II) complexes **13**-[Cu]₂ and **14**-

[Cu]₃ in the HPNP cleavage in water. The HPNP transesterification in the presence of **14**-[Cu]₃ follows a Michaelis-Menten kinetics. The substrate binds to the catalyst with a $K_{\text{ass}} = 500 \text{ M}^{-1}$ and it is converted into product with a $k_{\text{cat}} = 7.6 \times 10^{-4} \text{ s}^{-1}$.

The complex **14**-[Cu]₃ was also investigated as a nuclease mimic in the dinucleotide cleavage in water (pH 7.0) showing a remarkable selectivity for UpU and UpG dinucleotides. Compared with the uncatalyzed reactions the rate enhancements measured for these dinucleotides are in the order of 7×10^3 .

The data reported in this chapter point out the difficulty in the design of nuclease mimics. Despite the fact that all catalysts described are based on the same scaffold (the calix[4]arene) very different results in terms of cooperativity of the metal centers are obtained by changing both the ligating groups and the metal ion, whose coordination geometry can strongly influence the multinuclear catalysis.

6.6 Experimental part

General information

Spectrophotometric measurements were carried out on either a double beam Perkin Elmer Lambda18 or on a diode array Hewlett Packard 8453 spectrophotometer. HPLC analyses were performed on an Agilent 1100 Series liquid chromatograph fitted with a UV-Vis detector operating at 264 nm. Kinetic runs monitored by HPLC were carried out in the presence of 4-methoxybenzoic acid as an internal standard. Samples were analyzed on a Supelcosil LC-18 DB column (25 cm × 4.6 mm I.D., particle size 5 μm). Error limits of rate constants are in the order of ±5% (time-course kinetics) and ±10% (initial rate method). Nonlinear least-squares calculations were carried out using the program SigmaPlot 2002 for Windows, Version 8.0 (SPSS, Inc.).

Materials

The synthesis of compounds **7**, **11**, **12**, **13** and **14** is described in Chapter 5. Compounds **4**,²⁵ **5**,²⁵ **6**,²⁵ **8**,²⁵ and **10**²⁶ were obtained according to literature procedures. 1,5,9-Triazacyclododecane **9** was a commercial sample (Sigma-Aldrich) used without further purification. Dinucleotides UpU, GpG, ApG were purchased from Sigma-Aldrich, while UpG, CpC, GpA, GpU, CpA, CpG were from Dharmacon Research (Lafayette, CO). The aqueous solutions were prepared using deionized (Millipore) distilled water.

Water solubility of **14**-[Cu]₃ by UV-spectrophotometry

Calculated volumes of a $2.00 \times 10^{-2} \text{ M}$ solution of the calixarene **14** in ethanol and of a 0.276 M solution of CuCl₂ in water were added into a cuvette containing 2mL of water

(in the cuvette: $[\text{Cu}^{2+}]/[\text{calix}] = 3.0$). The molar absorptivity (ϵ) value of $1958 \text{ M}^{-1}\text{cm}^{-1}$ for complex **14**- $[\text{Zn}]_3$ was obtained from the linear regression of the absorbances at 360 nm plotted versus concentration. A $9.93 \times 10^{-3} \text{ M}$ water solution of **14** and a 0.276 M water solution of Cu^{2+} were prepared. $54 \mu\text{L}$ of the Cu^{2+} solution were added to $500 \mu\text{L}$ of the calixarene one obtaining a green solution. After ca. 20 min a precipitate was formed and the solution was filtered on nylon filters (Chemtek $0.200 \mu\text{m}$, 4 mm). $100 \mu\text{L}$ of the saturated solution were added to 2 mL of water in a cuvette and its absorbance at 360 nm was measured ($A_{360} = 0.495$). After further addition of $50 \mu\text{L}$ of the saturated solution the absorbance was $A_{360} = 0.739$. From these data we could calculate the **14**- $[\text{Zn}]_3$ concentration in the saturated solution ($5.35 \times 10^{-3} \text{ M}$).

Kinetics of HPNP transesterification

Transesterification of:

- 0.2 mM HPNP (in 50% (v/v) CH_3CN - 20 mM aqueous HEPES buffer, 25 °C, pH 7) in the presence of 1 mM **4**- $[\text{Zn}]$, **5**- $[\text{Zn}]$, **6**- $[\text{Zn}]_2$, **7**- $[\text{Zn}]_2$ and **8**- $[\text{Zn}]_3$,
 - 0.15 mM HPNP (in 50% (v/v) CH_3CN - 20 mM aqueous HEPES buffer, 25 °C, pH 7) in the presence of 0.2 mM **9**- $[\text{Zn}]$, **10**- $[\text{Zn}]$, **12**- $[\text{Zn}]_2$, **13**- $[\text{Zn}]_2$ and **14**- $[\text{Zn}]_3$,
 - 0.15 mM HPNP (in 20 mM aqueous HEPES buffer, 25 °C, pH 7) in the presence of 0.2 mM **10**- $[\text{Cu}]$, **12**- $[\text{Cu}]_2$, **13**- $[\text{Cu}]_2$ and **14**- $[\text{Cu}]_3$,
- was monitored by UV-Vis spectrophotometry, following the *p*-nitrophenol release at 400 nm.

Dinucleotide cleavage

In a typical experiment calix[4]arene **14** ($10 \mu\text{L}$, 50 mM in EtOH) and CuCl_2 ($56 \mu\text{L}$, 26.7 mM in H_2O) were added to $450 \mu\text{L}$ of 20 mM HEPES solution pH 7 and thermostated at 50 °C. After 45 min 3',5'-NpN ($10 \mu\text{L}$, 5 mM in H_2O) was injected (final concentration 0.95 mM **14**- $[\text{Cu}]_3$, 0.095 mM 3',5'-NpN). Aliquots ($80 \mu\text{L}$) of the reaction mixture were quenched with an excess of EDTA ($80 \mu\text{L}$, 50 mM) and the *p*-hydroxybenzoic acid ($50 \mu\text{L}$, 0.16 mM) was added as internal standard. After filtration, the solution was injected into a C-18 reversed-phase column and eluted with 0–15% MeCN in H_2O containing 0.1% CF_3COOH (linear gradient, flow rate = 0.9 mL min^{-1}). The eluent was monitored at 254 nm.

6.7 References and notes

- (1) Menger, F. M.; Ladika, M. *J. Am. Chem. Soc.* **1987**, *109*, 3145.
- (2) Breslow, R.; Singh, S. *Biorg. Chem.* **1988**, *16*, 408-417.

- (3) Worm, K.; Chu, F. Y.; Matsumoto, K.; Best, M. D.; Lynch, V.; Anslyn, E. V. *Chem. Eur. J.* **2003**, *9*, 741-747.
- (4) Oivanen, M.; Kuusela, S.; Lönnberg, H. *Chem. Rev.* **1998**, *98*, 961-990.
- (5) Witzel, H.; Barnard, E. A. *Biochem. Biophys. Res. Commun.* **1962**, *7*, 289.
- (6) Liu, S. H.; Hamilton, A. D. *Chem. Commun.* **1999**, 587-588.
- (7) Komiyama, M.; Kina, S.; Matsumura, K.; Sumaoka, J.; Tobey, S.; Lynch, V. M.; Anslyn, E. *J. Am. Chem. Soc.* **2002**, *124*, 13731-13736.
- (8) Yashiro, M.; Ishikubo, A.; Komiyama, M. *Chem. Commun.* **1997**, 83-84.
- (9) The catalytic measurements described in this chapter were performed in collaboration with R. Salvio in the laboratories of Prof. L. Mandolini at the University "La Sapienza" of Rome.
- (10) We repeated the experiments with complexes **4**-[Zn], **5**-[Zn], **6**-[Zn]₂ and **8**-[Zn]₃ already performed by Molenveld in "Molenveld, P.; Stikvoort, W. M. G.; Kooijman, H.; Spek, A. L.; Engbersen, J. F. J.; Reinhoudt, D. N. *J. Org. Chem.* **1999**, *64*, 3896-3906", and substantially confirmed them. The rate enhancement found in the presence of **6**-[Zn]₂ resulted slightly higher (k_{rel} of 68,000 instead of 56,000), while the one measured in the presence of **8**-[Zn]₂ resulted lower (k_{rel} of 36,000 instead of 64,000).
- (11) Since the reported k_{obs} are pseudo-first-order rate constants, the comparison of the data in Table 6.2 with that in Table 6.3 has to take into account the concentration of the catalyst used in the measurements, 1mM and 0.2mM, respectively.
- (12) Young, M. J.; Chin, J. *J. Am. Chem. Soc.* **1995**, *117*, 10577-10578.
- (13) Hegg, E. L.; Burstyn, J. N. *Coord. Chem. Rev.* **1998**, *173*, 133-165.
- (14) Reichenbach-Klinke, R.; König, B. *J. Chem. Soc., Dalton Trans.* **2002**, 121-130.
- (15) Itoh, T.; Hisada, H.; Usui, Y.; Fujii, Y. *Inorg. Chim. Acta* **1998**, *283*, 51-60.
- (16) Zompa, L. J. *Inorg. Chem.* **1978**, *17*, 2531-2536.
- (17) In "Riedo, T. J.; Kaden T. A. *Helv. Chim. Acta*, **1979**, *62*, 1089-1096" the second order formation rate constant for the complex [12]aneN₃-Cu(II) at pH 5 was reported ($k = 23 \text{ M}^{-1} \text{ s}^{-1}$). The k value at pH 7 is certainly higher, because the second amino group of every triaza ligand is already partially deprotonated. However, considering the low k value reported, we waited 1 h for the formation of di- and trinuclear complexes **12**-[Cu]₂, **13**-[Cu]₂ and **14**-[Cu]₃.
- (18) Catrina, I. E.; Hengge, A. C. *J. Am. Chem. Soc.* **1999**, *121*, 2156-2163.
- (19) Kirby, A. J.; Jencks, W. P. *J. Am. Chem. Soc.* **1965**, *87*, 3209-3224.
- (20) Bunton, C. A.; Gillitt, N. D.; Kumar, A. *J. Phys. Org. Chem.* **1996**, *9*, 145-151.
- (21) Liu, T.; Schneider, H.-J. *Supramol. Chem.* **2002**, *14*, 231-236.
- (22) Rossi, P.; Felluga, F.; Tecilla, P.; Formaggio, F.; Crisma, M.; Toniolo, C.; Scrimin, P. *Biopolymers* **2000**, *55*, 496-501.
- (23) Kimura, E.; Shiota, T.; Koike, T.; Shiro, M.; Kodama, M. *J. Am. Chem. Soc.* **1990**, *112*, 5805-5811.
- (24) Li, Y.; Breaker, R. R. *J. Am. Chem. Soc.* **1999**, *121*, 5364-5372.
- (25) Molenveld, P.; Stikvoort, W. M. G.; Kooijman, H.; Spek, A. L.; Engbersen, J. F. J.; Reinhoudt, D. N. *J. Org. Chem.* **1999**, *64*, 3896-3906.
- (26) HubschWeber, P.; Youinou, M. T. *Tetrahedron Lett.* **1997**, *38*, 1911-1914.

Oligoribonucleotide cleavage by copper(II) triazacalix[4]arene complexes

*This chapter deals with the oligoribonucleotide cleavage by copper(II) triazacalixarene complexes, the ability of which to activate the phosphate diester bonds was already investigated in the transesterification of hydroxypropyl p-nitrophenylphosphate (HPNP) and RNA dimers (Chapter 6). Oligonucleotides **6-8**, containing all possible sixteen dinucleotide bonds, and oligonucleotides **9-11**, where the most reactive dinucleotide bonds are placed in different positions within the oligomeric sequence, were used as substrates. The calixarene complexes **3**-[Cu]₂, **4**-[Cu]₂ and **5**-[Cu]₃ showed high catalytic activity due to a significant synergy of the metal centers. An important contribution to the catalysis seems to come from the calixarene skeleton, which probably gives rise to hydrophobic interactions with the bases and creates an apolar environment around the oligomer that might favor a hydrogen bonding network favorable for catalysis. Contrary to what observed for ribodinucleotides, where UpU and UpG were cleaved faster, the reactivity order found for the metallocatalysts indicates selectivity for YpN dinucleotides, where Y is a pyrimidine. CpA is in every case the most reactive dinucleotide. Its ability to be cleaved depends on its position in the oligonucleotide, increasing when the bond is located more towards the 5'-terminal position.*

7.1 Introduction

RNA dinucleotides (RNA dimers) are largely used as substrates in the study of the catalytic properties of nuclease mimics. They resemble more closely the RNA polymers compared to other RNA models, but have only one reaction site and product formation can be easily followed by HPLC. However, it must be considered that the reactivity of a phosphate bond inserted in a polyribonucleotide structure is strongly influenced by other factors, such as the stacking of the bases,¹ the RNA secondary structure,²⁻⁴ intramolecular hydrogen bonds⁵ and sugar ring conformation⁶. Besides these factors, which affect the inherent reactivity of the phosphate bonds, the polyanionic structure of the oligonucleotide chain offers several binding sites for a metal complex and this can influence both the selectivity and the rate enhancement of the cleavage.

7.1.1 Structural and base-pair sequence effects on the nonenzymatic cleavage of oligoribonucleotides

The in-line conformation, in which the attacking 2'-oxyanion group and the 5'-leaving group are co-linear with the phosphorus atom, is a prerequisite for the dinucleotide transesterification (chapter 2.3.1). The two most important contributions to the in-line character of an internucleotide linkage are the rotation angles around the C3'-O3' (ϵ) and around the O3'-P (ζ) bonds (Figure 7.1 A).² The third structural parameter is the torsion angle of the bond connecting the C2' and C3' carbons (ν).

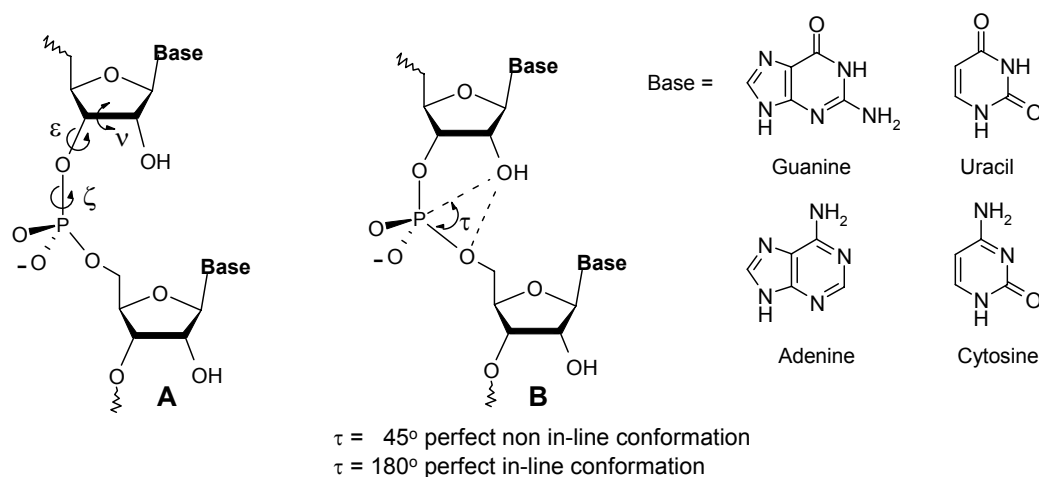


Figure 7.1

When the system is flexible, in the case of RNA dimers at any given time, each of these bonds can adopt one of a continuum of torsion angles. As a result, there may exist a continuum of structural states that range from a perfect non-in-line conformation ($\tau = 45^\circ$) to a perfect in-line conformation ($\tau = 180^\circ$), where τ defines the 2'-oxygen -P- 5'-oxygen angle (Figure 7.1 B). However, several structural factors and secondary structures (backbone

conformation, base stacking, loops, bulges, etc) influence the flexibility of a dinucleotide bond within an oligomer and this changes its reactivity.

In addition to the in-line conformation also the interatomic distance between the 2'-oxygen nucleophile and the phosphorous electrophile influences the rate of transesterification. A short interatomic distance, less than 3.25 Å, has been suggested to increase the frequency of productive collisions and therefore accelerate the cleavage.^{2;7} The same three torsion angles that determine the in-line conformation also establish the "attack distance". Variations in both the in-line orientation and the interatomic distance between reactive groups define the "in-line fitness" (F) of a particular RNA linkage.² The chemical stability of RNA duplexes compared to single-stranded RNAs is a proof of the importance of the in-line conformation in the rate of RNA cleavage. In the A-form helix, the 2'-oxyanion and the 5'-leaving group are precluded from adopting an in-line conformation, and the linkage is very resistant to transesterification. By studying several RNAs Breaker² concluded that by organizing an RNA linkage for in-line attack the rate enhancement is at least 10-20 times larger compared to a flexible RNA and 10³-10⁴ fold that of an A-form helix.

Solvent (H⁺, H₂O and OH⁻) catalyzed reactions. Lönnberg has studied the hydrolysis of oligomers which contain only one ribofuranoside unit, while the rest of the nucleotides are 2'-O-methylated. In this way only one phosphodiester bond can be cleaved by intramolecular transesterification. Data on the reactivity of specific dinucleotide bonds inserted in an oligonucleotide chain were obtained. Secondary structures, such as a seven-nucleotide hairpin loop, that do not affect significantly the conformational freedom of the phosphate bonds, have only a modest effect on their reactivity.³ On the other hand secondary structures that constrain the system can have much more influence.⁴ A phosphodiester bond in the middle of a four-nucleotide bulge is cleaved two or three times less readily than one inserted in a five-nucleotide bulge. When the phosphodiester bond is moved next to the double helical stem the cleavage rate decreases by a factor of ten.

Analogous substrates not forming stable secondary structures were used to investigate the effect of the base sequence on the reactivity of phosphodiester bonds. Some data obtained by Lönnberg *et al.*⁸ are reported in Table 7.1. They show a strong influence of the base sequence on the reactivity of the phosphodiester bonds. A more than 100-fold difference in reactivity is observed between oligonucleotides 5'-GGGUAN↓AAGUGC-3' (entry 4 and 13-15), all having the same base sequence with the exception of 5'-ribonucleoside of the phosphodiester bond cleaved. The 5'-ApA-3' bond is very stable also within oligonucleotide 5'-GGGUAUA↓AGUGC-3' (entry 13, 16). The 5'-UpA-3' bond is intrinsically the most reactive (entry 4-8), but within some oligonucleotides it shows reduced reactivity (entry 10, 11). The molecular environment also affects the cleavage rate of the 5'-CpA-3' bond and up to a 35-fold difference in reactivity may be observed (entry 14 and 17).

Table 7.1 Observed pseudo-first-order rate constants for the cleavage of oligonucleotides in CHES buffer, pH 8.5, at 35 °C.⁸

Entry	Sequence	$k, 10^{-7} s^{-1}$
1	UpU	2.2
2	5'-UUUUUU U UUUUUUU3'	0.9
3	UpA	1.5
4	5'-GGGU AU AAGUGC3'	14.6
5	5'-GGGU UU AAGUGC3'	31.7
6	5'-GGGA AU AAGUGC3'	43.2
7	5'-GGGU AU AUGUGC3'	43.8
8	5'-GGGU AU AAGUUC3'	30.1
9	5'-GUGU AU AAGUGC3'	1.2
10	5'-CCCC AU AACCCC3'	<0.2
11	5'-UCUCA AU AACUCU3'	2.5
12	5'-GGG U AUAGUGC3'	0.9
13	5'-GGGU AA AAGUGC3'	<0.2
14	5'-GGGU AC AAGUGC3'	0.3
15	5'-GGGU AG AAGUGC3'	0.5
16	5'-GGGU AUA AGUGC3'	<0.2
17	5'-GGGU AC AAGUUC3'	10.6

The ribonucleotide cleaved is indicated with a bold letter and the position of the strand scission with a vertical line.

The effect of the base composition on the stability of RNA phosphodiester bonds is attributed to stacking interactions that can prevent the 2'-OH and the leaving group to adopt the in-line conformation for the transesterification reaction. The stacking propensity of uracyl with its neighbors is generally weaker than that of any other of the three bases.⁹ Possibly more important than the stacking between the neighboring bases is the stacking farther in the molecule that has an influence on the overall structure of the oligomer.¹ Moreover, stabilization of the transition state (TS) has frequently been speculated to originate from hydrogen bonding,^{5;8} but also an enhanced base stacking in the TS with respect to the substrate seems to play an important role.¹⁰

Ammonium and metal ion catalyzed cleavage. Beside the structural factors that influence the inherent reactivity of phosphodiester bonds, also the polyanionic character of the oligonucleotide plays an important role when the transesterification is catalyzed by ammonium, metal ions or metal ion complexes. By studying the reactivity of different hexanucleotides in the presence of polyamines, such as spermine and spermidine, and cofactors, such as polyvinylpyrrolidone (PVP), Kierzek¹¹ found that the bonds pyrimidine-p-A and pyrimidine-p-C were especially susceptible to hydrolysis. The order of reactivity that he

observed was UA>CA>YC>YG>YU, where Y is a pyrimidine. The results of an extensive investigation allowed to conclude that only single-stranded fragments are cleaved, that at least two ammonium groups are necessary, and the optimal distance between them is 0.5-0.6 nm, corresponding to the distance between 2-3 carbons in a polymethylene chain. The presence of the ammonium ions in the catalysts increases their binding to the oligonucleotides inducing an active oligomer conformation, which is most abundant at a specific concentration of each polyamine. A very important role in reactivity is also played by the presence of a hydrogen bonding network that enhances the reactivity of a specific dinucleotide. In the case of YpA interactions between the 6-amino group in adenosine and the 2'- or 4'-oxygen of the 5'-pyrimidine or to an oxygen of the phosphate group should play a major role. Such hydrogen bonding may accelerate the reaction by abstracting the proton from the attacking 2'-OH, and/or by protonating the anionic phosphodiester.^{12;13} The polymeric cofactors can affect reactivity through non-specific interactions with the oligonucleotides, which change their conformation, or by excluding water molecules and creating a more apolar environment which makes the hydrogen bonding stronger.

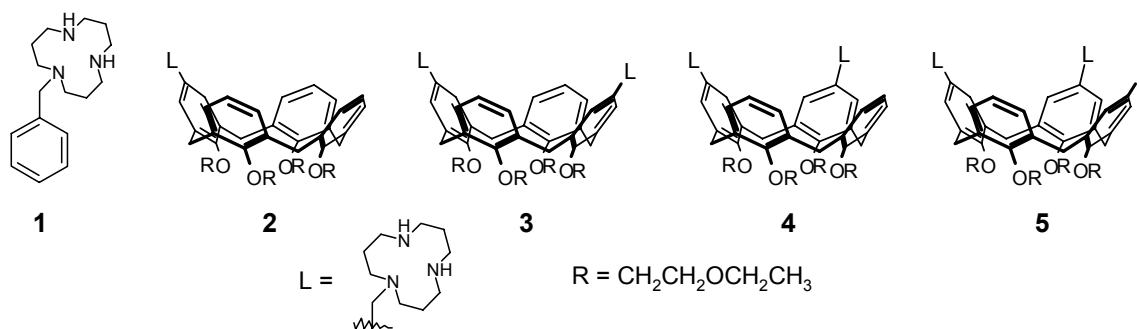
Studies of the hydrolysis of RNA by metal ions have revealed that dimers undergo a slower nucleophilic cleavage compared to that of longer RNA molecules. Even if phosphodiester bonds within poly-U oligomers in the absence of metal ions react approximately as fast as those within dinucleoside monophosphate UpU, in line with the low propensity of the uracyl to the stacking, metal ion catalyzed transesterification of poly-U showed a 5- to 20-fold rate enhancement over UpU.¹⁴ Even larger differences in the rate enhancements have been observed for the cleavage of ApA (slow) and poly(A)₁₂₋₁₈ (much faster) catalyzed by a Cu-terpyridine complex.¹⁵ ApAp is hydrolyzed about 2 orders of magnitude more rapidly than ApA in the presence of Zn(II), indicating the participation of the neighboring phosphate groups in the metal ion promoted hydrolysis of RNA.¹⁶ The considerably faster cleavage of phosphodiester bonds in oligonucleotides compared with dinucleotides is attributed to enhanced metal ion binding to the polymeric substrates, which in the case of free metal ions may act as a multidentate ligand.

Different from the results obtained in absence of metal ions, small bulge structures appear to have only a modest influence on the rate of Zn²⁺ or [12]aneN₃-[Zn²⁺] ion-promoted cleavage.⁴ The cleavage rates of phosphodiester bonds in different positions within bulges of various size differ by less than one order of magnitude by using Zn²⁺ as a catalyst, and less than a factor of five by using the [12]aneN₃-Zn(II) complex, where the less efficiently cleaved dinucleotide bonds are those close to the stem. These data reveal once again the importance of the stability of the metal ion-substrate complex on the efficiency of the catalysis. Even if in the bulge the dinucleotide bonds are less flexible, the adjacent phosphate groups might be closer than in the linear strand, forming a site with a higher negative charge that enhances the metal ion binding.⁴

7.1.2 Contents of the chapter

For the reasons given above, even if the use of RNA dimers as substrates for the screening of RNA cleavage agents and mechanistic studies is widespread, the results cannot accurately predict the relative abilities of metal complexes to cleave polyribonucleotide substrates. Moreover, the activity of metal catalysts that showed a remarkable selectivity for specific dinucleotides¹⁷⁻²⁰ has never been investigated in oligonucleotide cleavage and, as a consequence, in the literature there is no information on how the selectivity of supramolecular metal catalysts changes going from a RNA dimer to a RNA oligomer.

In Chapter 6 the catalytic activity of the copper(II) complexes of calix[4]arenes **3-5**, functionalized with 1,5,9-triazacyclododecane ([12]aneN₃), was described for the dinucleotide transesterification and compared to that of the monomer complex [12]aneN₃-[Cu]. Complexes **4**-[Cu]₂ and **5**-[Cu]₃ showed a selectivity for UpU and UpG cleavage. In this chapter the nuclease activity of metallo(II) complexes of compounds **1-5** in the cleavage of six-, seven- and seventeen-base oligomers will be reported.²¹



7.2 Catalytic activity of Cu(II)-triazacalix[4]arene complexes in oligonucleotide cleavage

The oligonucleotides **6-8** (Figure 7.2) were initially chosen to investigate the nuclease activity of Cu(II)-triazacalix[4]arene complexes in RNA oligomer cleavage. In these three oligomers all possible 16 dinucleotide bonds are present allowing an extensive screening of the efficiency and selectivity of the catalysts. The oligonucleotides have a radioactive phosphate (³²P), that was introduced in the 5'-terminal position by reaction with * γ -ATP and T4 polynucleotide kinase.²²

To avoid contamination from natural nucleases, everything that came into contact with the solutions of oligonucleotides, calixarenes and buffer was sterilized and used only once. The reactions of oligonucleotide cleavage were carried out in water (15 mM PIPES buffer, pH 7.4, I = 0.07, sodium dodecyl sulfate (SDS) 50 μ M) at 50 $^{\circ}$ C in the presence of 50 μ M Cu(II) calixarene complexes. The formation of products was followed by submitting small aliquots of the reaction mixture to gel-electrophoresis separation. The dried gel was exposed to a Kodak

phosphor screen that was analyzed by a Personal Molecular Imager (Bio-Rad). The images of the spots given by the radioactivity of ^{32}P were quantified with Quantity-One software from Bio-Rad.

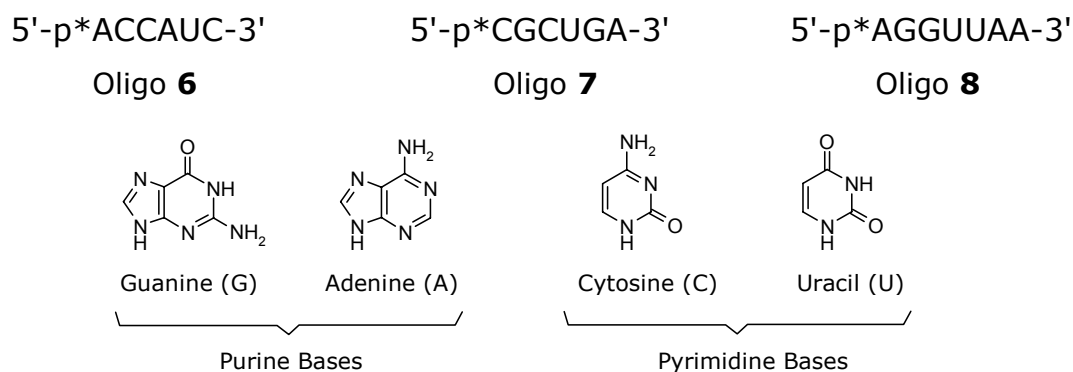


Figure 7.2

The fragments visible to the Bio-Rad analysis are only those containing the $5'\text{-}^{32}\text{P}$ -end-label. The identification of the cleavage products was carried out by comparison with the products obtained from the basic hydrolysis of the oligonucleotides. The basic hydrolysis gives two fragments for each phosphate cleavage, corresponding to the $2',3'$ -cyclic phosphate and to the acyclic $3'$ -phosphate, the former moving slightly slower than the latter.²³ Instead, when the metal calixarene complexes catalyze the phosphate cleavage only one fragment corresponding to the $2',3'$ -cyclic phosphate is visible on the denaturing gel, meaning that the reaction is a transesterification by the intramolecular attack of $2'\text{-OH}$. The spots on the gel corresponding to substrates and products were quantitatively analyzed to evaluate the mole fractions at different time intervals, which allowed the evaluation (see Appendix and Experimental part) of the k_{obs} values for the cleavage of oligonucleotides **6**, **7** and **8** in the presence of complexes **1**-[Cu], **2**-[Cu], **3**-[Cu]₂, **4**-[Cu]₂ and **5**-[Cu]₃ which are listed in Table 7.2.

The data in Table 7.2 can be analyzed in two different ways. Information on the cooperativity of the metal centers can be obtained by comparing the activity of the different catalysts for the same dinucleotide bond (Table 7.3). On the other hand, information on the selectivity of a catalyst are obtained by comparing the k_{obs} values for different dinucleotide bonds measured with the same catalyst (Table 7.4).

Table 7.2 Observed pseudo-first-order rate constants (k_{obs} , s^{-1}) for the transesterification of oligonucleotides **6-8** at 50 °C, pH 7.4, catalyzed by Cu(II) complexes of the ligands **1, 2, 3, 4** and **5**.^a The letters subscript to the k indicate the dinucleotide bond to which the value is referred.

Substrate Catalyst	Oligo 6 5'-ACCAUC-3'	Oligo 7 5'-CGCUGA-3'	Oligo 8 5'-AGGUUAA-3'
1 -[Cu]	$k_{CA} = 4.6 \times 10^{-7}$ $k_{CC} < 2.0 \times 10^{-7}$ ^b	- ^c	- ^c
2 -[Cu]	$k_{CA} = 5.8 \times 10^{-6}$ $k_{CC} = 3.0 \times 10^{-7}$	$k_{CG} < 2.0 \times 10^{-7}$ ^b $k_{CU} < 2.0 \times 10^{-7}$ ^b $k_{UG} < 2.0 \times 10^{-7}$ ^b	$k_{UA} < 2.0 \times 10^{-7}$ ^b
3 -[Cu] ₂	$k_{CA} = 1.3 \times 10^{-5}$ $k_{CC} = 2.8 \times 10^{-6}$	$k_{CG} = 3.7 \times 10^{-6}$ $k_{CU} = 1.3 \times 10^{-6}$ $k_{UG} = 4.2 \times 10^{-7}$	$k_{UA} = 5.2 \times 10^{-6}$
4 -[Cu] ₂	$k_{CA} = 3.5 \times 10^{-5}$ $k_{CC} = 4.6 \times 10^{-6}$	$k_{CG} < 2.0 \times 10^{-7}$ ^b $k_{CU} < 2.0 \times 10^{-7}$ ^b $k_{UG} < 2.0 \times 10^{-7}$ ^b	$k_{UA} = 1.3 \times 10^{-5}$
5 -[Cu] ₃	$k_{CA} = 8.2 \times 10^{-5}$ $k_{CC} = 1.1 \times 10^{-5}$	$k_{CG} = 6.4 \times 10^{-6}$ $k_{CU} = 1.1 \times 10^{-6}$ $k_{UG} = 1.1 \times 10^{-6}$	$k_{UA} = 9.5 \times 10^{-6}$

^a [Cat] = 50 μ M, [Oligonucleotide] < 0.2 nM, in 15 mM PIPES, I = 0.07 (NaCl), SDS 50 μ M.

^b After 5 h of incubation, less than 0.5% product was present.

^c Measurement not carried out.

Error limits = \pm 15%.

CpA is the most reactive bond with all of the calixarene catalysts. Since it was possible to measure the pseudo-first order rate constants for the cleavage of CpA by the benzyltriaza metal complex **1**-[Cu], this value was used to calculate the relative k_{obs} values for CpA cleavage of calixarene catalysts (Table 7.3). Interestingly, the activity of the mononuclear calixarene **2**-[Cu] is 12-fold higher than that of the benzyltriaza complex **1**-[Cu], indicating that the calixarene moiety plays a positive role in the catalytic process. It is possible that this effect is due to a hydrophobic environment created by the calixarene around the bond to be cleaved, as a consequence of enhanced substrate binding due to hydrophobic interactions with some of the aromatic bases. The activity of the 1,3-dinuclear calixarene **3**-[Cu]₂ in the cleavage of the CpA bond of oligo **6** is about twice that of **2**-[Cu], meaning that the diametral metal centers do not significantly cooperate in the catalysis. A certain degree of cooperativity, even if quite modest ($k_{obs}^{1,2-di}/k_{obs}^{mono} = 6$) is observed with the 1,2-dinuclear complex **4**-[Cu]₂. The trinuclear complex **5**-[Cu]₃ is 14 times more reactive than the mononuclear, but only 2.3 times more than **4**-[Cu]₂, a result that might be simply reflect a statistical advantage of the trinuclear over the 1,2-dinuclear catalyst.

Table 7.3 Observed pseudo-first-order rate constants for the cleavage of CpA, CpC and UpA dinucleotide bonds and relative rate accelerations with respect to the k_{obs} measured with the least efficient catalyst.^a

Catalyst	5'-AC Cp AUC-3' Oligo 6		5'-AC Cp CAUC-3' oligo 6		5'-AGGU Up AA-3' Oligo 8	
	k_{obs} (s ⁻¹)	$k_{obs}/k_{obs(1-[Cu])}$	k_{obs} (s ⁻¹)	$k_{obs}/k_{obs(2-[Cu])}$	k_{obs} (s ⁻¹)	$k_{obs}/k_{obs(3-[Cu]_2)}$
1 -[Cu]	4.6 x 10 ⁻⁷	1	-	-	-	-
2 -[Cu]	5.8 x 10 ⁻⁶	12.5	3.0 x 10 ⁻⁷	1	-	-
3 -[Cu] ₂	1.3 x 10 ⁻⁵	28	2.8 x 10 ⁻⁶	9.3	5.2 x 10 ⁻⁶	1
4 -[Cu] ₂	3.5 x 10 ⁻⁵	76	4.6 x 10 ⁻⁶	15.3	1.3 x 10 ⁻⁵	2.5
5 -[Cu] ₃	8.2 x 10 ⁻⁵	178	1.1 x 10 ⁻⁵	36.7	9.5 x 10 ⁻⁶	1.8

^a [Cat] = 50 μM, [Oligonucleotide] < 0.2 μM, in 15 mM PIPES, I = 0.07 (NaCl), SDS 50 μM.
Error limits = ± 15%.

No cleavage of the CpC bond could be detected using **1**-[Cu] as a catalyst. Therefore the k_{rel} values in Table 7.3 for this bond are relative to the k_{obs} measured with the mononuclear **2**-[Cu] catalyst. In this case a high synergism of the metal centers in **3**-[Cu]₂, **4**-[Cu]₂ and **5**-[Cu]₃ is observed. Once again the trinuclear complex is the most active compound, but only twice as effective as the 1,2-dinuclear **4**-[Cu]₂ and therefore a trimetallic catalysis seems unlikely. In the case of the UpA linkage in oligo **8** the rate of cleavage in the presence of the mononuclear calixarene **2**-[Cu] was too low to be measured and the k_{rel} for this bond are calculated using the k_{obs} found with the 1,3-dinuclear complex **3**-[Cu]₂, which is the least efficient catalyst. In UpA cleavage the 1,2-dinuclear calixarene **4**-[Cu]₂ is more efficient than the trinuclear complex, even if the rate enhancements observed with the three calixarene metal complexes **3**-[Cu]₂, **4**-[Cu]₂ and **5**-[Cu]₃, are in a close range of values. For the catalysts **3**-[Cu]₂, **4**-[Cu]₂ and **5**-[Cu]₃, the relative rate accelerations with respect to the least reactive dinucleotide are reported in Table 7.4. The selectivity in the phosphodiester bond cleavage can be qualitatively seen in Figure 7.3, which shows the gel-electrophoresis of oligonucleotides **6**, **7** and **8** cleaved in the presence of **5**-[Cu]₃. Lanes 1, 8 and 14 represent the basic hydrolysis of oligonucleotides **6**, **7** and **8**, respectively (20 min incubation, at 50 °C in 0.1 M NaOH solution). The spot at the top is the uncleaved oligonucleotide, and the spots below are the products of cleavage of a nucleotide from the 3'-terminal position. At the right side of the lanes of the basic hydrolysis the samples of the reactions carried out in the presence of the Cu(II) triazacalixarene complex **5**-[Cu]₃ are reported (the last point is taken at 5 h after the addition of the catalyst).

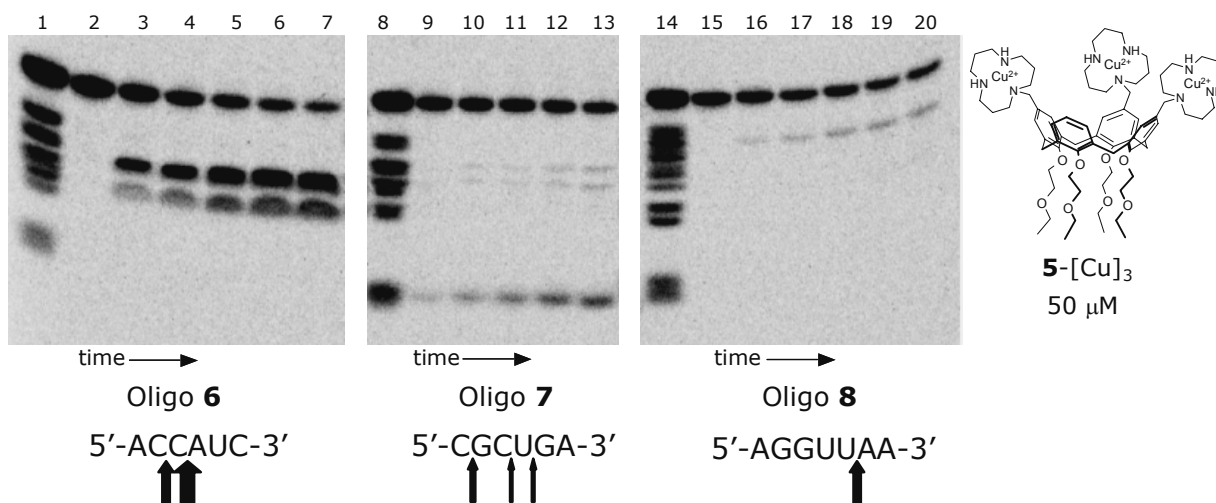


Figure 7.3 Gel-electrophoresis of the cleavage of oligo **6**, **7** and **8** catalyzed by 50 μM **5**-[Cu]₃. The lanes represent the following conditions: Lane 1: Basic hydrolysis of oligo **6** (20 min at 50 °C, NaOH 0.1 M). Lanes 2-7: cleavage of the oligonucleotide **6** in the presence of 50 μM **5**-[Cu]₃ at 50 °C in 15 mM PIPES, pH 7.4. Time points are 10 s, 1 h, 2 h, 3 h, 4 h and 5 h, respectively. Lane 8: Basic hydrolysis of oligo **7** (20 min at 50 °C, NaOH 0.1 M). Lanes 9-13: cleavage of the oligonucleotide **7** in the presence of 50 μM **5**-[Cu]₃ at 50 °C in 15 mM PIPES, pH 7.4. Time points are 1 h, 2 h, 3 h, 4 h and 5 h, respectively. Lane 14: Basic hydrolysis of oligo **8** (20 min at 50 °C, NaOH 0.1 M). Lanes 15-20: cleavage of the oligonucleotide **8** in the presence of 50 μM **5**-[Cu]₃ at 50 °C in 15 mM PIPES, pH 7.4. Time points are 10 s, 1 h, 2 h, 3 h, 4 h and 5 h, respectively. The arrows below the oligonucleotide sequences indicate the phosphate bonds that are cleaved; their thickness indicates the efficiency in the cleavage of the selected bond.

The most reactive bonds have always a pyrimidine nucleotide in 5' position. However, not every YpN bond, where Y is a pyrimidine, is cleaved, since no reaction of UpU in oligo **8** and UpC in oligo **6** was observed. The order of reactivity of the dinucleotide bonds is similar for all the calixarene catalysts. The most reactive phosphate bond is that which links the cytidine and adenosine in oligonucleotide **6**. The selectivity for CpA is remarkable. It undergoes cleavage 30 times faster than UpG in the presence of **3**-[Cu]₂, and even a higher selectivity was found with the trinuclear catalyst **5**-[Cu]₃, which catalyzes CpA cleavage 74 times more efficiently than UpG cleavage. Surprisingly, the 1,2-dinuclear catalyst **4**-[Cu]₂, which in the cleavage of oligonucleotides **6** and **8** is more active than its 1,3-diametral regioisomer **3**-[Cu]₂, does not cleave CG, CU and UG bonds in oligonucleotide **7** (Table 7.2, Figure 7.4). Therefore the selectivity of **4**-[Cu]₂ for CpA with respect to UpG, CpU and CpG is much higher, reaching a value of no less than 380.

Table 7.4 Observed pseudo-first-order rate constants for the selected dinucleotide cleavage in oligonucleotides **6-8** catalyzed by **3**-[Cu]₂, **4**-[Cu]₂ and **5**-[Cu]₃ and relative rate accelerations with respect to the least reactive dinucleotide.^a

Substrate	3 -[Cu] ₂		4 -[Cu] ₂		5 -[Cu] ₃	
	<i>k</i> _{obs} (s ⁻¹)	<i>k</i> _{obs} / <i>k</i> _{obs(UG)}	<i>k</i> _{obs} (s ⁻¹)	<i>k</i> _{obs} / <i>k</i> _{obs(UG)}	<i>k</i> _{obs} (s ⁻¹)	<i>k</i> _{obs} / <i>k</i> _{obs(UG)}
UG	4.2 × 10 ⁻⁷	1	<2.0 × 10 ⁻⁷	1	1.1 × 10 ⁻⁶	1
CU	1.3 × 10 ⁻⁶	3.1	<2.0 × 10 ⁻⁷	1	1.1 × 10 ⁻⁶	1
CG	3.7 × 10 ⁻⁶	8.8	<2.0 × 10 ⁻⁷	1	6.4 × 10 ⁻⁶	5.8
UA	5.2 × 10 ⁻⁶	12.4	1.3 × 10 ⁻⁵	> 65	9.5 × 10 ⁻⁶	8.6
CC	2.8 × 10 ⁻⁶	6.7	4.6 × 10 ⁻⁶	> 230	1.1 × 10 ⁻⁵	10
CA	1.3 × 10 ⁻⁵	30	3.5 × 10 ⁻⁵	> 380	8.2 × 10 ⁻⁵	74.5

^a [Cat] = 50 μM, [Oligonucleotide] < 0.2 μM, in 15 mM PIPES, I = 0.07 (NaCl), SDS 50 μM. Error limits = ± 15%.

The order of reactivity is CA>UA>CG>CC> CU>UG with **3**-[Cu]₂, CA>CC>UA>>CG,CU,UG with **4**-[Cu]₂, and CA>CC>UA>CG>CU=UG with **5**-[Cu]₃.

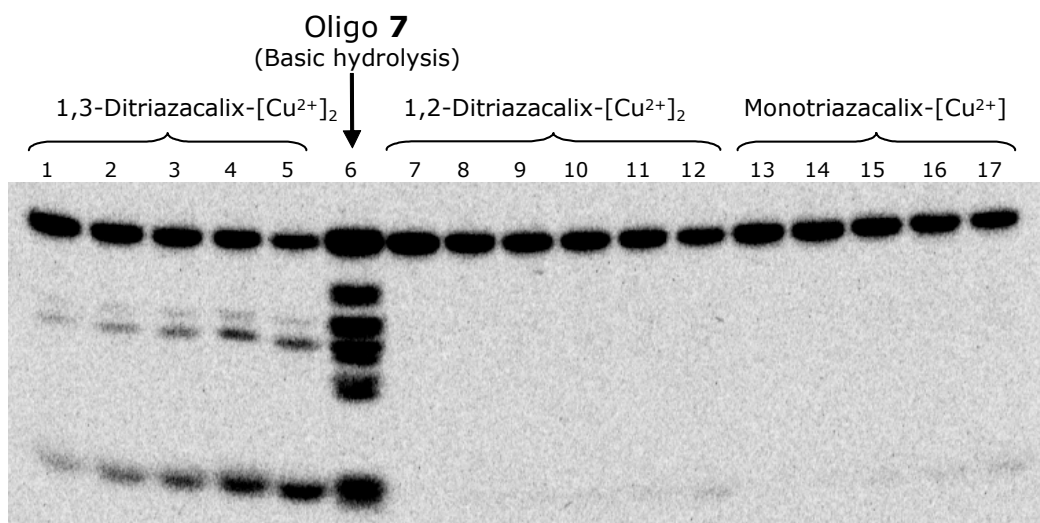


Figure 7.4 Gel-electrophoresis of the cleavage of oligonucleotide **7** catalyzed by 50 μM **3**-[Cu]₂, **4**-[Cu]₂, **2**-[Cu]. The lanes represent the following conditions: Lanes 1-5: cleavage of the oligonucleotide **7** in the presence of 50 μM **3**-[Cu]₂ at 50 °C in 15 mM PIPES, pH 7.4. Time points are 1 h, 2 h, 3 h, 4 h and 5 h, respectively. Lane 6: Basic hydrolysis of oligo **7** (20 min at 50 °C, NaOH 0.1 M). Lanes 7-12: cleavage of the oligonucleotide **7** in the presence of 50 μM **4**-[Cu]₂ at 50 °C in 15 mM PIPES, pH 7.4. Time points are 10 s, 1 h, 2 h, 3 h, 4 h and 5 h, respectively. Lanes 13-17: cleavage of the oligonucleotide **7** in the presence of 50 μM **2**-[Cu] at 50 °C in 15 mM PIPES, pH 7.4. Time points are 1 h, 2 h, 3 h, 4 h and 5 h, respectively.

This selectivity is not in accordance with that observed in the transesterification of RNA dimers (Chapter 6). Dinucleotides UpU and UpG were the most reactive dimers in the presence of the complex **5**-[Cu]₃, but when UpU is within an oligomeric sequence it is not

appreciably cleaved. The transesterification of UpG within the oligonucleotide **7** is instead observed, even if it is the least reactive dinucleotide bond among those cleaved.

The observed selectivity for pyrimidine-pN dinucleotides, where N is any base, which is similar to that shown by some nucleases as e.g. the pancreatic ribonuclease A (even if with our catalysts the UpU and UpC bonds are not cleaved), and the discrepancy with the behaviour of RNA dimers could suggest the presence of some contaminating nucleases. Therefore, additional experiments were carried out to exclude this possibility. The solution of the oligonucleotides did not show any cleavage even after 20 h of incubation at 50 °C in 15 mM PIPES, SDS 50 μM. The metal solution was freshly prepared with milliQ sterile water before every experiment. Moreover, the oligonucleotides incubated with 150 μM Cu(II) did not show the selective cleavage observed with the calixarene metal complexes. These results show that any possible contaminant would result only from the solutions of the catalysts, which, however, were obtained from a dichloromethane solution and stocked in ethanol, where bacterial proliferation is prevented. A solution of compound **3**, diluted with water to reach a 70% EtOH composition, was purified by ultrafiltration, to remove globular molecules larger than 3 KDa.^{24;25} The catalytic activity of **3**-[Cu]₂ before and after filtration was exactly the same. Moreover, the order of catalytic efficiency is definitely related to the number and positions of the metal centers, namely, trinuclear > 1,2- and 1,3-dinuclear > mononuclear, which should not be observed in the presence of catalytically active contaminants.

For the CG cleavage of oligonucleotide **7** at 25 °C in the presence of **5**-[Cu]₃ the k_{obs} is 1/10 of that measured at 50 °C, and this cannot be well explained if the catalysis was given by a natural enzyme, that should work better at room temperature than at 50 °C where it should be partially denaturated.

Finally, the reactions in the presence of the metal free azacalixarenes show very little cleavage of the oligonucleotides **6-8**. Therefore, all these data strongly suggest that the catalytic activity is due to the metal complexes and the presence of any contaminants in the calixarene stock solutions can be excluded.

It is not easy to find a satisfactory explanation for the observed selectivity, since many factors can affect the intrinsic reactivity of phosphate bonds within oligonucleotide sequences (chapter 7.1.1). As already noted, the highest rate in the cleavage of oligonucleotides catalyzed by calixarene complexes is observed for CpA, which was completely unreactive in the case of the **5**-[Cu]₃ catalyzed cleavage of RNA dimers (see Chapter 6). However, the observed selectivity is partially in agreement with the results of Kierzek^{5;11;23;26} discussed previously (Chapter 7.1.1), although there the most reactive bond was UpA instead of CpA. The positively charged calixarene metal ion complexes, like the ammonium ions of the biogenic polyamines spermine, spermidine and putrescine, might complex the oligoribonucleotides, inducing a conformational rearrangement which exposes the CpA bond

to cleavage. It cannot be ruled out that also the calixarene platform might play a positive role in the catalysis by non-specific apolar binding to the oligonucleotide, as suggested by the observation that, in the cleavage of oligo **6**, the mononuclear calixarene complex **2**-[Cu] is 12 times more active than the benzyltriazacalix complex **1**-[Cu]. Indirect evidence suggests that the calixarene complexes can indeed bind strongly to the oligonucleotides. In fact, when aliquots of the reactions were analyzed by gel-electrophoresis without removing the calixarene, the oligonucleotide could not penetrate into the gel and the entire radioactivity remained in the wells. Removal of the calixarene by CH₂Cl₂/H₂O extraction before the analysis allowed a normal run of the oligonucleotide on the denaturing gel.

Since the reactivity of a phosphodiester bond can be strongly influenced by the sequence in which it is inserted,⁸ three other substrates (**9-11**) were subsequently investigated in order to evaluate if the cleavage selectivity found with oligonucleotides **6-8** was due to their particular sequence and/or to the relative position of the dinucleotide within the oligomer.



Oligo **9**



Oligo **10**



Oligo **11**

In oligo **9** and **10** CpA is at the beginning and at the end of the sequence, respectively, whereas CC is at the beginning of the sequence in oligo **10** and at the end in oligo **9**. Oligo **11**, instead, has the same sequence of oligo **6**, but with UpA in the position of CpA, to compare the reactivity of CpA and UpA in the same sequence. Kinetic measurements were carried out under the same conditions used for oligonucleotides **6-8**. The pseudo-first order constants measured in the presence of complexes **2**-[Cu], **3**-[Cu]₂, **4**-[Cu]₂ and **5**-[Cu]₃ are listed in Table 7.5.

Table 7.5 Observed pseudo-first-order rate constants (k_{obs} , s^{-1}) for the transesterification of oligonucleotides **9-11**, catalyzed by Cu(II) complexes of **2**, **3**, **4** and **5** at 50 °C, pH 7.4.^a The letters subscript to the k indicate the dinucleotide bond to which the value is referred.

Substrate Catalyst	Oligo 9 5'-CAGGCC-3'	Oligo 10 5'-CCGGCA-3'	Oligo 11 5'-ACUAUC-3'
2 -[Cu]	$k_{CA} = 7.1 \times 10^{-6}$	$k_{CC} < 2.0 \times 10^{-7}$ $k_{CG} < 2.0 \times 10^{-7}$ $k_{CA} < 2.0 \times 10^{-7}$	$k_{UA} = 2.1 \times 10^{-6}$
3 -[Cu] ₂	$k_{CA} = 1.1 \times 10^{-4}$	$k_{CC} = 1.5 \times 10^{-5}$ $k_{CG} = 3.2 \times 10^{-6}$ $k_{CA} = 1.0 \times 10^{-5}$	$k_{UA} = 5.0 \times 10^{-5}$
4 -[Cu] ₂	$k_{CA} = 1.3 \times 10^{-4}$	$k_{CC} = 7.5 \times 10^{-5}$ $k_{CG} = 1.7 \times 10^{-5}$ $k_{CA} = 5.0 \times 10^{-5}$	$k_{UA} = 2.5 \times 10^{-5}$
5 -[Cu] ₃	$k_{CA} = 3.0 \times 10^{-4}$	$k_{CC} = 1.7 \times 10^{-5}$ $k_{CG} = 2.1 \times 10^{-6}$ $k_{CA} = 1.1 \times 10^{-5}$	$k_{UA} = 5.1 \times 10^{-5}$

^a [Cat] = 50 μ M, [Oligonucleotide] < 0.2 nM, in 15 mM PIPES, I = 0.07 (NaCl), SDS 50 μ M.
Error limits = \pm 15%.

The cleavage selectivity found with oligonucleotides **6-8** was observed also with oligonucleotides **9-11**, and this is also visible in the gel-electrophoresis depicted in Figure 7.5 for the reactions of **9-11** in the presence of **3**-[Cu]₂. The selectivity is therefore not due to the particular sequence in which the dinucleotides are inserted. However, the sequence has a strong influence on the rate enhancements. Comparing for instance the pseudo first order constant found for UpA cleavage in oligo **8** and in oligo **11** in the presence of **5**-[Cu]₃ ($k_{obs} = 9.5 \times 10^{-6} s^{-1}$ and $k_{obs} = 5.1 \times 10^{-5} s^{-1}$, respectively) UpA in oligo **8** is cleaved about 5 times more slowly than in oligo **11**. Because in both cases UpA is in the middle of the oligonucleotide, this difference in reactivity is probably due to an effect of the sequence more than to an effect of the position of the scissile bond. It could be suggested that, compared to **11**, the stacking in oligo **8** is stronger because of the higher number of purine bases and the substrate is more stabilized.

Another example of the effect of the sequence is observed in the CpG cleavage catalyzed by the 1,2-dinuclear complex **4**-[Cu]₂. While similar rate enhancements were found for the transesterification of this bond with **3**-[Cu]₂ and **5**-[Cu]₃ both in oligo **7** and oligo **10**, in the case of the 1,2-dinuclear complex **4**-[Cu]₂ large differences were observed. For the cleavage of CG in oligonucleotide **10** a $k_{obs} = 1.7 \times 10^{-5} s^{-1}$ was found, while less than 0.5% of product was observed after 5 h for the reaction in oligonucleotide **7** ($k_{obs} < 2.0 \times 10^{-7} s^{-1}$). This means that the CG bond in oligonucleotide **10** is not intrinsically more reactive, but the base sequence might favor a productive binding with the catalyst **4**-[Cu]₂.

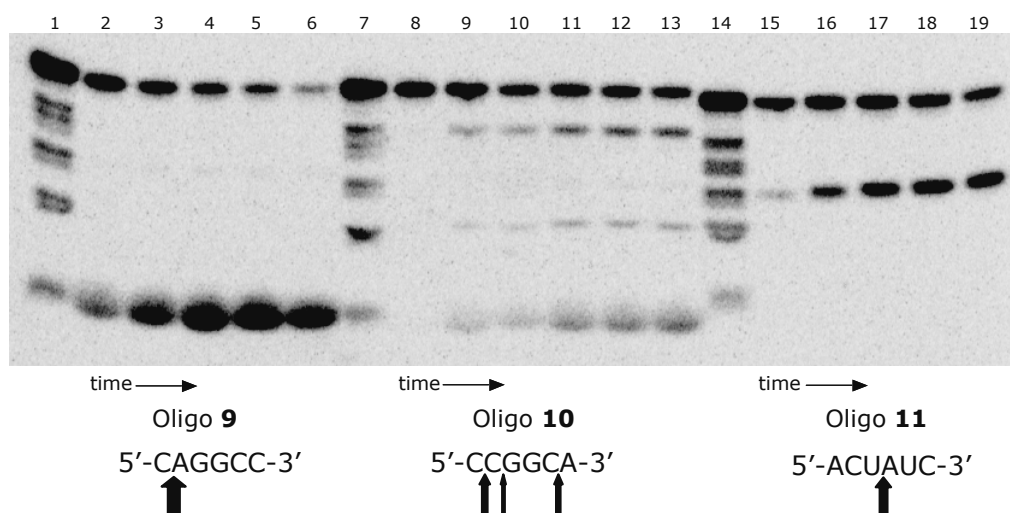


Figure 7.5 Gel-electrophoresis of the cleavage of oligonucleotides **9**, **10** and **11** catalyzed by $50 \mu\text{M}$ **3**-[Cu]₂. The lanes represent the following conditions: Lane 1: Basic hydrolysis of oligonucleotide **9** (20 min at 50 °, NaOH 0.1 M). Lanes 2-6: cleavage of the oligonucleotide **9** in the presence of $50 \mu\text{M}$ **3**-[Cu]₂ at 50 °C in 15 mM PIPES, pH 7.4. Time points are 1 h, 2 h, 3 h, 4 h and 5 h, respectively. Lane 7: Basic hydrolysis of oligo **10** (20 min at 50 °, NaOH 0.1 M). Lanes 8-13: cleavage of the oligonucleotide **10** in the presence of $50 \mu\text{M}$ **3**-[Cu]₂ at 50 °C in 15 mM PIPES, pH 7.4. Time points are 10 s, 1 h, 2 h, 3 h, 4 h and 5 h, respectively. Lane 14: Basic hydrolysis of oligonucleotide **11** (20 min at 50 °, NaOH 0.1 M). Lanes 15-19: cleavage of the oligonucleotide **11** in the presence of $50 \mu\text{M}$ **3**-[Cu]₂ at 50 °C in 15 mM PIPES, pH 7.4. Time points are 30 min, 2 h, 3 h, 4 h and 5 h, respectively. The arrows below the oligonucleotide sequences indicate the phosphate bonds that are cleaved and their thickness indicates the efficiency in the cleavage of the selected bond.

Beside the effect of the sequence, the reactivity of the phosphodiester bonds is dependent on their position within the oligonucleotide. This factor is particularly relevant in CpA transesterification with all calixarene catalysts, but especially with **5**-[Cu]₃. Table 7.6 shows the relative rate accelerations for CpA cleavage in the presence of **5**-[Cu]₃ with respect to the k_{obs} measured for oligo **10**. When CpA is moved toward the 5' terminal position its reactivity highly increases. The CpA linkage in oligonucleotide **9** is 27-fold more reactive than in oligonucleotide **10**, where it is placed in the 3' terminal position. All these data could indicate an interaction of the catalyst with the phosphate in 3' position important for the formation of the Michaelis complex, and also a favorable interaction with the terminal 5' phosphate group, less hindered and doubly charged compared to the other phosphate groups.

Table 7.6 Relative rate accelerations for the cleavage of CpA bond catalyzed by trinuclear complex **5**-[Cu]₃ with respect to the k_{obs} found for oligonucleotide **10**.

Substrate	k_{rel}
5'-CCGG CpA -3' Oligo 10	1
5'-AC CpA UC-3' Oligo 6	7.7
5'- CpA GGCC-3' Oligo 9	27.3

The kinetic analysis of hydrolysis of **10** revealed that the fragment 5'-CCGGC formed by CpA cleavage becomes also a substrate for the transesterification of CpC. Instead, cleavages of CA and CC in the oligo **6** are parallel reactions. The two products 5'-ACC and 5'-AC derive from the starting substrate and even if the fragment 5'-ACC, given by CA cleavage, could become a substrate for the CC cleavage, this is not observed, or at least it has a much slower rate (see Appendix 7.4). This could be an indication of the importance of non-cyclic phosphate in 3' position adjacent to the scissile bond for a productive binding of the calixarene catalysts. In fact in 5'-ACC the CC dinucleotide is in 3' terminal position and has a 2',3',-cyclic phosphate. The phosphate in the 3' position could be a binding site for one of the metal centers, without being a reaction site, and the other Cu(II) (or the other two) of the catalyst could activate the hydrolysis of the adjacent phosphate.

Table 7.7 shows the relative rate accelerations in the presence of **2**-[Cu], **3**-[Cu]₂, **4**-[Cu]₂ and **5**-[Cu]₃ with respect to the k_{obs} measured with the mononuclear catalyst **2**-[Cu] for the cleavage of CpA in oligo **9** and UpA in oligo **11**. The superiority of di- and trinuclear catalysts compared with the mononuclear catalyst indicates that in all cases the metal ions work together in a cooperative fashion. However, even if with both substrates the most efficient catalyst is the trinuclear complex **5**-[Cu]₃, its activity does not significantly differ from that of the dinuclear ones. The activity of **5**-[Cu]₃ in UpA cleavage is practically the same of that of 1,3-dinuclear complex **3**-[Cu]₂, while in CpA cleavage **5**-[Cu]₃ is a little bit more than twice as efficient as the dinuclear complex **4**-[Cu]₂.

Table 7.7 Relative rate accelerations with respect to the k_{obs} measured with the mononuclear catalyst **2**-[Cu] for the cleavage of CpA and UpA bonds within oligoribonucleotides **9** and **11** ($k_{rel} = k_{obs}/k_{obs(2-[Cu])}$).

Catalyst	5'- Cp AGGCC-3' Oligo 9	5'-ACU Up AUC-3' Oligo 11
	k_{rel}	k_{rel}
2 -[Cu]	1	1
3 -[Cu] ₂	15.4	23.8
4 -[Cu] ₂	18.3	11.9
5 -[Cu] ₃	42.3	24.2

The cleavage of CpA phosphodiester bond in oligonucleotide **9** catalyzed by **5**-[Cu]₃ was used to investigate the dependence of the rate enhancement on the concentration of the catalyst. The experiments showed a good linearity in the concentration range 5-50 μM. However, increasing the concentration of **5**-[Cu]₃ to 150 μM we observed rate enhancement significantly lower than that measured with 50 μM catalyst. This can only be explained when calixarene aggregates are formed that prevent catalysis or when a partial precipitation of the catalyst takes place. Although at first sight the latter hypothesis seems unlikely, because the water solubility measured for **5**-[Cu]₃ (Chapter 6) is high, the complexes between **5**-[Cu]₃ and the oligonucleotide could be much less soluble as a consequence of charge neutralization.

The oligonucleotide **12** (Figure 7.6) was used to investigate the activity of copper(II) calix[4]arene complexes with an oligomer composed of more than 6-bases, closer to a natural RNA. Oligo **12** is a 17-mer oligomer, labeled in 5' with a radioactive phosphate (³²P). Among its six pyrimidine-p-N bonds, five belong to CpA dimeric units, for which our catalysts have shown the highest efficiency (Table 7.2 and 7.5), and one is a UpC linkage, that in oligonucleotide **6** was not efficiently cleaved by any of our catalysts. The measurements on oligonucleotide **12** could not be carried out under the same conditions used for oligonucleotides **6-11**. Only a small part of the radioactivity was detected on the gel electrophoresis, whereas a major part of the radioactivity remained in the wells of the gel and probably precipitation also occurred in the reaction tubes. This was attributed to formation of cluster complexes, arising from strong interactions between the catalysts and the substrate. The concentration of SDS was therefore increased to 150 μM, and that of the catalyst decreased to 10 μM. Under these conditions the cleavage of **12** in the presence of **3**-[Cu]₂ and **4**-[Cu]₂ at 50 °C, in PIPES 15 mM could be studied and the gel electrophoresis is depicted in Figure 7.6. The selectivity for CpA dinucleotide was confirmed and other bonds

were not cleaved. Analysis of the cleavage of α and β CpA bonds was not easy because of the low intensity of the spots corresponding to the products.

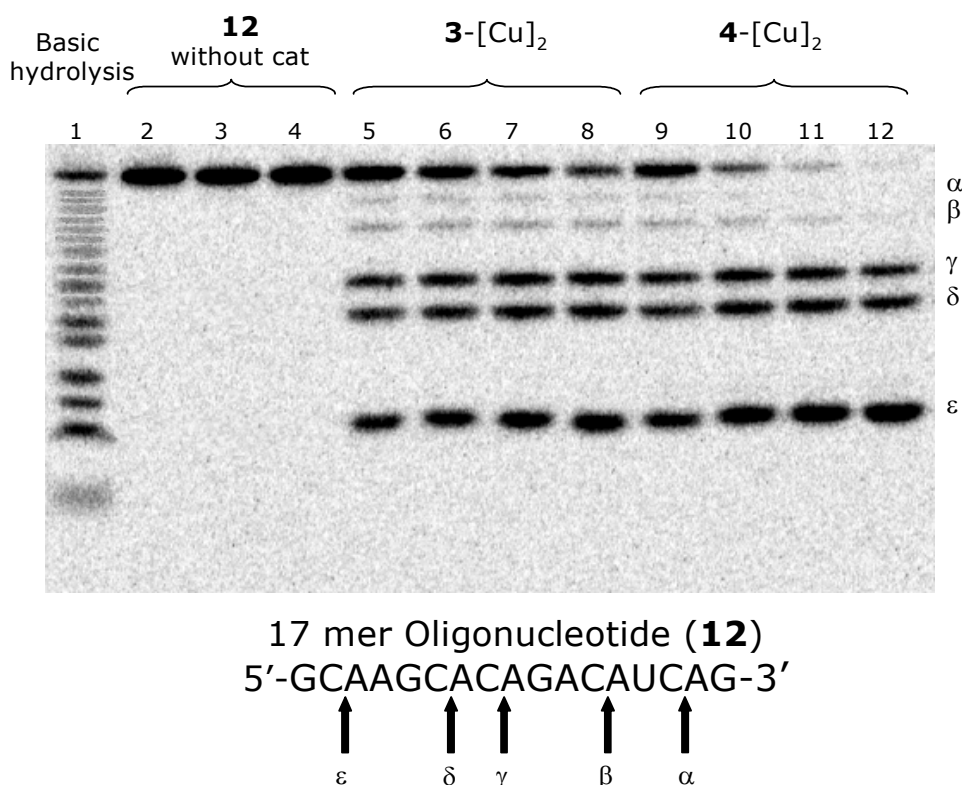


Figure 7.6 Gel-electrophoresis of the cleavage of oligonucleotide **12** catalyzed by $10 \mu\text{M}$ **3**-[Cu]₂ and **4**-[Cu]₂. The lanes represent the following conditions: Lane 1: Basic hydrolysis (20 min at 50 °, NaOH 0.1 M). Lanes 2-4: oligonucleotide **12** in 15 mM PIPES, pH 7.4, SDS 150 μM at 50 °C. Time points are 20 s, 3 h and 6 h, respectively. Lanes 5-8: reaction in the presence of $10 \mu\text{M}$ **3**-[Cu]₂ at 50 °C in 15 mM PIPES, pH 7.4, SDS 150 μM . Time points are 1 h 50 min, 3 h 15 min, 4.5 h and 6 h 15 min, respectively. Lanes 9-12: reaction in the presence of $10 \mu\text{M}$ **4**-[Cu]₂ at 50 °C in 15 mM PIPES, pH 7.4, SDS 150 μM . Time points are 1 h 50 min, 3 h 15 min, 4.5 h and 6 h 15 min, respectively. The arrows below the oligonucleotide sequence indicate the phosphate bonds that are cleaved.

The cleavages of γ , δ and ϵ CpA bonds catalyzed by **3**-[Cu]₂ are parallel reactions, as shown by the fact that by fitting the experimental points (Figure 7.7) we obtained the same value of k_{obs} (see Appendix). Actually, the ratios of the products $[5'\text{-GC}]/[5'\text{-GCAAGC}]$ and $[5'\text{-GC}]/[5'\text{-GCAAGCAC}]$ increase very slowly in the time, meaning that 5'-GCAAGC and 5'-GCAAGCAC tend to become substrate for the cleavage of ϵ CpA. However, the process is slow and was not taken into account in the calculation of the kinetic constants. The bonds CpA γ , δ and ϵ are cleaved with similar efficiency, but faster than the CpA α and β close to the 3' terminal position of the oligomer, confirming the results obtained with the shorter oligonucleotides.

Table 7.8 Observed pseudo-first-order rate constants (k_{obs} , s^{-1}) for the transesterification of oligonucleotides **12**, catalyzed by Cu(II) complexes of **3** and **4** at 50 °C, pH 7.4.^a The bold letters indicate the dinucleotide bond to which the value is referred.

Catalyst	5'-GCAAGCA CpA ...	5'-GCAAG CpA CA...	5'-GC CpA AAGCACA...
	(γ)	(δ)	(ϵ)
	k_{obs}	k_{obs}	k_{obs}
3 -[Cu] ₂	1.26×10^{-5}	1.21×10^{-5}	1.82×10^{-5}
4 -[Cu] ₂	4.4×10^{-5}	5.0×10^{-5}	4.5×10^{-5}

^a [Cat] = 10 μ M, [Oligonucleotide] < 0.2 nM, in 15 mM PIPES, I = 0.07 (NaCl), SDS 150 μ M. Error limits = \pm 10%.

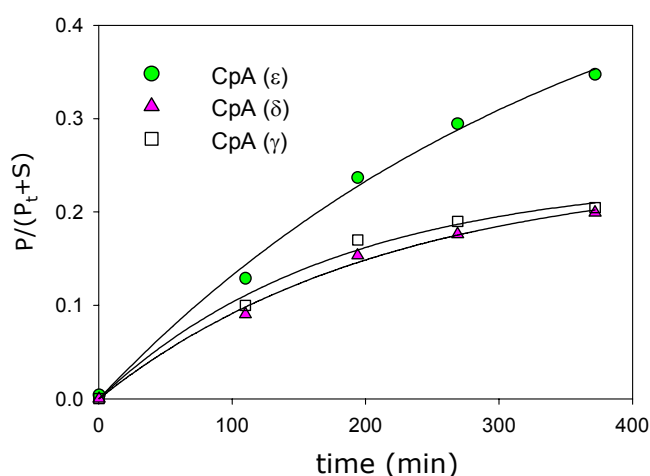


Figure 7.7 Molar fractions of 5'-GC (CpA (ϵ) cleavage), 5'-GCAAGC (CpA (δ) cleavage) and 5'-GCAAGCAC (CpA (γ) cleavage) as function of time for the reaction of oligonucleotide **12** catalyzed by 10 μ M **3**-[Cu]₂.

Also in the case of the reaction catalyzed by **4**-[Cu]₂ the three k_{obs} values measured for the cleavage of CpA γ , δ and ϵ bonds are similar (Table 7.8), but differently from what was observed with **3**-[Cu]₂ the fragments given by the cleavage of CpA γ and δ became substrates for the cleavage of CpA ϵ (Figure 7.8). The two fragments react to give 5'-GC with a pseudo-first order constant $k_{obs} = 4.7 \pm 0.3 \times 10^{-5} s^{-1}$, meaning that the cleavage of CpA (ϵ) is catalyzed with the same efficiency both for the substrate **12** and for the two fragments. It could be hypothesized that in the case of the reaction catalyzed by **3**-[Cu]₂ the products remain complexed to the catalyst and cannot undergo further cleavage, while in the reaction catalyzed by **4**-[Cu]₂ the products are released fast in the medium undergoing further reaction. The different behavior suggests that the two catalysts, even if selective for the same bonds, bind to the substrate in a different way.

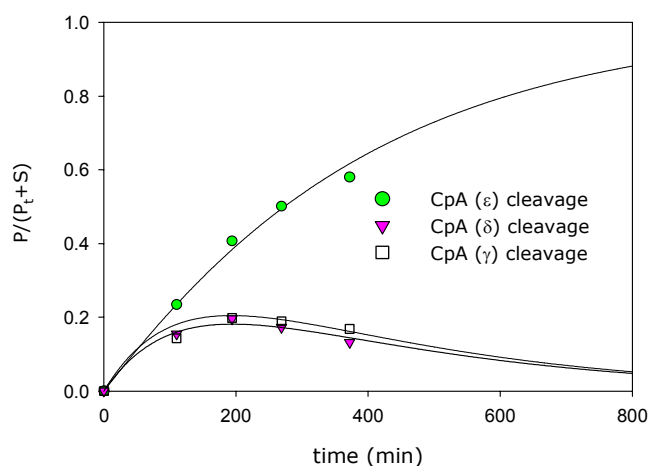


Figure 7.8 Molar fractions of 5'-GC (CpA (ϵ) cleavage), 5'-GCAAGC (CpA (δ) cleavage) and 5'-GCAAGCAC (CpA (γ) cleavage) as function of time for the reaction of oligonucleotide **12** catalyzed by 10 μ M **4**-[Cu]₂.

7.3 Conclusions

In this chapter the catalytic activity of copper(II) triaza calix[4]arene complexes was investigated in oligonucleotide cleavage. The reactions were carried out in water pH 7.4 (15 mM PIPES) and at 50 °C. The calixarene based complexes **3**-[Cu]₂, **4**-[Cu]₂ and **5**-[Cu]₃ are very efficient catalysts in the cleavage of phosphodiester bonds within an oligomer. The efficiency of these catalysts is provided by two factors. One is the cooperative action of the metal centers, and the other one, whose relative importance was not evaluated, is the apolar calixarene skeleton that could interact with the aromatic bases or create an apolar environment around the oligomer that increases the activity of the hydrogen bonding network around the catalytic center.

A more important property of these catalysts is the selectivity of the cleavage. Dinucleotide bonds having a pyrimidine base in 5' position are cleaved more rapidly. The order of reactivity is CA>UA>CC>CG>CU>UG with **3**-[Cu]₂, CA>CC>UA with **4**-[Cu]₂, and CA>CC>UA>CG>CU~UG with **5**-[Cu]₃. CpA is the most reactive bond with all the catalysts. This result is unprecedented and can be explained assuming a strong binding of the calixarene complexes to the oligonucleotides, which stabilizes a conformation where the CpA dimmer unit is more exposed to the cleavage. The ability of calixarene catalysts to cleave phosphodiester CpA bonds in oligonucleotides strongly depends on their position in the oligomer. It is higher when CA is in the 5' terminal position and lower when it is placed in the 3' terminal position, showing differences in reactivity of up to 27 times. Some literature data suggest that the pyrimidine-p-N bonds within a oligonucleotide are intrinsically more susceptible to cleavage and this could explain the observed selectivity and the discrepancy of

these results with the data for UpU and UpG in RNA dimer cleavage found with the same catalysts (Chapter 6).

The reactivity of dinucleotides within an oligomeric sequence is affected by many factors that can change dramatically the efficiency and selectivity of the catalyst. The data reported in this chapter represent one of the first examples in the literature of site specific RNA oligonucleotide cleavage of supramolecular metallo-catalysts lacking other recognition groups.

7.4 Experimental part

General information and Materials

The synthesis of compounds **2**, **3**, **4** and **5** is described in Chapter 5. Compound **1** was synthesized according to literature procedures.²⁸ Oligonucleotides were purchased from Dharmacon Research (Lafayette, CO). 1,4-Piperazinediethane sulfonic acid (PIPES) was purchased from Fluka. Oligonucleotides were ³²P-5'-end-labeled with T4 polynucleotide kinase according to standard procedures.²⁹ Concentrations of radioactive oligonucleotides were determined from specific activities; concentrations of nonradioactive oligonucleotides were determined using extinction coefficients at 260 nm estimated by the nearest neighbor method³⁰. Unless otherwise stated, measurements were carried out in 15 mM PIPES±NaOH, adjusted to pH 7.4 at the final reaction temperature. The ionic strength was adjusted to ~0.07 M with NaCl. Divalent metal chlorides (>99.99%) were from Aldrich. Solutions of transition metal chlorides were used immediately after preparation. The aqueous solutions were prepared using deionized (Millipore) distilled water.

Solutions

TBE is a water solution containing tris(hydroxymethyl)aminomethane (TRIS) (89 mM), boric acid (89 mM) and EDTA (2.5 mM). 10 mL of stop solution are composed of formamide (9 mL), TBE (1 mL), EDTA (50 µL, 0.5 M, final concentration 2.5 mM). Polyacrylamide gels are made from acrylamide and N,N'-methylene bisacrylamide (bisacrylamide). 1 L of "gel-mix" contains TBE (100 mL), 40% acrylamide solution (500 mL, acrylamide/bisacrylamide 29:1), urea (420 g) and water till final volume (~ 70 mL). 80 mL of acrylamide gel-mix are polymerized adding 0.5 mL of 10% ammonium persulfate aqueous solution and 50 µL of N,N,N',N'-tetramethylethylenediamine. The gel running buffer is a solution of TBE diluted ten times in water.

Measurement of the pseudo-first order rate constants for oligonucleotide cleavage

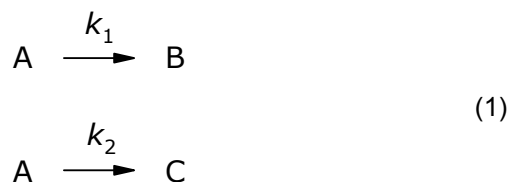
Substrates were heated at 90 °C for 2 min to disrupt potential aggregates, spun briefly in a microfuge and equilibrated for 10 min at the reaction temperature, in a thermostated water bath. The reactions were carried out in polypropylene sterilized micro test tubes, kept inside

metal boxes completely plunged in a thermostated water bath. After adding the desired concentration of divalent metal ions to the deoxyribozyme tube, reactions were initiated by adding the substrate (total volume of the reaction mixture: 40 ml). Samples were collected at appropriate time intervals and quenched by adding formamide and excess EDTA. Radiolabeled substrates and products were separated on 7M urea/20% polyacrylamide gels and quantitated using a Personal Molecular Imager (Bio-Rad). Reaction time-courses were fit to the appropriate kinetic equation using Sigma Plot (SPSS Inc.).

In a typical experiment calix[4]arene **5** (10 μ L, 1 mM in EtOH) and CuCl₂ (20 μ L, 1.5 mM in H₂O) were added to 149 μ L of 15 mM PIPES solution pH 7.4. The solution was kept overnight at room temperature to ensure a complete complex formation and then thermostated at 50 °C. After 1 h the oligonucleotide (20 μ L, concentration between 0.05 and 0.5 nM depending on the radioactivity of ³²P-end label, in H₂O) and SDS (1.5 μ L, 7 mM in H₂O) were injected (final concentration 50 μ M **14**-[Cu]₃, oligonucleotide between 0.005 and 0.05 nM, 50 μ M SDS). Aliquots (25 μ L) of the reaction mixture were injected in 30 μ L of CH₂Cl₂ and 1.5 μ L of 0.5 M EDTA solution (50 mM). The solutions were vortexed, centrifugated and 4 μ L of the aqueous phase were taken and quenched in 5.6 μ L of stop solution. These solutions were successively loaded into the wells of the polyacrylamide-gel. After the run, the gel was dried and exposed to a Kodak phosphor screen that was analyzed by a Personal Molecular Imager (Bio-Rad). Cleavage reactions with rate constants $k_{\text{obs}} > 3 \times 10^{-5} \text{ s}^{-1}$ were obtained by analyzing the data of the overall exponential development of the reaction, while $k_{\text{obs}} < 3 \times 10^{-5} \text{ s}^{-1}$ were obtained by initial rate methods.

7.5 Appendix

In the case of two parallel first order reactions, where one substrate **A** give products **B** and **C** according to scheme (1), the concentrations of the products **B** and **C** at any time are given by equations (2) and (3).²⁷ Comparing equations (2) and (3) both **B** and **C** rise exponentially with a rate constant equal to (k_1+k_2) , because the rates depend on the concentration of **A**, which decreases exponentially with a rate constant equal to (k_1+k_2) . Moreover, at all times the ratio of products **B** and **C** is $\mathbf{B/C} = k_1/k_2$.



$$B = \frac{k_1}{k_1 + k_2} A_0 [1 - e^{-(k_1 + k_2)t}] \quad (2)$$

$$C = \frac{k_2}{k_1 + k_2} A_0 [1 - e^{-(k_1 + k_2)t}] \quad (3)$$

In the case of the reaction of oligonucleotide **6**, **A** is the substrate, **B** is the fragment 5'-ACC arising from CpA cleavage and **C** is the fragment 5'-AC given by CpC cleavage. Plotting the molar fractions of 5'-ACC and 5'-AC as function of time (Figure 7.7), for the reaction catalyzed by **5**-[Cu]₃, and fitting them with an exponential function the same value of k_{obs} for the cleavage of CpA and CpC is measured, meaning that the two reactions are parallel. Since $k_{\text{obs}} = k_1 + k_2$ and knowing that the ratio of the products is k_1/k_2 , we calculated the pseudo-first order rate constants (k_1 and k_2) relative to the single processes.

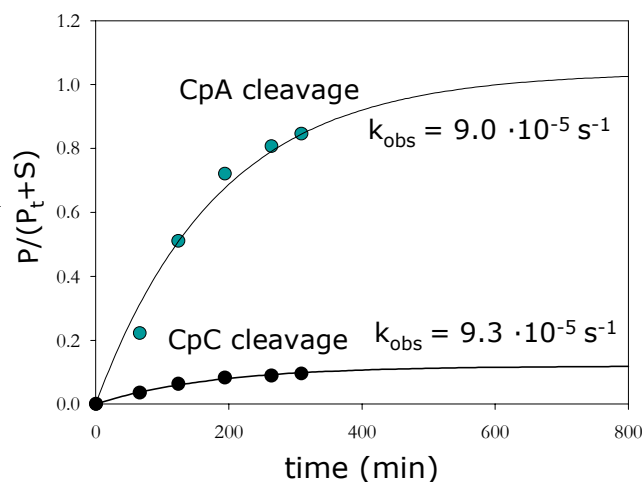


Figure 7.9 Molar fractions of 5'-ACC (CpA cleavage) and 5'-AC (CpC cleavage) as function of time for the reaction of oligonucleotide **6** catalyzed by 50 μM **5**-[Cu]₃.

A different picture was obtained in the case of the oligonucleotide **10** cleavage. Figure 7.8 shows the molar fractions of the products as function of time for the reaction of **10** catalyzed by **4**-[Cu]₃. It appears clear that the cleavage of CpA, CpG, and CpC are not three parallel reactions. The concentration of the fragment given by CpA cleavage at first raises, but at a certain point starts decreasing meaning that it becomes a substrate for further cleavage.

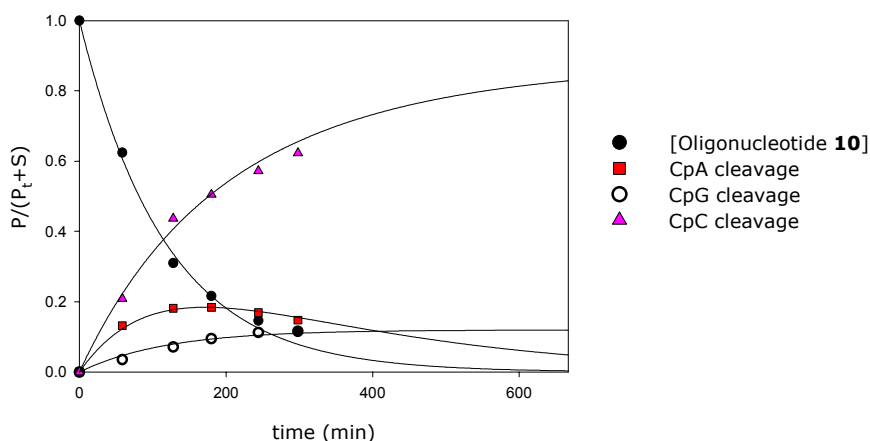
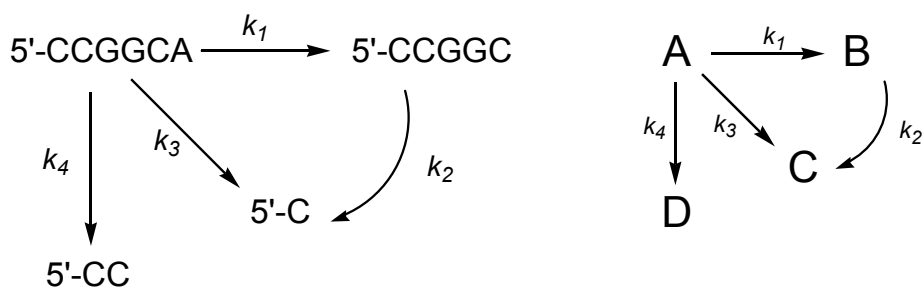


Figure 7.10 Molar fractions of substrate, 5'-CCGGC (CpA cleavage), 5'-CC (CpG cleavage) and 5'-C (CpC cleavage) as function of time for the reaction of oligonucleotide **10** catalyzed by 50 μM **4**-[Cu]₂.

The data were fitted considering the Scheme 7.1, where beside the three parallel reactions (k_1 , k_3 , and k_4) the consecutive reaction from 5'-CCGGC to 5'-C was taken into account. For simplicity the reaction of 5'-CCGGC to 5'-CC and the reaction of 5'-CC to C were neglected, because they are slow compared to the others.



Scheme 7.1

A is the substrate and **B**, **C**, **D** the products of the reaction (Scheme 7.1). The differential equations describing this reaction scheme are:

$$\frac{dA}{dt} = -k_1A - k_4A - k_3A = -(k_1 + k_4 + k_3)A = -k_T A \quad (4)$$

$$\frac{dB}{dt} = k_1A - k_2B \quad (5)$$

$$\frac{dC}{dt} = k_2B + k_3A \quad (6)$$

$$\frac{dD}{dt} = k_4A \quad (7)$$

Integration of differential equation (4) gives the time dependent concentration of A:

$$A = A_0 \exp(-k_T t) \quad (8)$$

Substitution of this solution into equation (7) yields the differential equation:

$$\frac{dD}{dt} = k_4 A = k_4 A_0 \exp(-k_T t) \quad (9)$$

and its integration gives (10)

$$D = k_4 A_0 \int_0^t \exp(-k_T t) = \frac{k_4 A_0}{k_T} (1 - \exp(-k_T t)) \quad (10)$$

The concentration of B is given by (11)²⁷:

$$B = \frac{A_0 k_1}{k_2 - k_T} (e^{-k_T t} - e^{-k_2 t}) \quad (11)$$

Finally since by the mass balance is $A+B+C+D=A_0$, the equation for C can be obtained.

$$C = A_0 - A - B - D$$

$$C = A_0 \left(1 - e^{-k_T t} - \frac{k_1}{k_2 - k_T} (e^{-k_T t} - e^{-k_2 t}) - \frac{k_4}{k_T} (1 - e^{-k_T t}) \right) \quad (12)$$

7.6 References and notes

- (1) Li, Y.; Breaker, R. R. *J. Am. Chem. Soc.* **1999**, *121*, 5364-5372.
- (2) Soukup, G. A.; Breaker, R. R. *RNA* **1999**, *5*, 1308-1325.
- (3) Zagorowska, I.; Mikkola, S.; Lönnberg, H. *Helv. Chim. Acta* **1999**, *82*, 2105-2111.
- (4) Kaukinen, U.; Bielecki, L.; Mikkola, S.; Adamiak, R. W.; Lönnberg, H. *J. Chem. Soc., Perkin Trans. 2* **2001**, 1024-1031.
- (5) Kierzek, R. *Nucleic Acids Res.* **1992**, *20*, 5073-5077.
- (6) Kværnø, L.; Wengel, J. *Chem. Commun.* **2001**, 1419-1424.
- (7) Torres, R. A.; Bruice, T. C. *Proc. Natl. Acad. Sci. U. S. A.* **1998**, *95*, 11077-11082.
- (8) Kaukinen, U.; Lyytikäinen, S.; Mikkola, S.; Lönnberg, H. *Nucleic Acids Res.* **2002**, *30*, 468-474.
- (9) Kaukinen, U.; Venalainen, T.; Lönnberg, H.; Perakyla, M. *Organic & Biomolecular Chemistry* **2003**, *1*, 2439-2447.
- (10) Kaukinen, U.; Lönnberg, H.; Perakyla, M. *Organic & Biomolecular Chemistry* **2004**, *2*, 66-73.
- (11) Kierzek, R. *Meth. Enzymol.* **2001**, 657-675.
- (12) Oivanen, M.; Kuusela, S.; Lönnberg, H. *Chem. Rev.* **1998**, *98*, 961-990.
- (13) Kosonen, M.; Yousefi-Salakdeh, E.; Strömberg, R.; Lönnberg, H. *J. Chem. Soc., Perkin Trans. 2* **1998**, 1589-1595.
- (14) Kuusela, S.; Lönnberg, H. *J. Chem. Soc., Perkin Trans. 2* **1994**, *2*, 2301-2306.
- (15) Stern, M. K.; Bashkin, J. K.; Sall, E. D. *J. Am. Chem. Soc.* **1990**, *112*, 5357.

- (16) Butzow, J. J.; Eichhorn, G. L. *Biochemistry* **1971**, *10*, 2019-2027.
- (17) Komiyama, M.; Kina, S.; Matsumura, K.; Sumaoka, J.; Tobey, S.; Lynch, V. M.; Anslyn, E. J. *Am. Chem. Soc.* **2002**, *124*, 13731-13736.
- (18) Liu, S. H.; Hamilton, A. D. *Chem. Commun.* **1999**, 587-588.
- (19) Yashiro, M.; Ishikubo, A.; Komiyama, M. *Chem. Commun.* **1997**, 83-84.
- (20) Molenveld, P.; Engbersen, J. F. J.; Reinhoudt, D. N. *Angew. Chem. Int. Ed. Engl.* **1999**, *38*, 3189-3192.
- (21) The measurements described in this chapter were carried out in the laboratories of Prof. Peracchi, at Biochemistry Department of the University of Parma, in collaboration with R. Salvio.
- (22) T4 Polynucleotide Kinase (T4 PNK) is a polynucleotide 5'-hydroxyl kinase that catalyzes the transfer of the gamma-phosphate from ATP to the 5'-OH group of single- and double-stranded DNAs and RNAs, oligonucleotides or nucleoside 3'-monophosphates.
- (23) Kierzek, R. *Nucleic Acids Res.* **1992**, *20*, 5079-5084.
- (24) Podyminogin, M. A.; Vlassov, V. V.; Giege, R. *Nucleic Acids Res.* **1993**, *21*, 5950-5956.
- (25) Zenkova, M.; Beloglazova, N.; Sil'nikov, V.; Vlassov, V.; Giege, R. *Meth. Enzymol.* **2001**, *341*, 468-490.
- (26) Bibillo, A.; Figlerowicz, M.; Kierzek, R. *Nucleic Acids Res.* **1999**, *27*, 3931-3937.
- (27) Cox, B. G. *Modern Liquid Phase kinetics*; Oxford Science Publications: 1994.
- (28) HubschWeber, P.; Youinou, M. T. *Tetrahedron Lett.* **1997**, *38*, 1911-1914.
- (29) Maniatis, T.; Fritsch, E. F.; Sambrook, J. *Molecular Cloning: A Laboratory Manual*; Cold Spring Harbor: New York, 1982.
- (30) Cantore, C. R.; Warshaw, M. M.; Shapiro, H. *Biopolymers* **1970**, *9*, 1059-1077.

Summary

Supramolecular catalysis is the main topic of this thesis. New calix[4]arene-based metallo-catalysts were synthesized by linking one, two or three ligating groups at the upper rim of the calixarene skeleton. The catalytic activity of the copper, zinc or barium complexes was investigated in phosphoryl and acyl transfer reactions.

Previous research had revealed that the calix[4]arene motif is an interesting scaffold to build multifunctional enzyme models, thanks to its ability to opportunely preorganize the catalytic functions at the upper or lower rim. Moreover, even when blocked in the cone structure, it maintains a residual conformational mobility, and this allows the calixarene based catalysts to adapt themselves to the changes of the substrate geometry in the transition state. An important aspect is the development of water-soluble catalysts. For this purpose a supramolecular approach was used, which exploits the interaction between adamantyl calix[4]arenes and β -cyclodextrins (β -CD). The interaction between some of these calixarene derivatives and polyvalent β -CDs and β -CD self-assembled monolayers (SAMs) was also studied in solution and at surfaces, respectively.

A general introduction to enzyme catalysis and its origins is reported in the first part of Chapter 2. The mechanisms of the phosphoryl and acyl transfer reactions, with particular attention to the role of metal ions, are explained in the second part of this chapter and examples of natural nucleases and peptidases that exploit divalent ions are described. Recent examples of synthetic mono-, di- and trinuclear metal catalysts for the cleavage of phosphates, amides and esters are reviewed in the third part, underlining the factors that influence the cooperativity of the metal ion centers.

Chapter 3 describes three different approaches to solubilize in water a calixarene compound bearing three 2,6-bis[(dimethylamino)methyl]pyridine groups at the upper rim. Its zinc complex had previously shown good catalytic activity in the phosphodiester cleavage in EtOH/H₂O 35%. Water solubility is an essential property of nuclease mimics because, ultimately, their activity has to be studied on natural substrates such as RNA under physiological conditions. In order to make this compound soluble in water we introduced adamantyl units at the calixarene lower rim and exploited the formation of inclusion complexes with β -CDs in water. It was found that the adamantyl group (Ad) is incompatible with the reactions needed to attach the pyridine units at the upper rim. However, it was possible to prepare some water soluble *p*-guanidinium di- and tetraadamantyl calix[4]arenes and to study the calix[Ad]- β -CD interactions in solution by microcalorimetry and at the surface of β -CD SAMs by surface plasmon resonance. When the spacer between the Ad group and the calixarene is more than twelve atoms, all four adamantyl moieties can be included by

β -CDs without interference among binding sites, and with intrinsic binding constants in the range $2.9\text{-}5.4 \times 10^4 \text{ M}^{-1}$. Another approach towards a water-soluble calixarene-based catalyst consisted in the introduction of six hydroxyl groups at the upper rim of a trispyridine catalyst, obtaining a compound with a solubility of $2 \times 10^{-4} \text{ M}$. However, studies of Zn(II) complexation in pure water revealed that the binding constant of the 2,6-bis[(dimethylamino)methyl]pyridine chelating units is too low to ensure a quantitative formation of the complex at millimolar concentration.

In [Chapter 4](#) the procedure to obtain a calix[4]arene with two functional groups such as alcohols, formyls or carboxylic acids in the 1,2-proximal positions is described. These compounds are important intermediates for the synthesis of catalysts bearing metal ions in proximal positions. Novel difunctional calix[4]arene ligands were prepared by introducing two monoaza-18-crown-6 in the 1,2-proximal or 1,3-diametral positions of the calix[4]arene upper rim. The Ba^{2+} complexes of these compounds were investigated as catalysts in the ethanolysis of esters endowed with a carboxylate anchoring group. For the first time a direct comparison between diametral and proximal calix[4]arene supramolecular catalysts was performed. Even if in both cases the metal centers are able to cooperate, the proximal calixarene catalyst is largely superior to its diametral regioisomer. One of the parameters that mostly influence the reactivity is the distance between the carboxylate and the ester carbonyl groups, but other factors, favoring the proximal catalyst, are also involved.

[Chapter 5](#) describes, in the first part, the synthesis of a calix[4]arene equipped with two 2,6-bis[(dimethylamino)methyl]pyridine ligating groups in the proximal positions in order to compare the catalytic activity with those of similar catalysts reported in the literature. In the second part, the synthesis of a new class of ligands ([12]aneN₃-calixarenes) is described. These compounds were synthesized by functionalizing the calix[4]arene upper rim with one, two (in diametral or proximal positions) or three triazacyclododecane ([12]aneN₃) macrocycles. The [12]aneN₃ is a ligating group for divalent transition metal ions which is much stronger and more hydrophilic than the 2,6-bis[(dimethylamino)methyl]pyridine, thus allowing a higher stability and an easier solubilization in water of the calixarene metal complexes. The catalytic activity of the Zn(II) complexes of the pyridine-calixarenes and [12]aneN₃-calixarenes was investigated in the methanolysis of aryl esters. The measurements, carried out in methanol at pH 10.4, show that the two classes of catalysts have similar catalytic properties. The presence of a carboxylic anchoring group on the substrate is necessary to obtain high rate enhancements, which, in some cases, reach values up to 10^5 in the presence of 1 mM catalyst. The 1,2-proximal calix[4]arene complexes are much more effective than their 1,3-diametral isomers. The two metal centers in proximal positions can cooperate better in the catalytic process, as one coordinates the carboxylate group present on the substrate and the other activates the attacking methoxide anion. The higher rate enhancements obtained with the trinuclear catalysts were explained by taking into

account the statistical advantage of these compounds over the corresponding 1,2-dinuclear ones. Only in the case of the trinuclear Zn(II) pyridine-calixarene complex with the *p*-carboxyphenyl acetate a significant contribution of the third Zn(II) ion in the activation of the ester carbonyl group was found. The Zn(II) complexes of the 1,2-proximal disubstituted and trisubstituted [12]aneN₃-calixarenes, show a remarkable shape selectivity for *m*-carboxyphenyl acetate over its *para*-isomer. The reactions follow Michaelis-Menten kinetics with the formation of a catalyst-substrate complex that reacts to give the product.

Chapter 6 reports, in the first part, the activity of Zn(II) and Cu(II) [12]aneN₃-calixarene complexes in the cleavage of phosphodiester bonds in the RNA hydroxypropyl-*p*-nitrophenyl phosphate ester (HPNP). The choice of copper(II) metallo-catalysts was due to the fact that [12]aneN₃-calixarene Cu(II) complexes are more soluble in water and show higher cooperativity in the activation of the phosphate bond of HPNP compared to the corresponding Zn(II) complexes. The rate enhancement of HPNP transesterification catalyzed by the trinuclear Cu(II) calixarene measured as a function of the substrate concentration showed Michaelis-Menten kinetics, where the substrate binds to the catalyst with a $K_{\text{ass}} = 500 \text{ M}^{-1}$ and it is converted into product with a $k_{\text{cat}} = 7.6 \times 10^{-4} \text{ s}^{-1}$. In the second part of the chapter, the catalytic activity of the Cu(II) trinuclear complex in dinucleotide cleavage is reported. A remarkable selectivity for UpU and UpG dinucleotides was observed, e.g. UpU is cleaved 40 times faster than GpA. Compared to the uncatalyzed reactions, the rate enhancements measured for the cleavage of UpU and UpA are in the order of 7×10^3 .

In Chapter 7 the catalytic activity of Cu(II) [12]aneN₃-calix[4]arene complexes in oligonucleotide cleavage was investigated. The reactions were carried out at 50°C, [cat] = 50 μM, and the substrates were six-, seven- and seventeen-base oligomers radiolabeled with ³²P in 5'-position. Both the two dinuclear and the trinuclear copper complexes are very efficient catalysts in the cleavage of phosphodiester bonds within an oligomer. Beside the cooperative action of the metal centers, also the calixarene apolar skeleton seems to play an important role in the catalytic process. Its action is probably due to the creation of an apolar environment around the oligonucleotide that favors hydrophobic interactions along with hydrogen bonding useful for the phosphate cleavage. Phosphodiester bonds having a pyrimidine nucleotide in the 5'-position are cleaved faster. In all the investigated cases, CpA is the most reactive bond with all the catalysts, and the ease with which this bond can be cleaved depends also on its position in the oligonucleotide, increasing when the bond is closer to the 5'-terminal position. The results indicate that the reactivity and selectivity data obtained with RNA models or dinucleotides cannot be simply extended to larger oligonucleotides or RNAs, since with macromolecular substrates many other factors could come into play.

Samenvatting

Supramoleculaire katalyse is het hoofdonderwerp van dit proefschrift. Nieuwe, op calix[4]areen gebaseerde metallo-katalysatoren zijn gesynthetiseerd door een, twee of drie metaalbindende groepen aan de bovenrand van het calixareenskelet te bevestigen. De katalytische activiteit van hun koper-, zink- of bariumcomplexen in fosforyl- en acyl-overdrachtsreacties is bestudeerd.

Eerder onderzoek heeft aangetoond dat het calix[4]areen motief een interessant geraamte vormt voor de constructie van multifunctionele enzymmodellen, dankzij het vermogen van calixarenen om de katalytische functies aan de boven- of onderrand op te arrangeren. Ondanks de vaste kegelstructuur behoudt de calixareen bovendien een residuele conformationele beweeglijkheid, en dit laat toe dat de op calixareen gebaseerde katalysatoren zich aanpassen aan de veranderingen in de geometrie van het substraat in de overgangstoestand. Een belangrijk aspect is de ontwikkeling van wateroplosbare katalysatoren. Voor dit doel werd een supramoleculaire benadering gebruikt, die de interactie tussen adamantylcalix[4]arenen en β -cyclodextrines (β -CD) uitbuit. De wisselwerking tussen enkele van deze calixareenderivaten en polyvalente β -CD's and β -CD 'self-assembled monolayers' (SAMs, zelf-geassembleerde monolagen) werd tevens respectievelijk in oplossing en op oppervlakken bestudeerd.

Een algemene inleiding over enzymkatalyse en zijn oorsprong wordt gegeven in het eerste deel van Hoofdstuk 2. De mechanismen van de fosforyl- en acyl-overdrachtsreacties, met speciale aandacht voor de rol van metaalionen, worden uitgelegd in het tweede deel van dit Hoofdstuk, en voorbeelden worden gegeven van natuurlijke nucleasen en peptidasen die divalente ionen uitbuiten. In het derde deel wordt een overzicht gegeven van recente voorbeelden van synthetische mono-, di-, en tri-nucleaire metaalkatalysatoren voor de splitsing van fosfaten, amiden, en esters, welke de factoren onderstreep die de coöperativiteit tussen de metaalioncomplexen beïnvloeden.

Hoofdstuk 3 beschrijft drie verschillende benaderingen om een calixareenverbinding met drie 2,6-bis[(dimethylamino)methyl]pyridine-groepen aan de bovenrand oplosbaar te maken in water. De hiervan afgeleide zink-complexen hebben voorheen reeds goede katalytische activiteit laten zien in de fosfodiëster splitsing in EtOH/H₂O 35%. Oplosbaarheid in water is een essentiële eigenschap van nuclease mimics aangezien hun activiteit uiteindelijk op natuurlijke substraten zoals RNA, en onder fysiologische condities, bestudeerd moet worden. Om deze verbindingen oplosbaar te maken in water hebben we adamantyleenheden ingevoerd aan de onderrand van de calixarenen en hebben we de vorming van insluitingscomplexen met β -CDs in water gebruikt. De adamantylgroep (Ad) bleek niet

kompatibel te zijn met de reacties die nodig zijn om de pyridine-eenheden aan de bovenrand te bevestigen. Het was evenwel mogelijk om enkele wateroplosbare *p*-guanidinium di- en tetraadamantyl-calix[4]arenen te bereiden en de calix[Ad]- β -CD interacties te bestuderen met behulp van microcalorimetrie in oplossing en via 'surface plasmon resonance' op het oppervlak van β -CD SAMs. Wanneer de spacer tussen de adamantylgroep en de calixareen langer is dan twaalf atomen kunnen alle vier de adamantylgroepen door β -CDs worden ingesloten zonder interferentie van andere bindingsposities en met intrinsieke bindingskonstanten in het bereik van $2.9\text{-}5.4 \times 10^4 \text{ M}^{-1}$. Een andere benadering om wateroplosbare op calixareen gebaseerde katalysatoren te verkrijgen omhelsde de invoering van zes hydroxylgroepen aan de bovenrand van een trispyridine katalysator, waardoor een verbinding werd verkregen met een oplosbaarheid van $2 \times 10^{-4} \text{ M}$. Complexatiestudies met Zn(II) in zuiver water onthulden echter dat de bindingskonstante van de chelerende 2,6-bis[(dimethylamino)methyl]pyridine-eenheden te laag is om kwantitatieve vorming van het complex te garanderen bij millimolaire concentraties.

In Hoofdstuk 4 wordt de procedure beschreven om een calix[4]areen te verkrijgen met twee functionele groepen zoals alcoholen, formylgroepen, of carbozuren, op de 1,2-proximale posities. Deze verbindingen zijn belangrijke tussenproducten voor de synthese van katalysatoren met metaalionen in de proximale posities. Nieuwe bifunctionele calix[4]areenliganden werden bereid door twee monoaza-18-kroon-6 in te voeren op de 1,2-proximale of de 1,3-diametrale posities aan de bovenrand van de calix[4]areen. De Ba^{2+} complexen van deze verbindingen werden onderzocht als katalysatoren voor de ethanolysen van esters voorzien van een verankerende carboxylaatgroep. Voor de eerste keer werd een directe vergelijking tussen diametrale and proximale supramoleculaire calix[4]areen-katalysatoren uitgevoerd. Ookal zijn in beide gevallen de metaalcentrums in staat om te coöpereren, toch is de proximale calixareen-katalysator vele malen beter dan zijn diametrale regioisomeer. Een van de parameters die de reactiviteit het meest beïnvloedt is de afstand tussen de carboxylaatgroepen en de ester-carbonylgroepen, maar er zijn ook andere factoren betrokken ten gunste van de proximale katalysator.

Hoofdstuk 5 beschrijft, in het eerste gedeelte, de synthese van een calix[4]areen uitgerust met twee metaalbindende 2,6-bis[(dimethylamino)methyl]pyridine-groepen in de proximale posities om hun katalytische activiteit te kunnen vergelijken met die van soortgelijke katalysatoren die in de literatuur vermeld zijn. In het tweede gedeelte wordt de synthese van een nieuwe klasse liganden ([12]aneN₃-calixarenen) beschreven. Deze verbindingen werden bereid door de calix[4]arenen aan de bovenrand te funktionaliseren met één, twee (in de diametrale of proximale posities), of drie triazacyclododecane ([12]aneN₃) macrocycli. De [12]aneN₃ is een ligerende groep voor divalente overgangsmetaalionen, die veel sterker is en meer hydrofiel dan 2,6-bis[(dimethylamino)methyl]pyridine, wat een verhoging toelaat van de stabiliteit van de resulterende calixareen-metaalcomplexen, en deze gemakkelijker

oplosbaar maakt in water. De katalytische activiteit van de Zn(II) complexen van de pyridine-calixarenen en [12]aneN₃-calixarenen werd onderzocht voor de methanolysen van arylesters. De metingen, die in methanol werden uitgevoerd bij pH 10.4, tonen aan dat de twee klassen van katalysatoren soortgelijke katalytische eigenschappen bezitten. De aanwezigheid van een verankerende carboxylgroep op het substraat is nodig om grote reactiesnelheidsverhogingen te bewerkstelligen, die in enkele gevallen waarden tot wel 10⁵ bereiken bij een katalysatorconcentratie van 1 mM. De 1,2-proximale calix[4]areen-complexen zijn veel effectiever dan hun 1,3-diametrale isomeren. De twee metaalcomplexen in proximale posities kunnen beter coöpereren in het katalytische proces aangezien er één de carboxylaatgroep op het substraat coördineert en de ander het aanvallende methoxide-ion activeert. De grotere verbeteringen in reactiesnelheid, verkregen met de trinucleaire katalysatoren, kunnen worden verklaard door rekening te houden met het statistische voordeel van deze verbindingen tegenover de corresponderende 1,2-dinucleaire complexen. Alleen in het geval van het trinucleaire Zn(II) pyridine-calixareencomplex met *p*-carboxyfenylacetaat werd een beduidende bijdrage van het derde Zn(II) ion aan de activering van de ester-carbonylgroep gevonden. De Zn(II)-complexen van de 1,2-proximale digesubstitueerde and trigesubstitueerde [12]aneN₃-calixarenen vertonen een buitengewone vormselectiviteit voor *m*-carboxyfenylacetaat tegenover zijn *para* isomeer. De reacties volgen Michaelis-Menten kinetiek waarbij een katalysator-substraatcomplex wordt gevormd, dat vervolgens verder reageert tot de producten.

In Hoofdstuk 6 wordt in het eerste deel de activiteit beschreven van Zn(II)- en Cu(II)-[12]aneN₃-calixareencomplexen in de splitsing van fosfodiësterbindingen in RNA hydroxypropyl-*p*-nitrofenylfosfaatester (HPNP). Het gebruik van koper(II) metalokatalysatoren is te wijten aan het feit dat [12]aneN₃-calixareen-Cu(II) complexen oplosbaarder zijn in water en een hogere coöperativiteit vertonen in de activering van fosfaatbinding van HPNP, in vergelijking tot de corresponderende Zn(II)-complexen. De verbetering in reactiesnelheid voor de door het trinucleaire Cu(II)-calixareen complex gekatalyseerde om-verestering, gemeten als een functie van de substraatconcentratie, vertoonde Michaelis-Menten kinetiek, waarbij het substraat aan de katalysator bindt met $K_{\text{ass}} = 500 \text{ M}^{-1}$ en in produkt wordt omgezet met $k_{\text{cat}} = 7.6 \times 10^{-4} \text{ s}^{-1}$. In het tweede deel van het Hoofdstuk wordt de katalytische activiteit van het trinucleaire Cu(II)-complex in de splitsing van dinucleotiden beschreven. Er werd een buitengewone selectiviteit voor UpU en UpG dinucleotides waargenomen; UpU werd 40 maal sneller gesplitst dan GpA. De reactiesnelheidsverhogingen waargenomen voor de splitsing van UpU en UpA zijn in de orde van 7×10^3 ten opzichte van de ongekatalyseerde reacties.

In Hoofdstuk 7 werd de katalytische activiteit van Cu(II)-[12]aneN₃-calix[4]areen-complexen in de splitsing van oligonucleotiden bestudeerd. De reacties werden uitgevoerd bij 50°C, [cat] = 50 μM, en de substraten waren zes-, zeven-, en zeventien-basenlange radio-

gelabelde oligomeren met ^{32}P op de 5'-positie. Zowel de twee dinucleaire als de trinucleaire koper complexen zijn zeer efficiënte katalysatoren voor de splitsing van fosfodiëster bindingen in oligomeren. Naast de coöperatieve actie van de metaalcentra's lijkt ook het apolaire calixareengeraamte een belangrijke rol te spelen in het katalytische proces. Zijn werking is waarschijnlijk te danken aan de vorming van een apolaire omgeving rond de oligonucleotide, welke een hydrofobe interactie bevordert zowel als waterstofbindingen die van nut zijn voor de fosfaatsplitsing. Dinucleotidebindingen met een pyrimidinebase op de 5'-positie worden sneller gesplitst. In alle onderzochte gevallen en met alle katalysatoren is CpA de meest reactieve binding, en hoe makkelijk een binding gesplitst kan worden hangt ook af van de positie in de oligonucleotide; hoe dichterbij de binding zich bij de 5'-terminale positie bevindt, hoe makkelijker deze te splitsen is. De resultaten geven aan dat de reactiviteits- en selectiviteitsgegevens die verkregen zijn met RNA-modellen of dinucleotiden niet eenvoudigweg kunnen worden toegepast op grotere oligonucleotiden of RNAs, aangezien er bij macromoleculaire substraten weer vele andere factoren komen kijken.

Acknowledgements

The project of this thesis was born as a collaboration between the groups of Prof. D. N. Reinhoudt, Prof. R. Ungaro and Prof. L. Mandolini and I have worked in the three different groups. This has allowed me to know many people and to learn something from all of them and I would like to thank all the colleagues and friends, who made this Ph.D. period so interesting, nice and enjoyable.

First of all David Reinhoudt, my promoter, who made this kind of project possible, by funding this research. Thanks for supervising me during these four years, for all the stimulating meetings, the ideas and advices that you gave me, and for letting me the freedom of making my own choices within the project.

I would like to thank my Italian supervisors, Rocco Ungaro and my assistant promoter Alessandro Casnati. Avete saputo creare un gruppo di ricerca in cui si può lavorare ad alto livello, ma allo stesso tempo in un clima sereno, quasi familiare. Credo che questa cosa non sia sempre facile da ottenere, e mi ritengo fortunato di aver lavorato tanto tempo in questo gruppo. Grazie anche per la supervisione e gli stimoli che mi avete dato in questi quattro anni e per il lavoro di correzione della tesi.

As I previously said, this work has been a collaboration with the group of Prof. Mandolini (University of Rome, "La Sapienza"), where most of the catalytic measurements were carried out, and where I spent a couple of months. I would like to thank all the people of this group with whom I have worked. Luigi Mandolini, per avermi ospitato nel suo gruppo, per i numerosi consigli e soprattutto per la carica di ottimismo che sapeva trasmettere durante i meeting, anche quando inizialmente i risultati non erano tanti. Roberta Cacciapaglia, bravissima ricercatrice e soprattutto persona di una gentilezza estrema. Grazie per tutte le spiegazioni sulla catalisi e per aver corretto parte della tesi. Thanks to Stefano Di Stefano, who carried out the catalytic measurements with monoaza-18-crown-6-calixarenes shown in Chapter 4. Ho ammirato la passione con cui ti dedichi alla ricerca, e che sai trasmettere a chi lavora con te. I would like to thank Riccardo Salvio for the measurements of methanolysis described in Chapter 5. Moreover, I collaborated with him for all the catalytic measurements of cleavage of phosphodiester bonds (Chapters 6 and 7). Con te ho praticamente diviso tutti i successi e gli insuccessi di questa tesi. Grazie per le spiegazioni che colmavano le mie lacune sulla cinetica e per avermi insegnato a fare misure di catalisi.

I am grateful to Prof. Alessio Peracchi, of the Biochemistry Department of the University of Parma, who very kindly has put at my disposal his laboratory for the measurements reported in Chapter 7. Thanks for all the explanations on the RNA's world and the discussions on the interpretation of the results. Grazie anche a Maria, che mi ha insegnato a fare i gel di elettroforesi, e per la sua canora compagnia in laboratorio.

Thanks to Susanna Del Ciotto, who worked with me to the synthesis of the adamantylcalix[4]arenes.

Grazie a Laura P., Laura B., Uta e Iain, che hanno letto e corretto la concept thesis. Iain, grazie anche per tutte le volte che hai risolto i miei problemi con il computer. Uta, sei una persona veramente fuori dall'ordinario, e conoscerti è stata una sorpresa continua. Laura P. e Laura B., quanto tempo abbiamo passato insieme a chimica (e non solo)? Grazie per la vostra amicizia che non è mai venuta meno e anche per l'aiuto nella preparazione della copertina.

Grazie a Sander per il samenvatting, e per tutte le volte che mi hai aiutato con l'olandese.

I would like to thank all the people of the SMCT group, who have made the period spent in Enschede so special. Thanks to all the staff members, in particular way to Jurriann Huskens and Mercedes Crego Calama. Un sincero ringraziamento a Francesca, che avendo appena scritto la tesi mi ha dato utili consigli; Alessio, grazie per la bici e le cene che spezzavano la monotonia delle minestre in busta; Tommaso, per le volte in cui cercavi di spronarmi ad essere più determinato; Marta, con cui ho condiviso lo stress degli ultimi mesi; Barbara, l'unica a conoscere il segreto dell'ISBN; e tutti gli altri: Lourdes, Irene, Miguel, Fernando, Soco, Monica, Emiel, Maria, Henk, Alart, Roberto, Steffen, thank everybody for your friendship and your help.

Un grazie ai miei paraninfi, Olga, sempre piena di energia e allegria, e pronta ad aiutarmi per qualsiasi cosa avessi bisogno, grazie per le lezioni di spagnolo (yo canto, tu cantas, el canta...), un giorno lo imparerò; Mirko, maestro di traduzioni (a 'l bidel), ironia e pirateria, grazie per le cene e i tapper per il giorno dopo (ma l'orchestra sta ancora suonando?).

Passiamo ora al laboratorio di Parma. Prima di tutto vorrei ringraziare Francesco Sansone, in parte artefice di questo Ph.D., una guida del lab. 192, a cui poter sempre chiedere consigli e suggerimenti, chimici e non. Grazie a Stefano, il primo che ho seguito nel suo lavoro di tesi di laurea. Quando ti eri laureato, ho temuto che come tanti altri saresti sparito, e invece eccoci qua, ancora amici, dopo vacanze, serate, grigliate. Grazie a Cecco, ormai papà, Ivan e Leni, che sono venuti in Olanda a trovarmi dopo un viaggio di 17 ore (record!!!) e per la splendida serata a Goor, Federico, altro dell'élite, in fondo mi hai sopportato bene durante l'ultimo anno, e tutti gli altri, Davide, Emiliano, Marco, Barbara, Ombretta, Gigi, Silvia, Sambo, Giovanni, Mira, Elisa, Luca, Nicola, Colo, Mario, Margot. Grazie agli altri chimici non del 192, Luciano, per avermi trascinato in ferrate e arrampicate, che altrimenti non avrei mai fatto, e Matteo.

Grazie infine alla mia famiglia, che mi ha sempre appoggiato in tutte le scelte, senza farmi mai mancare il suo supporto.

Andrea

The author

Andrea Sartori was born in Parma (Italy) on the 5th of November 1973. In 1987 he obtained his diploma at the Liceo Classico "G. D. Romagnosi" in Parma. In November 1997 he graduated, magna cum laude, in Chemistry at the Department of Organic and Industrial Chemistry at the University of Parma under the supervision of Prof. Rocco Ungaro and Prof. Alessandro Casnati with a thesis entitled "New ditopic receptors based on calix[4]arenes, for the simultaneous complexation of cations and anions".

From January 1999 to March 2000, after his military service, he worked at the Department of Physics of the University of Parma under the supervision of Prof. M. Riccò with a grant of the Istituto Nazionale di Fisica della Materia (INFN) on the preparation and study of superconducting and magnetic properties of C₆₀ compounds obtained by intercalation of metal cations in the fullerene lattice.

In May 2000 he joined the supramolecular chemistry and technology group of Prof. Dr. Ir. David N. Reinhoudt at the University of Twente (NL) as a PhD student. The research was carried out partially at the University of Twente and partially at the University of Parma in the group of Prof. Rocco Ungaro, and in collaboration with the group of Prof. Luigi Mandolini (University of Rome "La Sapienza", Italy). The results of the research conducted during the period 2000-2004 are described in this thesis.